UNIVERSITY *of* SHEFFIELD

Department of Civil and Structural Engineering

Triaxial Behaviour of Partially Saturated Granular Soils at Low Stress Levels

by

Talib H. Salman

A thesis submitted to the University of Sheffield in Partial fulfilment for the degree of Doctor of Philosophy

Supervisors: Dr. W F Anderson and Dr. I C Pyrah

June, 1995

Summary

Granular soil is used as a backfilling material in trenches that are prepared for the installation, repair and replacement of service pipes. The soil is likely to be partially saturated and subjected to low stress levels (<100 kPa), as it exists at shallow depths (about 5 m below the ground)

A new double-wall triaxial cell has been designed for testing partially saturated granular specimens, with height/diameter equal to 375 mm/150 mm, at low stress levels. The cell is able to make separate measurements and control of the pore air and pore water pressures. It was designed to make specimen stress and strain measurements internally. A conventional triaxial cell was modified to carry out tests on saturated granular specimens of the same dimensions at low stress levels. Two gradings of Limestone, fine and coarse, with maximum particle sizes of 5 mm and 20 mm respectively were used in the triaxial tests.

The experimental results showed that the suction in the range 25 kPa to 75 kPa can have an effect on the volume, stiffness and shear strength of partially saturated granular soils at low stress levels. The results also showed that there is a linear relationship between q and $(p-u_a)$ for the unsaturated soils or $(p-u_w)$ for the saturated soils. And Fredlund's equation cannot be used to predict the shear strength of partially saturated granular soils at low stress levels, if the value of ϕ' is taken from tests carried out on saturated specimens. The results also showed that there was a relationship between q, $(p-u_a)$, suction, specific volume and water content, all at failure.

ACKNOWLEDGMENTS

I would like to express my sincere gratitude to my supervisors Dr. W F Anderson and Dr. I C Pyrah for their guidance and suggestions during the experimental work and writing up this thesis. I wish to thank Dr. S J Wheeler for his help with the discussion of this thesis. My thanks also go to the technical staff at Sheffield University, Mr. P L Osborne and Mr. M Foster for their suggestions in the designing and development of the experimental apparatus for this research.

Also I would like to thank my wife for her encouragement during this research. My special thanks also go to my parents and in-laws for their help and support. Finally I would like to thank Mr N Ahmed for allowing me using his company's computer, laser printer and photocopier.

Table of Contents

List of Figures

Chapter 6

Chapter 7

List of Plates

List of Tables

List of Symbols

a_c	Corrected area of the specimen at strain ε.
c' and ϕ'	Effective shear strength parameters of a soil at saturation
D	Specimen Diameter
d	Mean grain size
d_e	Specimen diameter at the end of consolidation
d_{im}	Initial membrane diameter
d_{max}	Maximum grain size of a soil
E_m	Membrane elastic modulus
H	Specimen Height
h	Height of water rise in the capillary tube
g	Gravity acceleration
M	Membrane elastic modulus at 10% extension
M_i	Initial elastic modulus at 1% extension.
$p-u_a$	Net mean stress
$p-u_w$	Effective mean stress
q	Deviator stress
r	Curvature or capillary tube radius
T	Surface tension
t_m	Membrane thickness
u_a	Pore air pressure

u_w	Pore water pressure
$(u_a - u_w)$	Suction
V_i	Initial specimen volume
ΔV_c	Volume Change during the consolidation stage
ΔV_e	Volume Change during the equalisation stage
ΔV_{ec}	Volume Change during the equalisation and consolidation combined stage
ΔV_s	Volume Change during the shearing stage
Δv_m	Volumetric strain due to membrane penetration
α	The tangential angle between surface tension force and capillary tube
χ	A parameter equals unity at 100% saturation and zero at zero saturation.
ε	Axial strain
ϕ' and c'	Effective shear strength parameters of a soil at saturation
ϕ^b	The slope of the τ vs. $(u_a - u_w)$, curve
γ_w	Water density
σ	Total Stress
$(\sigma - u_a)$	Net normal stress
σ'	Effective Stress
σ_{om}	Initial confining stress due to membrane
σ_{1m}	Axial stress due to membrane restraint
σ_3	Cell pressure
$(\sigma_3 - u_a)$	Net cell pressure
$(\sigma_3 - u_w)$	Effective cell pressure
τ	Shear strength
v	Specimen specific volume

Chapter 1

Introduction

Most research on the behaviour of granular soils has been carried out on dry or saturated granular soil at high stress levels (>100 kPa). Little work has been done to investigate the behaviour of partially saturated granular soil (coarse sand and gravel) at low stress levels (<100 kPa). The reason may be due to the fact that the value of suction in partially saturated soils decreases as the size of the soil particle increases and the effect of suction on granular soil behaviour may be thought to insignificant. This may be true when dealing with partially saturated granular soil at high stress levels, but at low stress levels (<100 kPa), the value of the suction may be of the same order of magnitude as applied stresses and thus be important. This has led to a gap in the knowledge and understanding of the behaviour of partially saturated granular soils at low stress levels.

Some construction activities are carried out at shallow depths where the soil is likely to be partially saturated and subjected to low stress levels. Such activities include the installation, repair and replacement of service pipes, which take place at no more than five metres below the ground surface. These service pipes are installed in trenches which sometimes are backfilled with imported granular soil. Post-construction settlement of reinstatements across highways are often of such magnitude that repair to the road surface has to be carried out some time after initial reinstatement.

This thesis describes tests that were carried out on partially saturated and saturated granular soils at low stress levels to examine the strength and stiffness of these soils. Two

soil gradings (fine and coarse) were used, which had maximum grain sizes of 5 mm and 20 mm respectively. The objectives of this research were:

(i) to carry out a review of the work that has already been done on the behaviour of partially saturated soils and on factors and errors that affect the triaxial cell design and triaxial test procedures.

(ii) to design a new double-wall triaxial cell for testing partially saturated granular specimens.

(iii) to carry out different types of tests on partially saturated and saturated granular specimens at low stress levels, to obtain high quality and reliable data on the strength and stiffness of partially saturated granular soil at low stress levels.

Chapters 2 and 3 of this thesis review the work that has been done on partially saturated soils, and the factors and errors affecting triaxial cell design and test procedures. In Chapter 4 a description of the experimental apparatus that was used in the current research is given. Chapter 5 describes the methods used to calibrate the measuring devices and the equations that were used to correct the test results. The bulk properties of the test material, the test programme and the test procedures are detailed in Chapter 6. The test results are given in Chapter 7 and discussed in Chapter 8. Finally conclusions and recommendation for further work are listed in Chapter 9.

Chapter 2

Literature Review:

Behaviour and Properties of Partially Saturated Soils

2.1 Introduction

Partially saturated soil, or unsaturated soil, has behaviour and properties different to saturated soil, due to the existence of air in the soil pores in addition to water. Equations that were developed to describe the behaviour of saturated soils may not be adequate to describe the behaviour of unsaturated soils. A review of the literature on the behaviour of unsaturated soil and comparisons with that for saturated soils is reported in this chapter

2.2 Unsaturated Soil - General

By definition an element of unsaturated soil contains soil particles, water and gas (usually air). As the air content increases the degree of saturation decreases. At zero degree of saturation the soil is dry, while at 100% saturation the soil is saturated by water only and the soil has no air content. At degrees of saturation below about 80-90%, close to the optimum water content of the soil, the air voids may be continuous. At higher degrees of saturation the air voids are in the form of occluded bubbles (Fredlund, 1979 and Bocking and Fredlund, 1980)

Fredlund and Morgenstern (1977) defined unsaturated soil as a four phase system, Solid, Water, Air and Contractile Skin (or Air-Water interface). The reason that the contractile skin is defined as an independent phase is because it has a definite boundary surface and it has different properties from the other phases, such as its ability to exert a tensile pull and behave like an elastic membrane.

2.3 Held Water in Soil

There are different ways in which water may exist in soil. These are (i) aqueous vapour, (ii) free water and (iii) held water. Vapour exists in the air voids and can move through the air voids due to pore water pressure and temperature gradients. Free water exists as groundwater which is influenced by gravity forces. Held water is the water which is retained above the water table. Held water can be divided into three types (Croney, 1952, Jumikis, 1962, Barden, 1965 and RRL, 1968):

i. Chemically Combined Water. This water is regarded as part of the soil solids and cannot be removed by drying the soil.

ii. Adsorbed Water. Each soil particle has electrical charges (mainly negative) on its surface. A water molecule behaves as a dipole, as shown in Fig. 2.1, which has positive charge at one end and negative charge at the other end. Charges on the soil particles attract water molecules. Also these attracted water molecules, attract other water molecules and so on, as shown in Fig. 2.1. The attractive forces on the soil particle surface can extend further than the first layer of water molecules, but decrease as distance from the particle surface increases. These attractive forces are called the "Adsorptive Forces". The amount of water held in the soil depends on the specific surface area of the

soil particles. The smaller the particle size of the soil the larger the specific surface area and the larger the amount of water which can be held and vice versa (Lambe, 1953, Jumikis, 1962, RRL, 1968 and Lambe and Whitman, 1976). The layers of water molecules closest to the soil particle are rigidly held against the particle surface, and are not affected by gravity and can only be removed by drying at 110°C temperature or above. Outer layers of water molecules are also unaffected by gravity, but can move under electrical or thermal action. For clays, Lambe (1953) reported that the layer thickness of the strongly attracted water molecules to the soil particle was of the order of 10 water molecules . He also reported that the effect of adsorptive forces becomes insignificant at a distance of 200 water molecules from the particle surface. This phenomenon is called the "Electrical Double Layer".

iii. Water Held by Surface Tension and Capillarity. Water can also be held in the soil pores and around the points of particle contacts. This is due to the surface tension effect. Soil pores act as channels and when dry soil is placed on water, water will rise due to capillary action through these channels to different heights, because the channels have non-uniform diameters. Assuming a uniform channel diameter (Fig. 2.2), the rise in water , h , will be

$$h = 2\,T\cos\alpha \,/\, \rho_w\, r\, g \qquad (2.1)$$

where T is the surface tension, r channel radius, α the tangential angle between surface tension and channel (Fig. 2.2), g gravity acceleration and ρ_w water density. The smaller the radius the greater the height of capillary rise. If a drop of water is added to a point of contact of two soil grains as shown in Fig. 2.3, water will be held at this point under surface tension action. The surface tension forces try to pull the two grains together. The value of the surface tension force is the same as that holding water in a capillary tube (Fig. 2.2), providing r is same for both cases, and the smaller the radius, r (the smaller amount of water) the higher the pull (Jumikis, 1962 and RRL, 1968).

2.4 Suction

Croney(1952) defined soil suction as the reduction of pore water pressure, below atmospheric pressure, which arises mainly from the surface tension and adsorptive forces (section 2.3) which cause water to be held in the soil above the water table.

Although suction in soil is made up from several components, Marshall, as reported by Aitchison (1960), suggested that only two components, matrix and osmotic, need to be considered. Krahn and Fredlund (1972) showed that their sum gives the total suction. Matrix suction is the difference between the pore air and pore water pressures. This type of suction is due to surface tension and adsorptive forces (section 2.3). Osmotic suction is a result of differing ionic concentrations in the pore water. Aitchison (1960) concluded from the work of different authors that osmotic suction can be neglected for total suctions up to 220 atmospheres. Alonso et al. (1987) reporting work of other authors, stated that only matrix suction is relevant in governing the geotechnical behaviour of unsaturated soil. Also they reported experimental evidence that there was a volume change in the soil once a solute is introduced to the soil , but it has no effect on strength. They showed that the solute type and concentration may affect the volumetric behaviour but not through a solute suction term.

Due to the fact that adsorptive forces depend on specific surface area of the soil, (section 2.3), these forces may have insignificant effect on coarse soils, such as sand, due to the small specific surface area of the soil. This means that the surface tension forces may be the dominant forces for coarse soils while the adsorptive forces may be the dominant forces in fine soils, such as clay, due to the large specific area of these soils (Brackley, 1973 and Alonso et el., 1987).

Authors, such as Croney and Coleman, 1948 and 1960, Olson and Leonard, 1965, Barden and Sides, 1970 and Krahn and Fredlund, 1972, showed that there was a relationship between suction and soil moisture (water) content for different types of soil, as shown in Fig. 2.4. As the soil moisture content decreases, suction increases. The figure shows that, at a certain water content, the smaller the grain size the larger the suction, as was discussed in the previous paragraph. Different researchers, such as Croney (1952), reported that this relationship (suction and moisture content) is not the same for wetting and drying cycles as shown in Fig. 2.5. This hystersis effect may arise because the release of water from the larger pores is to some extent controlled by the surrounding smaller pores, during the drying process. Jones and Hurt (1978) have also shown this hystersis effect for coarse granular soils, with a maximum grain size of 38 mm.

The relationship between moisture content and suction indicates that, when other conditions such as temperature are constant, variation in the moisture content at any point in the soil will produce a suction gradient. Water will move towards the higher suction to return the soil to equilibrium. This movement of water can be upwards if the difference in suction is greater than the gravity force (Croney, 1952, Gardener, 1960, Croney and Coleman, 1960 and RRL, 1968). Movement of water may occur either through the liquid or vapour phases or both (Croney and Coleman, 1948 and Randkivi and U'u, 1976). Croney and Coleman (1948) produced a relationship between suction and vapour pressure, as vapour pressure decreases, suction increases.

Temperature has an effect on suction. The increase in temperature produces movement in the liquid and vapour phases towards the cold regions. This movement reduces the water

content and vapour pressure at the hot region, which in turn increases suction at the hot region and decreases suction at the colder region (Taylor and Cary, 1960 and Mohamed et al., 1992). Olson and Leonard (1965) and Krahn and Fredlund (1972) showed that for clay and sandy clay soils, the variation in dry density has little effect on suction. Olson and Leonard (1965) also showed that the type of compaction can have an effect on suction with kneading compaction giving higher suctions than static compaction.

2.5 Suction Effect on Soil Structure

In granular soils, as the water content decreases from saturation, menisci (contractile skin) between air and water will develop due to the difference between air and water pressures. With a further reduction in water content, air will enter soil voids and menisci will recede into the particle contacts as shown in Fig. 2.6a. These menisci help in making the soil structure more stable by pulling the soil particles to each other, as was discussed section 2.3.

Fig. 2.7 shows results of oedometer tests carried out on saturated and unsaturated silts, the saturated curve is below the unsaturated curve. The graph shows clearly the effect of suction in making the soil stiffer than the saturated soil, as the deformation of unsaturated soil is less than that of saturated soil under same stress increase. If the unsaturated soil is inundated with water under constant applied stress, at point A in Fig. 2.7, the soil collapses (sudden reduction in void ratio) until its void ratio becomes close to that of the saturated soil. The reason for this collapse is due to the removal of menisci, or surface tension, which were supporting the soil structure before inundation (Jennings and Burland, 1962 and Blight, 1965).

Suction in a clay soil also makes the soil structure stiffer and more stable, but a different structure to that of granular soil is developed during drying from saturation, because the adsorptive forces in the clay soil are the dominant forces, (section 2.4). Jennings and Burland (1962), Burland (1965), Barden and Sides (1970) and Brackley (1973, 1975) stated that as clay dries and menisci are drawn into the soil matrix, the clay structure tends to form into "Packets" of clay particles as shown in Fig. 2.6b. These packets act as small grains, similar to those of granular soil, and are saturated with water. If water is introduced to the soil it can be absorbed due to the remaining adsorptive forces in the soil particles, until the suction in the packets is balanced by the suction of the water in the inter-packet voids.

Fig. 2.8 shows a graph of void ratio against the applied stress of unsaturated clay when it is inundated with water. The figure shows that under low applied stresses the soil swells and under high applied stresses the soil collapses. This is due to the fact that packets absorb water during inundation and swell (increase in the packet's volume) producing a pressure called the swelling pressure. When the swelling pressure is higher than the applied stress, the soil swells. When the swelling pressure is lower than the applied stress, the soil collapses either due to packet deformation or packet slippage or a combination of both.

2.6 Modelling Unsaturated Soil

After the success of the principle of effective stress to describe the behaviour of saturated soils which was presented by Terzaghi, some authors, such as Bishop (1959), Jennings

(1960) and Aitchison (1960), tried to extend the principle of effective stress to unsaturated soils. The equation below, which was proposed by Bishop (1959), received more attention than other equations, because it included the pressure in the air phase:

$$\sigma' = (\sigma - u_a) + \chi(u_a - u_w) \qquad (2.2)$$

where σ' is the effective stress, σ is the total stress, u_a is the pore air pressure, u_w is the pore water pressure and χ is a parameter which equals unity at 100% saturation and zero at zero saturation. $(\sigma - u_a)$ and $(u_a - u_w)$ are often called the net normal stress and suction respectively.

Bishop et al. (1960) and Bishop and Donald (1961) examined the validity of the above equation by performing triaxial tests on compacted shale clay, boulder clay and silt soils and found that the equation appeared to explain the shear strength behaviour of unsaturated soils. Jennings and Burland (1962) performed oedometer tests on silts and clay soils. They stated that Equation 2.2 could not explain fully the volume change behaviour for unsaturated soils. They showed that there was no unique relationship between void ratio and effective stress for most unsaturated soils below a critical degree of saturation. The critical degree of saturation was about 20% for course granular soils, 40-50% for silts and upwards of 85% for clayey soils. These limitations were also confirmed by Bishop and Blight (1963).

Blight (1965) found that the value of χ not only differed from soil to soil but also depended on the type of test. He proposed two methods to evaluate χ. Each method yielded different values of χ, but no decision was made on which method was more correct. He stated that it was theoretically possible for the value of χ to be greater than

one in unsaturated soil close to saturation, and this was confirmed experimentally by Guilhuti and Satiju (1981).

Maytas and Radhakrishna (1968) abandoned the effective stress concept for unsaturated soils and expressed the soil behaviour as a direct function of two independent stress variables, $(\sigma-u_a)$ and (u_a-u_w), rather than in terms of one single effective stress, as in Equation 2.2. Different authors also recommended the use of these stress variables in expressing the unsaturated soil behaviour, such as Bishop and Blight (1963), Blight (1965), Burland (1965) and Fredlund and Morgenstern (1976, 1977).

Maytas and Radhakrishna (1968) showed experimentally that two (state) surfaces can be obtained if the void ratio or the degree of saturation was plotted against the stress variables, $(\sigma-u_a)$ and (u_a-u_w), as shown in Fig. 2.9. These surfaces were unique for non-decreasing degree of saturation and soil not permitted to swell, and the surfaces are independent of the stress path followed. They indicated that the above two restrictions arise from the fact that hysteresis in the soil (section 2.4) introduced certain non-unique characteristics. Hysteresis may not be the significant factor in this non-uniquness in the state surfaces, it may be due to the elasto-plastic nature of the soil behaviour when is loaded and unloaded.

Fredlund et al. (1978) introduced the equation below to describe the shear strength of unsaturated soils in terms of the stress variables:

$$\tau=c'+(\sigma-u_a)\tan\phi'+(u_a-u_w)\tan\phi^b \qquad (2.3)$$

where τ is the shear strength, c' and ϕ' are the effective shear strength parameters of the soil at saturation and ϕ^b is the slope of the τ vs. $(u_a - u_w)$, curve. The above equation is an extension of the Mohr-Coulomb failure envelope as shown in a three dimensional diagram in Fig. 2.10. Fredlund et al. assumed the failure envelope to be planar with ϕ' and ϕ^b constants. They re-analysed the data reported by Bishop et al. (1960) for the compacted shale clay specimens for suctions below 132 kPa and values of the net cell pressure, $(\sigma_3 - u_a)$, up to 163 kPa, where σ_3 is the cell pressure, and for compacted boulder clay of suctions up to 171 kPa and $(\sigma_3 - u_a)$ up to 381 kPa. They concluded that the failure envelope was planar. This conclusion was also confirmed by Ho and Fredlund (1982) for sand soils.

Escario and Sa'ez (1986) performed tests on clay and sand soils using a modified direct shear apparatus at suctions higher than 70 kPa and $(\sigma_3 - u_a)$ higher than 100 kPa. They showed that the failure envelope (Equation 2.3) cannot be planar, because ϕ^b was found to be variable and not constant as was suggested be Fredlund et al. (1978). This finding was also confirmed by Escario (1989) for high stress levels.

Fredlund et al. (1987) also confirmed the above findings but they showed from the analysis that was carried out on the results that were produced by Bishop et al. (1960) at low stress levels, that the failure envelope was planar, but for higher stress levels the failure envelope was not planar. It may be seen that the work of Escario and Sa'ez (1986) was at higher stress levels (>100 kPa) and high suctions on soil grain sizes up to sand, while the work of Bishop et al. (1960) was on low to intermediate stress levels and low suction on fine soils. No work was carried out at low stress levels for coarser soils to study the validity of Equation 2.3.

Toll (1990) coupled the shear and volume change behaviour within a single framework. His framework is based on the critical state model for saturated soils, but incorporating the additional variables which are needed to formulate unsaturated soil behaviour. He carried out tests on saturated and unsaturated lateritic gravel (about 9% clay content) at high stress levels (>100 kPa) and confirmed that ϕ^b (Equation 2.3) was not constant. Wheeler and Sivakumar (1992) carried out series of triaxial tests on compacted kaolin. They provided evidence of a critical state framework for unsaturated soils, which may be useful in the predictions of unsaturated soil behaviour.

2.7 Behaviour of Coarse Granular Soils

Work on granular soils has concentrated on testing either saturated or dry soils at high stress levels (>100 kPa). Little work has been done to study the behaviour of unsaturated granular soils under different values of suction. The reason may be due to the fact that suction in the coarse granular soils is very low compared with that of clay soils, and thus may be assumed to have an insignificant effect on the soil behaviour. Anderson et al. (1993) reported that suctions for coarse grading soils, with maximum grain size of 37.5 mm, could be as high as 38 kPa, for water content of about 4% (optimum water content was about 6%). This low value of suction could be significant for unsaturated granular soils at low stress levels (<100 kPa). The current research was to investigate the triaxial behaviour of unsaturated granular soils at low stress levels.

The effect of confining pressure on the soil strength of granular soils has been discussed by different authors. Skermer and Hillis (1970), Marachi et al. (1972), Charles and Watts (1980) and Al-Hussaini (1983) showed that for tests on coarse granular soil carried out at high stress levels, that the value of the angle of shearing resistance, ϕ', decreased at

decreasing rate with increasing confining pressure. At very high values of confining pressure (>4 MPa), the curve of ϕ' vs. confining pressure tend to flatten. Skermer and Hillis (1970) showed that at high confining pressures, there was particle breakdown. The particle breakdown increased with decreasing particle size and increasing confining pressure (Al-Hussaini, 1983). For low values of confining pressures, triaxial tests were carried out on saturated fine granular soils (sand) by Ponce and Bell (1971) and Fukushima and Tatsuoka (1984). They showed that the value of ϕ' increased as the confining pressure decreased. Fukushima and Tatsuoka (1984) showed that the increase in ϕ' with the decreasing of confining pressure tend to be very small for confining pressures lower than about 50 kPa, in particular this change was found to be even smaller for confining pressures lower than 10 kPa.

The above authors also showed that the soil stiffness increases as confining pressure increases. The effect of confining pressure on soil stiffness was also studied by Indraratna et al. (1993), as they carried out triaxial tests on saturated greywacke rockfill soil, with maximum grain size of 38.1 mm. They showed that the tangent Young's modulus, for confining pressures above 100 kPa, increased as the confining pressure was increased.

Authors such as Al-Hussaini (1983) and Indraratna et al. (1993) showed that for tests on coarse granular soils carried out at high stress levels, that the compressibility increased with increasing maximum particle size. Also they showed that the volumetric strain increased at a decreasing rate with increasing confining pressure and decreasing density. This conclusion was also reached by Fukushima and Tatsuoka (1984) for saturated sand tested at low stress levels, but the compressibility was very low at confining pressures below 50 kPa. Goodwin (1991) showed that the compressibility of coarse granular soils, tested at low stress level using a modified one dimensional compression cell, decreased

with increasing suction, which may show the effect of suction in producing a stiffer soil structure.

2.8 Effect of Suction on Soil Stiffness

Little work has been done to relate suction to soil stiffness. Authors, such as Wu et al. (1984, 1985) found a relationship between shear modulus and the degree of saturation. As the degree of saturation increased the shear modulus increased. Yoshida et al. (1991) showed that the stiffness of sand and silt soils increased with increasing degree of saturation, although no measurements of suction were carried out. Alonso et al. (1987) reviewed the work of different authors and stated that there was a relationship between the shear modulus and suction, and indicated that for larger values of suction (up to 3 MPa) there was a power relationship between the initial shear modulus and suction.

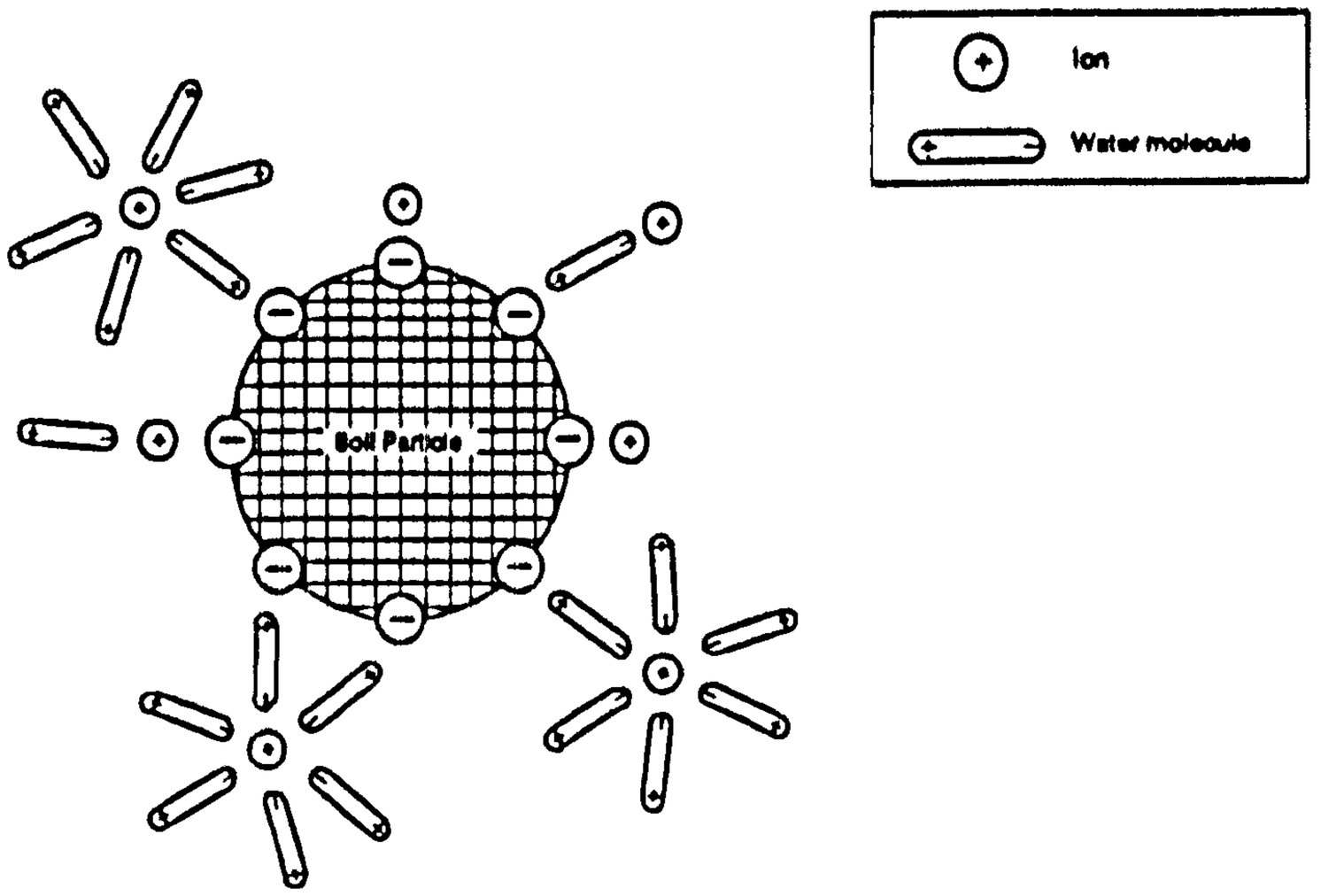

Fig.2.1- Arrangement of water molecules around a soil particle

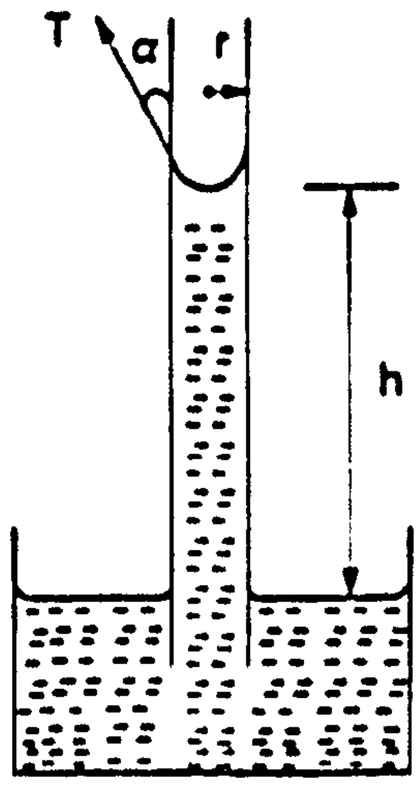

Fig.2.2- Capillary action

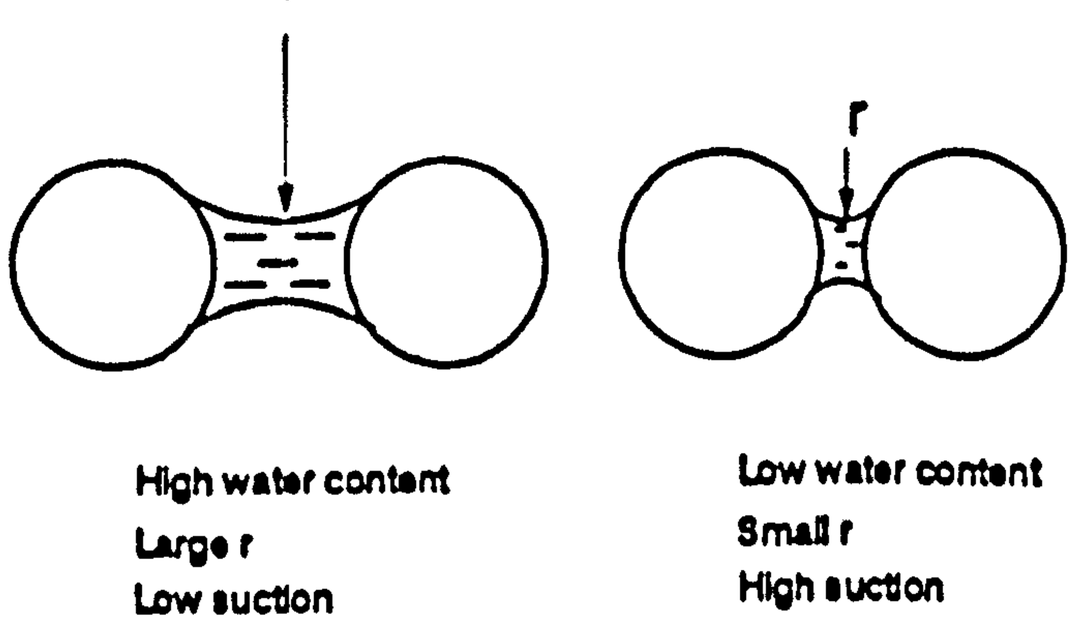

Fig.2.3- Held water between two soil particles

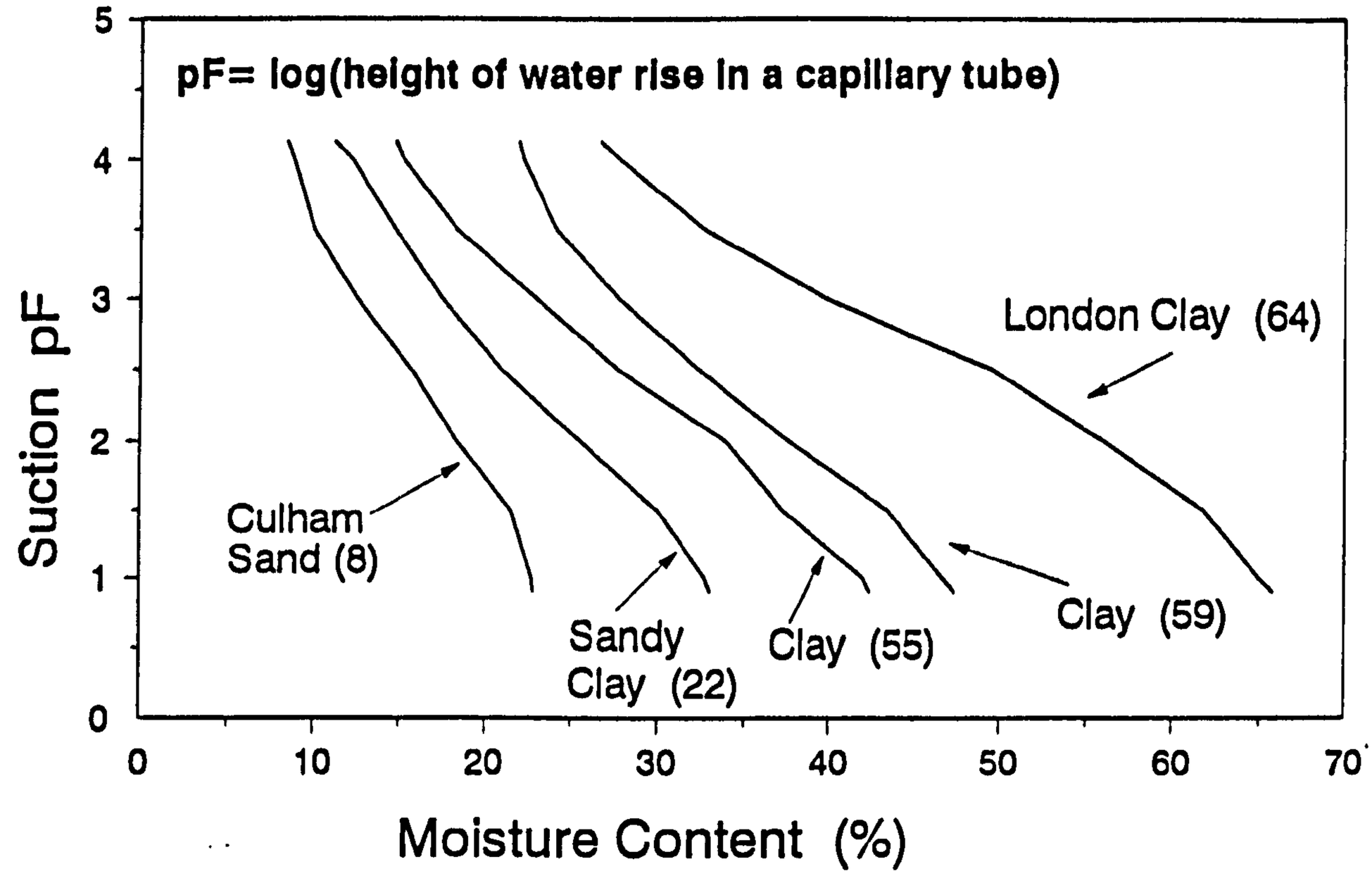

Fig. 2.4- Comparison of soil moisture suction (drying) curves for five soils. Clay content for each soil is shown beside the soil title (after Croney and Coleman, 1948)

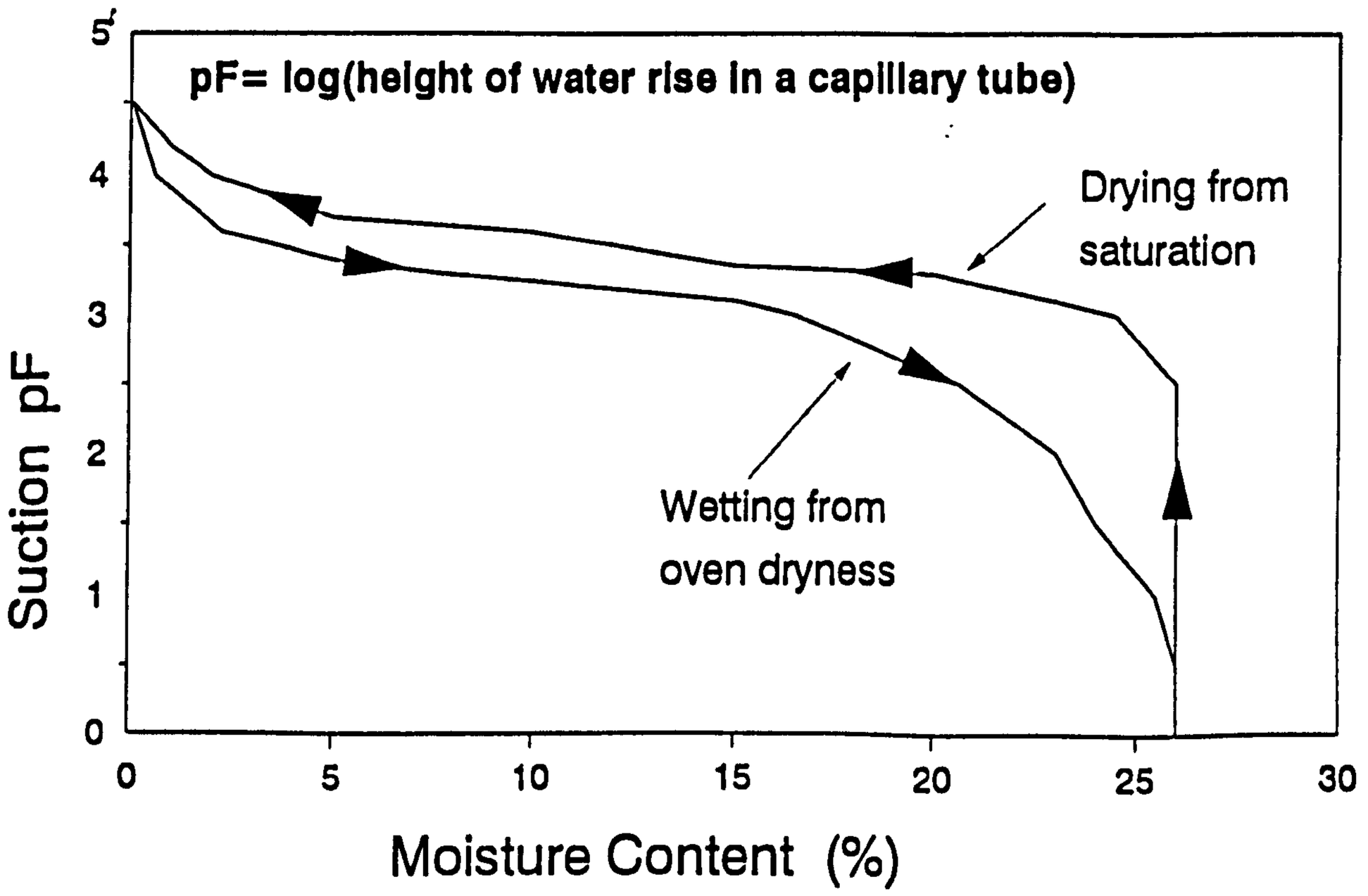

Fig. 2.5- Relationship between suction and moisture content for soft chalk specimen (after Croney, 1952)

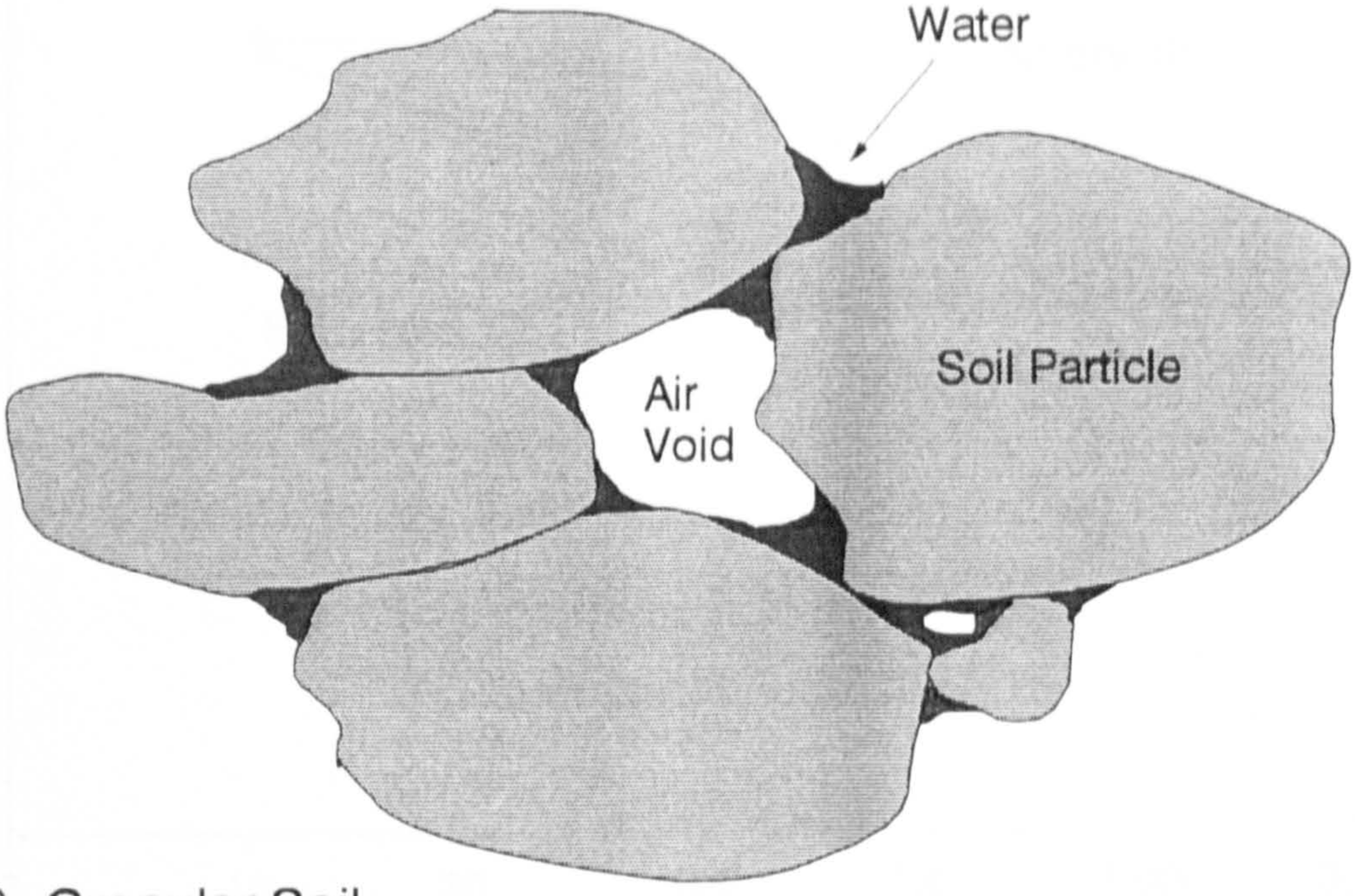

(a) Granular Soil

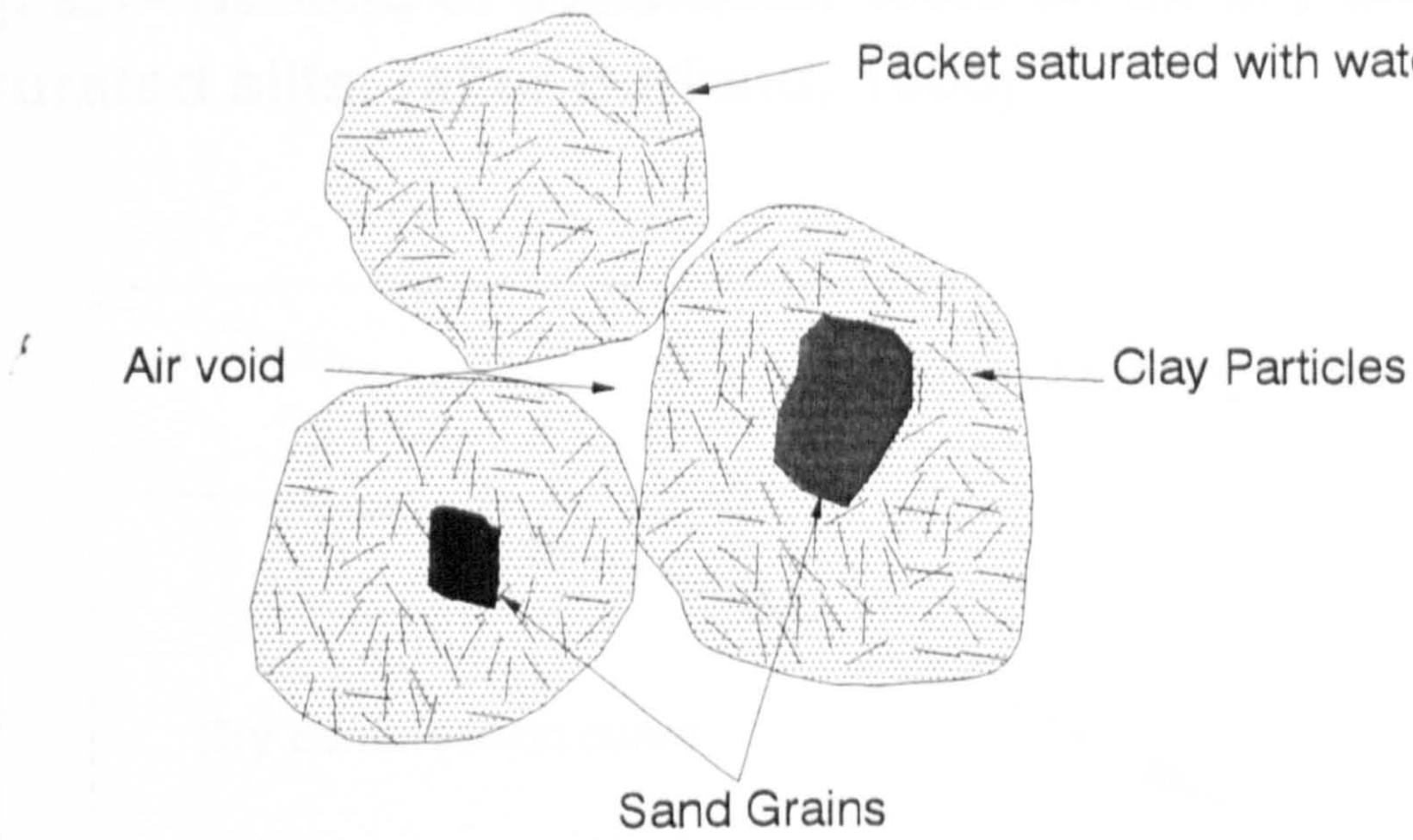

(b) Clay Soil

Fig. 2.6- Particle arrangement for unsaturated (a) granular and (b) clay soils

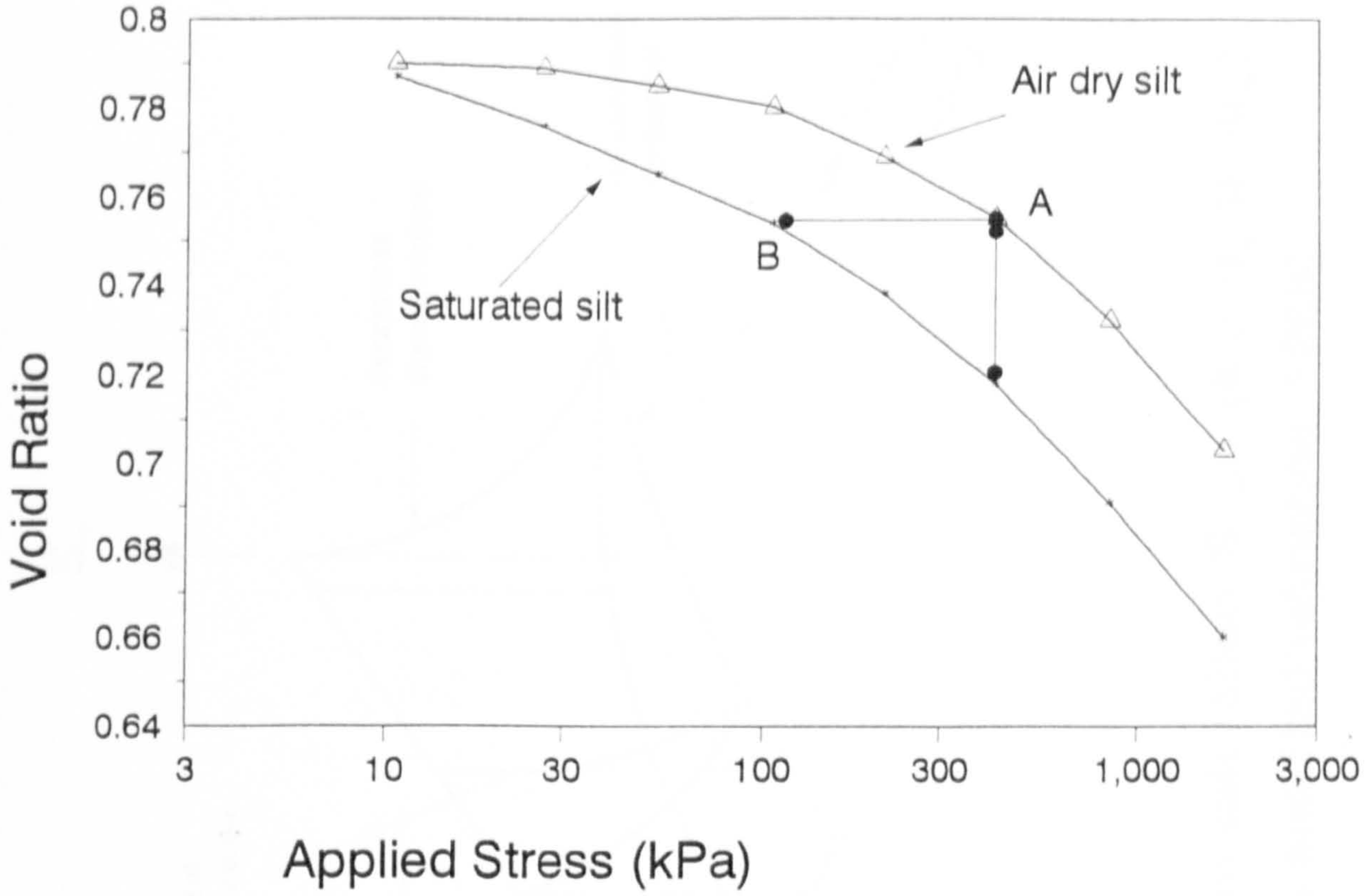

Fig. 2.7- Results of oedometer tests on air dry and saturated silts. (after Burland, 1965)

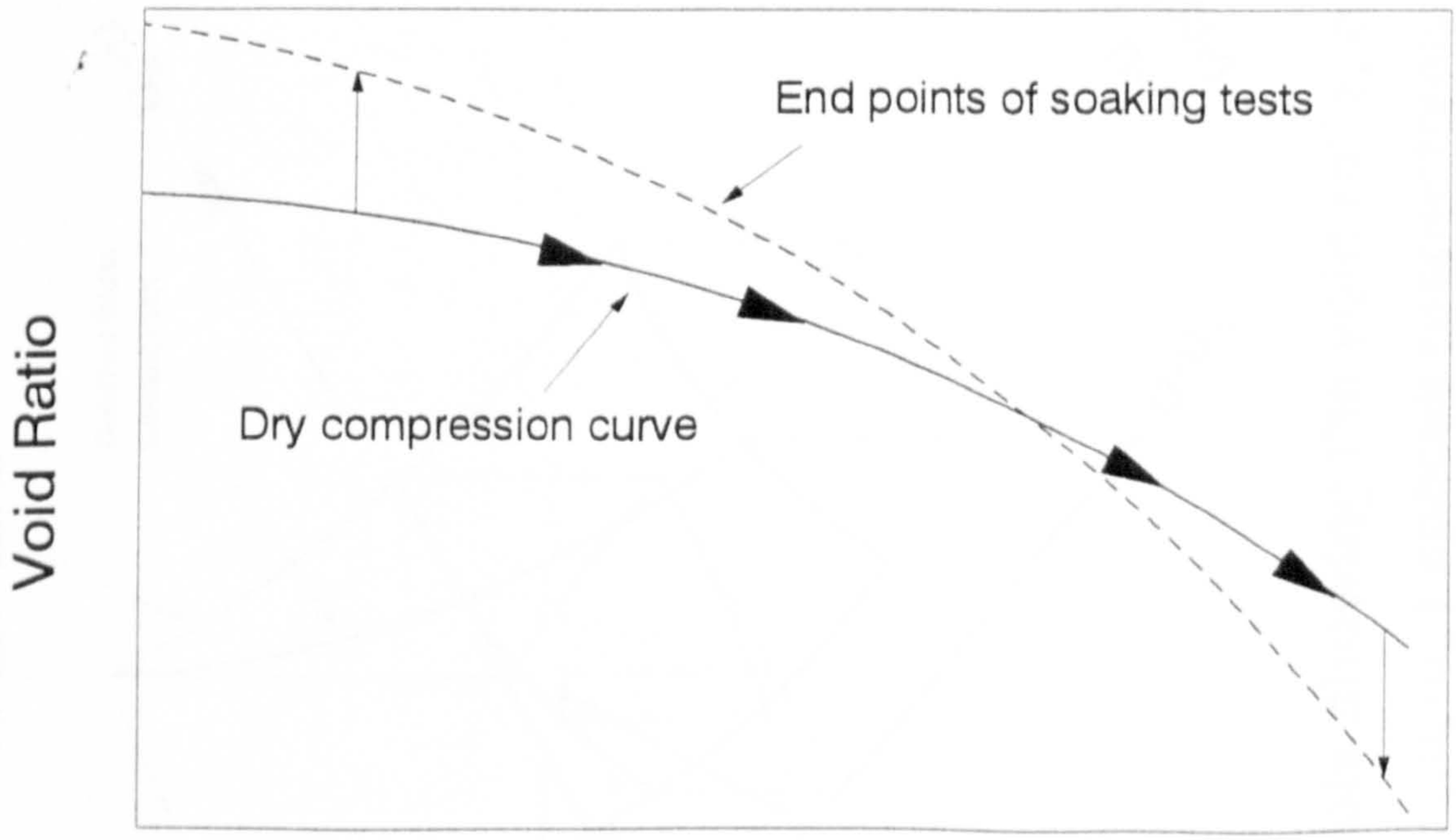

Fig. 2.8- Void ratio changes due to wetting up a dry soil at various applied stresses (after Burland, 1965)

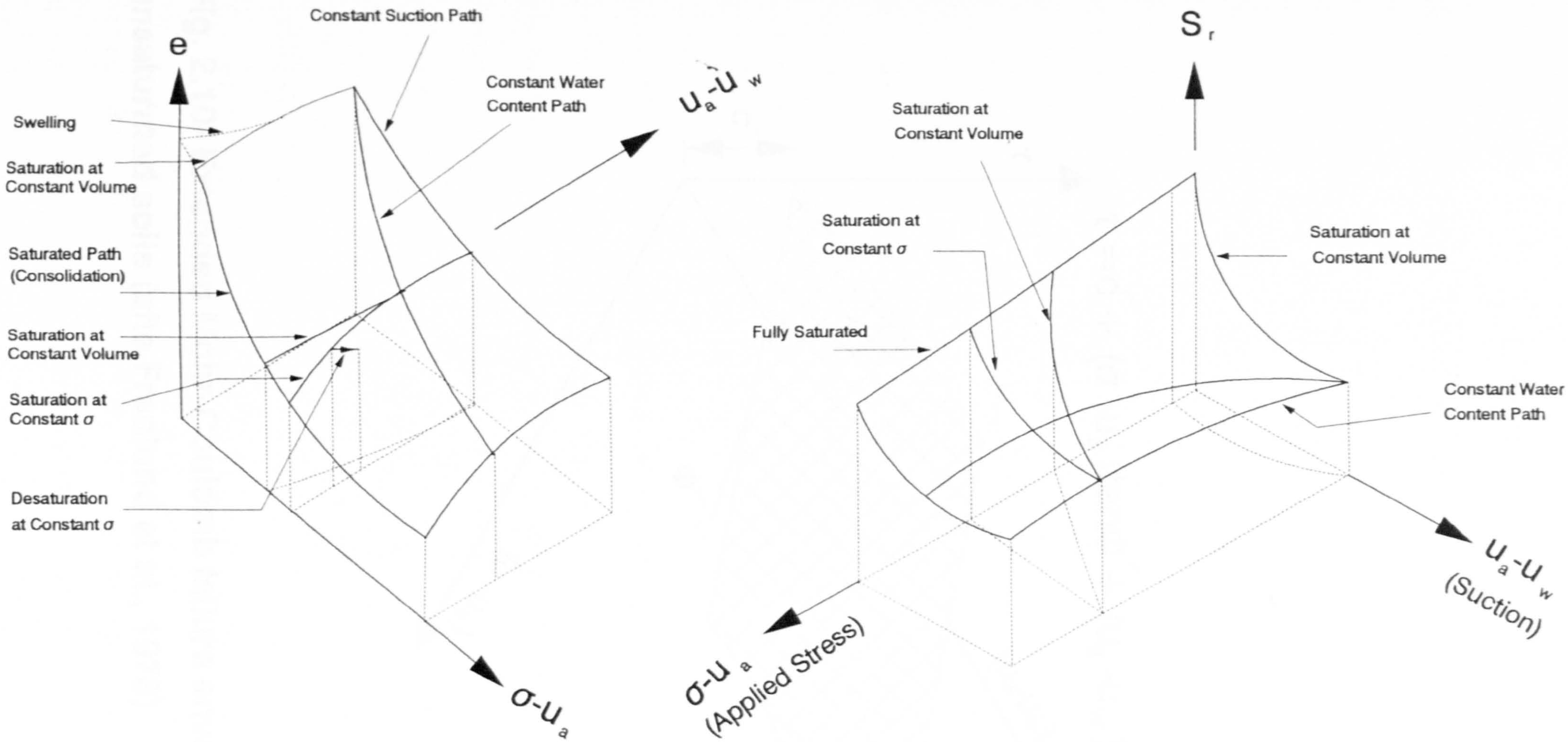

Fig. 2.9- Plots showing the void ratio, e, and degree of saturation, S_r ,in ($e,\sigma-u_a,u_a-u_w$) and ($S_r,\sigma-u_a,u_a-u_w$) spaces respectively (after Matyas and Radhakrishna, 1968)

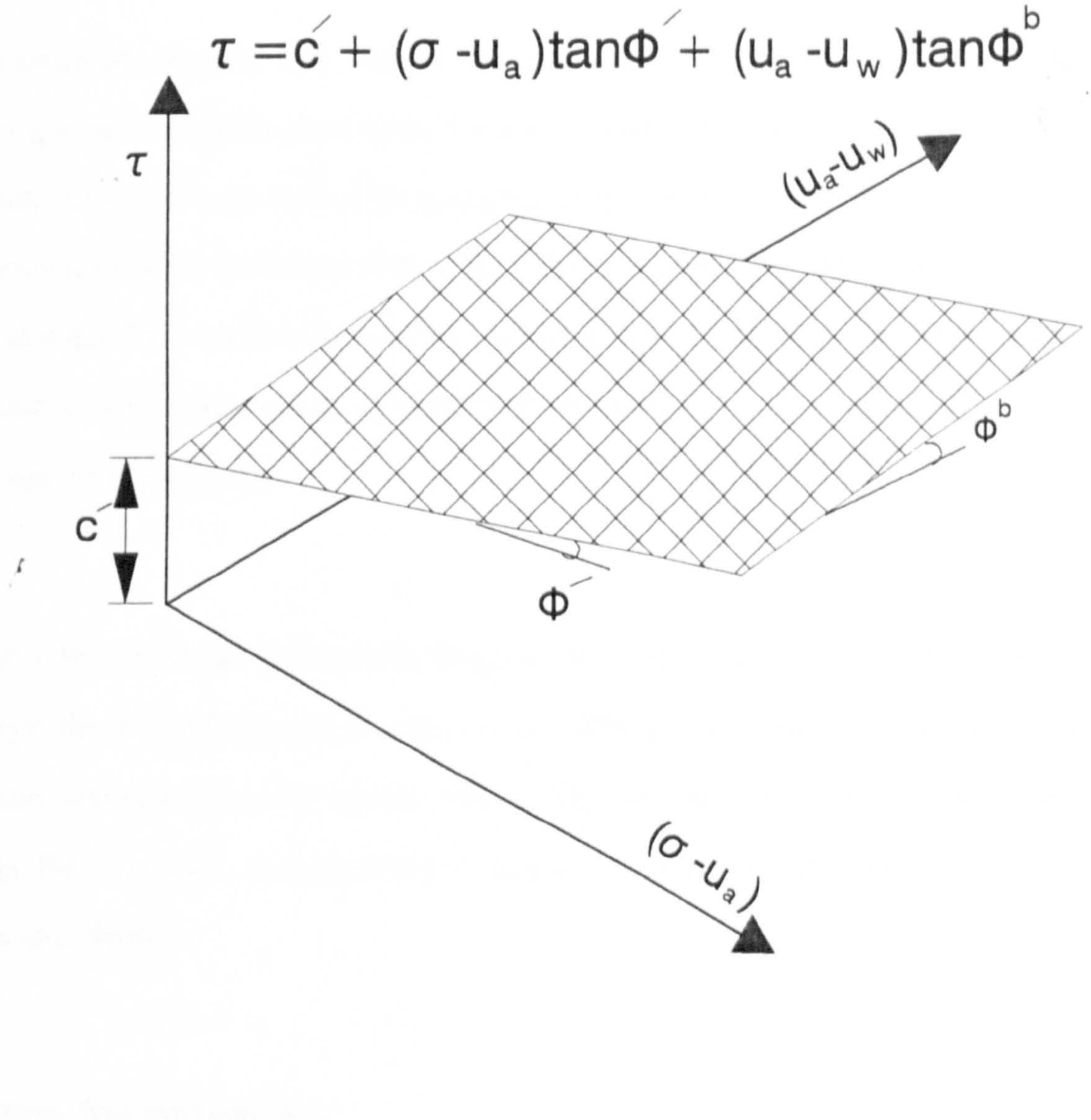

Fig. 2.10- Extended Mohr-Coulomb failure envelope for unsaturated soils (afte Fredlund et at., 1978)

Chapter 3

Literature Review: Triaxial Cell Design Considerations

3.1 Introduction

Testing unsaturated granular soils cannot be done using the conventional triaxial cell, because the specimen negative pore water pressure (suction) cannot be measured directly and specimen volume change cannot be measured in the same way as for saturated soils, due to the existence of air in the soil voids. Also, the specimen dimensions should be large enough so that the large particle size of the granular soil do not affect the soil strength. For these and other reasons (such as measuring the specimen strains internally), a new triaxial cell had to be designed.

In this chapter the errors and factors affecting triaxial testing and cell design are reviewed to help design the new triaxial cell so that it is versatile in use, allows for easy specimen setting up and testing and has few testing errors. Also the decisions that have been made in designing the new cell and choosing a certain technique for specimen testing are discussed in this chapter.

3.2 Suction Measurements

There are different methods for measuring the negative pore water pressure (suction). Some of them measure the suction directly such as the suction plate technique while others measure the suction indirectly, such as thermal conductivity sensors, psychrometer or filter paper. Descriptions of these devices are given by Fredlund and Rahardjo (1988).

Devices which measure the suction indirectly are not used in the current research because of the long time they take to reach equilibrium, and the accuracy of measurement is not adequate, especially at low suctions (<100 kPa). Also some of them, such as the psychrometer, require very small temperature variations (<±0.1°C) to give accurate readings of suctions. It was decided to use the direct method of measuring suction in the current research.

Fig. 3.1a shows the suction plate method. When the unsaturated soil is placed on a saturated high air entry ceramic stone, the soil pore water will link with that of the ceramic stone and pore water pressure is measured by a measuring device (such as pressure transducer). The ceramic stone, when its pores are saturated with water, acts as a filter by preventing air entering the pore water pressure measuring system by the action of surface tension up to a certain negative pore water pressure, which depends on the size of the ceramic stone pores. Above that pressure (usually called the Air Entry Value, AEV) air can enter the stone pores and affects the pore water pressure measurements. Therefore, ceramic stones can be used to separate the water pressure from the air pressure (atmospheric), so that an independent measurement of soil pore air and water pressures, below the AEV, can be made. The suction plate technique is only suitable for suction measurements up to about 100 kPa suction, as it has been found that water cavitates (i.e. air comes out of solution in the measuring system) at this suction (Olson and Langfelder, 1965 and Bocking and Fredlund, 1980).

Hilf (1956) measured higher suctions using the suction plate technique by increasing the air pressure above atmospheric pressure, as shown in Fig. 3.1b, to the point where the pore water pressures were all positive. He assumed that increasing the air pressure by a fixed amount will increase the pore water pressure by the same amount, so that the

difference between pore air and water pressures (suction) will remain constant. This technique is called the "Axis Translation Technique". Olson and Langfelder (1965) and Bocking and Fredlund (1980) showed that this technique was correct for soils containing continuous air voids (below a degree of saturation of about 85%), because the air pressure does not compress the water and soil particles significantly, provided it is less than 3.5 MPa, which means that the radius of curvature of the air-water menisci (Fig. 2.3) does not change significantly, and the difference between pore air and water pressures remains constant.

Fredlund and Rahardio (1988) stated that this technique only measures the matrix suction (section 2.4). Although this technique measures one component of the total suction (which is equal to the sum of the matrix and osmotic suctions, see section 2.4), this technique was used in the current research, and osmotic suction was assumed to have insignificant effect, as was shown in section 2.4.

3.3 Specimen Dimensions

The size of the specimen should be large enough so that the specimen stress and strain measurements reflect the soil behaviour and to ensure it is representative. In this section the factors influencing the choice of the specimen dimensions are reviewed.

3.3.1 Specimen Diameter

The diameter of the specimen, D, depends on the size of the maximum grain size, d_{max}, of the soil. Researchers have used the ratio D/d_{max} to specify the specimen diameter according to its maximum grain size. The method used to determine an acceptable

D/d_{max} is to carry out series of tests for different values of D/d_{max} , either by changing the specimen diameter for one soil gradation, or by changing d_{max} and keeping D constant, and finding the minimum D/d_{max} ratio at which the change in strength is negligible.

Holtz and Gibbs (1956) suggested D/d_{max} to be 4.3 or more for soil containing 20% gravel, and 8 or more for soil containing 50% gravel. Marachi (1969) stated that "judging from the data presented by Holtz and Gibbs (1956), it seems reasonable to conclude that if the material gradation is such that the proportion of particles in the maximum sieve size range is 30% or less and the ratio D/d_{max} is 6, then there is no effect of the specimen size on the test". NIRR Council of Science and Industrial Research, South Africa (1969), have suggested a ratio of specimen diameter to the *mean* particle diameter to be 9.2 or more (d_{max} is larger than the mean particle diameter, i.e. D/d_{max} will be less than 9.2).

To design a triaxial cell suitable for testing a soil with d_{max} up to 20 mm, according to Marachi (1969), with D/d_{max} equal to 6, the specimen diameter should be no less than 120 mm, providing that the proportion of particles in the maximum sieve size range is 30% or less. The coarser soil used in this research has d_{max} of 20 mm, and the proportion of the particles in the maximum sieve size range was less than 30% as will be seen in chapter 6. Therefore to be conservative the ratio D/d_{max} was chosen to be 7.5 so that the sample diameter was 150 mm.

3.3.2 Specimen Height

It is known that a specimen barrels during shearing, which is evidence of non-uniform deformations along the specimen due to the effect of the end friction between the soil and the top cap and base pedestal. The height of the specimen should be large enough so that the friction at the specimen ends does not affect the soil strength.

Kirkpatrick and Belshaw (1968) and Kirkpatrick and Younger (1970) inserted lead shot between soil particles of a sand specimen, and used an X-ray technique to measure the lead shot movements during specimen shearing. They showed two different zones, as shown in Fig 3.2. The first zone is called the Dead Zone, which consisted of a cone at each end of the specimen. The cone height was about same as the radius of the specimen. The soil particles in this zone did not move due to end friction. The second zone was between the two cones as shown in Fig. 3.2, where the soil particles were free to move and were not affected by the end friction. This zone is called the Dilating Zone. The existing of these zones due to end friction are responsible for the barrelling behaviour of the specimen during shearing.

Different authors, such as Rowe and Barden (1964), Bishop and Green (1965), Lee (1978), Norris (1981) and Tatsuoka et al. (1984), have reported attempts to reduce the end friction by using lubrication to make the specimen deform uniformly. Lubrication consists of one or more layers of rubber membrane disc with silicone grease in between. It is suggested that the ratio of specimen height to diameter , D/H, can be reduced to one, when end lubrication is used. Although this method gives uniform deformation of the specimen, the authors mentioned above stated that it has the following disadvantages:

1. The silicone grease squeezes out during specimen compression, especially for slow rates of shearing , and this may reduce the lubricant efficiency.
2. The coarse particles of a granular soil can penetrate the lubricant and reduce its efficiency.
3. Using multiple layers of lubricant increases bedding errors between the specimen and the top cap and the base pedestal, and may induce a slip in the lubricant.

Rowe and Barden (1964), Bishop and Green (1965), Lee (1978), Goto and Tatsuoka (1988) and Ueng et al. (1988) showed that for drained tests on saturated sand, specimens

with well lubricated ends gave lower peak strengths at higher axial strains than those tested using unlubricated ends. Also they showed that the volume changes of the specimens with lubricated ends were higher than those without lubrication. For undrained tests on saturated soils, the end friction affects the measurements of pore water pressure. A pore water pressure gradient occurs between the dead and dilating zones within the specimen, so a slower rate of shearing is required to allow for pore water pressure equalisation between the centre and the ends of the specimen. Lee (1978) and Gens (1982) showed that there was no difference in the soil shear behaviour between lubricated and unlubricated ends for small axial strains (<4%), but the difference became significant at large axial strains.

Bishop and Green (1965) showed that specimens of height to diameter D/H=1 with well lubricated ends had similar strength to those of D/H=2 without lubricated ends. Goto and Tatsuoka (1988) carried out series of tests on sand to find the best ratio of D/H that reduced the effect of end friction. They used three types of specimens, as shown in Fig. 3.3. In type A, the specimen ends were lubricated and the top cap was fixed to the piston (Fixed Cap), while type B was similar to type A but the specimen ends were not lubricated. In type C, the specimen ends were not lubricated and the top cap was not fixed to the piston, as shown in Fig. 3.3, but could rotate if the specimen rotated during shearing (Rotated Cap), as in the conventional triaxial cell. They used different values of D/H and soil density, and came to the following conclusions:

1. The difference in the angle of shearing resistance, ϕ', between types A and B for dense specimens (void ratios <0.7) with D/H=2, was about 1°, while there was no difference for loose specimens (void ratios >0.8).

2. For type B, as D/H increased from 2 to 2.7, ϕ' became the same as that for type A. They suggested the use of D/H=2.5 of type B for dense soils, so that the value of ϕ' can be free from the effects of end friction, but the overall stress-strain behaviour may still be affected.

3. ϕ' values for type C were located between those for types A and B, but those with D/H=2.4 were closer to those for type A.

They showed that, when using a rotated cap, the specimen rotated during shearing but the rotation was negligible for dense specimens, because the dense specimens failed at lower axial strains than that for loose specimens, during which the cap rotation was very small.

In the current research, end lubrication was not used for the following reasons:

1. The lubrication may hinder measurement of soil suction, as it reduces the contact area between the high air entry ceramic stone (section 3.2) and the specimen.
2. Grease may squeeze into the ceramic stone and block its pores
3. Thicker lubrication is needed due to the existence of coarse soil particles; this may introduce further bedding errors.
4. The test duration is very long (14 to 25 days), which means that all of the grease may be pushed from between the membrane rubber discs.
5. There may be difficulties during placing and centring the specimen on the pedestal.

It was decided to use a rotated top cap as shown in Fig. 3.3, type C, because the specimen used in the current research was dense with void ratio <0.4. Also using a fixed top cap is not recommended because it may damage the load cell (axial stress measuring device), fitted at the bottom of the piston, if the specimen tries to rotate.

3.4 Cell Fluid

The choice of a cell fluid (i.e. the fluid surrounding the specimen and used to apply the cell pressure) depends on the following

1. Fluid Properties. The fluid should be safe to use, have a suitable viscosity for easy cell filling and emptying, should not attack the rubber membrane containing the specimen, have a low air solubility to prevent air leakage, have molecules which are large enough that they do not leak through the rubber membrane and should not suck out specimen pore water.

2. Type of Test. There are three basic types of triaxial test which can be carried out on unsaturated soils. First, is the pore air and water undrained test (Undrained Test), with the cell pressure kept constant. In this type of test, air leakage through the rubber membrane, is the main problem. If the cell fluid has high air solubility, air can leak through the membrane from the specimen to the cell fluid or vice versa, and can cause a variation in the pore air pressure and pore air volume change. The second type of test is the water undrained test (Constant Water Content Test), during which the pore air and cell pressures are kept constants. In this type of test, air leakage is not a problem as long as the air volume is not measured. The third type of test is the Drained Test, during which pore air, pore water and cell pressures are kept constant. In all three types of test, water leakage through the rubber membrane from the cell fluid to the specimen can occur.

Authors such as Leroueil et al. (1988) suggested using silicone oil as a cell fluid because it is safe to use and has large molecules so that there is very little leakage through the rubber membrane when compared with other fluids, as shown in Table 3.1. This type of cell fluid may not be suitable for an undrained test on unsaturated soil because its air solubility is higher than water, which cannot prevent air leakage. Bishop et al. (1960) used mercury as a cell fluid to reduce both air and water leakage, because mercury has a very low air

solubility. Fredlund and Morgenstern (1977) and Head (1982) suggested using a nylon film and aluminium foil between two membranes to eliminate air and water leakage. Head (1982) suggested using two rubber membranes and a thin layer of silicone grease in between to reduce water leakage and reduce the rate of air leakage through membrane.

Although mercury and silicone oil are recommended to reduce water and air leakage, it was decided to use de-aired water instead in the current research for the following reasons:

1. The new triaxial cell is very large, with a capacity of about 60 litres, so it would be expensive to buy such a large volume of mercury or silicone oil. Also, due to their high viscosity, it would take a longer time to fill or empty the cell than with de-aired water.

2. Only constant water content and drained tests were planned for the current research, and the pore air volume change was not to be measured. This means air leakage was not a pfoblem. Also the water leakage was reduced by using two thick rubber membranes (0.5 mm thickness each) with a silicone grease layer in between them.

3. According to Leroueil et al. (1988), the air leakage through the rubber membrane used in the current research, could be 1.7 cc per 100 kPa pressure per week per 0.5 mm thick ungreased membrane (calculated from Table 3.1). This would cause insignificant error in the measurements of the specimen volumetric strains (about 0.004 %/week), because the specimen used in the current research was quite large.

3.5 Double-Wall Triaxial Cell

The volume change of a saturated specimen is measured by measuring the water entering or leaving the specimen. For an unsaturated specimen, this method cannot be adopted, because the specimen voids are filled with air and water. Some authors, such as Bishop and Donald (1961), measured the specimen volume change by measuring the volume

change of the cell fluid surrounding the specimen. Adopting this method, corrections have to be made to the specimen volume change due to change in the triaxial cell volume due to creep and cell pressure variations which cause cell expansion and contraction.

Wheeler (1988) developed a double-wall triaxial cell to eliminate these errors in the specimen volume change measurements. The double-wall cell consists of two perspex cylinders, one inside the other, as shown in Fig. 3.4. By introducing same pressures inside the inner perspex (Inner Cell) and the gap between the two perspex walls (Outer Cell), the resultant pressure on the inner perspex wall is zero. Zero resultant pressure on the inner wall means zero volume change of the inner perspex due to creep and cell pressure variation. Therefore measurements of the cell fluid of the inner cell should reflect the specimen volume change.

3.6 Direct Measurement of Axial Strain

Measuring the axial strain of the specimen externally (or between the top cap and base pedestal) may not be accurate due to the bedding errors and end friction (section 3.3.2) which cannot be fully avoided. Burland and Symes (1982) and Jardine et al. (1984) have developed a technique to overcome this problem. They measured the axial strain over the middle part of the specimen using an immersible gauge, as shown in Fig. 3.5. This method is likely to give representative results of the soil behaviour as the middle part of the specimen, the dilating zone (section 3.3.2), is not affected by bedding errors and end friction.

Burland and Symes (1982) stated that movement between the specimen and membrane can occur during a test, but this can be ignored for small strain tests. They suggested that for large strains, the brass footings of the mounting system (Fig. 3.5) should be fitted with

pins which penetrate the specimen to fix the mounting system, instead of using glue, to avoid the membrane slippage. Gens (1982) drew a fine grid on the membrane of a clay specimen and monitored the vertical movement of the intersections of the grid, and found that there was no movement between specimen and membrane up to about 4% axial strains.

In the current research, the axial and lateral strains were measured internally over the middle part of the specimen using LVDTs, as will be described in chapter 4. The technique suggested by Burland and Symes (1982), to use pins that penetrate the specimen to avoid membrane slippage, was not adopted in the current research for the following reasons:

1. From trial tests carried out on the granular soil used in the current research it was found that pins were not stable in granular soils, as the membrane can pull the pins (with the mounting system) and affect strain measurements.

2. It was also found from the trial tests, that failure occurred at about 1% axial strain, at which strain membrane slippage may be ignored according to Gens (1982). Therefore the mounting system was glued to the membrane

3.7 Specimen Rubber Membrane

In this research a Latex rubber membrane, 0.5 mm thickness, was used around the specimen to separate the soil from the cell fluid. Using such a membrane may produce some errors in the measurements of the specimen volume change, suction, water content and axial and lateral stresses. These errors are due to air and water leakage, membrane penetration and membrane restraint. Air and water leakage have already been discussed in section 3.4, while membrane penetration and restraint will be described in the following subsections.

3.7.1 Membrane Penetration

The rubber membrane can penetrate into the interstices between the outer particles of the specimen, as shown in Fig. 3.6, due to an increase in the cell pressure which pushes the membrane towards the specimen. Membrane penetration causes errors in the measurements of specimen volume change.

Frydman et al. (1973) showed that the major factor influencing the membrane penetration for any applied pressure was the particle size. This was also confirmed by Kiekbush and Schuppener (1977), who showed that membrane penetration did not become zero for very fine soils, such as clay. Molenkamp and Langer (1981), Baldi and Nova (1984) and Kramer et al. (1990) developed theoretical equations to determine the volumetric strain due to membrane penetration, Δv_m. These equations are as follows:

Molenkamp and Langer (1981)	$\Delta v_m = 0.160\,(4d/D)\,[\sigma_3 d / E_m t_m]^{1/3}$	(3.1)
Baldi and Nova (1984)	$\Delta v_m = 0.125\,(4d/D)\,[\sigma_3 d / E_m t_m]^{1/3}$	(3.2)
Kramer et al. (1990)	$\Delta v_m = 0.231\,(4d/D)\,[\sigma_3 d / E_m t_m]^{1/3}$	(3.1)

where σ_3 is the cell pressure, d the mean grain size, D the specimen diameter, E_m the membrane elastic modulus and t_m is the membrane thickness. E_m can be found using the Henkel and Gilbert (1952) method. The above authors found, using the developed equations, that the volumetric strain due to membrane penetration was inversely proportional to the specimen diameter and it increased with increasing particle size.

3.7.2 Membrane Restraint

The rubber membrane can produce axial and lateral stresses to the specimen before and during shearing. Mathematical equations were suggested which can be used to correct for the membrane restraint, these will be discussed in the following subsections.

3.7.2.1 Initial Confining Stress

This is the stress applied by the membrane to the specimen before applying the cell pressure. LaRochelle et al. (1988) suggested the equation below to determine the initial confining stress, σ_{om},

$$\sigma_{om} = 2M_i \frac{d_o - d_{im}}{d_o d_{im}} \qquad (3.4)$$

where d_o is the specimen diameter at the end of consolidation, d_{im} is the initial membrane diameter and M_i is the initial elastic modulus at 1% extension.

3.7.2.2 Axial and Lateral Stresses during Shearing

The restraint of the membrane in a bulging type failure was first studied by Henkel and Gilbert (1952). They suggested two methods of correction, the first one being called the "Compression Shell" method. In this method they assumed that the specimen deformed as a right cylinder and the rubber membrane acted as a compression shell. The correction to the measured compressive stress, σ_{1m}, due to membrane restraint is :

$$\sigma_{1m} = \frac{\pi d_o M \varepsilon}{a_c} \qquad (3.5)$$

where M is the membrane elastic modulus at 10% extension (LaRochelle et al. 1988), ε is the axial strain and a_c is the corrected area of the specimen at strain ε. LaRochelle et al. (1988) suggested using the above equation where the cell pressure was high enough to hold the membrane firmly against the specimen, i.e. no buckling (wrinkling) in the membrane is likely to occur.

The second method is called the "Hoop Theory" method. This method assumes that as specimen deforms, the membrane buckles. The increase in the specimen diameter will induce a hoop tension in the membrane which will act as an increase in the cell pressure. To correct for the confining stress due to membrane restraint, the equation below can be used:

$$\sigma_{3m} \cong \frac{M\varepsilon}{d_o} \qquad (3.6)$$

LaRochelle et al. (1988) suggested that Equation 3.6 can be used where the rubber membrane is not held firmly against the specimen, i.e. membrane buckles during specimen shearing. LaRochelle et al. (1988) presented a modification to Equation 3.6. They showed that the equation below can give a good correction for the membrane restraint:

$$\sigma_{3m} = \sigma_{om} + 0.75\frac{M\sqrt{\varepsilon}}{d_o} \qquad (3.7)$$

Cell Liquid	Range of Measured Flow Through the Rubber Membrane cc/week
De-aired water	-0.23 to +0.25
Glycerine	-1.45 to -1.76
Castor oil	-0.25 to -0.41
Liquid paraffin	-0.04
Silicone oil	-0.04 to 0.05

(+) is flow of liquid from the cell to the specimen

Rubber latex membrane thickness = 0.3 mm.

Specimen height/diameter = 100/50 mm.

Table 3.1- Flow of liquid through a rubber latex membrane (after Lerouiel et al., 1988)

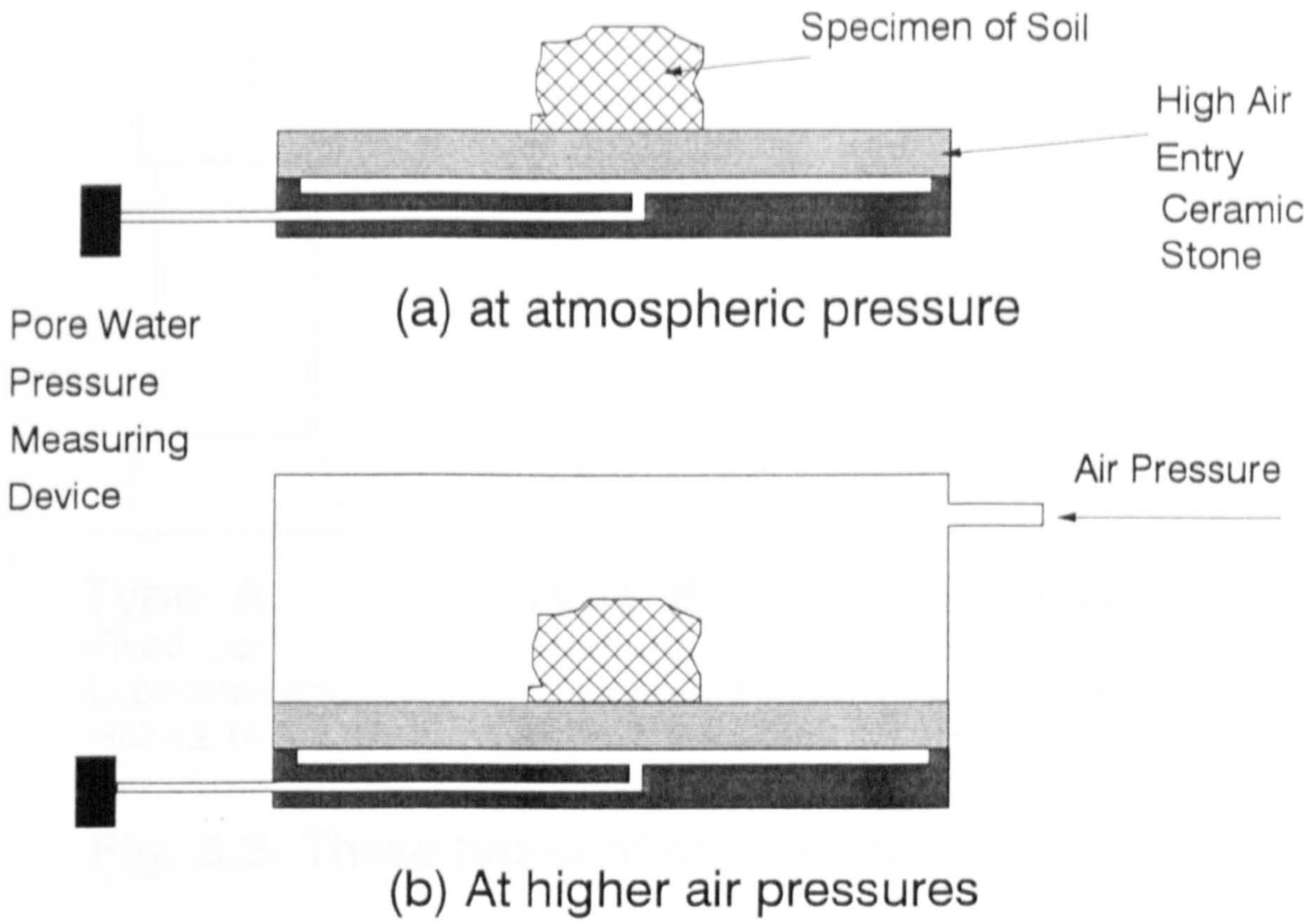

Fig. 3.1- Suction plate method for measuring soil suction at (a) atmospheric and (b) higher air pressures

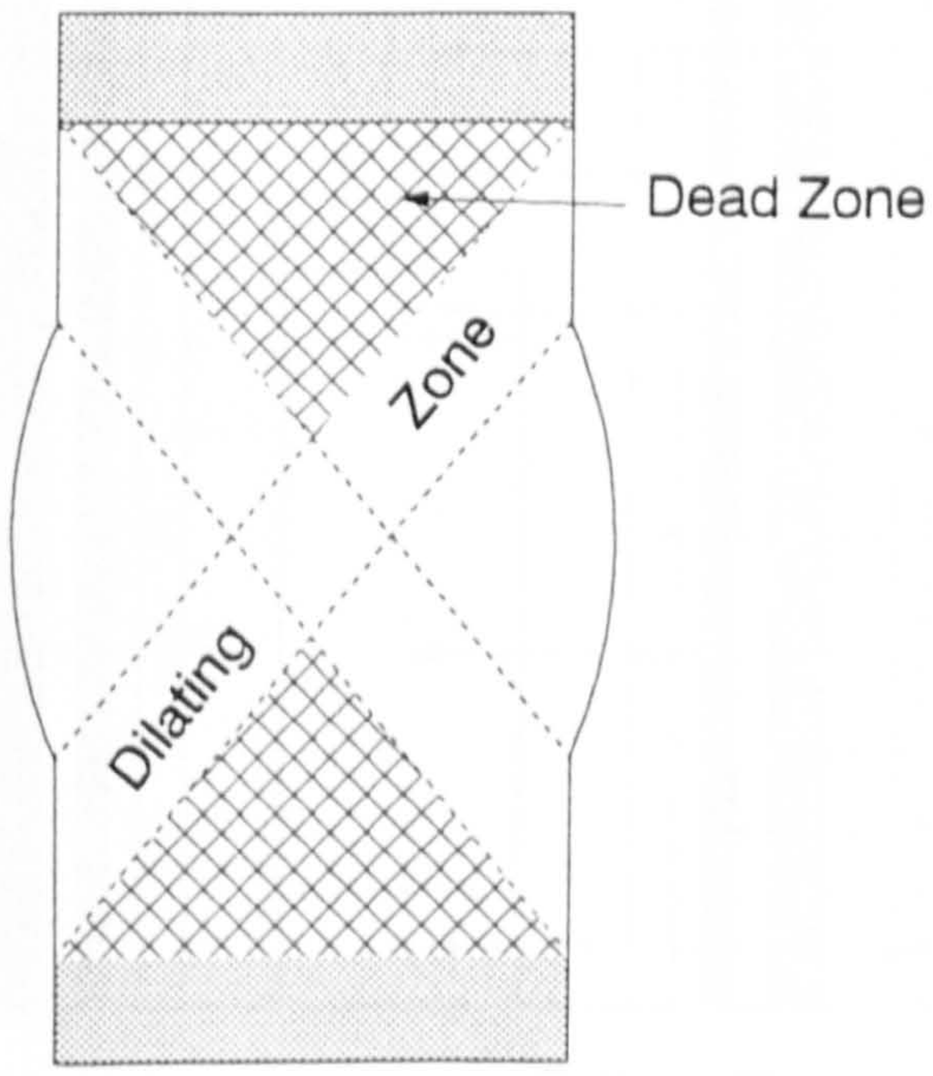

Fig. 3.2- Non-uniform deformation during shearing a specimen of soil.

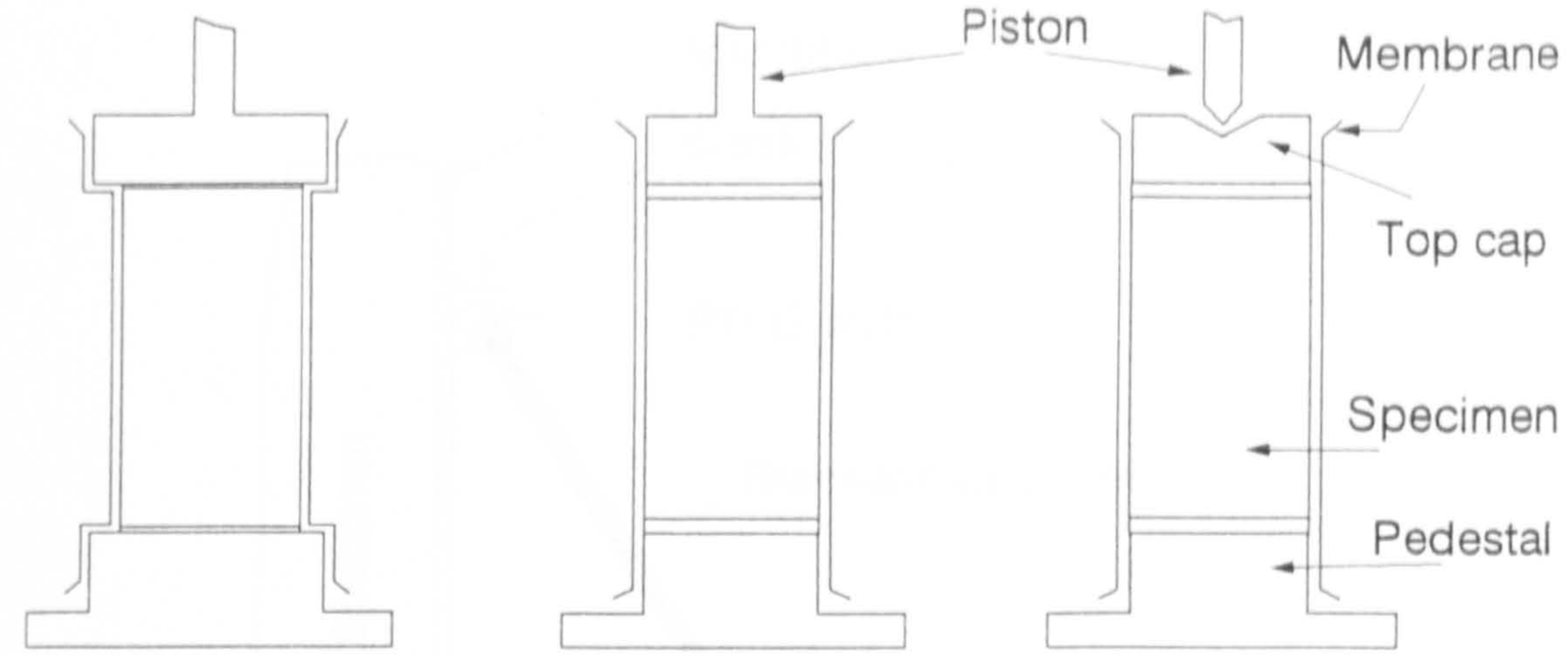

Type A
-Fixed cap
-Lubricated ends
-H/D=2.14 & 2.57

Type B
-Fixed cap
-Unlubricated ends
-H/D=2, 2.4 & 2.67

Type C
-Rotated cap
-Unlubricated ends
-H/D=2 & 2.4

Fig. 3.3- Three types of end connctions

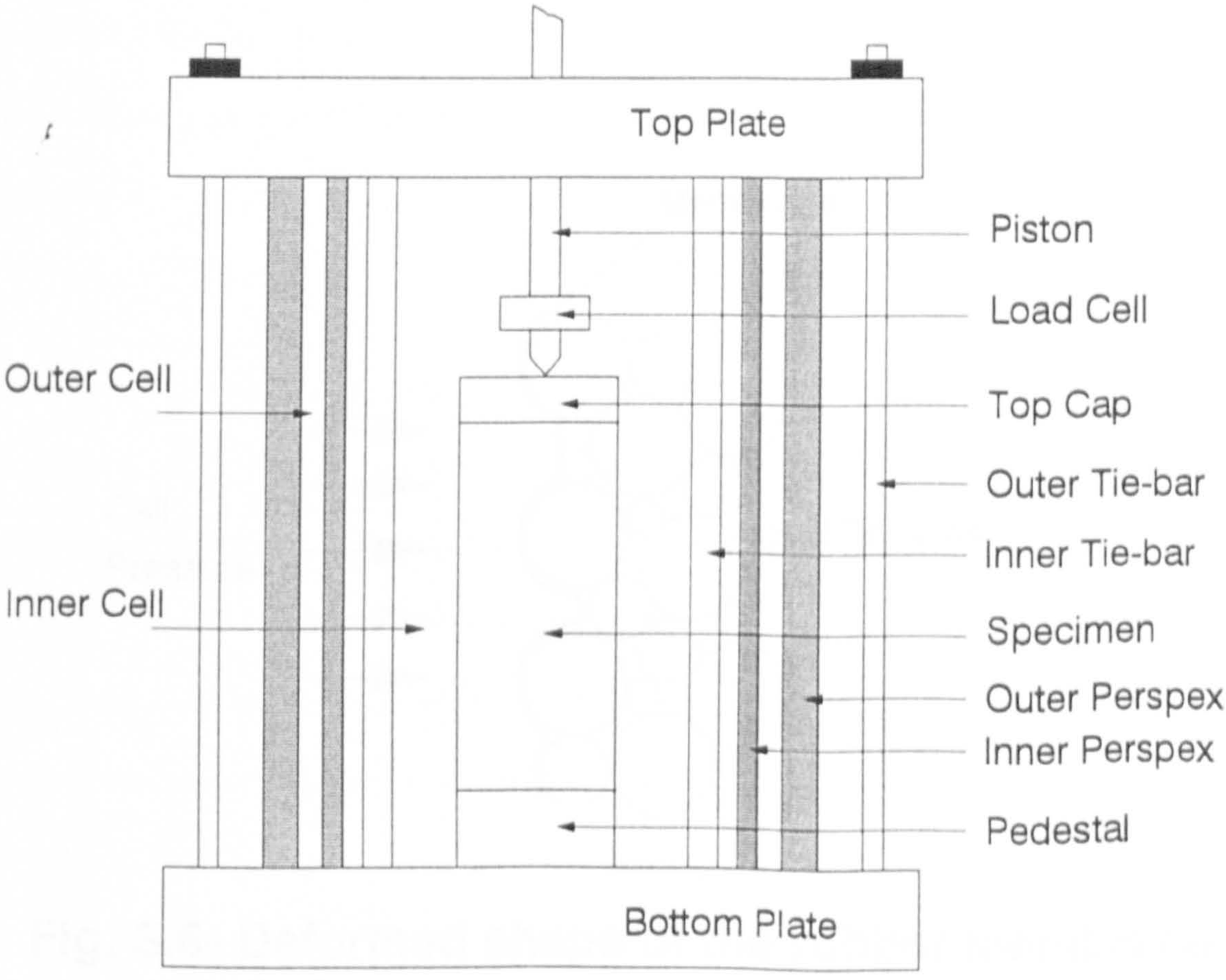

Fig. 3.4- Double-wall triaxial cell

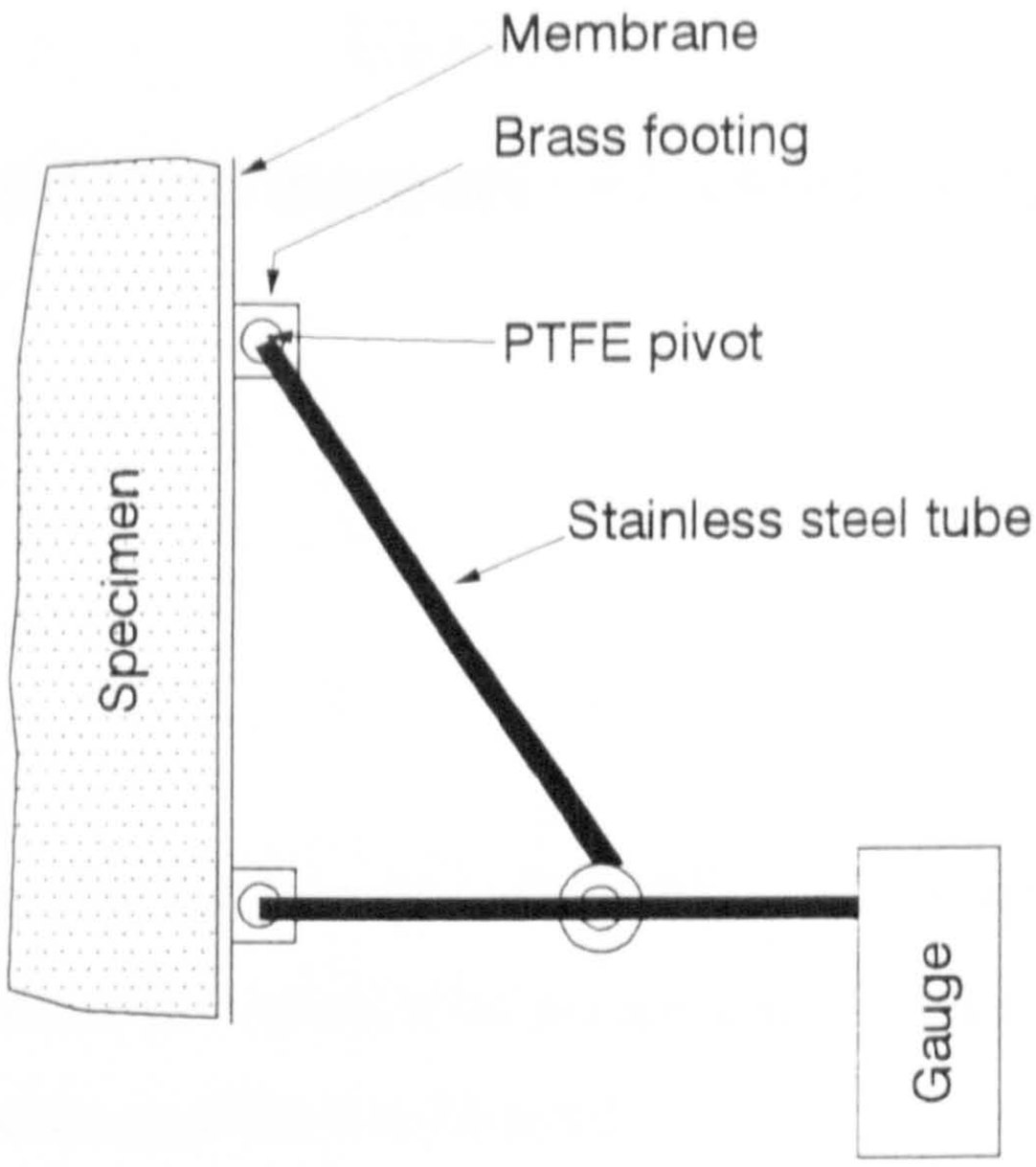

Fig. 3.5- Construction of electrolevel gauge (after Jardine et al., 1982)

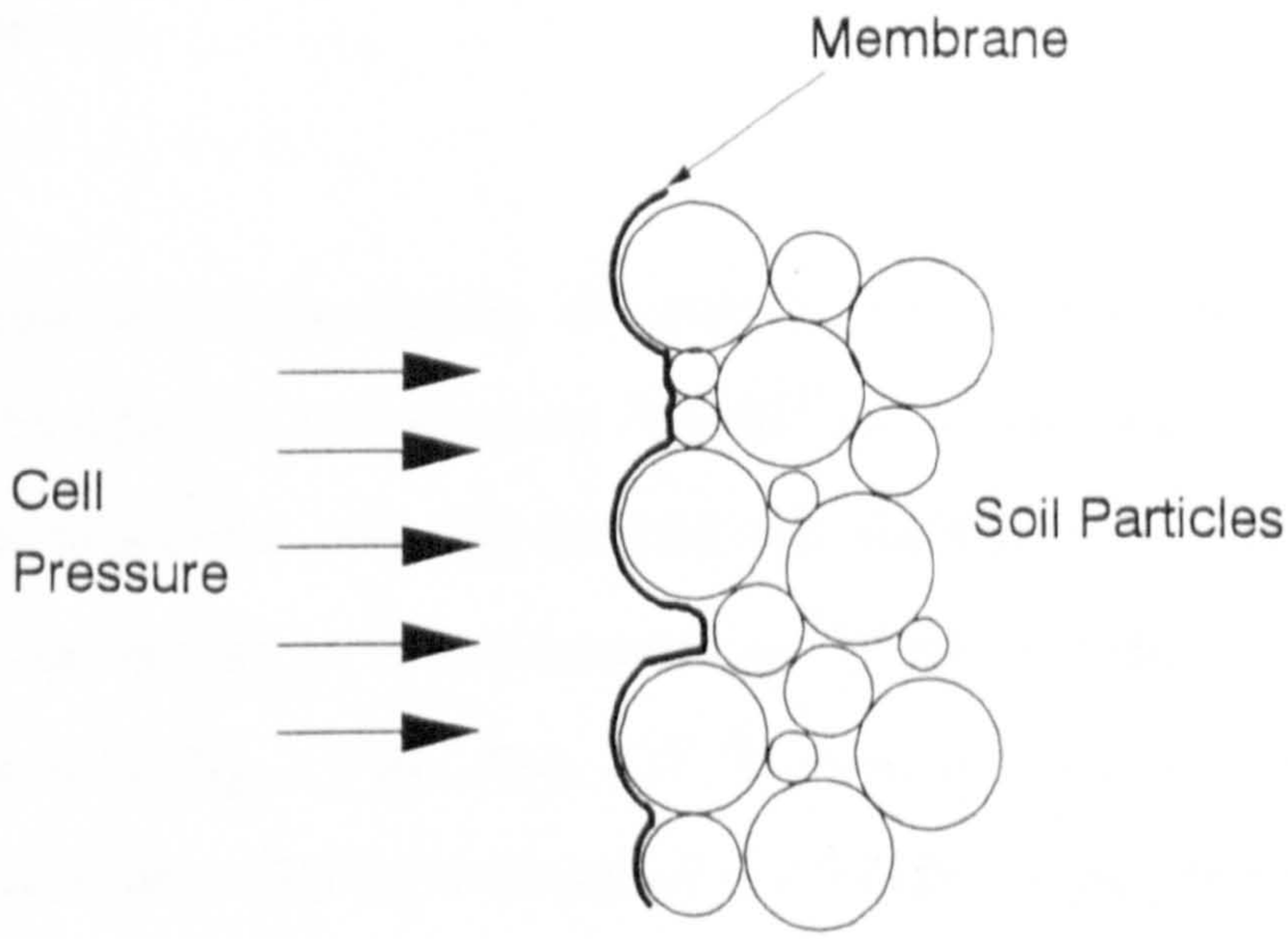

Fig. 3.6- Deformed shape of the rubber membrane when the cell pressure is increased

Chapter 4

Description and Development of Experimental Apparatus

4.1 Introduction

In the previous chapter, the literature on factors affecting the design of the triaxial cells and tests was reviewed with discussion of the decisions made towards the design of a new triaxial cell. These decisions are listed in Table 4.1.

In the current research, two triaxial cells were used. The first one was a 150 mm specimen diameter double-wall triaxial cell, as shown in Fig. 4.1 and Plate 4.1, which was designed especially for this research at the University of Sheffield. This cell will be called the *Double-Wall Triaxial Cell* in this thesis. It was only used for testing unsaturated granular soils and was placed in a new 100 kN loading machine for shearing the specimen as shown in Plate 4.1.

The second triaxial cell was an existing 150 mm diameter specimen conventional triaxial cell, which will be called the *Conventional Triaxial Cell* in this thesis. It was only used for testing saturated granular soils, and the body was modified by inserting an aluminium tube to increase the cell height to accommodate a 150 mm diameter by 375 mm height specimen, as shown in Fig. 4.2 and Plate 4.2. All other cell features were similar to a conventional triaxial cell. This cell was placed in a 50 kN loading machine as shown in Plate 4.2.

In the following sections a description of the double-wall triaxial cell design and the plumbing and logging systems for both cells will be given.

4.2 Double-Wall Triaxial Cell Design

Fig. 4.1 shows all of the components of the double-wall triaxial cell, which was designed to withstand a working pressure of 1500 kPa. The cell consists of different components that are assembled during specimen setting up. The axis translation technique (Section 3.2) is used for measuring the suction by increasing the specimen pore air pressure above atmospheric pressure to the point where the pore water pressure measurements taken at the base of the specimen are positive. A high air entry ceramic stone is fixed to the base pedestal to separate air from water and enables the measurements of the pore water pressure be carried out independently (Section 3.2).

4.2.1 Cell Components

A. Inner and Outer Cells. The cell was designed as a double wall cell which consists of two perspex cylinders one inside the other, which makes two cells , inner and outer cells, as was described in Section 3.5. Both cells are connected to one line of pressure supply, so that the same pressure is introduced to both cells to eliminate any volume change which would occur in the inner cell water due to cell pressure variations and cell creep (Section 3.5). The diameter of the inner cell is 342 mm, and the width of the gap between the inner and outer cells is 10 mm. Both perspex cylinders are cut into two parts, the lower and upper parts (Fig. 4.1), to fit into a metal ring which is used to fix three LVDTs for the lateral strain measurements, details of which are given later in this section.

B. Top and Bottom Plates. The bottom plate (Fig. 4.1) is made from aluminium and is clamped in three places to the loading machine platen to prevent it from tilting. These clamps are not removed at any time during test. Another single clamp prevents the cell from rotation during tightening up of the cell nuts and screws. This clamp is removed prior to starting the test. Four holes are drilled horizontally in the bottom plate. Two of them are drilled to the pedestal for the pore water pressure measurements and ceramic stone

flushing (to remove air bubbles that develop below the ceramic stone). The other two holes are drilled to the inner and outer cells for applying cell pressure.

The top plate consists of two concentric pieces of aluminium, the outer and the inner plates. The outer top plate rests on both the inner and outer perspex cylinders, while the inner top plate rests on three inner tie-bars (Fig. 4.1). A stainless steel top ring fits in the gap between the inner and outer top plates, as shown in Fig. 4.1. It is placed after filling the cell with de-aired water and three clamps seal it in position . Holes are made in the outer and inner top plates for bleeding air and passing through transducer wires.

C. The Piston Bushing. The piston bushing, which is made from aluminium with an inner brass sleeve (Fig. 4.1), is placed and tightened on the top face of the inner top plate. The bottom faces of the bushing and inner top plate are machined with a slope so that air can be flushed from the cell through a hole in the bushing when filling the cell, as shown in Fig. 4.1. The piston is made from stainless steel with the 25 kN load cell connected to its bottom.

D. Tie-bars. There are two sets of tie-bars, the outer and inner tie-bars, for connecting the top and bottom plates, as shown in Fig. 4.1. The outer tie-bars consist of 12 stainless steel 16 mm diameter rods. The inner tie-bars consist of three stainless steel 30 mm diameter rods.

E. Top Cap and Base Pedestal. Both are made from stainless steel to withstand the large loads that are applied to the specimen during shearing. Two O-ring grooves are made around each of their side faces, to help seal the membrane. There are two holes in the top cap, one to supply the specimen pore air pressure, the other to inundate the

specimen from its top, if required. The top cap is not fixed to the piston but was designed so that it can rotate.

The base pedestal is tightened to the bottom plate by screws from underneath of the bottom plate. A spiral groove, for flushing the ceramic stone, is machined on its top face. This starts from the pedestal centre and goes to near the edge as shown in Plate 4.3. Two holes are drilled vertically in the base pedestal to meet the other two holes drilled in the bottom plate for pore water pressure measurements and ceramic stone flushing. One of the holes is at one end of the spiral groove, and the other hole is at the other end.

F. High Air Entry Ceramic Stone. The pore water pressure of the specimen was only measured at its bottom. A 1-bar air entry value ceramic stone (Section 3.2) is glued into a stainless steel ring using Araldite epoxy resin glue. The ring is tightened to the pedestal by 12 screws. An O-ring is fitted in a groove on the bottom face of the ring to prevent water and air leakage. The ratio of the area of the top face of the ceramic stone (122.2 mm diameter, not including the metal ring) to the specimen area (150 mm diameter) is 0.664. This ratio was made as large as possible to make good contact between the specimen and ceramic stone.

G. Middle Ring. Each perspex cylinder is divided into lower and upper parts (see part A in this section) with an aluminium ring between them as shown in Fig. 4.1. Three holes are drilled in the middle ring with 120° angles between them to position three LVDTs horizontally, as shown in Fig. 4.3, for specimen lateral strain measurements. The height of the centre of the middle ring is 15 mm below the centre of the specimen, so that when the specimen shortens during shearing, lateral strain measurements will always be close to the specimen mid-height position.

4.2.2 Axial and Lateral Strains Measurements

Six LVDTs of same type were used for measuring the specimen axial and lateral strains internally (three LVDTs each). The type of the LVDT used in the current research is called an Immersible Free Armature LVDT. A Free Armature LVDT is one in which the armature, which moves through a hole in the LVDT body, is not attached to the LVDT body by any sort of connection, such as a spring, and is free to move through the hole. This hole is open to the atmosphere at one end, i.e. water can enter the hole when the LVDT is immersed in water. The reason for choosing this type of LVDT was to prevent armature movement when the cell pressure is applied.

Each of the three LVDTs used for internal axial strain measurements was hung by a light spring (1 mm extension for 3.5 grams mass) from a rod attached to an inner tie bar, as shown in Fig. 4.4, to counter balance the LVDT weight and to help prevent membrane slippage (Section 3.6). The three LVDTs are clamped together by a special mounting arrangement, as shown in Fig. 4.5. The arrangement consists of three perspex curves, each one holding an LVDT. The curves are connected at each end by a rod, as shown in Fig. 4.6, so that the three curves move in one plane. Two rubber bands at the each of two perspex curve ends (Fig. 4.6) were fitted to push the curves against the specimen to prevent membrane slippage during testing. A similar arrangement was made for the axial LVDTs targets, these are made from perspex.

Although some authors, such as Gens (1982), suggested that membrane slippage may be ignored for axial strains up to 4% (Section 3.6), a test was carried out on a dummy concrete specimen to measure the amount of membrane slippage due to the pull force of the spring, which carries the LVDT, during specimen compression. Two rubber membranes with silicone grease in between (as was used in the real tests), were put around the dummy concrete specimen. A metal hanger was glued to the outer rubber membrane,

as shown in Fig. 4.7, to carry weights. It was found that there was no membrane slippage up to a mass of 7.7 grams, then a 0.02 mm membrane slippage occurred at mass of 10.2 grams.

If a mass of 7.7 grams is hung at the end of the spring that is used to suspend the LVDT, the spring will extend about 2.2 mm. This means that there will be no membrane slippage if the specimen axial displacement is below 2.2 mm. From trial tests carried out on the soil used in the current research , it was found that the failure strain was less than 1% (1.5 mm displacement) i.e. less than 2.2 mm, which indicates that the membrane slippage can be ignored below failure strain. It should be noted that the rubber bands used on the perspex curve ends (Fig. 4.6) help reduce membrane slippage even further.

The three LVDTs used for the lateral strain measurement are placed in the middle ring, as shown in Fig. 4.3. A 50 mm x 20 mm brass plate is glued to the membrane at the mid-height of the specimen to act as a target for each LVDT. A light spring is placed around the lateral LVDT armature (Fig. 4.3) so that the armature can move outwards during specimen contraction.

4.3 Plumbing System

4.3.1 Double-Wall Triaxial Cell Plumbing System

Fig. 4.8 shows a diagram for the plumbing system used for the double-wall triaxial cell. Description of the plumbing system will be started from the air pressure supply line (top left of Fig. 4.8) and working downwards.

i) Air Pressure Supply. Air Pressure is provided by a compressor, which through a pressure regulator, is able to provide a maximum of 700 kPa air pressure with ±1 kPa pressure variation in the laboratory.

ii) Specimen Pore Air Pressure System. For the purpose of axis translation technique (Section 3.2), the pore air pressure is provided by a line which runs from the air pressure supply line to the top cap of the specimen. The line consists of a pressure regulator for controlling the pore air pressure, pressure gauge, pressure transducer and water trap device which prevents any water entering the specimen from the air supply line and changing the specimen water content.

iii) Cell Pressure System. Two pressure regulators and two pressure gauges are connected to the air pressure supply line. One pressure regulator and gauge are for low range of cell pressures (0-1 bar), and the others are for high range of cell pressures (0-8 bar). These are connected to one line which then splits into two lines, which run to the inner and outer cells. The first line is connected to an air-water interface and to the outer cell. The second line is connected to a volume change unit (1000 cc capacity) and a pressure transducer, and then connected to the inner cell. The specimen volume change is measured by measuring the volume change of the inner cell water (Section 3.5) using the 1000 cc volume change unit.

iv) Pore Water and Back Pressure System. Two pressure regulators and two pressure gauges are connected together in a similar arrangement as that described for the cell pressure system, and have the same purpose as that described for cell pressure system. These are connected to the air pressure supply line and to a 100 cc specimen water content volume change unit, pressure transducer, and to the centre of the base pedestal. In test in which the specimen water content change was not measured, this line was closed and the pressure transducer line was opened to the specimen for pore water pressure measurement during the test.

v) Flushing System. During a test, air may dissolve in the specimen pore water and flow through the high air entry ceramic stone, and come out of solution underneath the

ceramic stone as bubbles. These bubbles produce errors in the measurements of the specimen water content change and pore water pressure. The purpose of the flushing system is to remove these air bubbles and collect them in a burette to measure their volume, so that the specimen water content change can be corrected. The flushing water is sent from an air-water interface flushing storage tank to the centre of the pedestal and follows the spiral groove on the base pedestal (Section 4.2.1E and Plate 4.3) to the other hole towards the edge of the pedestal, and then goes to a 10 cc capacity burette, where the air bubbles are collected. The flushing water is then collected from the burette by a line to an air-water interface flushing collector tank. A flow reversal unit is connected to this system to reverse the flow of water sent from the flushing storage tank, by passing the water from the other end of the spiral groove to remove any trapped air bubbles that may not be removed by flushing in one direction only. A pressure regulator and gauge are connected from the air pressure supply line to the flushing system to provide the flushing pressure which should have the same value as that of the pore water pressure before flushing, to prevent water entering the specimen during flushing.

vi) Filling and Emptying System. The triaxial cell, volume change units, air-water interface tanks and burette all are connected to two large de-aired storage tanks (30 litres capacity each) to be filled with de-aired water. The water is de-aired by two de-aerators (6 litre capacity each) and transferred to the de-aired storage tanks (which are at higher level than the de-aerators) though a line, by vacuuming the tanks. Also, the de-aired storage tanks and the other parts of the plumbing system are connected to a drainage line for emptying.

4.3.2 Conventional Triaxial Cell Plumbing System

Fig. 4.9 shows the plumbing system used for the conventional triaxial cell. The air pressure supply line is provided by the same compressor that provides the air pressure to the double-wall triaxial cell. The system can perform the following functions.

i) Triaxial Cell Emptying and Filling. The cell is connected to a water tap for filling. The same line is used to empty the cell water.

ii) Cell Pressure System. The cell pressure is only measured by a pressure gauge connected to the cell (i.e. no pressure transducer is connected to the cell pressure system). The pressure gauge is connected to a pressure regulator, which is connected to a large air-water interface tank and to the air pressure supply line

iii) Specimen Flushing and Back Pressure System. The pore water pressure is measured, as well as by a pressure gauge, by a pressure transducer fitted to the bottom plate of the triaxial cell. The pressure gauge is connected to the pressure supply line, and to an air-water interface tank, for storing de-aired water. The tank is connected to a pressure regulator and to a specimen volume change unit (100 cc capacity), which is connected to the base pedestal of the triaxial cell. The specimen volume change unit, which is also used to measure the volume of the flushing water during specimen saturation process is connected to a flow reversal unit to reverse the flow of water from the top cell of the unit to the bottom cell, and vice versa, so that the volume change measurements can be extended beyond the capacity of the unit (100 cc). An air drainage line is connected to the top cap of the specimen for draining the flushed specimen air during the saturation stage. The flushing water is sent from the air-water interface storage tank to the specimen and measured by the specimen volume change unit. A burette is connected to the air drainage line to measure the volume of the flushing water entering the air drainage line during specimen flushing, so that it can be subtracted from the volume of the flushed water.

4.4 Data Logging System

Transducers for each triaxial cell are connected to a data logging system, for automatic record of the transducer readings. Each cell has a different data logging system, which are described in the following subsections.

4.4.1 Double-Wall Triaxial Cell Data Logging System

Fig 4.10 and Plate 4.4 show the data logging system used for this cell. The system is linked to thirteen transducers, which were 3 LVDTs for internal lateral strain, 3 LVDTs for internal axial strain, one LVDT for external axial strain, 1000 cc specimen volume change unit, 100 cc specimen water content volume change unit, 25 kN load cell and 3 pressure transducers for cell, pore water and pore air pressure measurements.

Lotus 123-Measure software, release 2.0, was used to read and record data from the thirteen transducers. The software provides macros (command statements) which can be used to write a program, to perform the required functions.

Seven programs were written, three for transducer calibrations, one for monitoring the specimen pore water pressure during specimen setting up and three for reading data from the thirteen transducers during specimen equalisation (the specimen is left under low net cell pressure, $(\sigma_3 - u_a)$= 10 kPa, for pore water pressure to equalise along the specimen), consolidation and shearing stages, one program for each stage of a test.

The Calibration programs were as follows:

- **Program-1.** This program was used to record the volume change of the inner cell water under different values of pressure so as to make corrections to the readings obtained from the specimen volume change unit. The correction is described in more detail in Section 5.3.2.

- **Program-2.** This program was used for the calibration of all the transducers except the 1000 cc specimen volume change unit.

• **Program-3.** This program was used for calibrating the 1000c specimen volume change unit. This unit was calibrated using the 100 cc specimen water content volume change unit, as will be described in Section 5.2.2.

The other four programs, in addition to taking readings from transducers, can perform the following functions:

1) Show graphs of the transducer readings during a test without interrupting the program

2) Calculate the time for the next reading on an exponential basis starting at 9 seconds.

3) Save data on both hard and floppy discs

4) In case of power cut-off, the program can be re-run.

4.4.2 Conventional Triaxial Cell Data Logging System

An existing ADU (Autonotnous Data Unit), model EL26-600, ELE International, which is shown in Plate 4.5, was used to log data from four transducers, which were the LVDT for external axial strain, the 25 kN load cell, the pressure transducer for pore water pressure and the 100 cc volume change unit for measuring the volume of flushing water during the saturation stage and specimen volume change unit during a test. The system has facilities for transducer calibration.

Subject	Reference	Type of decision made in the triaxial cell design
Suction measurement	Section 3.2	High air entry ceramic stone (Suction Plate Method) is used. The pore air pressure is increased to the point where the pore water pressure measurements are positive (Axis Translation Method).
Specimen diameter	Section 3.3.1	150 mm, with maximum soil grain size of 20 mm.
Specimen height	Section 3.3.2	375 mm.
Type of top cap and piston connection	Section 3.3.2	Rotated top cap, i.e. top cap is not fixed to the piston.
End friction	Section 3.3.2	The contact between the specimen ends and the top cap and base pedestal is not lubricated.
Cell fluid	Section 3.4	De-aired water.
Test types	Section 3.4	Drained test and constant water content test.
Water leakage	Section 3.4	The water leakage, to or from the specimen, is reduced by using two Latex rubber membranes and a coat of silicone grease in between.
Triaxial cell type	Section 3.5	Double-wall triaxial cell.
Specimen volume change measurements	Section 3.5	It is measured by measuring the inner cell water volume change.
Specimen strain measurements	Section 3.6	The axial and lateral strains are measured internally.

Table 4.1- Summary of the decisions made for designing the double-wall triaxial cell.

Plate 4.1 (Left)- Double-wall Triaxial Cell

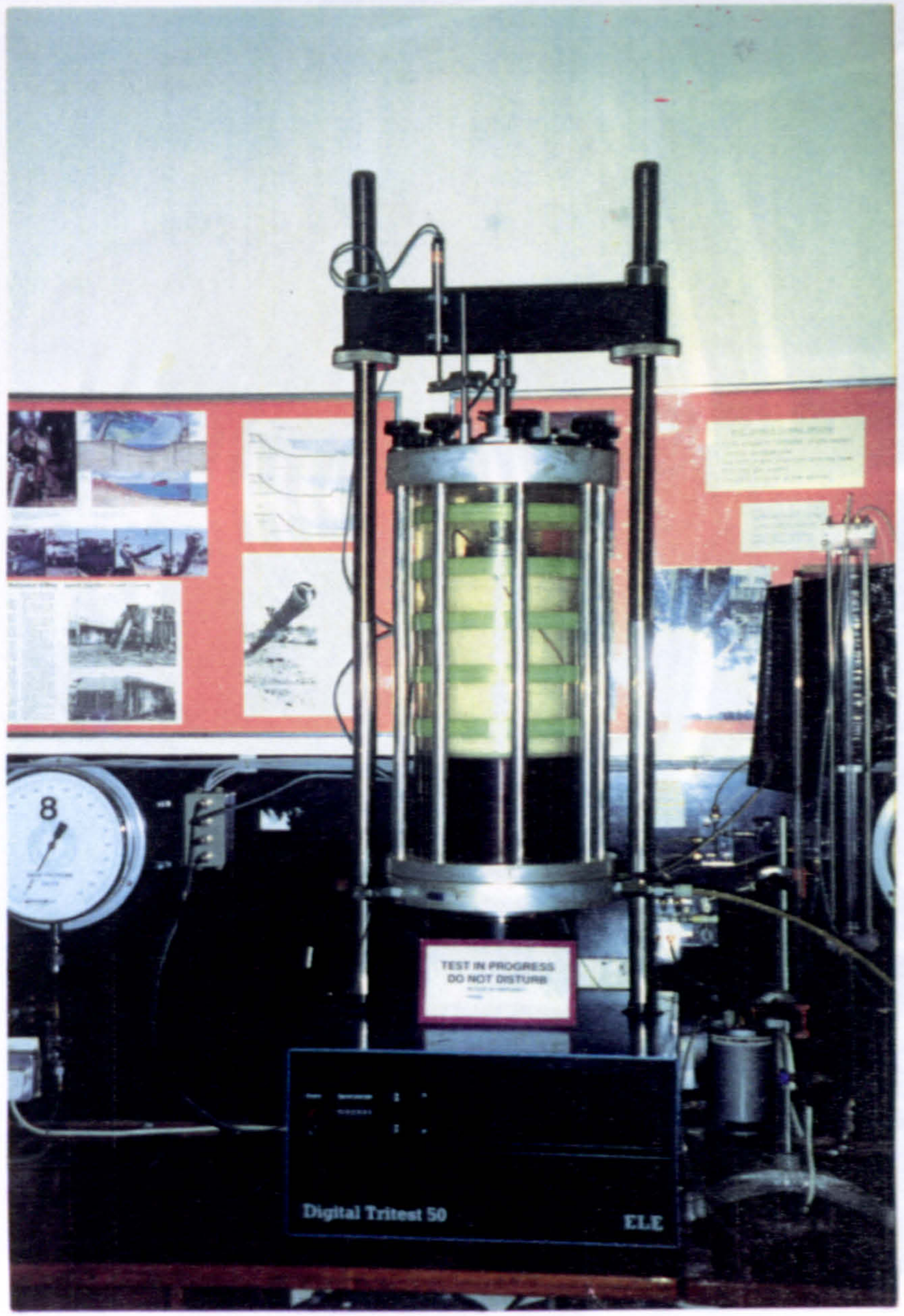

Plate 4.2 (Right)- Conventional Triaxial Cell

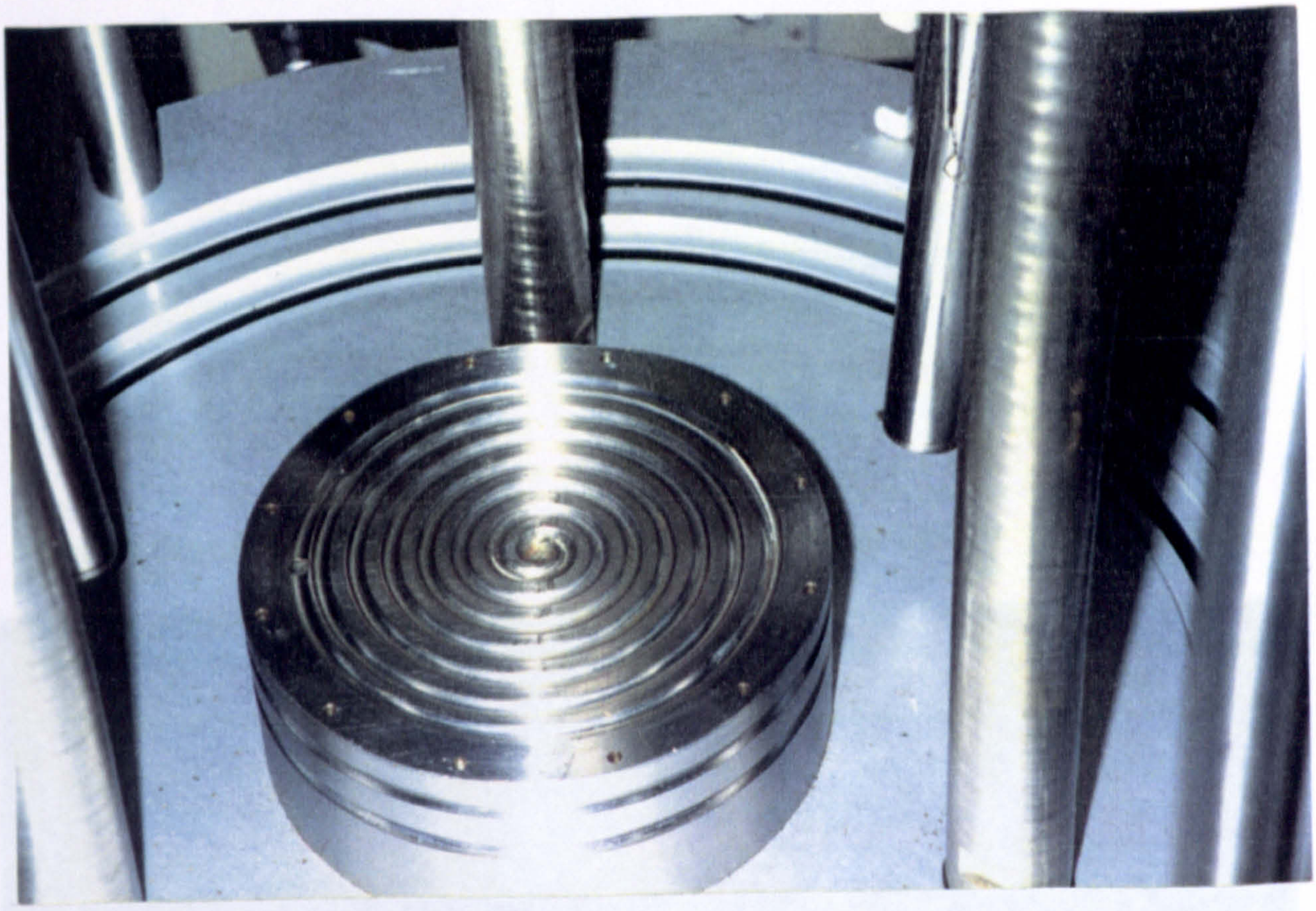

Plate 4.3- Spiral groove made on the top face of the base pedestal

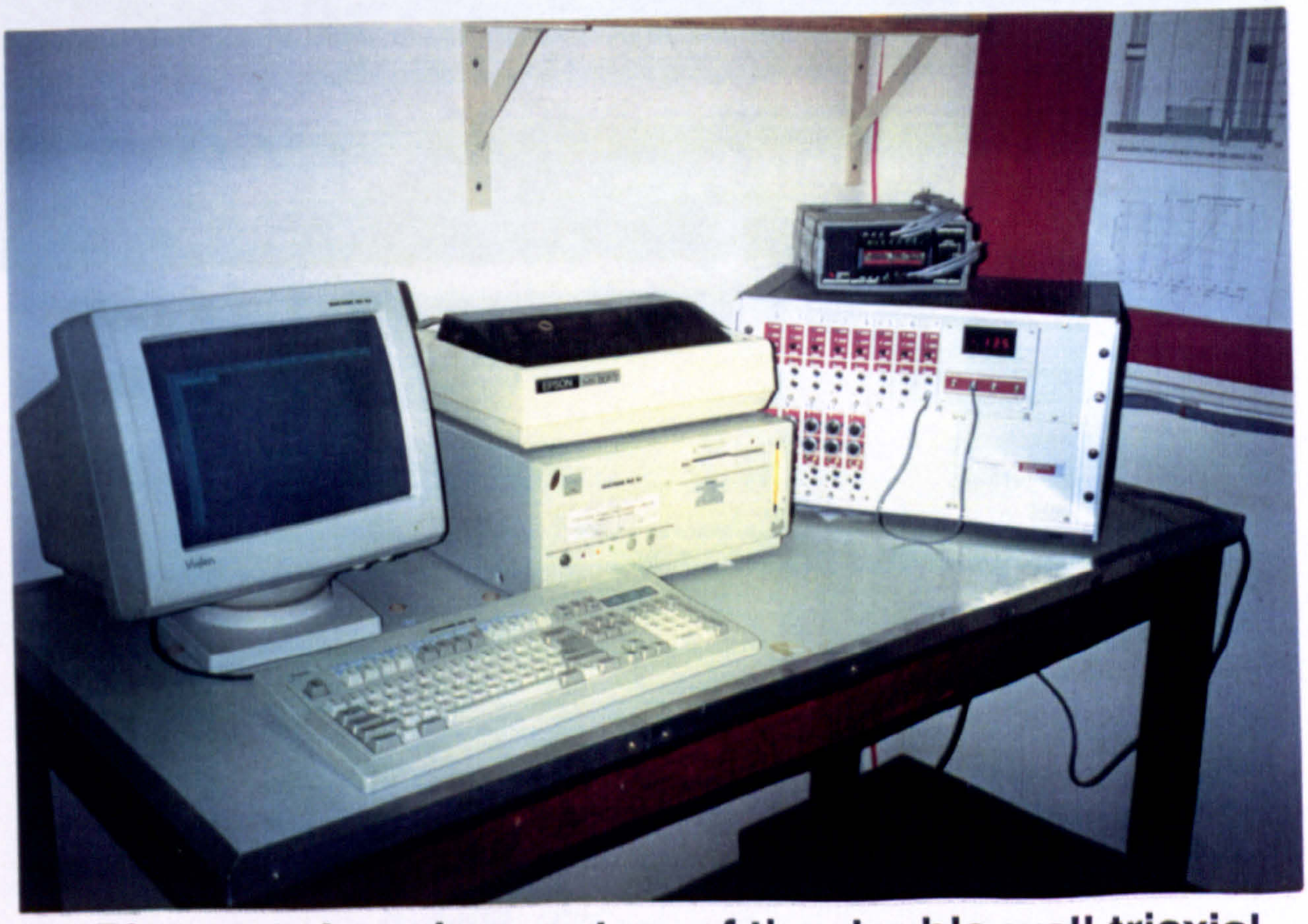

Plate 4.4- Logging system of the double-wall triaxial cell

Plate 4.5- Logging system of the conventional triaxial cell

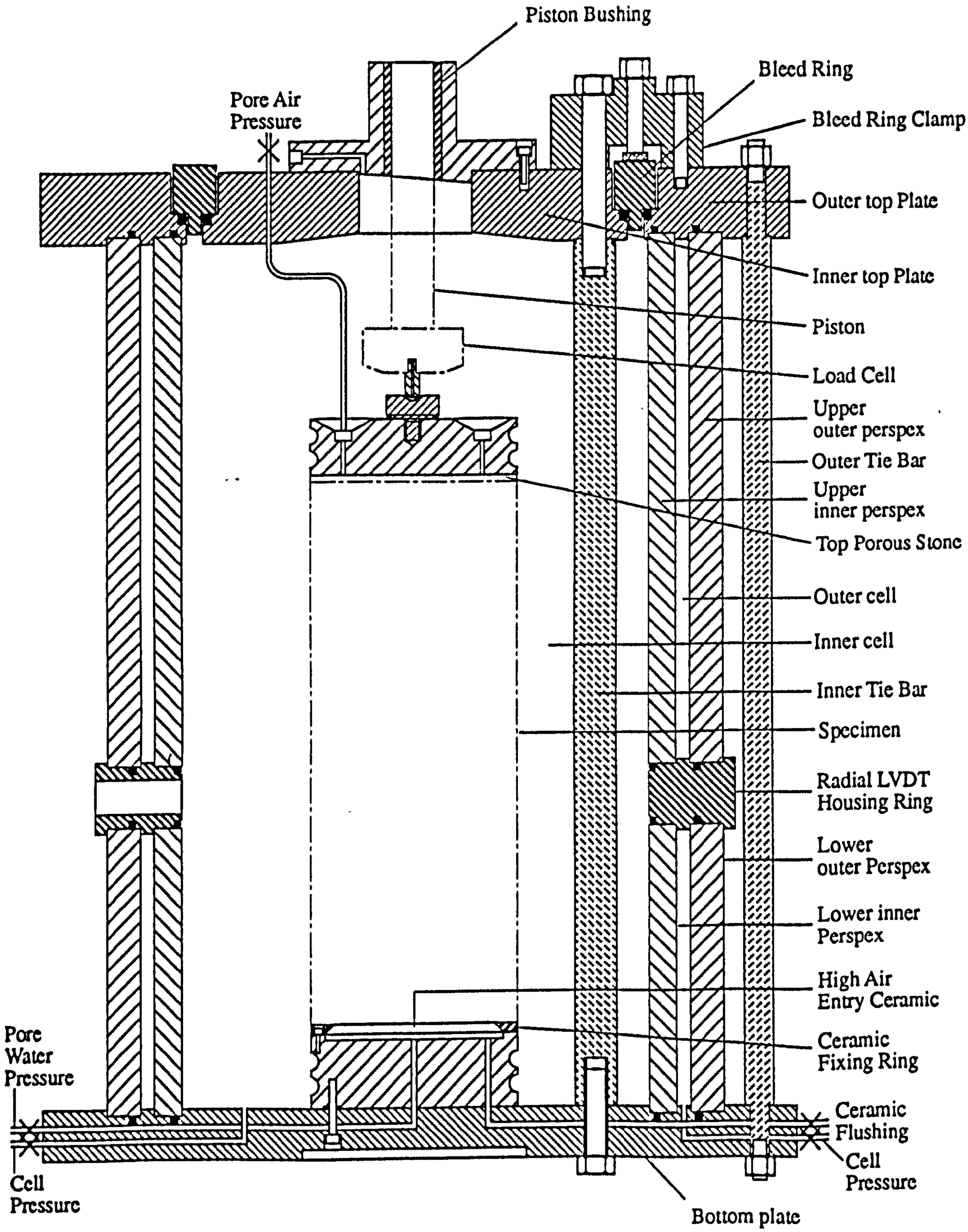

Fig. 4.1 Double-wall triaxial cell for testing unsaturated soils

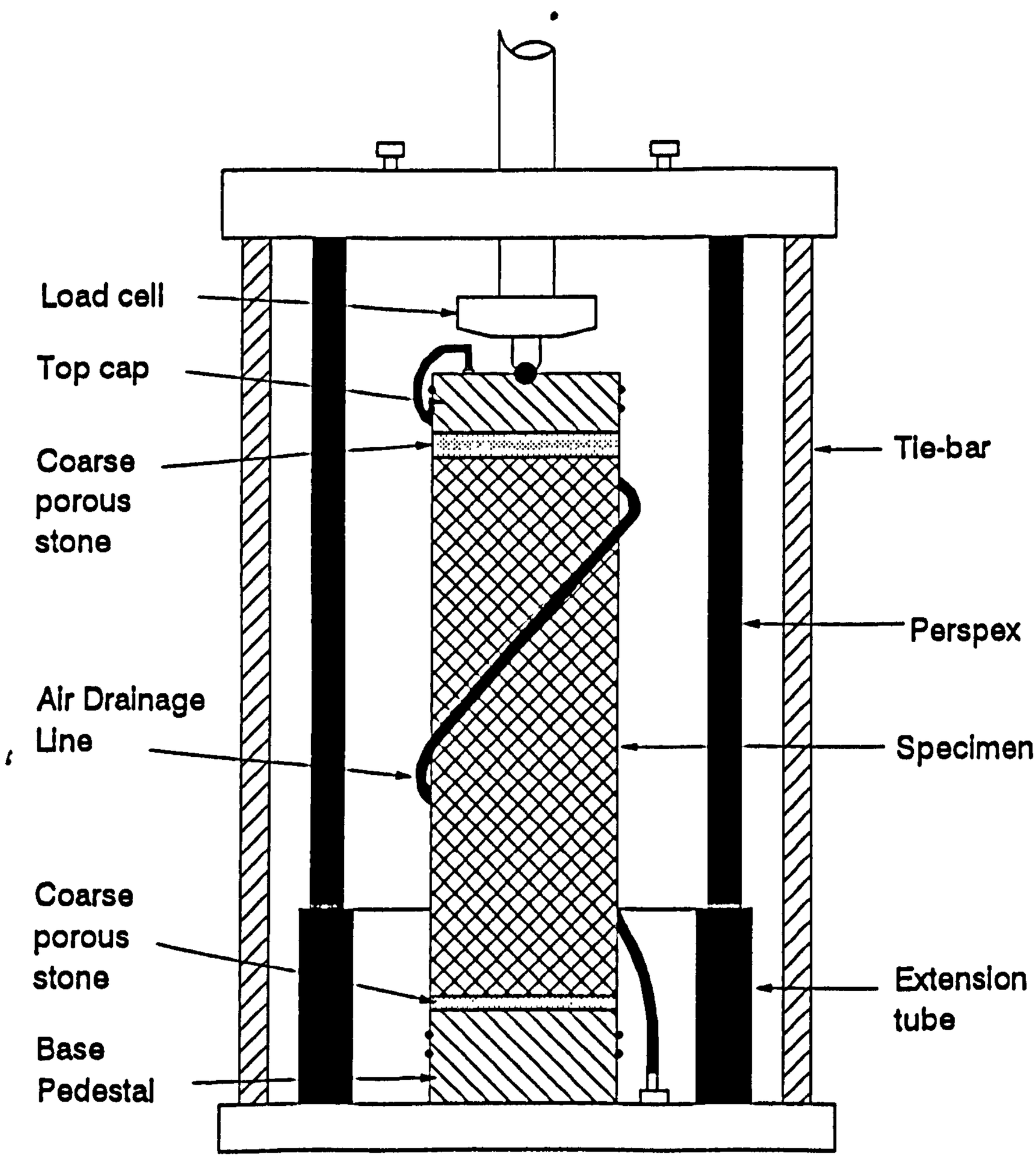

Fig. 4.2 -Conventional triaxial cell used for testing saturated specimens

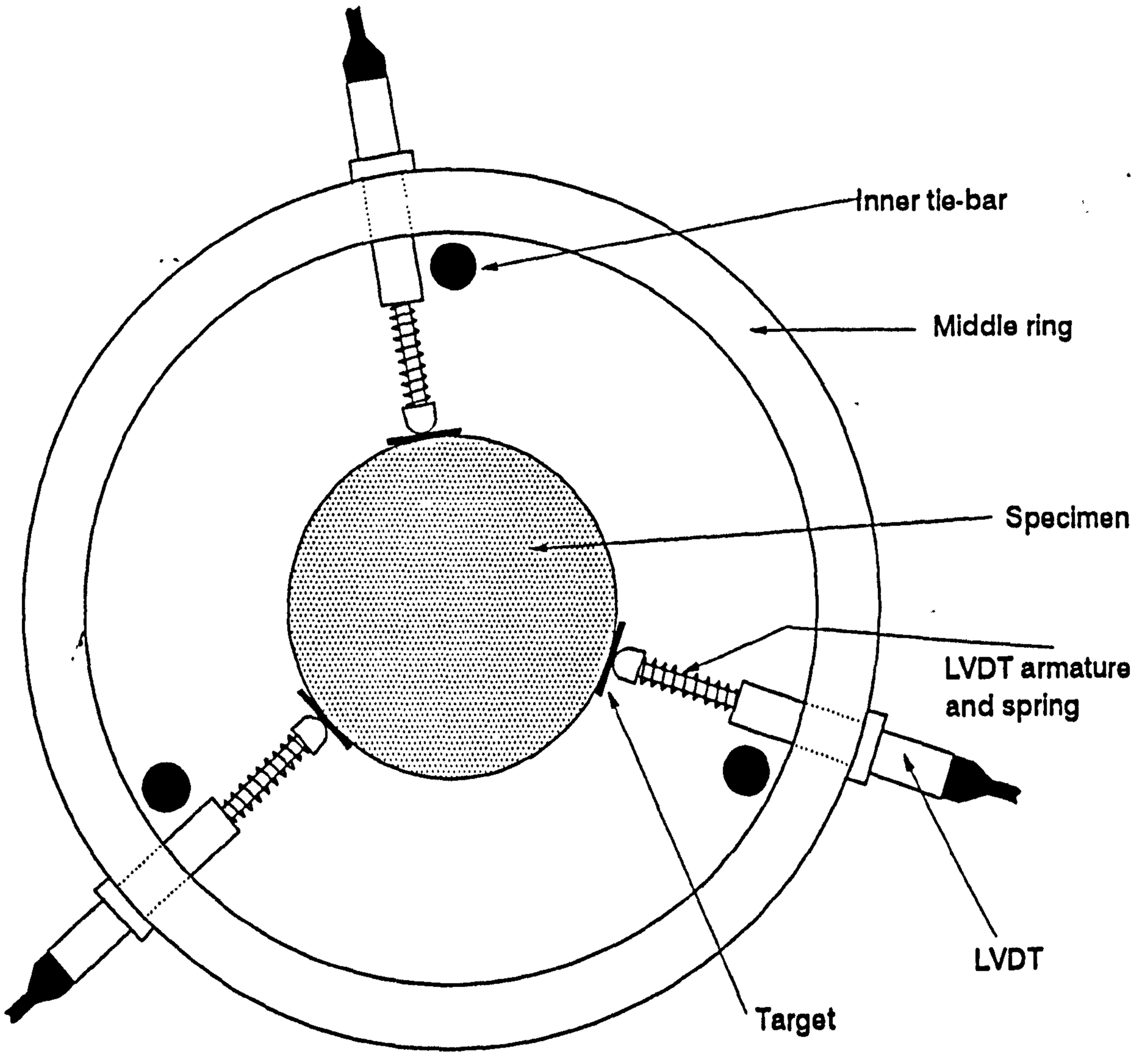

Fig. 4.3- Arrangement of the lateral LVDTs for the lateral strain measurements

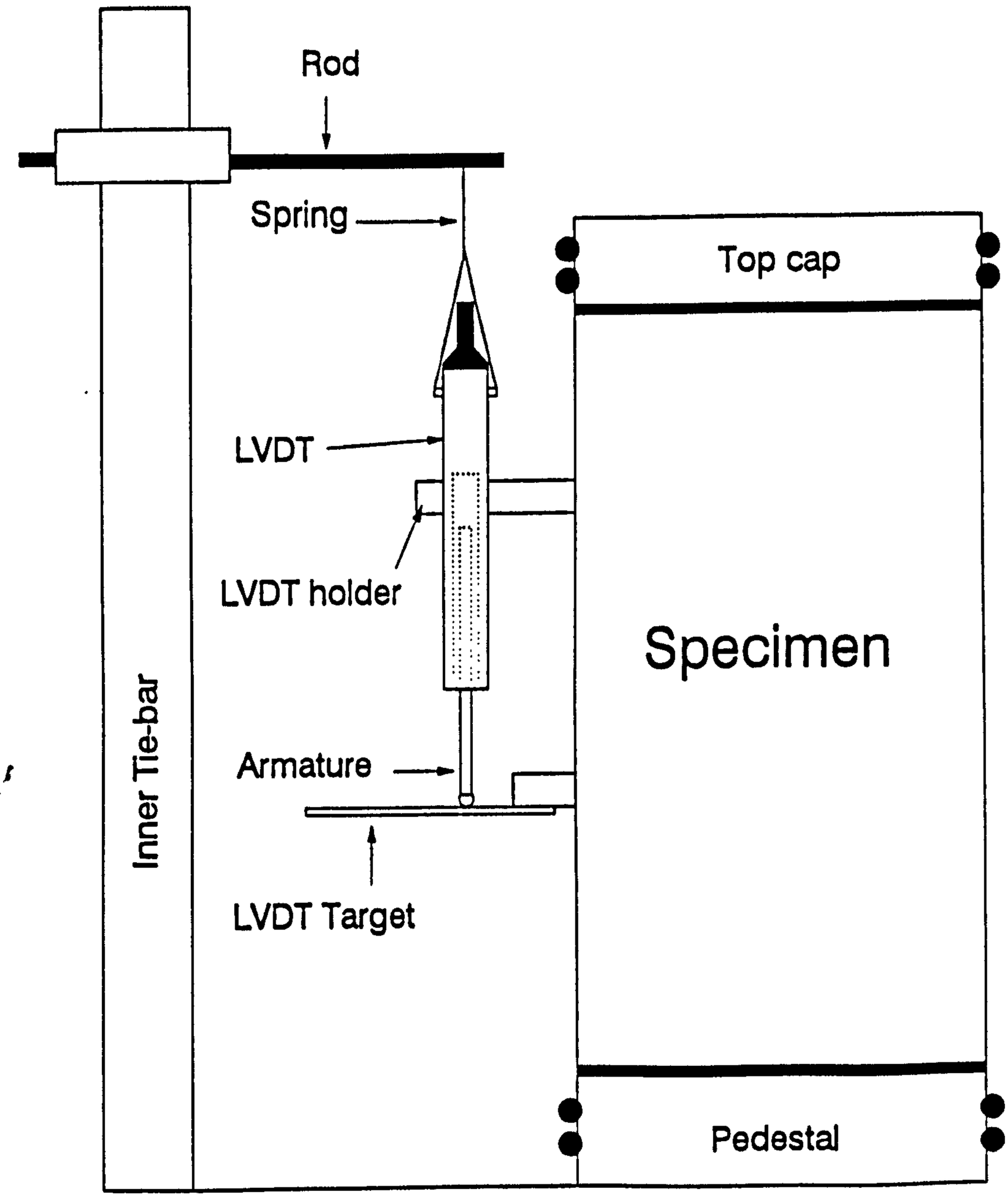

Fig. 4.4- Method of measuring the specimen internal axial strain

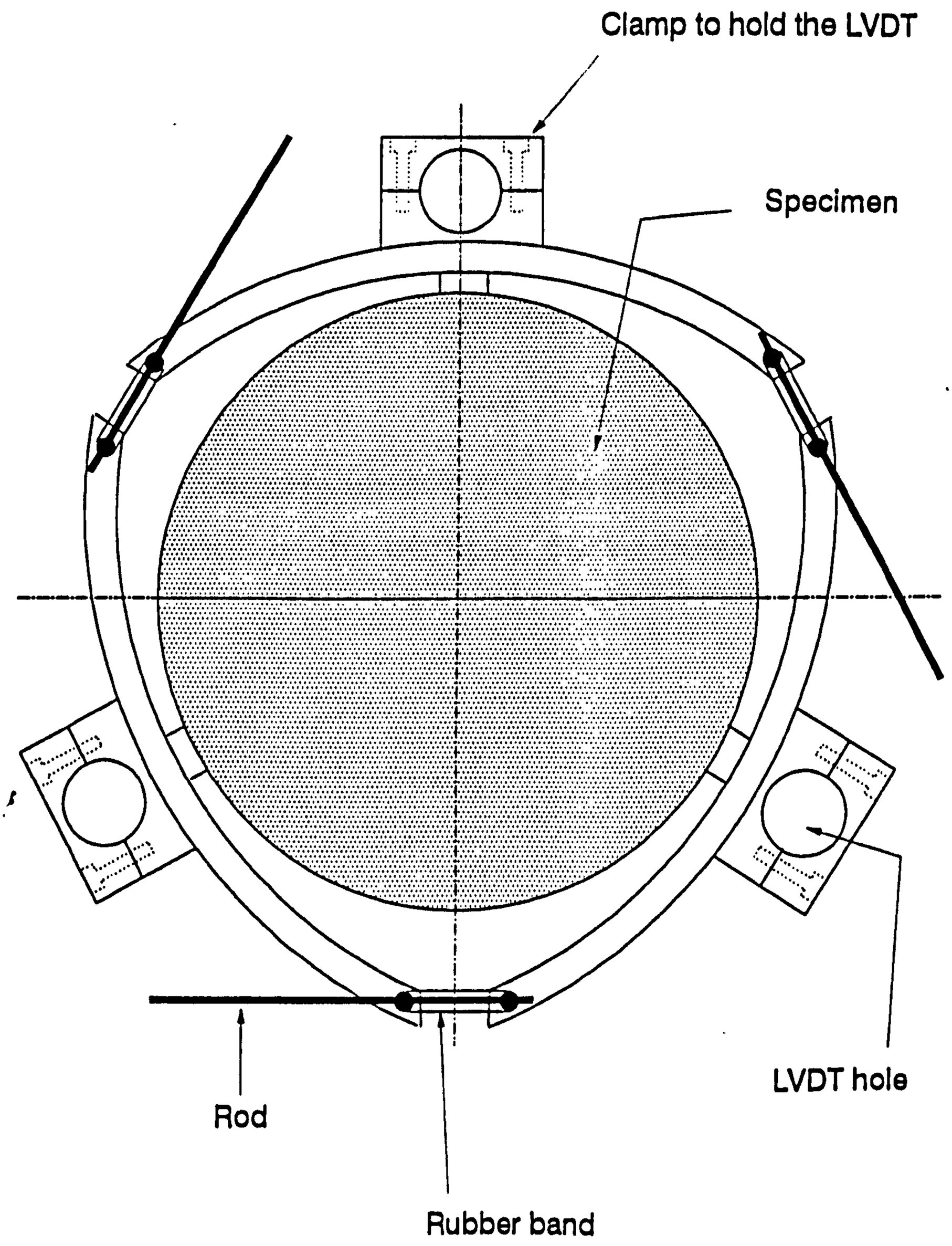

Fig. 4.5- Mounting system of the axial LVDTs used for the specimen internal axial strain measurements

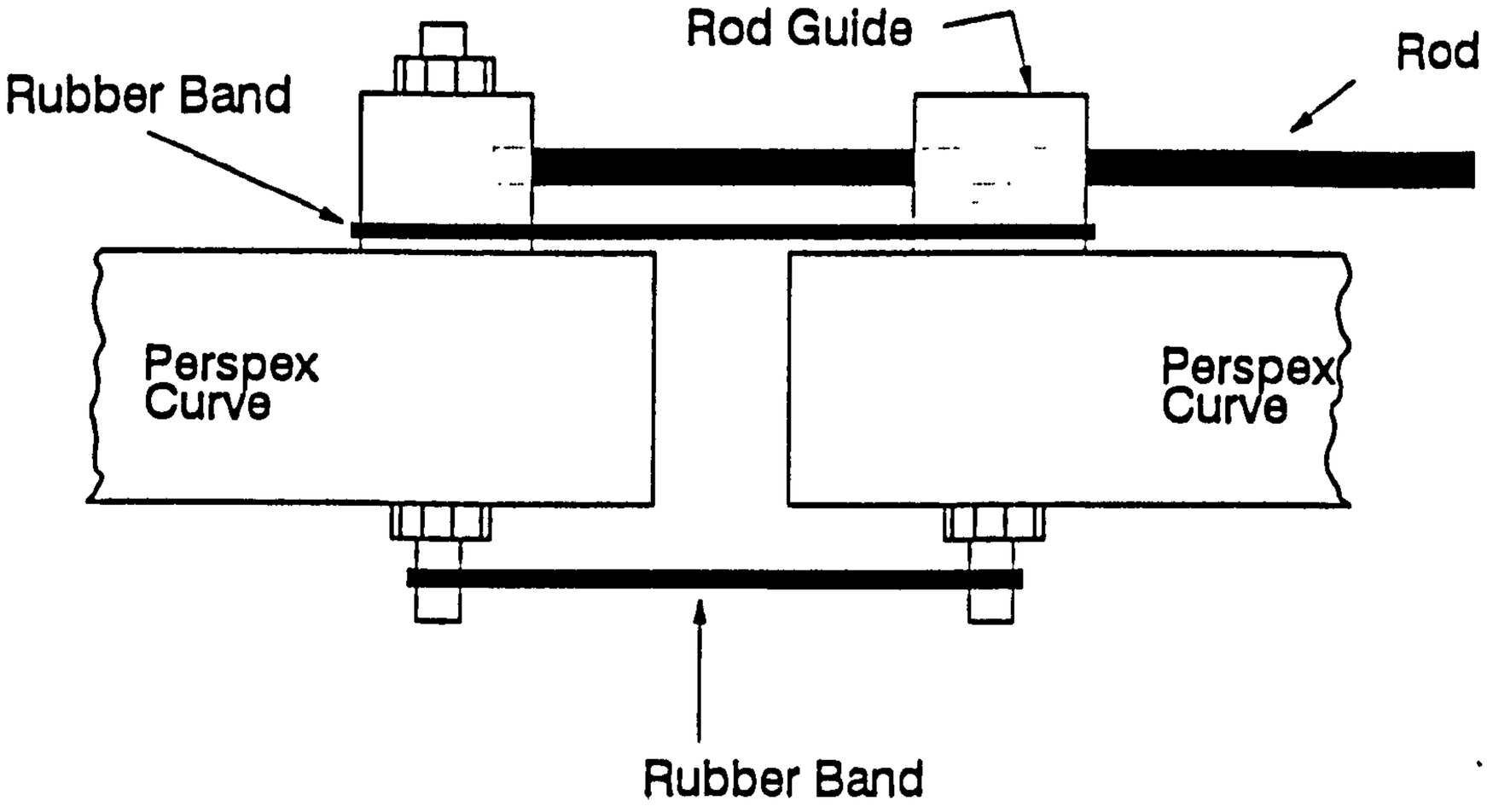

Fig. 4.6- Diagram shows the technique used to join the ends of the perspex curve holders

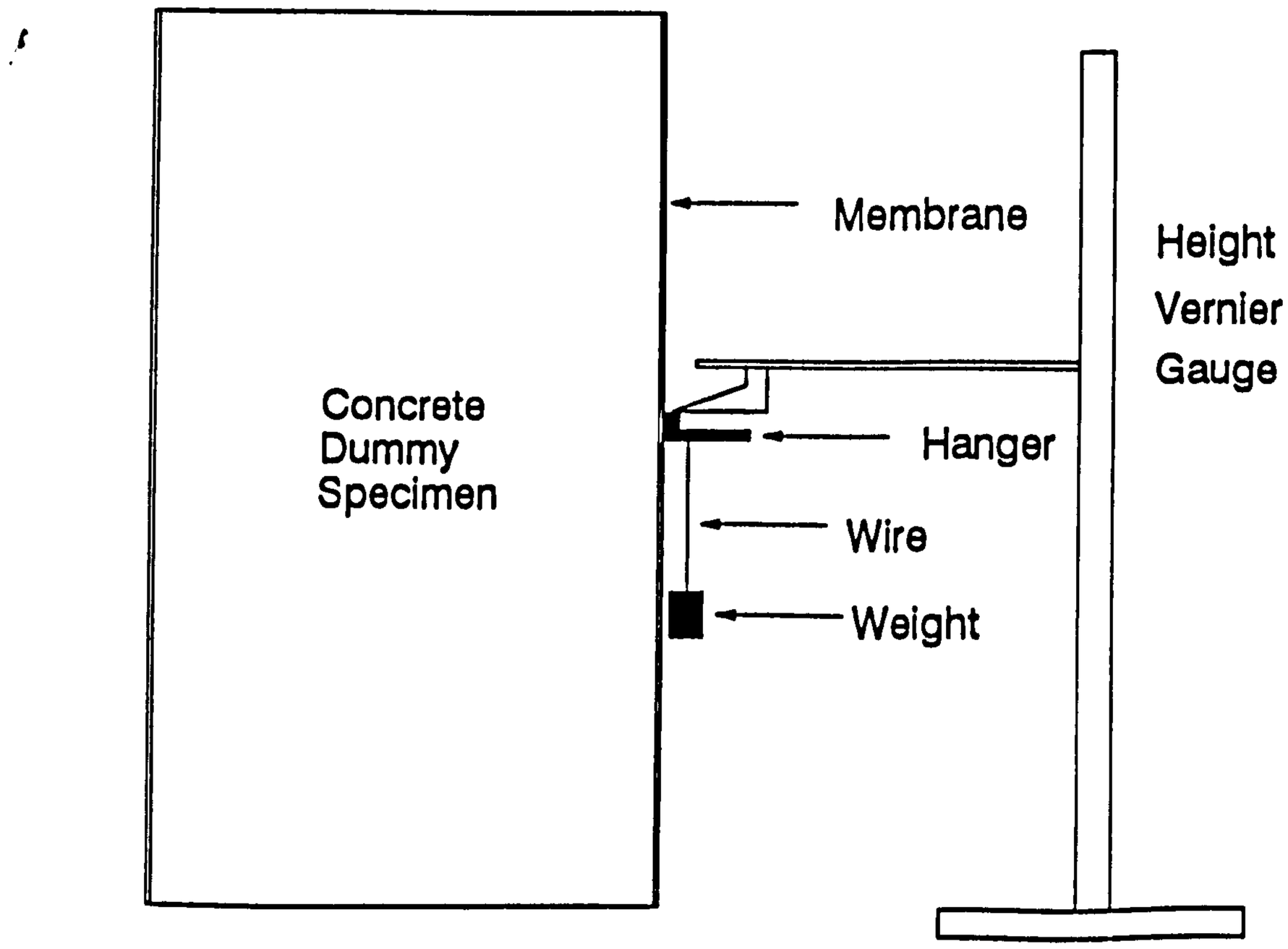

Fig. 4.7- Test arrangement for membrane slippage

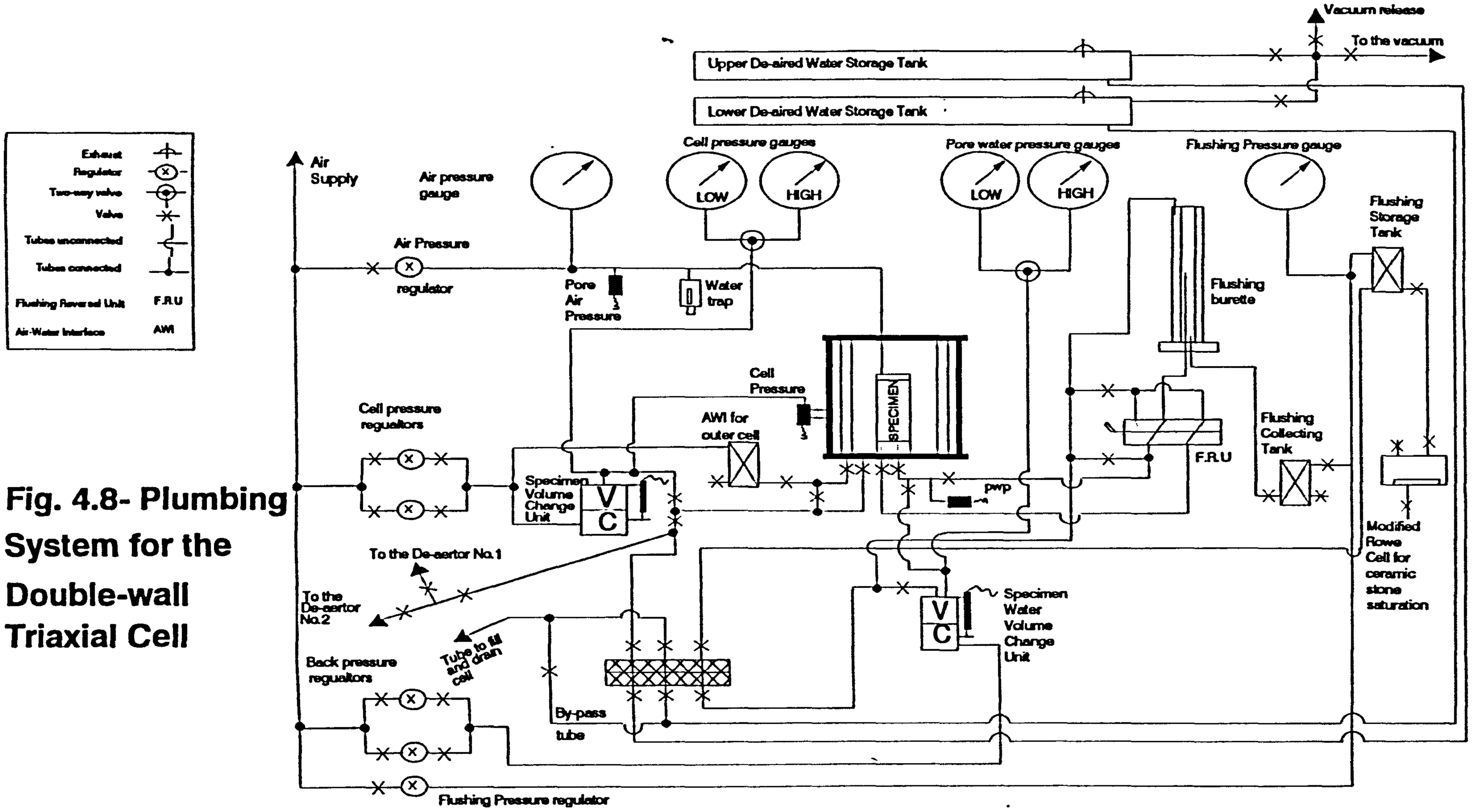

Fig. 4.8- Plumbing System for the Double-wall Triaxial Cell

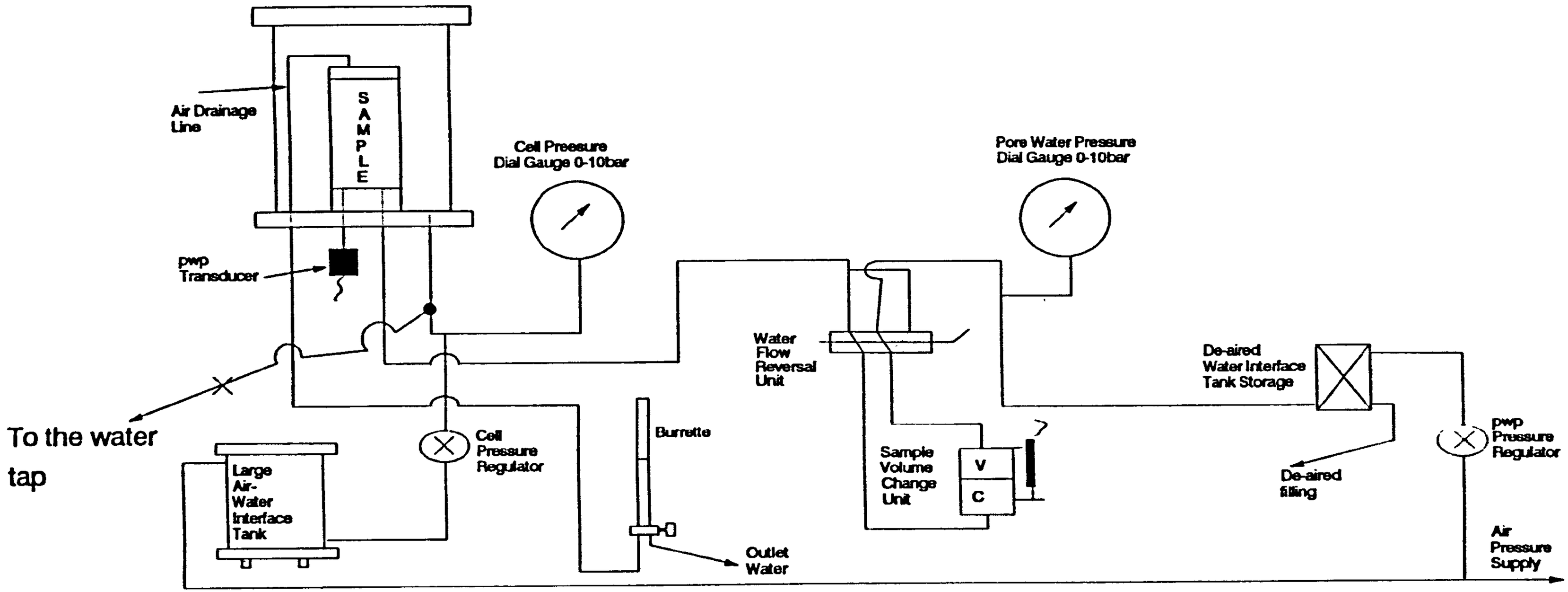

Fig. 4.9- Plumbing system for the conventional triaxial Cell

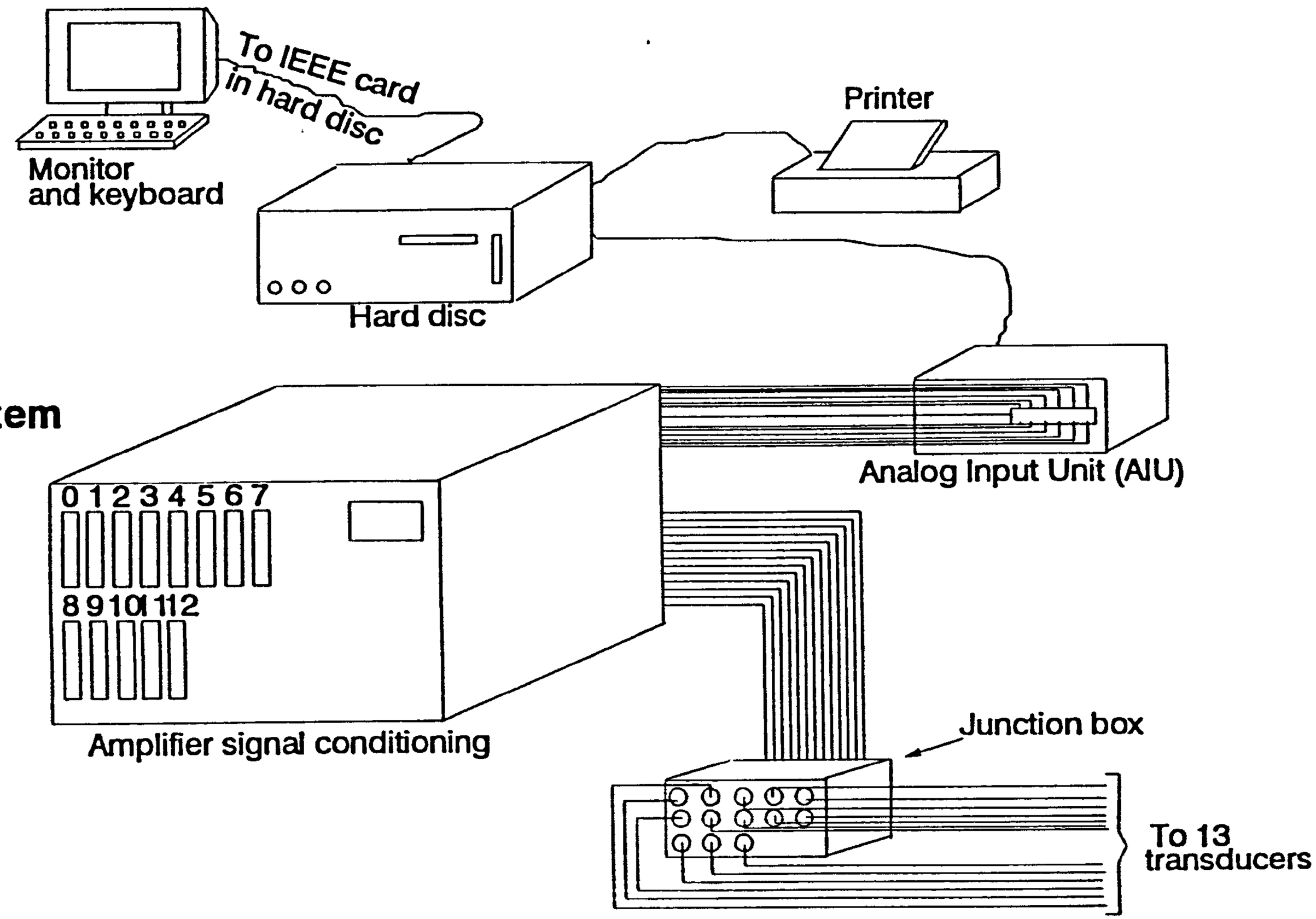

Fig. 4.10- Data logging system used for the double-wall triaxial cell

Chapter 5

Calibrations and Corrections

5.1 Introduction

Good test results depend on the quality of the measuring instruments . They should have the required accuracy and have little drift (variation in the calibration factor with time), and should be re-calibrated periodically, depending on the value of drift, to update the calibration factor. Also, good test results depend on a number of corrections being made to the results to improve their accuracy, such as correcting for the specimen volume change due to membrane penetration.

Description of the methods used to calibrate all of the measuring devices used for the unsaturated and saturated specimens triaxial tests, will be given in this chapter. Also, types of corrections made to the data are described.

5.2 Calibration

Tables 5.1 and 5.2 show lists for all measuring devices used in the double-wall and conventional triaxial cells respectively. Thirteen transducers were used for the double-wall triaxial cell for testing unsaturated specimen, seven LVDTs, 2 volume change units, one load cell and 3 pressure transducers. Four transducers, LVDT, volume change unit, load cell and pressure transducer, and one pressure gauge were used in the conventional triaxial

cell for testing saturated specimens. Tables 5.1 and 5.2 also show details of the measuring ranges and accuracy.

Computer programs were written for calibrating the measuring devices used in the double-wall triaxial cell (Section 4.4.1), while those used for the conventional triaxial cell were calibrated using built-in software in the logging system used for this cell (Section 4.4.2).

A linear regression technique was used to calculate the calibration factors. The accuracy of each transducer (scatter in the readings may be due to hysteresis) was calculated by dividing the maximum deviation from the best fit line, by the full measuring range of the transducer, which is shown with the calibration factors for all transducers in Tables 5.3 and 5.4. The drift (variation in the calibration factor with time) for each transducer was checked frequently by calibrating the transducers for a period of six months, and it was found that the drift was negligible for some transducers and small for others, apart from the cell pressure transducer, where the drift was high and varied linearly. It was therefore decided to repeat the calibration for all transducers every six months, apart from the cell pressure transducer which was re calibrated every two to three months. Tables 5.3 and 5.4 show the drift over the measured range for each transducer per six months. The drift was divided linearly by the time to correct the results of the tests carried out during two calibrations.

In the following subsections, a description of the method used to calibrate each type of measuring device will be given.

5.2.1 Displacement Transducers (LVDT)

Three types of LVDTs were used in the current research. The first type was the immersible LVDT, 25 mm range, which were used for measuring the internal axial and lateral strains (three LVDTs each) in the double-wall triaxial cell. The second type was one 100 mm range LVDT, which was used for measuring the specimen external axial strain in the double-wall triaxial cell. The third type was a 50 mm range LVDT used for measuring the specimen external axial strain in the conventional triaxial cell.

The LVDTs were left connected to the logging system for about one day before calibration to warm up. A Mitutoyo digital vernier, accurate to 0.0001 mm, was used to calibrate all the LVDTs, with 1 mm, 2 mm and 1 mm increment displacements for the first, second and third types respectively. The calibration factor for each LVDT was calculated from three cycles.

Each LVDT showed different values of accuracy, as shown in Tables 5.3 and 5.4. The maximum accuracies were 0.36%, 0.29% and 0.32% of the full scale, for types 1, 2 and 3 respectively, which correspond to a maximum error of 0.05% of the unsaturated specimen internal axial and lateral strains, 0.07% of the unsaturated specimen external axial strain and 0.04% of the saturated specimen external axial strain respectively.

The error due to drift of these LVDTs was negligible, with a maximum of 0.003% of the measured range (i.e. 0-3 mm, 0-5 mm and 0-5 mm for types 1, 2 and 3 respectively) per six months.

5.2.2 Volume Change Units

Three Imperial College type volume change units were used, two units were used in the double-wall triaxial cell , the first one was 1000 cc capacity for the measurements of the unsaturated specimen volume change, the second one was a 100c capacity for measuring the unsaturated specimen water content change. One 100 cc capacity unit was used in the conventional triaxial cell for measuring the saturated specimen volume change.

Before calibration, the volume change units were flushed and filled, with de-aired water and left under pressure connected to the logging system for at least two days, to force any trapped air bubbles into solution. They were then drained and re-filled with fresh de-aired water for another day. A 10 cc burette was used to calibrate both of the 100 cc capacity volume change units. The 1000 cc volume change unit was calibrated using one 100 cc volume change unit, as shown in Fig. 5.1. The small unit is filled with a measured volume of water and then sent to the larger unit, as described in detail in Fig. 5.1. The calibration factors for all units were determined using three filling-emptying cycles. The calibration process was repeated at different pressures and it was found that the calibration factors were virtually the same.

The accuracy of the 100 cc unit used for measuring the unsaturated specimen water content change was 0.025% of the full scale, which corresponds to about 0.0002% error in the specimen water content change, with no drift found. That of the 1000 cc volume change unit was 0.19% of the full scale which corresponds to 0.03% error in the measurements of the unsaturated specimen volumetric strain, with drift of 0.56 cc per six months when filled to its maximum capacity. The accuracy of the 100 cc unit used for measuring the saturated specimen volume change was 0.06% of the full scale, which corresponds to 0.0009% error in the volumetric strain of the saturated specimen, with no drift.

5.2.3 Load Cell

Similar load cells were used for the double-wall and conventional triaxial cells, and had a maximum load of 25 kN. Each load cell was connected to the logging system for 24 hours to warm up, then quickly twice loaded to the maximum load and unloaded before starting calibration. A 50 kN capacity Budenburg Oil Dead Weight Tester (Model 380), in conjunction with a loading frame (Model 500), accurate to 0.4% of the applied load, was used to calibrate the load cells.

The calibration started from 200N load, which was the smallest available load, then loaded to the maximum load, with 200N load increments, then unloaded in the same steps. The calibration factors were calculated from three loading-unloading cycles (Tables 5.3 and 5.4). The accuracy of each load cell was 0.07% of the full scale, which corresponds to a 1 kPa error in the deviator stress. The drift was very small, being equivalent to 28N per six months when loaded to its maximum load. This corresponds to 0.8 kPa error in the maximum deviator stress measured in these series of tests.

5.2.4 Pressure Transducer

Three pressure transducers, 700 kPa range, were used in the double-wall triaxial cell for the measurements of cell, pore water and pore air pressures, and one pressure transducer, 700 kPa range, was used in the conventional triaxial cell to measure the pore water pressure. The Budenburg oil dead weight tester (Model 380) was used to calibrate the pressure transducers. The transducers were connected for 24 hours to the logging system to warm up, then quickly twice loaded to the maximum pressure and unloaded before starting calibration. The calibration factor for each transducer was calculated from three loading-unloading cycles with 100 kPa increments.

The accuracy of the pressure transducers used in the double-wall cell were 0.17%, 0.12% and 0.06% of the full scale, which correspond to 1.2 kPa, 0.8 kPa and 0.4 kPa of the cell, pore water and pore air pressures respectively. For the pressure transducer used in the conventional triaxial cell the accuracy was 0.15% which corresponds to 1.1 kPa of the pore water pressure.

The drift of the cell pressure transducer used in the double wall triaxial cell was high and was 1.6 kPa per month over the measured range (0-200 kPa). For this reason this transducer was calibrated every two to three months. The drift of the double-wall triaxial cell pore water and air pressures transducers were 0.3 kPa per six months, over the measured range (0-100 kPa), while the drift in the conventional pore water pressure transducer was 0.7 kPa per six months, over the measure range (0-600 kPa)

5.2.5 Pressure Gauge

These were calibrated using the Budenburg oil dead weight tester. The accuracy of the pressure gauges was ±1 kPa. It should be noted that readings from the pressure gauges were only taken for the cell pressure of the saturated specimens, where no pressure transducer was used.

5.3 Corrections

Corrections were made to the measured unsaturated and saturated specimen volume changes, external axial strains, radial stresses and area. The volume change of the unsaturated specimen, which was measured by measuring the inner cell water volume change (Section 3.5), was corrected for errors due to membrane penetration (Section 3.7.1), piston penetration (as piston moved, it changed the inner cell water volume),

immediate volume change (due to the increase of the cell pressure) and water leakage. Volume change of the saturated specimen was only corrected for errors due to membrane penetration.

The area correction was made according to the method given by Head (1982), and the volume change due to piston penetration was determined by calculating the volume of the piston that moved into the cell during specimen compression. In the following subsections, a description is given of the methods used to obtain the other corrections.

5.3.1 Immediate Volume Change

When the cell pressure of the double-wall triaxial cell was increased, an immediate volume change occurred due may be to the compression of O-rings and water itself. The water compressibility is $4.8 \times 10^{-2}\,m^2/MN$, which means that the water in the inner cell can compress about 2.68 cc per 100 kPa pressure increase. Also extra immediate volume change can occur due to expansion of the inner cell volume, as the bottom and top plates (Fig. 4.1) bend outwards as the cell pressure is increased, and due to expansion of tubes and fittings.

The relationship between immediate volume change and cell pressure was found by filling the double-wall triaxial cell with de-aired water, then increasing the cell pressure 100 kPa steps up to 600 kPa pressure, and measuring any volume change which occurred. Fig. 5.2 shows this relationship which is non-linear. Two best fit equations were derived for different pressure ranges and these were used to correct volume change data from the tests as appropriate.

5.3.2 Water Leakage

Although all contacts between the double-wall triaxial cell components were fitted with greased O-rings to prevent water leakage, water leakage was not fully eliminated, as some volume change was measured when the cell (without the specimen) was left under pressure for some time. This water leakage may have occurred through valves, O-rings or may be due to perspex absorption (Sivakumar, 1993). Perspex absorption was unlikely to cause large water leakage because all the perspex cylinders were kept saturated in a water tank when not in use.

Tests were carried out to determine the rate of the water leakage from the inner cell, under different cell pressures, by filling the triaxial cell with de-aired water and then increasing the cell pressure and leaving it under this pressure for 3 to 4 days. Fig. 5.3 shows a typical graph of the volume change of the inner cell water under 200 kPa cell pressure. As can be seen from this figure that the rate of the volume change is constant. The variation of the volume change, ±0.4 cc, around the average line (Fig. 5.3) was due to the temperature variation (±1°C). Fig. 5.4 shows results of the tests carried out on the double-wall triaxial cell to determine the rate of the volume change due to water leakage under different cell pressures. It may be seen from this figure that the water leakage changes with cell pressure. The figure also shows an equation of the best fit line though the data.

Fig. 5.4 shows that there is a scatter in the measured rate of water leakage. This may be due to the fact that as the triaxial cell was dismantled and re-assembled, the channel shape, size and length, where water leakage was taking place through the O-rings and fittings, changed between one test and another under the same cell pressure, which in turn changed the rate of the water leakage. The maximum scatter was about ±0.009 cc/hour which corresponds to ±0.003% specimen volumetric strain per day. This means that there may be a maximum error in the specimen volumetric strain at failure of about ±0.003%

and ±0.02% for the slow and the very slow rates of strain used in the current research respectively (Section 6.3.3).

5.3.3 External Axial Strain Corrections

It was found that there was some compression in the loading machines used in the current research, during the specimen shearing stage. The compression of the loading machine under load can affect the accuracy of the measurements of the external axial strains. A mild steel tube of 2.54 mm wall thickness, 150 mm outer diameter and 375 mm height, was used as a dummy specimen to measure the loading machine compression under different values of applied load. After calibrating the dummy specimen to find its compression under load, it was placed in the triaxial cell between the top cap and base pedestal , and loaded to the maximum limit of the load cell, which was 25 kN. The displacements between the loading machine and triaxial cell were measured under each value of load by an LVDT, while the applied load was measured by the load cell. The loading machine compression was the difference between the measured displacement and the dummy steel compression.

The loading machine compression of the double-wall and conventional triaxial cells are shown in Figs. 5.5 and 5.6 respectively under different loads. The figures also show the best fitted line equations used for applying this type of correction to the unsaturated and saturated external axial strains.

5.3.4 Membrane Penetration and Restraint Corrections

Corrections to the volume change of the unsaturated and saturated specimens due to membrane penetration (Section 3.7.1) were made using Equation 3.3. This correction requires a value for the elastic modulus of the membrane rubber. Values of the elastic modulus for the rubber membrane, which was used for calculating the membrane

penetration and restraint, were obtained using the relationship, shown in Fig. 5.7, which was obtained experimentally using the method described by Henkel and Gilbert (1952).

Corrections for the specimen axial stress due to membrane restraint (Section 3.7.2) were not made because the membrane buckled during shearing and before failure, which means that the axial stress due to membrane restraint was negligible (Section 3.7.2). The specimen radial stress was corrected due to membrane restraint using Equations 3.4 and 3.7, and this correction had a maximum value of 0.7 kPa at failure

No. of Transducers	Transducer Type	Manufacture and Claimed Accuracy	Measuring Range	Type of Measurement
6	Free Armature, Immersible LVDT	RDP (0.5% F.S.)	0-25 mm	Specimen internal lateral and axial strains
1	LVDT	RDP (0.5% F.S.)	0-100 mm	Specimen external axial strain
1	Volume change unit	Imperial College (0.25% F.S.)	0-1000 cc	Specimen volume change
1	Volume change unit	Imperial College (0.05% F.S.)	0-100 cc	Specimen water content change
3	Pressure transducer	RDP (0.1% F.S.)	0-700 kPa	Specimen cell, pore air and pore water pressures.
1	Load cell	Wykehm Farrance (0.1% F.S.)	0-25 kN	Specimen deviator stress

LVDT= Displacement Transducer, F.S.= Full Scale

Table 5.1- Transducers used in the double-wall triaxial cell.

No. of Transducers	Type of Transducer	Manufacture and Claimed Accuracy	Measuring Range	Type of Measurement
1	LVDT	MPE (0.5% F.S.)	0-50 mm	Specimen external axial strain
1	Volume change unit	Imperial College (0.05% F.S.)	0-100 cc	Specimen volume change
1	Pressure transducer	Druck Ltd. (0.1% F.S.)	0-700 kPa	Specimen pore water pressure
1	Load cell	Wykehm Farrance (0.1% F.S.)	0-25 kN	Specimen deviator stress

LVDT= Displacement Transducer, F.S.= Full Scale

Table 5.2- Transducers used in the conventional triaxial cell.

Transducer Type	Measurements Type	Range	Calibration Factor	Accuracy (% F.S.)	R^2	Drift
LVDT	Internal lateral strai	0-25 mm	0.01249 mm/mV	0.16	0.99999	Negligible
LVDT	Internal lateral strai	0-25 mm	0.01238 mm/mV	0.34	0.99998	Negligible
LVDT	Internal lateral strai	0-25 mm	0.01243 mm/mV	0.19	0.99999	Negligible
LVDT	Internal axial strain	0-25 mm	0.01237 mm/mV	0.36	0.99998	Negligible
LVDT	Internal axial strain	0-25 mm	0.01239 mm/mV	0.33	0.99999	Negligible
LVDT	Internal axial strain	0-25 mm	0.01242 mm/mV	0.23	0.99999	Negligible
LVDT	External axial strain	0-100 mm	0.04994 mm/mV	0.29	0.99995	Negligible
V.C.U.	Specimen volu change	0-1000 cc	0.52153 cc/mV	0.19	0.99998	0.56 cc per six months over the full scale
Pressure Transducer	Cell pressure	0-700 kPa	0.0844 kPa/mV -297.0	0.17	0.99997	9.6 kPa per one month over the measured range (0-200 kPa)
Pressure Transducer	Pore water pressure	0-700 kPa	0.0830 kPa/mV -281.3	0.12	0.99999	0.3 kPa per six months over the measured range (0-100 kPa)
Pressure Transducer	Pore air pressure	0-700 kPa	0.0841 kPa/mV -291.4	0.06	0.99999	0.3 kPa per six months over the measured range (0-100 kPa)
Load Cell	Deviator stress	0-25 kN	2.82 N/mV	0.07	0.99999	28 N per six months over the full scale
V.C.U.	S.W.C.C	0-100 cc	0.0146827 cc/m	0.025	0.99999	Negligible

R = Correlation factor (degree of scatter), LVDT = Displacement Transducer, V.C.U. = Volume Change Unit, mV = milivolt, S.W.C.C = Specimen Water Content Change

Table 5.3- Calibration factors and accuracy of the transducers used in the double-wall triaxial cell.

Transducer Type	Measurements Type	Range	Calibration Factor	Accuracy (% F.S.)	R^2	Drift
LVDT	External axial strain	0-50 mm	0.03188 mm/mV	0.32	0.99999	Negligible
V.C.U	Specimen volumetric strain	0-100 cc	0.06840 cc/mV	0.06	0.99995	Negligible
Pressure Transducer	Specimen pore water pressure	0-700 kPa	0.61090 kPa/mV	0.15	0.99996	0.7 kPa per six months over the measured range (0-600 kPa)
Load Cell	Deviator stress	0-25 kPa	27.5553 mm/mV	0.07	0.99999	28 N per six months over the full scale

R = Correlation factor (degree of scatter), LVDT = Displacement Transducer, V.C.U. = Volume Change Unit, mV = milivolt

Table 5.3- Calibration factors and accuracy of the transducers used in the conventional triaxial cell.

Calibration Method

1- Both volume change units should be emptied. Close valves 1, 2 and 3.

2- Increase pressures to both volume change units, so that all pressure gauges have same readings.

3- Open valves 1 and 3 to fill unit 1, then close them.

4- Take readings for both units using the available program.

5- Open valves 2 and 3 to fill unit 2, then close them.

6- Take readings for both units.

7- Repeat steps 3 to 6, until unit 2 is full.

8- Increase the pressure on unit 2 so that it is 3 kPa higher than unit 1, then take readings for both units.

9- Open valves 2 and 3 to fill unit 1, then close them.

10- Take readings for both units.

11- Decrease pressure on de-aired water storage tank until it has a pressure 4 kPa below that of unit 1.

12- Open valves 1 and 3 to empty unit 1, then close them.

13- Take readings for both units.

14- Repeat steps 9 to 13 until unit 2 is empty.

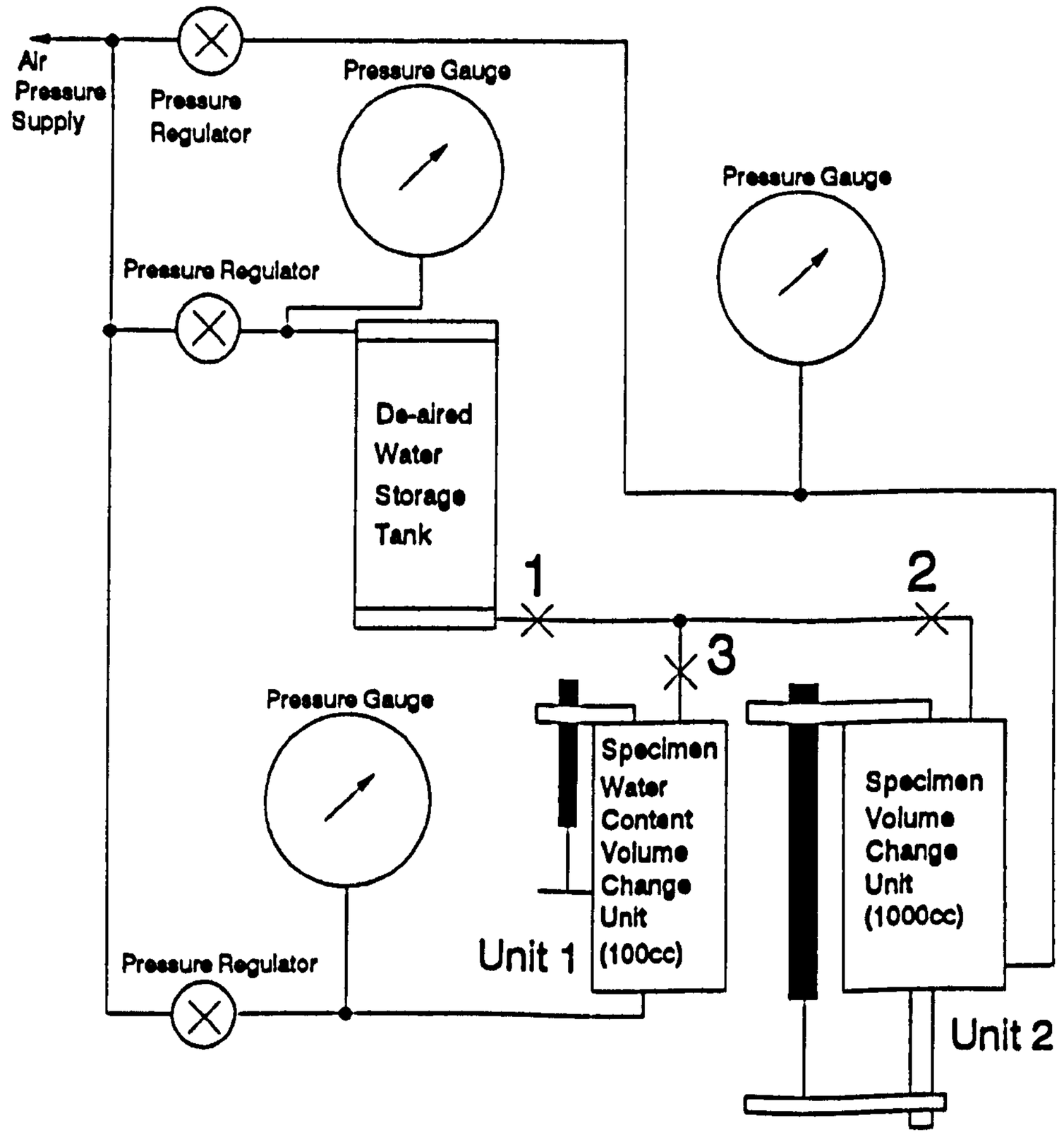

Fig. 5.1- Unsaturated specimen volume change unit calibration

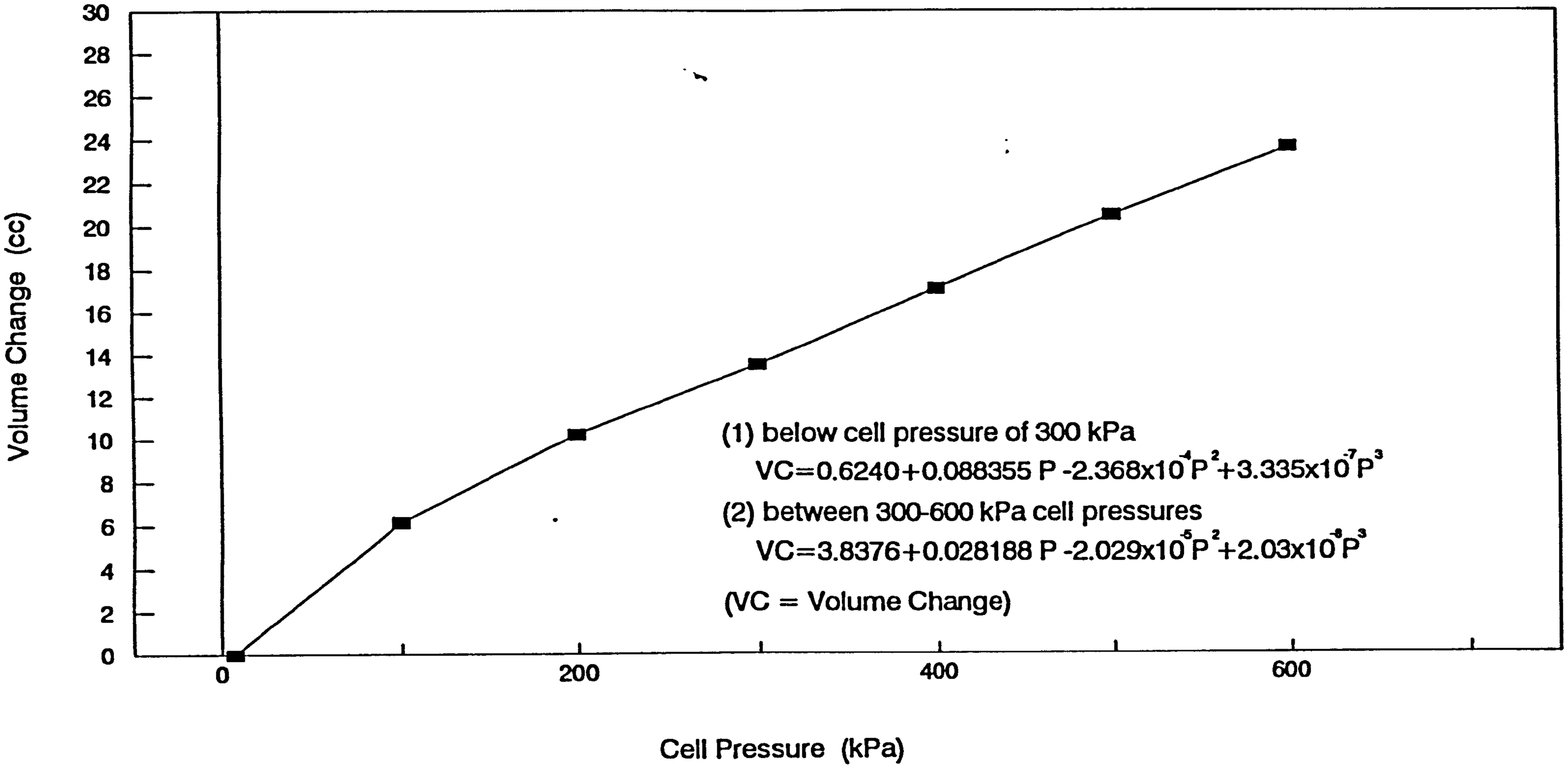

Fig. 5.2- Immediate change in the volume of the inner cell water of the double-wall cell, due to increase in the cell pressure.

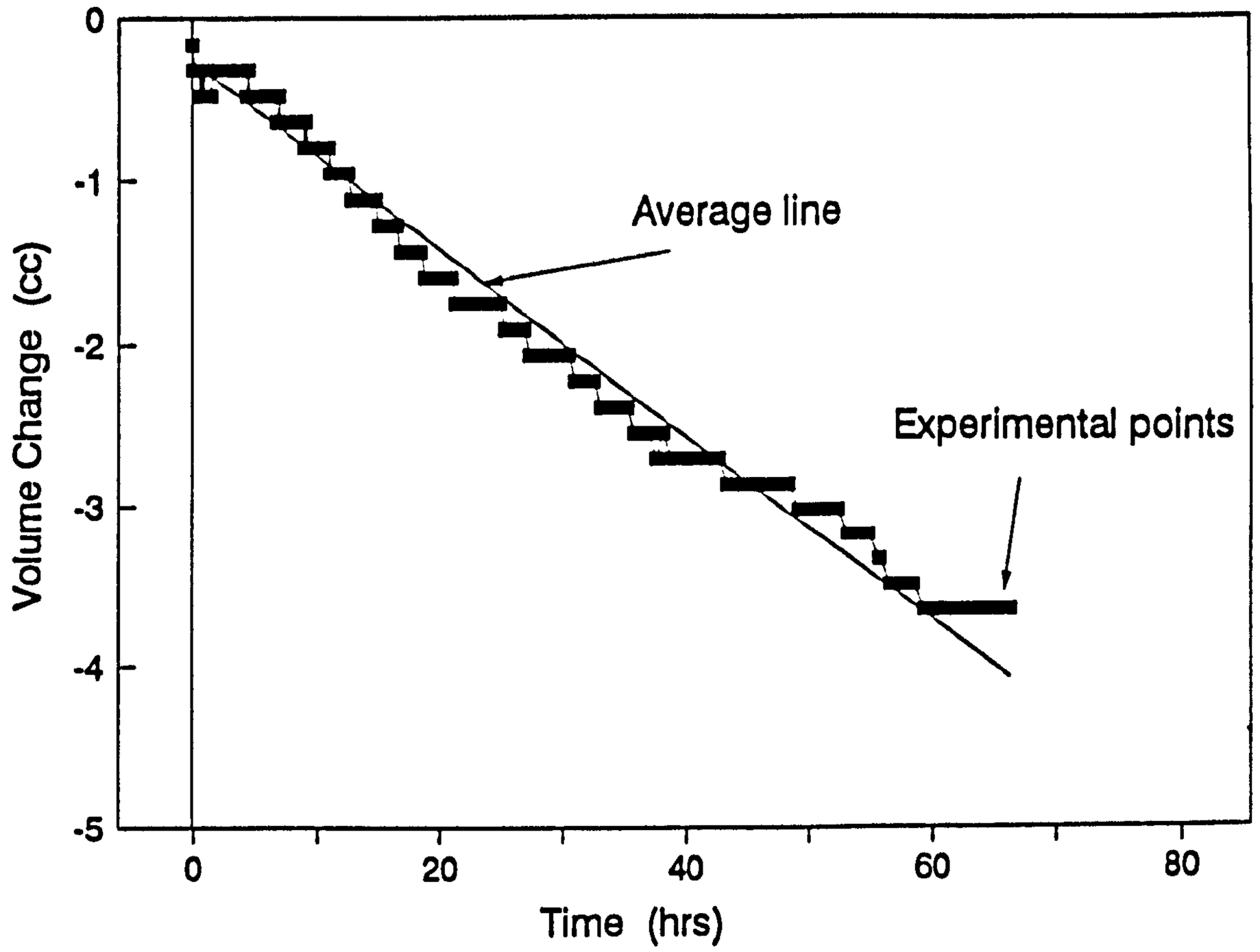

Fig. 5.3- Change in the volume of the inner cell water of the double-wall triaxial cell, at 200kPa cell pressure, due to water leakage

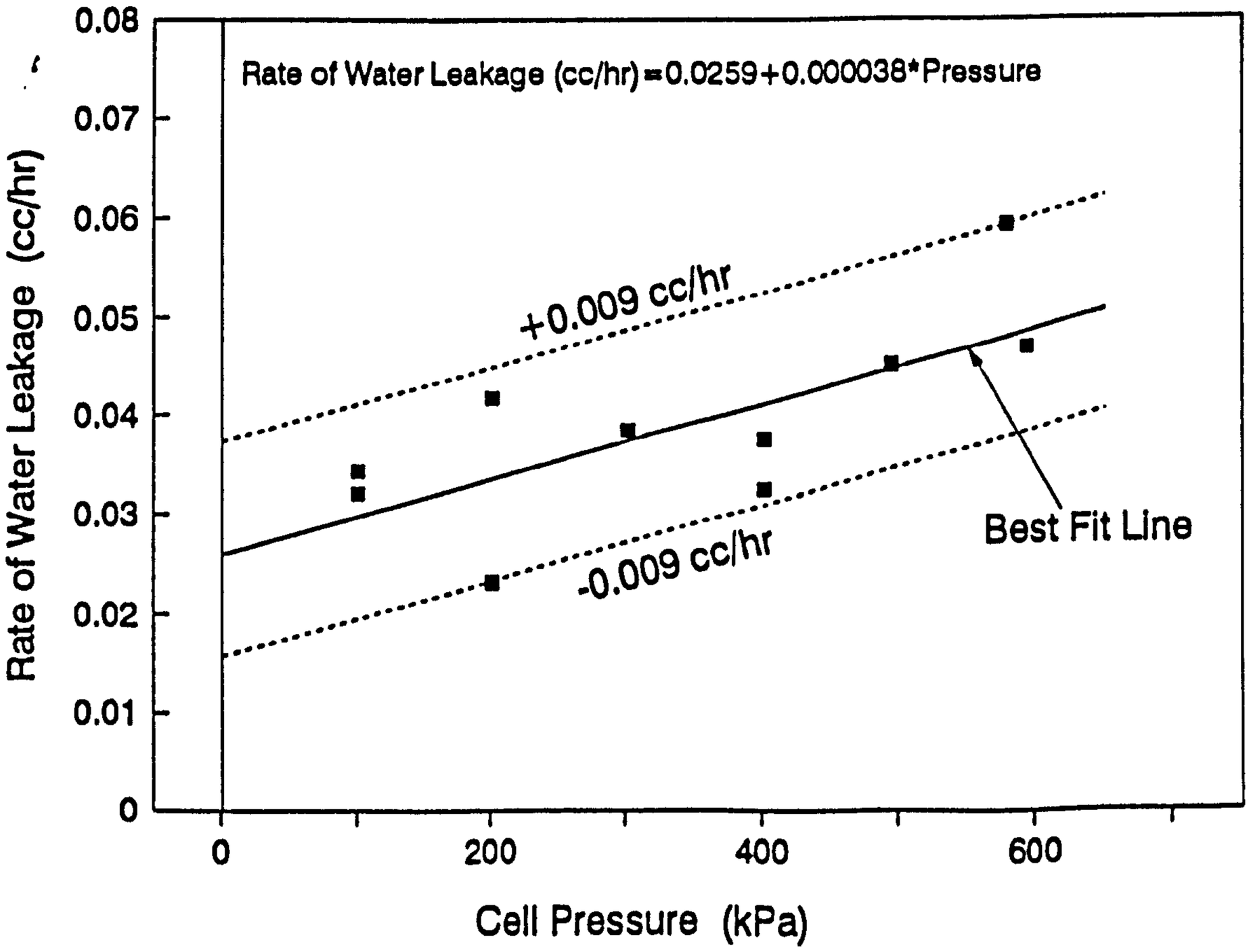

Fig. 5.4- Water leakge rate in the double-wall triaxial cell at different cell pressures.

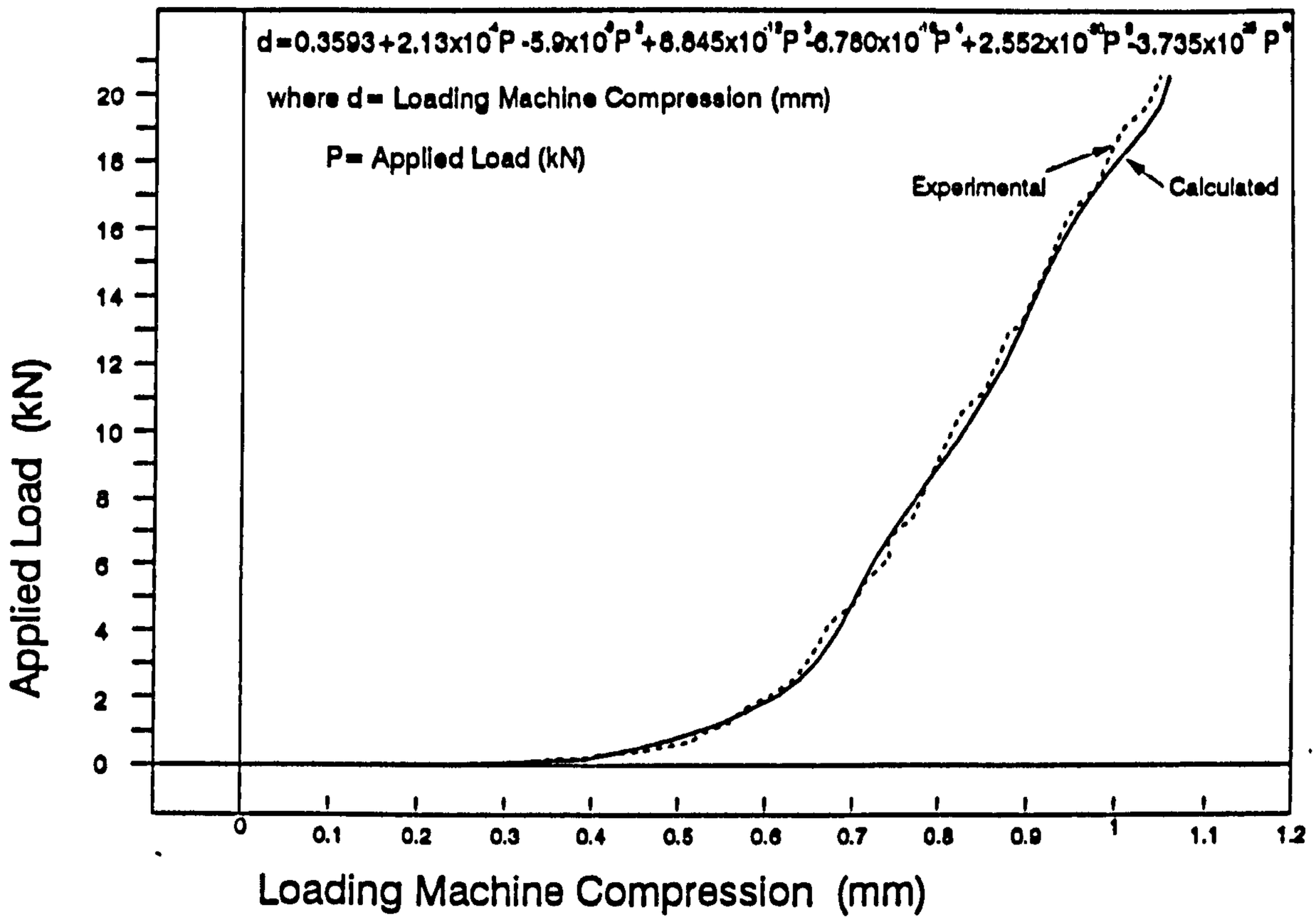

Fig. 5.5- Loading machine calibration graph for the double-wall triaxial cell.

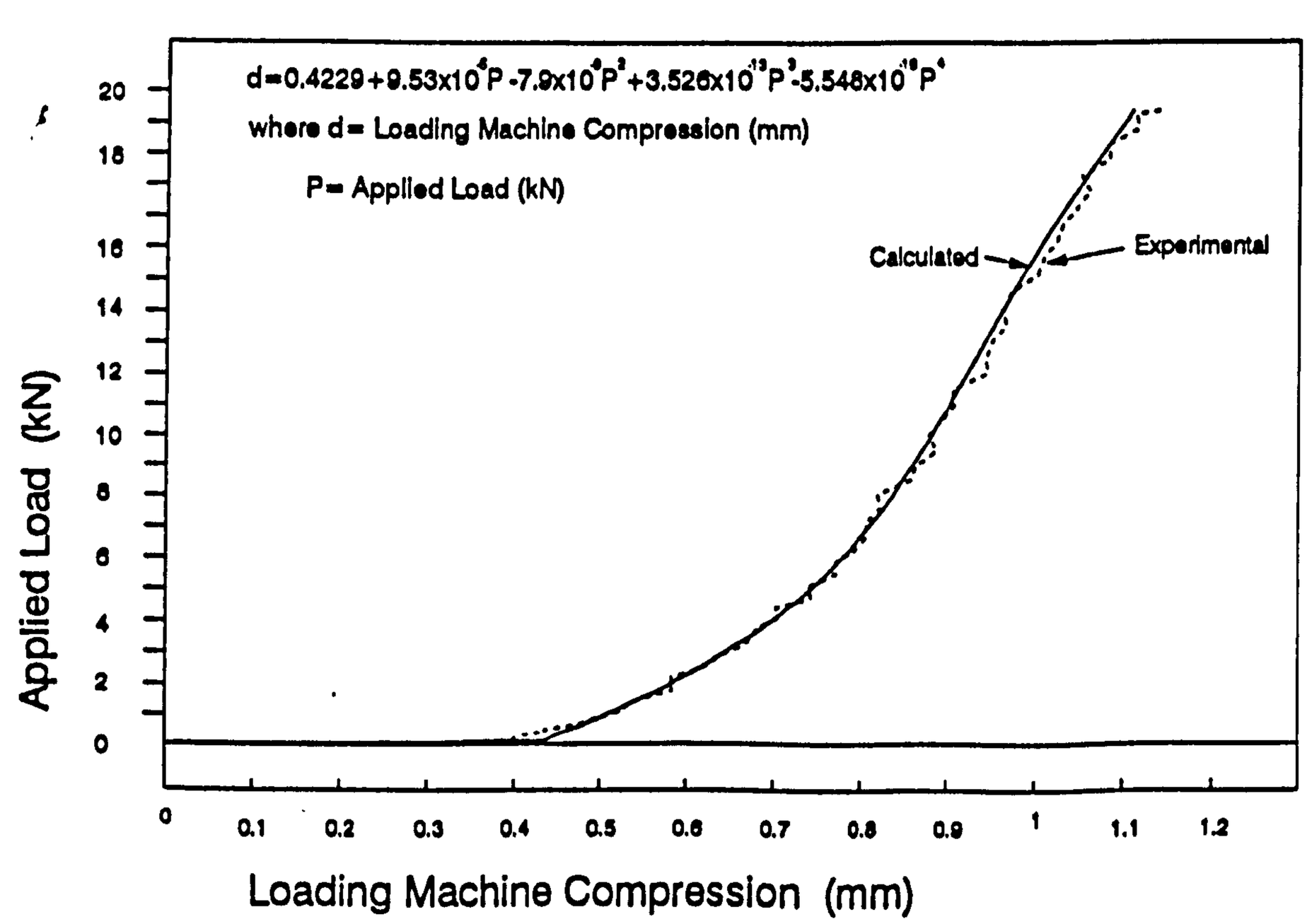

Fig. 5.6- Loading machine calibration graph for the conventional triaxial cell.

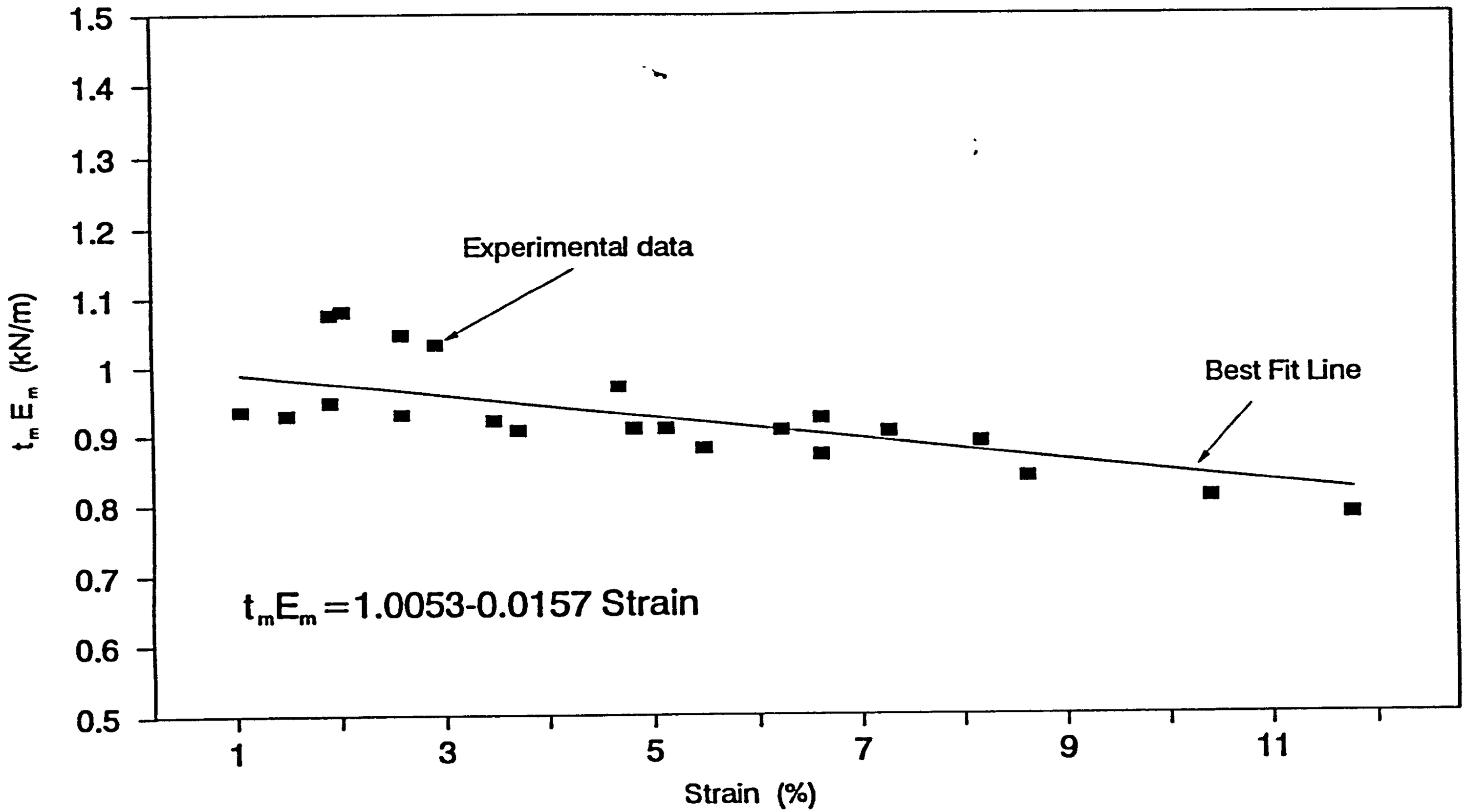

Fig. 5.7- Elastic modulus test on the rubber membrane (E_m and t_m are the elasic modulus and thickness of the membrane)

Chapter 6

Test Material, Test Programme and Test Procedures

6.1 Test Material

The soil used in the current research was Limestone aggregate supplied by North Tyne Roadstone Limited from Mootlaw Quarry, near Matfan, Northumberland. The soil belongs to the Upper Limestone Series of the Upper Carboniferous Period, is known locally as Blue Mountain Limestone and may be described as blue grey in colour, fine grained, with occasional veins of Calcite (Goodwin, 1991). The soil was supplied in bags in three size ranges, <5 mm, 5 mm-10 mm and 10 mm-20 mm, with grading as shown in Fig. 6.1.

Some of the remaining soil, with grain sizes greater than 5 mm, left from a previous research carried out by Goodwin (1991) was used in this research. While a new batch of soil for grain sizes less than 5 mm was brought from the same quarry that Goodwin brought his testing soil. However, Goodwin's soil with grain sizes <5 mm (Batch 1) was compared with the new batch of soil (Batch 2). The difference in grading between the two soils was found to be about 3-4%. Also a specimen of the soil from Batch 2 was analysed chemically and the comparison with Goodwin's Batch 1 is shown in Table 6.1. The Table shows some slight difference between both batches.

Fig. 6.2 shows the two soil gradings, *Fine* and *Coarse*, used in this research. The fine grading complies with the Department of Transport Specifications for Highway Works, 1986, clause 503 (Material for Bedding, Laying and Surrounding of Pipes) or its earlier

version, the Specification for Road and Bridge Work, 1975 (Goodwin, 1991). Table 6.2 shows the soil specifications which was reported by Goodwin (1991).

Most of the tests carried out in the current research concentrated on testing the fine grading soil, with only three tests being carried out on the coarse grading soil, due to time restraints.

6.1.1 Sample Preparation and Grading Tests

The fine grading soil used in this research was the same grading as that dispatched from the quarry as nominally less than 5 mm (Fig. 6.1). Four bags of this as supplied soil were mixed in a concrete mixer pan for 10 minutes, and riffled down to produce eight samples, each weighing about 19 kg. The method used for preparing eight samples of the coarse grading soil, each weighing about 20 kg, was by mixing 70%, 20% and 10%, of the total weight of the eight samples, from each of the three soil grain size ranges, <5 mm, 5 mm-10 mm and 10 mm-20 mm respectively, in a concrete mixing pan for 10 minutes. This mixture was then riffled down to eight samples.

At the beginning of the current research, two of the eight riffled samples from each grading batch were used for wet grading tests in accordance with BS1377 (1990). It was found that they had very similar grading, 2-3% variations. So, it was decided to use only one sample for grading test.

6.1.2 Compaction Tests

Specimens were compacted to different water contents to obtain a graph of dry density against water content. The method used for preparing the samples for the compaction tests was similar to that described in Section 6.1.1. Each sample was mixed with the

required water content and compacted in a mould, similar to that used for compacting a specimen for triaxial test, as will be described in detail in Section 6.3.1. Fig. 6.3 shows the dry density vs. water content curves of two sets of compaction tests on the fine and coarse grading soils. The coarse grading soil shows higher dry densities than the fine grading soil. It should be noted that the soil water content shown in the figure, and that will be used later in the rest of this thesis, is the total water content (i.e. the difference in water content of the soil when it is wet and oven dried at 110°C temperature).

Fig. 6.3 shows that the maximum dry densities for the fine and coarse grading soils are 2.200 Mg/m^3 and 2.305 Mg/m^3 at optimum water contents of 8.25% and 6.15% respectively. The figure also shows that both curves have similar shapes. It may also be seen that two of the tests carried out at water contents beyond the optimum water content, lie above the zero air content curve. This may be due to the flow of water to the bottom of the mould during compaction, which caused the first layer of the specimen to be compacted a higher water content than that of the last layer.

6.2 Test Programme

The test programme for the current research was divided into five series and trial tests, Table 6.3 shows a summary of the test programme and objectives of each test series. The method used to code each test is:

{Soil Grading Type, C or F}{Saturation, U or S}-{Test Series, A, B..or F}{Test No.}

where *C* is the coarse grading soil, *F* is the fine grading soil, *U* is the unsaturated soil and *S* is the saturated soil. For example test *FU-A1* is fine grading unsaturated specimen, series A, test number 1. All tests were conducted at the same water content (4%) to keep the initial dry density, before testing, the same for each soil grading. Also different

compaction water contents can lead to different soil structures (Barden and Sides, 1970), which may affect the interpretation of the results.

Different types of test were used in the current research. Fully drained shearing, consolidated constant water content shearing (no specimen water was allowed to drain and allowing specimen air to drain) and unconsolidated constant water content shearing tests, were used for unsaturated soils. Only fully drained shearing tests were used for the saturated specimens. Fully drained tests can be used to find the soil behaviour at constant values of suction, and finding relationships for the soil Young's modulus, Poisson's ratio, peak strength, specimen volume and water content at different values of suction and confining pressure. This can be very helpful in making a soil model to predict the soil behaviour. The reason for using the other two types of tests, is to compare the results of different types of test to find the effect of stress path on the soil behaviour.

Two triaxial cells were used. The first one was the double-wall triaxial cell, which was used to carry out two types of tests on the unsaturated soil, constant water content tests and drained tests (Section 3.4). The second one was the conventional triaxial cell, which was used to carry out drained tests on the saturated fine grading specimens. In the following subsections, descriptions of the test series will be given.

6.2.1 Trial Tests

At the start of the test programme, trial tests were carried out to help determine the test programme and to refine some of the techniques to be used in the current research. The purposes and conclusions of the trial tests were as follows:

1. Fine and coarse grading specimens were tested using a load ring instead of a load cell to find which load cell capacity would be suitable for testing these specimens. It was

found that using a 25 kN load cell gave a large enough load range and had the required sensitivity.

2. Due to the time available for this research, it was decided to concentrate on testing the fine grading soil at suctions up to 75 kPa, i.e. using a 1 bar high air entry ceramic stone (Section 4.2.1F). Tests were carried out at different specimen water contents to find a suitable initial water content that has a suction below 100 kPa. On the basis of these tests it was decided to use 4% as the initial water content.

3. Tests were carried out to establish a technique which would adequately seal the ceramic stone into its metal ring (Section 4.2.1F) as will be described in Section 6.3.2.

4. Tests were carried out to establish whether or not it was necessary to use pins to fix the perspex curves (Figs. 4.4 and 4.5) that hold the axial LVDTs for the internal axial strain measurements in position on the specimen. This technique was found to be unsuitable as the pins were unstable and were pulled by the specimen membrane during specimen compression, and this affected the internal axial strain measurements.

5. Specimens were sheared at fast rates of shearing (0.0035 mm/min and 1 mm/min), until the critical state was reached. It was found that the critical state started at internal axial strain above 6%. Due to the very slow rate of strain that was adopted in this research (0.00011 %/min) and also this research is to investigate the stiffness and soil behaviour at failure, it was decided to stop the shearing process one to two days after the failure stress was reached, i.e. the critical state for the tested specimens was not reached.

6. The pore water pressure parameter, B, (change in pore water pressure due to the change in cell pressure), of a saturated specimen, was checked against time for 10 days, to find its maximum value under 540 kPa back pressure. It was found that this value became constant with a value of about 0.94 some 3 to 4 days after starting the saturation stage of a test.

6.2.2 Test Series A

In this series, only fine grading soil specimens were tested. The main purpose of this series was to investigate the behaviour of unsaturated granular soil at low stress levels at different values of net cell pressure, $(\sigma_3 - u_a)$, and suction. In addition the results were examined to see whether Fredlund's equation (Equation 2.3), which suggests that the failure envelope (Fig. 2.10) for unsaturated soil is planar, could be applied to unsaturated granular soil at low stress levels.

All specimens had the same nominal initial conditions, as all specimens were compacted at the same water content and to the same dry density. Drained tests were carried out on these specimens by keeping the suction and cell pressure constants. The specimens were sheared at rate of strain 0.00011%/min, at three different suctions (25, 50 and 75 kPa) and different net cell pressures, $(\sigma_3 - u_a)$, as shown in Table 6.4.

After the specimen was set up in the double-wall triaxial cell, as will be described in Section 6.3.3, it was left under low net cell pressure, $(\sigma_3 - u_a)$= 10 kPa, to allow the applied suction to equalise throughout the specimen. Three values of suction were chosen, 25 kPa, 50 kPa and 75 kPa. Suctions up to 75 kPa were shown by Goodwin (1991), who carried out one-dimensional tests on unsaturated granular soil as that used in this research, to be realistic. During this stage (*Equalisation Stage*) the pore water and air pressure were set at constant values to give the suction at which the specimen was to be sheared, and the changes in the specimen water content were monitored. When there was no more specimen water content change, the cell pressure was increased to the pressure that the specimen was to be sheared to start the *Consolidation Stage*. During this stage the specimen water content change was monitored, when there was no more change the specimen was sheared

Due to the long time that these tests took, the equalisation and consolidation stages were combined for some tests to reduce the total test period from about 25 days to about 15 days. This will be discussed in more detail in Section 8.6. Table 6.4 shows the tests in which this combination was carried out.

6.2.3 Test Series B

The objectives of this series were firstly to examine the effect of combining the equalisation and consolidation stages on the subsequent behaviour of the soil. A second objective was to compare the results of this series (constant water content test) with those of series A (drained test) at the same rate of strain, to see how the results of both series corresponded.

Two unsaturated fine grading soil specimens were sheared at same initial suction and net cell pressure, $(\sigma_3 - u_a)$, as shown in Table 6.5, using the double-wall triaxial cell. The equalisation and consolidation stages were combined only for test FU-B1. Before shearing, the suction of the soil was brought to 25 kPa, for both specimens, by allowing the specimen water content to change to reach the required suction (drain test). When the required suction was achieved, no more specimen water content change was allowed (i.e. sheared at constant water content) and the specimens were sheared at a rate similar to that used in series A.

6.2.4 Test Series C

The aim of this series was to study the effect of the rate of strain on shearing behaviour by comparing the results of this series with those of series A and B. Two constant water content tests were carried out on the unsaturated fine grading soil specimens, as shown in Table 6.6, using the double-wall triaxial cell. The equalisation and consolidation stages were not combined for these tests, and the initial water content (after compaction) was not

allowed to change during the whole tests. Both tests were sheared at rate of strain 0.00093%/min, which was about nine times faster than that used for series A and B.

6.2.5 Test Series D

The aims of this series were to compare initial suction and behaviour of the coarse grading soil with those of fine grading soil (series D). Three constant water content tests were carried out on unsaturated coarse grading soil (Table 6.7) using the double-wall triaxial cell. A similar testing procedure and rate of strain was used to that used for series C.

6.2.6 Test Series E

The objectives of this series were to compare the behaviour of saturated and unsaturated soils at low stress levels, and to find whether Fredlund's equation (Equation 2.3) could be extended to the saturated soils, as was suggested by Fredlund et al. (1978), i.e. to find whether the values of c' and ϕ' for saturated specimens, can be used in Equation 2.3 to predict the shear strength of unsaturated granular soils at low stress levels. Drained tests were carried out on saturated fine grading specimens (Table 6.8), using the conventional triaxial cell. The initial conditions of these specimens (after compaction) were similar to those of series A to C. The specimens were saturated at low effective cell pressure (10 kPa), followed by the consolidated stage, and then sheared at a rate of strain similar to that used in series A.

6.3 Test Procedure

In this Section the test procedures used for setting up and testing the unsaturated and saturated specimens, using the double-wall and conventional triaxial cells respectively, will

be given. Before detailing the test procedures, the methods used to compact the specimens (which was same for the unsaturated and saturated specimens) and to seal and saturate the high air entry ceramic stone (Section 4.2.1F) will be described.

6.3.1 Mould Design and Specimen Compaction

The design of the mould was made to suit the double-wall triaxial cell. The mould was designed in such way that the specimen was compacted inside the mould on a solid base and then transferred to the base pedestal fitted with the ceramic stone by sliding, as will be described in the following paragraphs. This avoided the risk of breaking the ceramic stone.

Fig. 6.4 and Plate 6.1 show the mould and its base. The mould is made from aluminium tube, which is cut along its height into three pieces which can be assembled and tightened at their edges. These pieces are split apart after placing the compacted specimen on the base pedestal. A collar is fitted onto the mould top, to allow compaction of the soil higher than the mould height (specimen height). Then the specimen is trimmed to the right height when the collar is removed. Holes have been drilled through the mould wall at different heights so that plastic tubes can be connected to a vacuum pump which draws the rubber membrane against the mould's wall during compaction. This prevents the membrane trapping beneath the compaction hammer. The mould is tightened by three tie-bars (Fig. 6.4), onto one end of its base, which is made from steel. The other end of the mould base is machined as shown in Fig. 6.4, which can be placed around the base pedestal of the triaxial cell as shown in Plate 6.2, so that when the mould base is in level with the base pedestal, the mould (with the specimen inside) may be slid across its base to the pedestal. This prevents soil particles falling from the specimen and this in turn gives good contact between the specimen bottom and the ceramic stone. More details about the testing procedure will be given in Section 6.3.3. A stopper plate is fixed at the end of the mould base (Fig. 6.4) to make sure that the specimen is stopped when it is centred on the base pedestal.

The sample to be compacted was first oven dried at 110°C temperature for one day, and then weighed. Water, 4% of the dry weight of the sample, was properly mixed with the sample, in a large metal tray. The sample then double bagged, to prevent moisture loss, and stored for one day before compaction to allow moisture to be distributed evenly within the sample.

The mould with its collar were assembled and tightened together. Before placing the mould on its base, a filter paper was inserted around its inner wall face, then one membrane was inserted inside the mould, so that the filter paper was between the mould's wall and the membrane, and sealed by two O-rings at each end of the mould. The reason for inserting the filter paper was to distribute the vacuum pressure that was used during compaction equally along the membrane. The mould then was tightened to its base by the three tie-bars, weighed and connected to the vacuum line to draw the membrane against the mould wall to prevent it being trapped beneath the compaction hammer.

The sample was emptied on a large tray and re-mixed thoroughly. The soil was then compacted in 11 layers using a Kango hammer (Plate 6.3). Each layer was weighed before compaction (1.4 kg each) and compacted for 10 seconds (Plate 6.4) The Kango hammer was held by hand during compaction, with a small force applied to it to keep the hammer vertical. This method was found to give close dry densities, as will be discussed in Section 8.3. At the end of compaction the vacuum line was disconnected, the collar removed and the specimen trimmed to the mould's height. The top face of the specimen, which was still in the mould, was flattened by a light compaction. The mould was weighed to determine the mass of the specimen. Some of the soil (about 2 kg mass) was taken from the tray, and weighed, oven dried and then weighed again, to determine the water content of the specimen.

6.3.2 Ceramic Stone Sealing and Saturation

In the early stages of the project a number of different methods were used to seal the high air entry ceramic stone to its metal ring (Section 4.2.1F) using Araldite epoxy resin glue. Each method was checked after saturating the stone and before specimen testing to check for air leaks through the sealant. This check showed no air leakage for some of the method used to seal the ceramic stone, but the air leakage was developed during specimen testing, and some of the trial tests were lost for this reason.

Although the glue, when it set, was very strong, it was found that when applying the glue to both surfaces (the metal ring and ceramic stone), very fine pores left in the glue opened after the glue was set. These fine pores could not be eliminated even when the glue was applied carefully to both surfaces.

The best method that was found to give good sealing between the ceramic stone and metal ring, which seemed to eliminate all fine pores in the glue, was to place a 4 kg mass on the ceramic stone and its metal ring after applying the glue to their surfaces, then placing them in the oven for one day under 110°C temperature. The reason why this method was found to be successful may be due to the fact that the heat reduced the glue viscosity, which allowed the glue to flow into the fine pores and seal them.

The method used to saturate the ceramic stone after it was sealed to its metal ring, was to tighten the ring by screws to the base of the modified Rowe cell (Plate 6.5). Normal Rowe cell convoluted membrane was removed and the cell filled with de-aired water and connected to the flushing storage tank, as shown in the middle right of Fig. 4.8, for supplying pressure.

A new dry ceramic stone was left in the Rowe cell under 240 kPa pressure for two days. Some of the water was then allowed to drain slowly from the cell base through the ceramic stone for 15 minutes, and then stopped and left one more day under the same pressure. The water of the Rowe cell and flushing storage tank were replaced with fresh de-aired water and left under the same pressure for at least one more day before the ceramic stone was ready to be used in a triaxial test. To re-saturate a ceramic stone already used from a previous triaxial test, the stone was left under 240 kPa pressure in the modified Rowe cell for at least two days before it was used again for a triaxial test.

The ceramic stone was checked, after saturation and while it was fixed in the Rowe cell, to detect any air leaks. An air pressure line , with air pressure of 90 kPa, was connected to the base of the cell, and water was placed on the top of the ceramic stone. The air leakage was detected by observing any air bubbles coming out from the ceramic stone.

Two metal rings with ceramic stones were made, one to be used in the triaxial test after it was saturated, and the other one was left in the Rowe cell under pressure to be saturated and used for the following triaxial test.

6.3.3 Test Procedure for Unsaturated Specimens

Unsaturated specimens were tested in the new double-wall triaxial cell (Fig. 4.1). The perspex cylinders were always kept saturated in a water filled tank. Due to the large amount of water used to fill the triaxial cell (60 litres) which took five hours to be de-aired, the water was de-ionised and de-aired and kept less than one day in its two storage tanks (Section 4.3.1) under vacuum to keep it de-aired. The de-ionisation of water was to prevent the growth of algae during a test, which may affect the volume change measurements of the inner cell water. The bottom plate, base pedestal, inner top plate,

piston bushing and piston with load cell fixed at its end (Fig. 4.1), were placed on the loading machine. These components were not removed before and after specimen setting up and testing. All O-rings and their grooves were cleaned and smeared with silicone grease to prevent water leakage.

The piston was clamped from the top face of the inner top plate to prevent it falling downward. Before placing the ceramic stone on the base pedestal, the spiral groove, on the top face of the base pedestal (Plate 4.2), was flushed with de-aired water from the flushing storage tank (Section 4.3.1 and Fig. 4.8) to fill the groove.

A coarse metal porous disc was placed on the specimen while the specimen was in the mould, and the top cap was placed on the porous stone. Its side was greased with silicone grease to prevent water leakage between the top cap and the rubber membrane. The rubber membrane was rolled off the top of the mould and onto the top cap. A wooden block was placed on the bottom plate, as shown in Plate 6.6. The mould with its base and specimen (Fig. 6.4) was placed on the top of the wooden block, as shown in Plate 6.7, and the stopper plate (Fig. 6.4) was fixed at its base end, as shown in Plate 6.2. The height of the wooden block was made so that when the mould is placed on it, the top face of the mould base was level with the ceramic stone (Plate 6.2).

The computer program (Section 4.4.1) was run to monitor the specimen suction during setting up. The mould tie-bars (Fig. 6.4) were removed and the mould was pushed across its base to the ceramic stone until it was stopped by the stopper plate indicating that the specimen was centred on the ceramic stone, as shown in Plate 6.8. The mould base and stopper plate were then removed, as shown in Plate 6.9, and the side of the base pedestal was greased with silicone grease, to prevent water leakage between base pedestal and

rubber membrane. The rubber membrane was unrolled from the bottom of the mould and placed around the base pedestal and mould was then split apart and removed.

The rubber membrane was coated with silicone grease, to reduce water leakage, and a second rubber membrane was placed around it, to seal any holes in the first rubber membrane which may have developed during compaction. The technique used to placed the second membrane was to fold the membrane around a 50 mm wide and 156 mm diameter metal ring (Plate 6.10). The ring was placed around the base pedestal and one end of the membrane was held against the base pedestal while lifting the ring upward, as shown in Plate 6.11, until the top cap was reached. Two O-rings were placed around both the base pedestal and top cap to seal the two membranes.

The membrane was then marked for placing the axial strain LVDT perspex holder curves (Section 4.2.2 and Figs. 4.4 and 4.5). The axial LVDT holders and targets were placed around the specimen and glued to the membrane using super glue. The air line was connected to the top cap and the piston was lowered and brought into contact with top cap at its centre, as shown in Plate 6.12. The lower parts of the perspex cylinders and the middle ring (Section 4.2.1 and Fig. 4.1) were placed on the bottom plate. The lateral strain LVDTs (Fig. 4.3) were filled with de-aired water using a syringe, and then placed and tightened in their holes in the middle ring, and their targets were glued to the membrane. The glue was only applied to target centres. De-aired water was allowed to flow from the storage tanks to fill the inner cell up to the top edge of the middle ring. It was found that placing a thin layer of silicone grease in the perspex grooves, on the bottom plate, before placing the lower part of the perspex cylinders, could stop water leakage at this stage.

The axial LVDTs were de-aired and hung freely by their springs to their hangers (Fig. 4.4) and tightened in position as shown in Plate 6.13. Their verticality was checked by two

methods, first by eye with that of the tie-bars in more than one direction. The second method was to line them with an L-shaped ruler. It should be noted that part of each vertical LVDT was left immersed in the water to keep them de-aired while carrying out the rest of the setting up procedure.

The upper two perspex cylinders, outer tie-bars and outer top plate (Fig. 4.1) were placed in position and the outer tie-bars were then tightened. De-aired water was then run in to fill the inner and outer cells simultaneously. When the water level reached the top plate, the top ring (Fig 4.1) was placed and clamped to the top plate. The cross beam of the loading machine was placed in position and the external LVDT was fixed to the cross beam and its verticality was checked. The triaxial cell was raised on the loading machine platen to bring the piston into contact with the cross beam.

At this stage the specimen setting up was finished and the specimen equalisation stage was started by running the equalisation computer program (Section 4.4.1). For constant water content tests (Section 6.2.3) the pore air and cell pressures were gradually increased to 60 kPa and 70 kPa respectively, by keeping a net cell pressure, $(\sigma_3 - u_a)$, equal to 10 kPa, i.e. the pore water pressure was not controlled but was measured by the pore water pressure transducer (Section 4.3.1). The specimen water content was not allowed to change. For drained tests (Section 6.2.2), the pore air, pore water and cell pressures were gradually increased by keeping the net cell pressure, $(\sigma_3 - u_a)$, equal to 10 kPa and the suction, $(u_a - u_w)$, equal to the required suction that the specimen was to be sheared at. The pore air and cell pressures were increased to 90 kPa and 100 kPa respectively. The specimen water content was allowed to change, and this was measured using the 100 cc volume change unit (Section 4.3.1), to bring the soil to the required suction.

When the change in suction (constant water content test) or specimen water content (drained test) was less than 1 kPa or 0.05 cc respectively in 12 hours, the equalisation stage was stopped to start consolidating the specimen. The consolidation stage was started by running the consolidation computer program (Section 4.4.1), and then increasing the cell pressure to the require net cell pressure, $(\sigma_3 - u_a)$, that the specimen was to be sheared at. When the change in suction (constant water content test) or specimen water content (drained test) was as that at the end of the equalisation stage, the consolidation stage was stopped to start shearing the specimen. Both stages were combined into one stage for some of the drained tests (Section 6.2.2). Using this combined stage technique the pore air, pore water and cell pressures were increased after specimen setting up to that at which the specimen was to be sheared. When the change in specimen water content was less than 0.05 cc in 12 hours, this stage was stopped to start shearing the specimen.

The shearing stage was started by running the shear computer program (Section 4.4.1) and setting the loading machine at the required rate of strain. Two different rates of strain were used, 0.00011 %/min, for tests series A and B, and 0.00093 %/min, for tests series C and D. The choice of these rates of strain will be discussed in Section 8.4. The shearing stage was stopped one to two days after the specimen failure, i.e. the critical state for the soil was not reached (Section 6.2.1).

At the end of the test, the triaxial cell was dismantled and the specimen was cut horizontally into six parts. Because of the drying at the ends of the specimen, the 10 mm at each end of the specimen was cut off and discarded. The remaining of the specimen was divided horizontally into four approximately equal portions, and the water content of each portion was determined. This helps in finding the water content distribution along the specimen at the end of the test.

6.3.4 Test Procedure for Saturated Specimens

The base pedestal of the conventional triaxial cell was flushed with de-aired water. A metal coarse porous disc, which was de-aired by boiling it in a water tank for 30 minutes, was placed on the base pedestal. O-rings and their grooves were cleaned and smeared with silicone grease to prevent water leakage.

After specimen compaction, the mould's tie-bars (Fig. 6.4) were removed and the mould (with specimen) was removed from the its base and placed on the pedestal. It may be noted that the mould was not slid across its base to the pedestal as was done in the double-wall triaxial cell for the unsaturated specimen (Section 6.3.3). The reason for this was some soil particles may fall off the bottom of the specimen when the mould (with specimen) was removed from its base. This may leave an uneven surface at the bottom of the specimen, which may affect the suction measurements of the unsaturated specimen, because the contact area between the soil and the high air entry ceramic stone would be less than if the specimen bottom was flat. So, the unsaturated specimen was slid to make sure that its bottom surface was flat. However, this was not as important with the saturated specimen because the specimen was saturated with de-aired water to fill all of the voids.

After placing the mould on the pedestal, a second metal coarse porous disc was placed on the top of the specimen and the top cap was placed in position. The sides of the base pedestal and top cap were smeared with silicone grease, and both membrane ends were unrolled from the mould's ends and placed around the base pedestal and top cap. The mould was split apart and the membrane was coated with silicone grease to prevent water leakage. A second membrane was placed around the specimen using a similar technique as

that used for the unsaturated specimen (Section 6.3.3). Two O-rings were then placed at each end of the specimen to seal the membrane.

The air drainage line (Fig 4.9), which was used to drain the specimen air to the outside during specimen flushing, was connected to the top cap, and the triaxial cell body was placed on the bottom plate, and tightened by tie-bars. The LVDT was fixed to the cross beam of the loading machine, and the piston was brought into contact with the cross beam and top cap. The cell was then filled with tap water.

Before starting flushing the specimen with de-aired water to saturate it a file in the logging system was opened to take readings from the pore water pressure transducer and volume change unit (Table 5.2). A burette was connected to the other end of the air drainage line (Fig. 4.9) to measure the volume of water entering this line at the end of the flushing stage. This could be subtracted from the volume of the flushing water going into the specimen measured by the volume change unit and the change of specimen water content determined.

The cell pressure and pore water pressure were increased to 20 kPa and 15 kPa respectively and water allowed to enter the specimen from its bottom to flush it. Specimen air was drained through the air drainage line from the top of the specimen. When water started to flow through the air drainage line with no air bubbles this indicated the end of flushing and the air drainage line was closed.

A second file was set in the logging system to record the specimen pore water pressure and the volume of water that has entered the specimen during saturation. The cell and pore water pressure were gradually increased to 550 kPa and 540 kPa respectively to force any remaining air bubbles in the specimen to dissolve into the pore water. When the

pore pressure parameter, B, was found equal to 0.94, which was the maximum value that can be obtained with this pressure (Section 6.2.1), the specimen saturation stage was stopped.

A third file was opened in the logging system to record the change in the specimen volume and pore water pressure during consolidation stage. The cell pressure was increased to the value that the specimen was to be sheared at. When the change in specimen volume was less than 0.5 cc in 12 hours, the consolidation stage was stopped and a fourth file was opened to record the changes in the specimen volume, pore water pressure, deviator stress and external axial strain during the shearing stage. The loading machine was set at rate of strain 0.00011%/min, which was similar to that used for the drained test on the unsaturated specimens (series A). The shearing stage was stopped one to two days after the specimen failure.

Chemical	Percentage of Total, by Mass	
	Batch 1 (Goodwin, 1991)	Batch 2
$CaCO_3$	79.97	78.57
$MgCO_3$	11.50	8.67
SiO_2	2.80	5.99
$CaSO_4$	2.28	1.92
FeO_3	2.03	1.73
Al_2O_3	1.00	2.43
K_2O	0.12	0.31
MnO	0.06	0.05
P_2O_5	0.05	0.06
TiO_2	0.03	0.08
Na_2O	<0.10	<0.12
Total	99.84 exc. Na_2O	99.81 exc. Na_2O

Table 6.1- Results of the chemical analysis on Batch 1 and Batch 2 of the quarried limestone.

Strength	Aggregate crushing value =22 Aggregate impact value =18
Grain shape	Angular to sub-angular
Specific gravity	2.71

Table 6.2- Soil specification (Goodwin, 1991)

Series No.	Soil Type	Shear Test Type	Strain Rate %/min	Testing Objectives
A	F (U)	D	0.00011	(1)To investigate the triaxial behaviour of unsaturated granular at different values of cell pressure and suction, at low stress levels (<100 kPa). (2)To investigate the validity of Fredlund's equation (Equation 2.3) for unsaturated granular soil, at low stress levels.
B	F (U)	CWC	0.00011	(1)To examine the effect of combining the equalisation and consolidation stages on the subsequent soil behaviour. (2)To compare the results of different types of testing.
C	F (U)	CWC	0.00093	To examine the effect of rate of strain on the soil behaviour during shearing.
D	C (U)	CWC	0.00093	To compare the behaviour of the fine grading soil with that of coarse grading soil at low stress levels.
E	F (S)	D	0.00011	(1)To investigate the behaviour of saturated granular soil at low stress levels. (2)To compare the behaviour of saturated soil with that of unsaturated soil at low stress levels. (3)To check whether the values of c' and ϕ' for saturated soils can be used in Fredlund's equation to predict the shear strength of the unsaturated soil at low stress levels.

D = drained Test, CWC = Constant Water Content Test, F = Fine Grading Soil, C = Coarse grading Soil, U = Unsaturated Soil, S = Saturated Soil.

Table 6.3- Summary of the test programme and objectives.

Test No.	Initial Water Content %	Initial Degree of Saturation %	Initial Dry Density Mg/m^3	Applied Suction (u_a-u_w) kPa	Shearing net cell pressure (σ_3-u_a) kPa	Whether or not the E and C stages were combined
FU-A1	3.94	26.1	1.923	75	36.8	Yes
FU-A2	3.90	26.4	1.935	75	62.9	Yes
FU-A3	4.00	28.7	1.968	75	78.4	No
FU-A4	4.06	29.5	1.974	75	91.3	Yes
FU-A5	3.97	28.7	1.972	75	91.6	Yes
FU-A6	3.96	28.9	1.976	50	31.7	Yes
FU-A7	3.97	28.9	1.976	50	57.7	Yes
FU-A8	3.78	27.2	1.960	50	81.2	Yes
FU-A9	3.93	27.8	1.960	50	115.1	Yes
FU-A10	4.09	28.4	1.949	25	35.8	Yes
FU-A11	4.05	28.6	1.959	25	61.4	Yes
FU-A12	3.98	27.5	1.947	25	80.3	No
FU-A13	3.85	28.5	1.984	25	92.6	Yes
FU-A14	3.91	28.3	1.972	25	114.2	Yes

E and C stages are the Equalisation and Consolidation stages

Table 6.4- Initial conditions of the specimens of drained test series A.

Test No.	Initial Water Content %	Initial Degree of Saturation %	Initial Dry Density Mg/m^3	Applied Suction before shearing stage (u_a-u_w) kPa	Shearing net cell pressure (σ_3-u_a) kPa	Whether or not the E and C stages were combined
FU-B1	4.10	28.6	1.972	25	93.6	Yes
FU-B2	3.99	26.8	1.952	25	93.9	No

E and C stages are the Equalisation and Consolidation stages

Table 6.5- The initial conditions of the unsaturated fine grading specimens of test series B, which were sheared at constant water content.

Test No.	Initial Water Content %	Initial Degree of Saturation %	Initial Dry Density Mg/m^3	Shearing net cell pressure (σ_3-u_a) kPa	Whether or not the E and C stages were combined
FU-C1	3.93	27.7	1.958	64.9	No
FU-C2	3.89	32.5	2.047	84.6	No

E and C stages are the Equalisation and Consolidation stages

Table 6.6- The initial conditions of the unsaturated fine grading specimens of test series C, which were sheared at constant water content.

Test No.	Initial Water Content %	Initial Degree of Saturation %	Initial Dry Density Mg/m^3	Shearing net cell pressure (σ_3-u_a) kPa	Whether or not the E and C stages were combined
CU-D1	3.89	37.2	2.111	40.8	No
CU-D2	3.79	39.5	2.131	64.2	No
CU-D3	3.96	36.8	2.118	87.8	No

E and C stages are the Equalisation and Consolidation stages

Table 6.7- The initial conditions of the unsaturated coarse grading specimens of test series D, which were sheared at constant water content.

Test No.	Initial Water Content %	Initial Degree of Saturation %	Initial Dry Density Mg/m^3	Shearing effective cell pressure (σ_3-u_w) kPa
FS-E1	4.00	27.2	1.937	25.7
FS-E2	3.91	27.3	1.952	50.7
FS-E3	3.80	26.2	1.946	75.7
FS-E4	3.95	26.9	1.939	100.7
FS-E3	4.06	28.5	1.956	125.7

Table 6.8- The initial conditions of the saturated fine grading specimens of drained test series E.

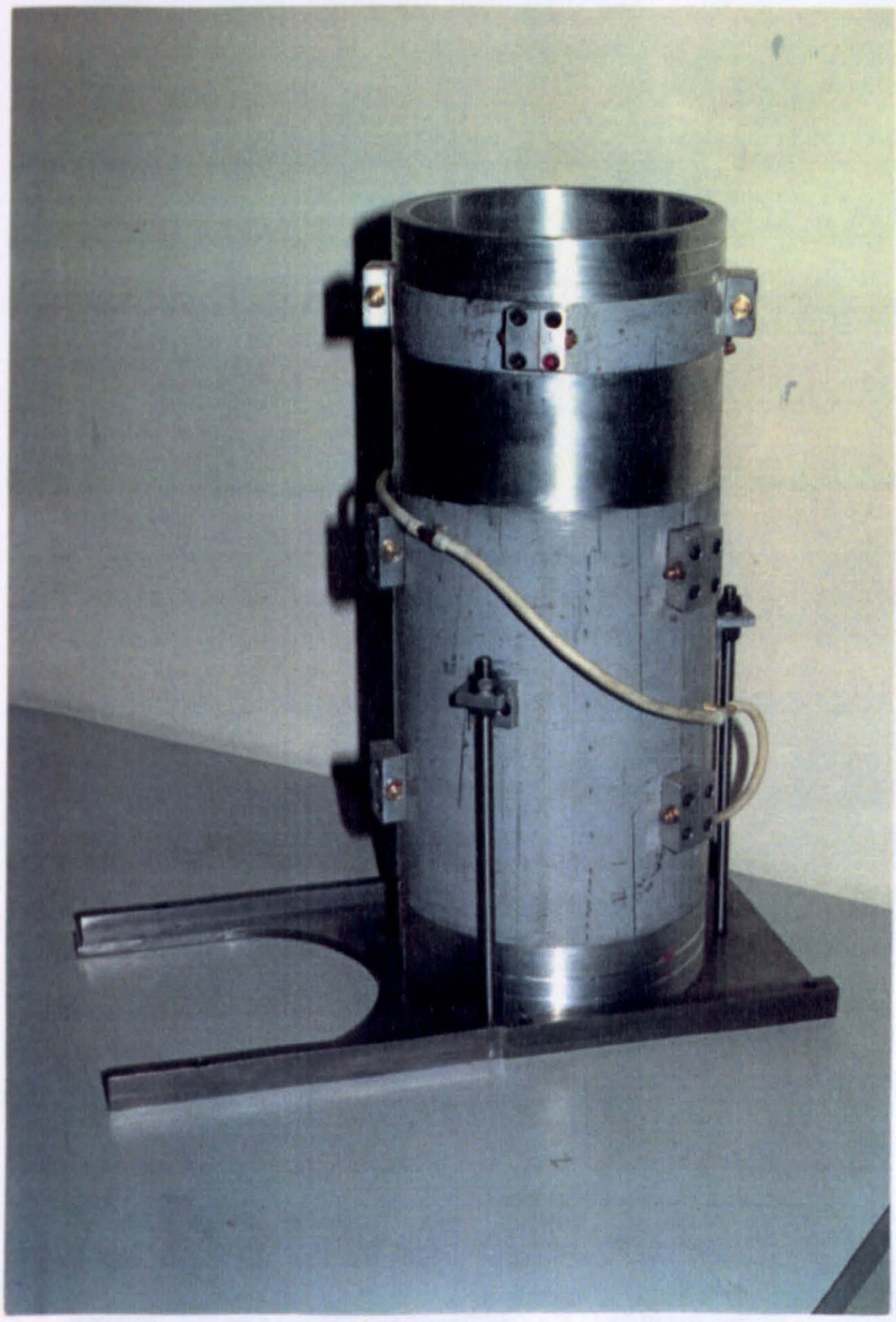

Plate 6.1 (Left)- Specimen Compaction Mould

Plate 6.2 (Bottom)- Mould base is placed around the base pedestal

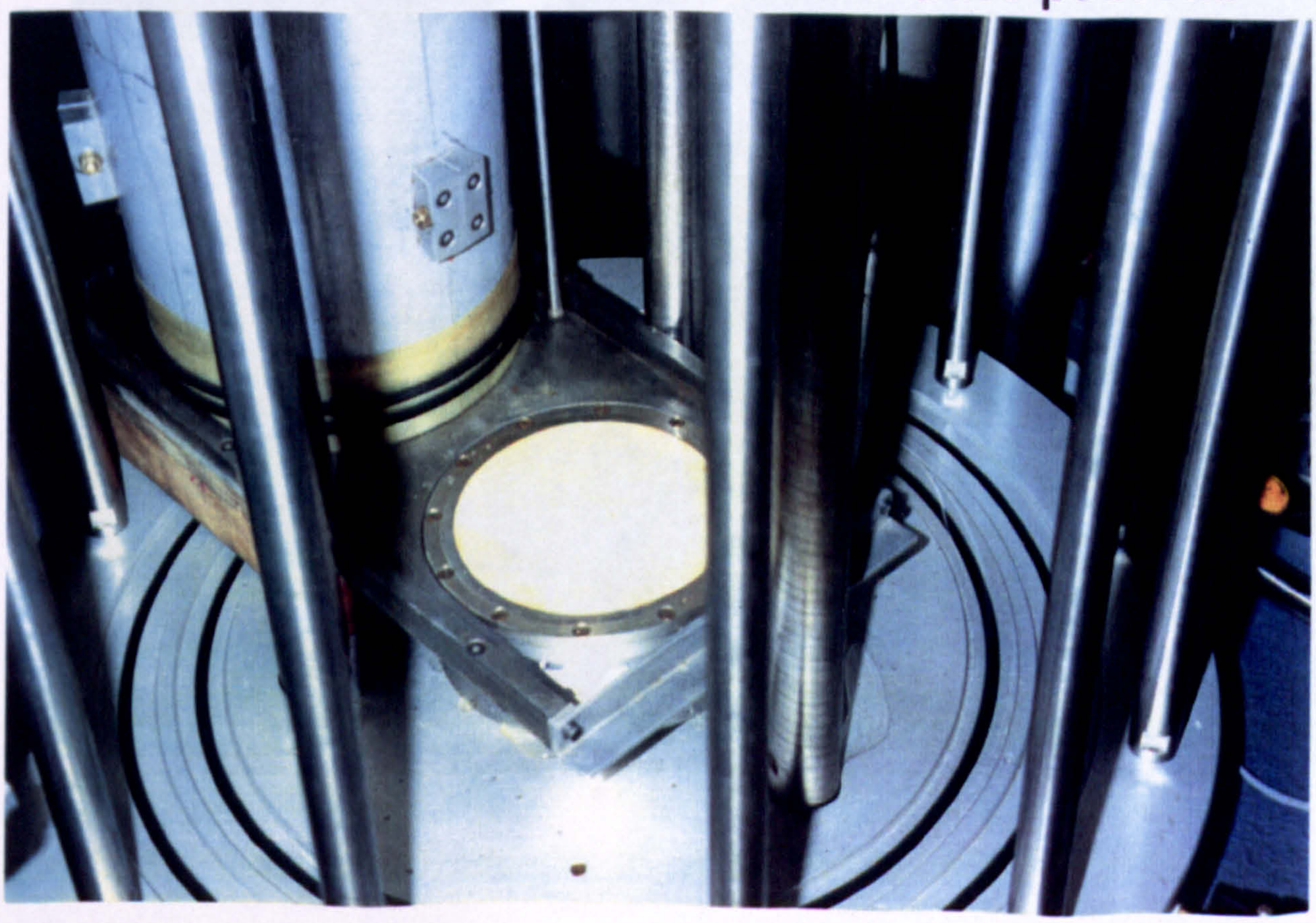

Plate 6.3- Kango compaction hammer, mould and vacuum pump

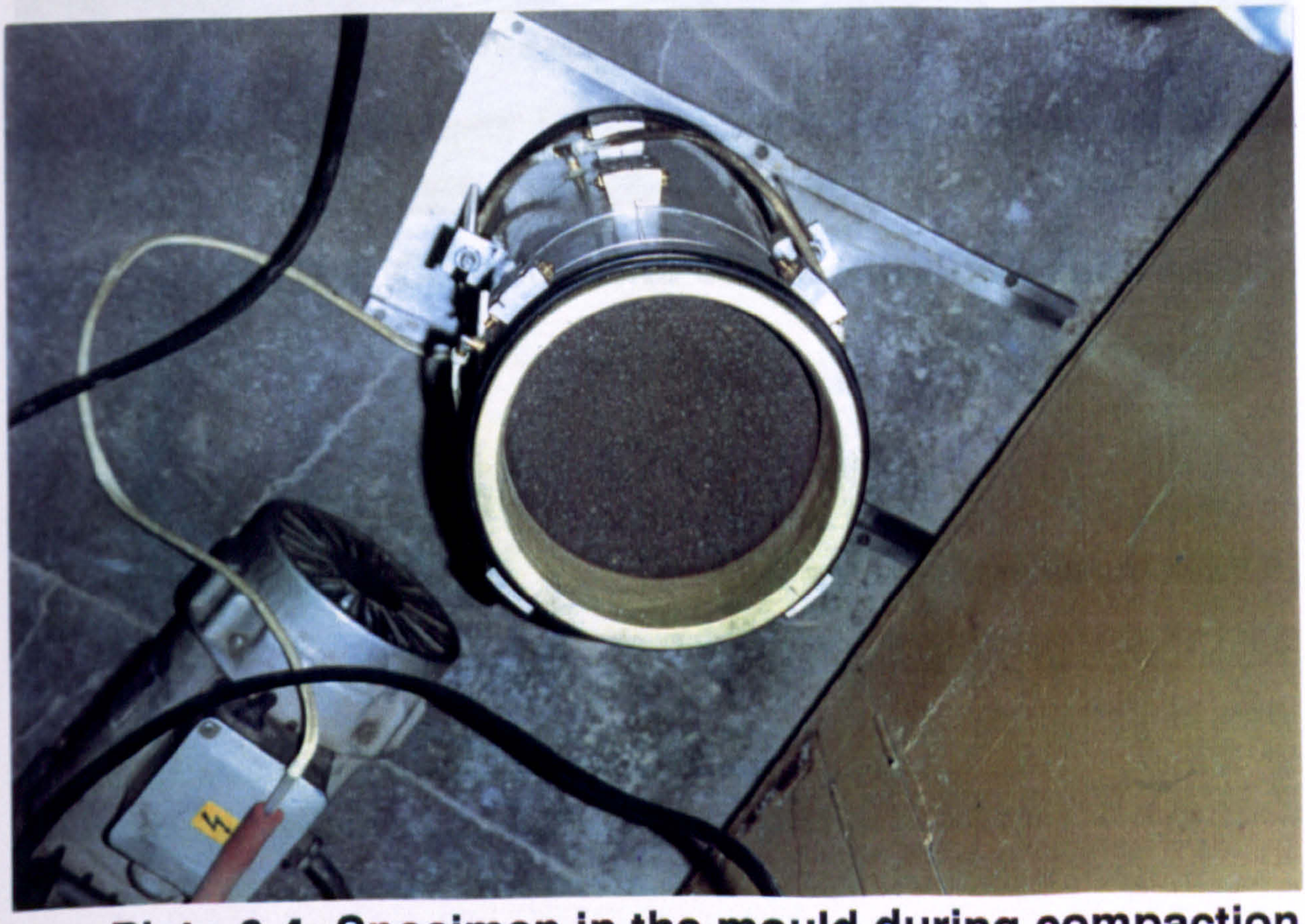

Plate 6.4- Specimen in the mould during compaction

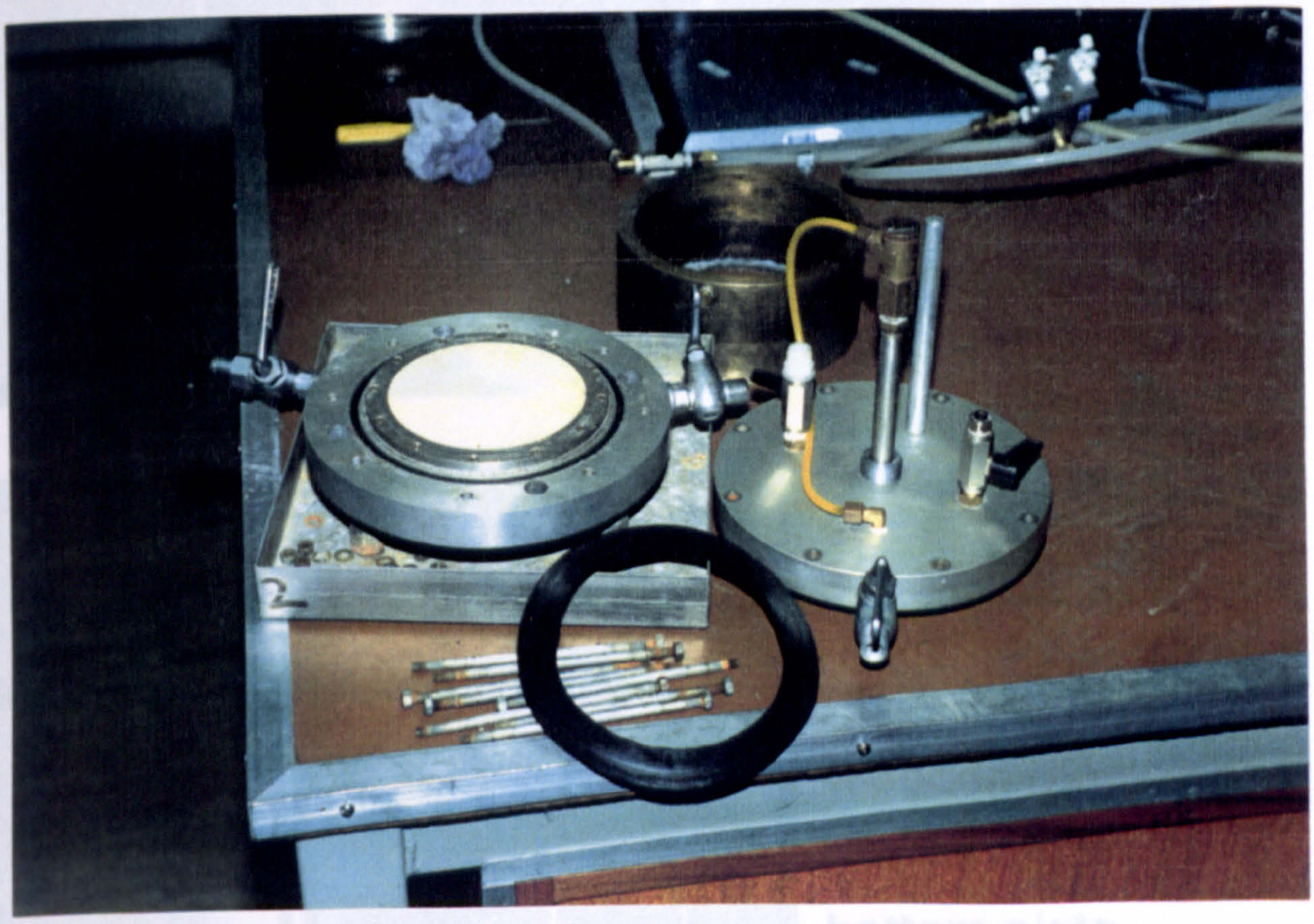

Plate 6.5- Components of the modified Rowe cell

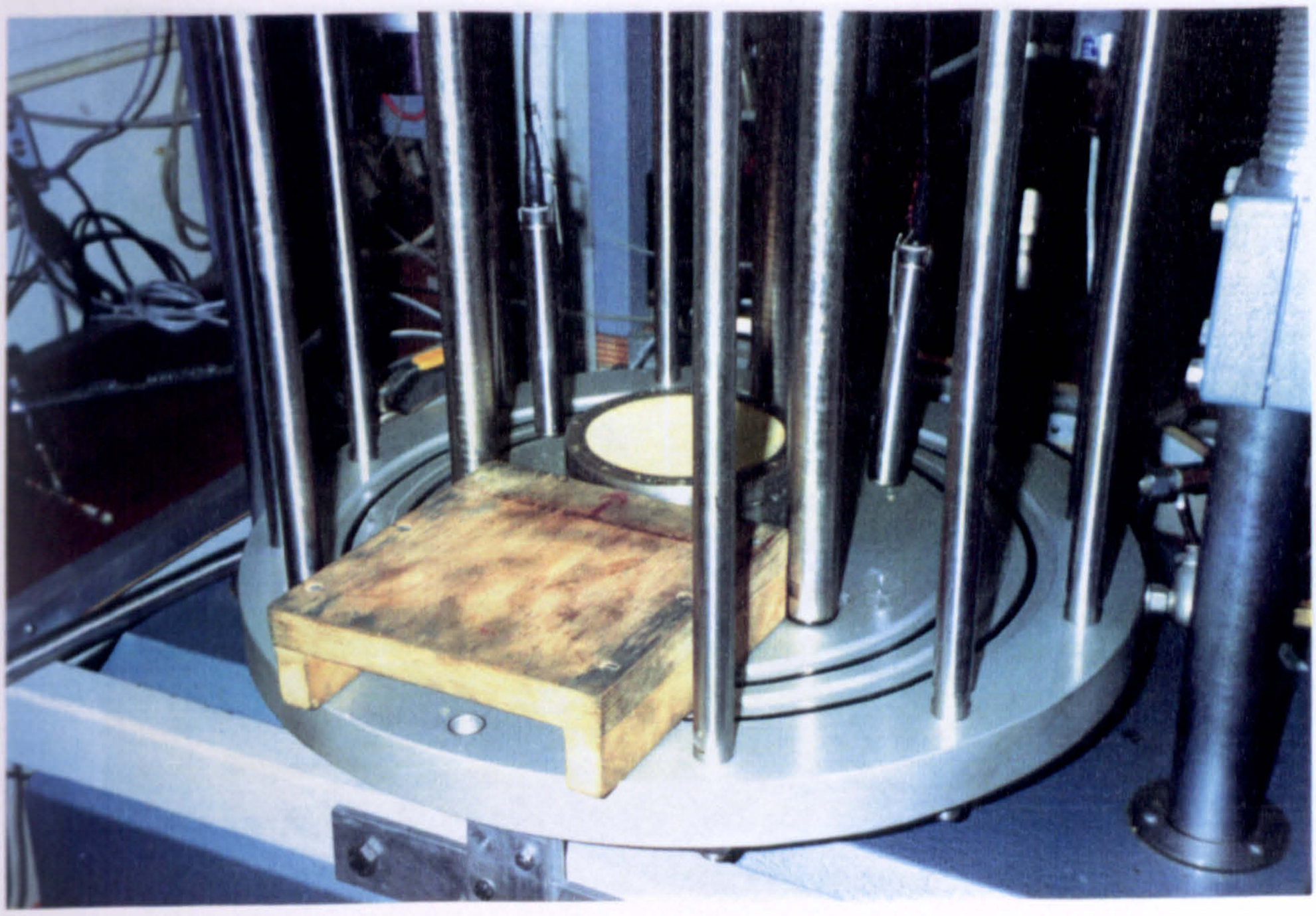

Plate 6.6 (Top)- Wooden block is placed on the bottom plate before placing the mould

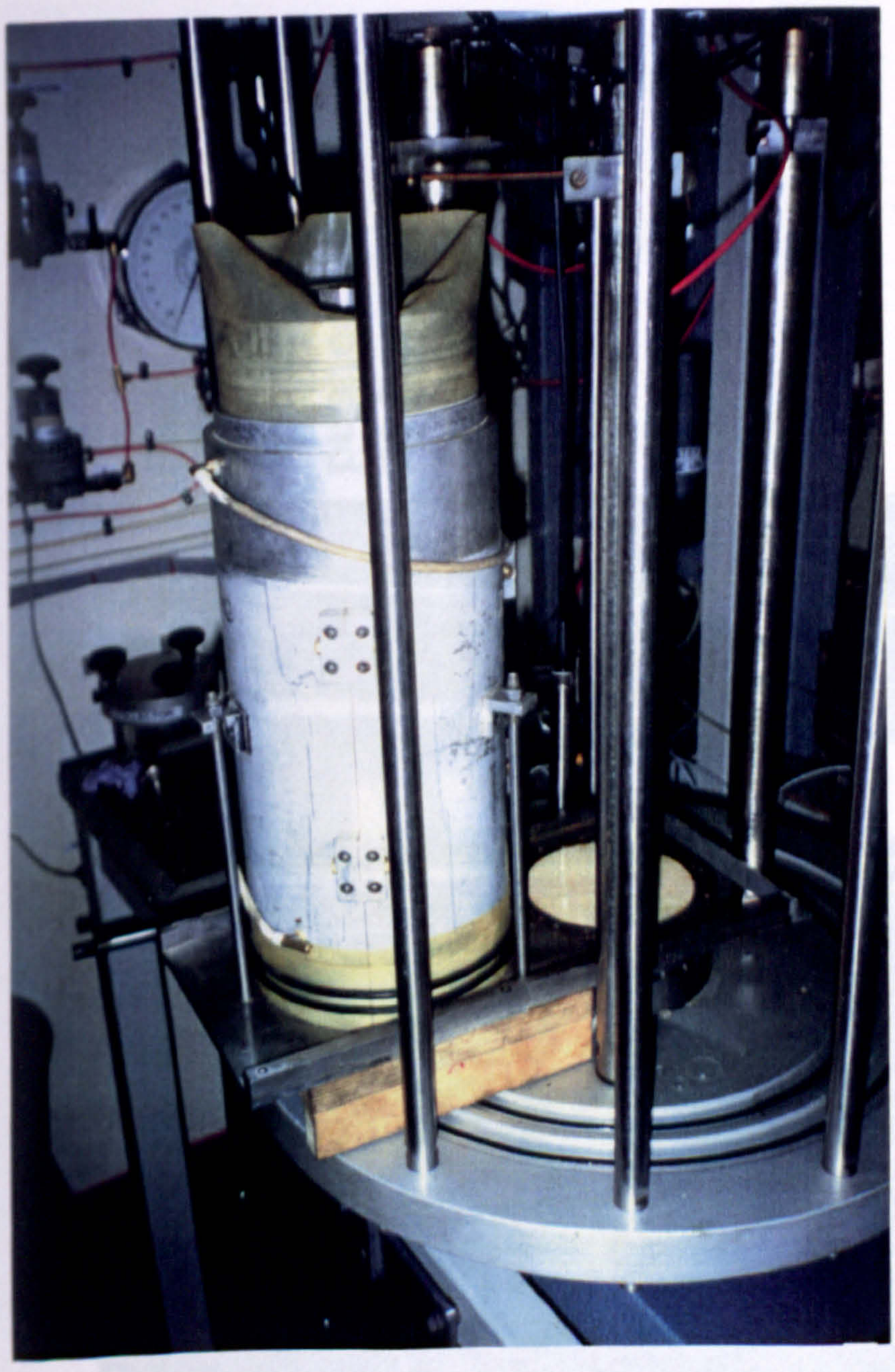

Plate 6.7 (Left)- Mould is placed on the wooden block

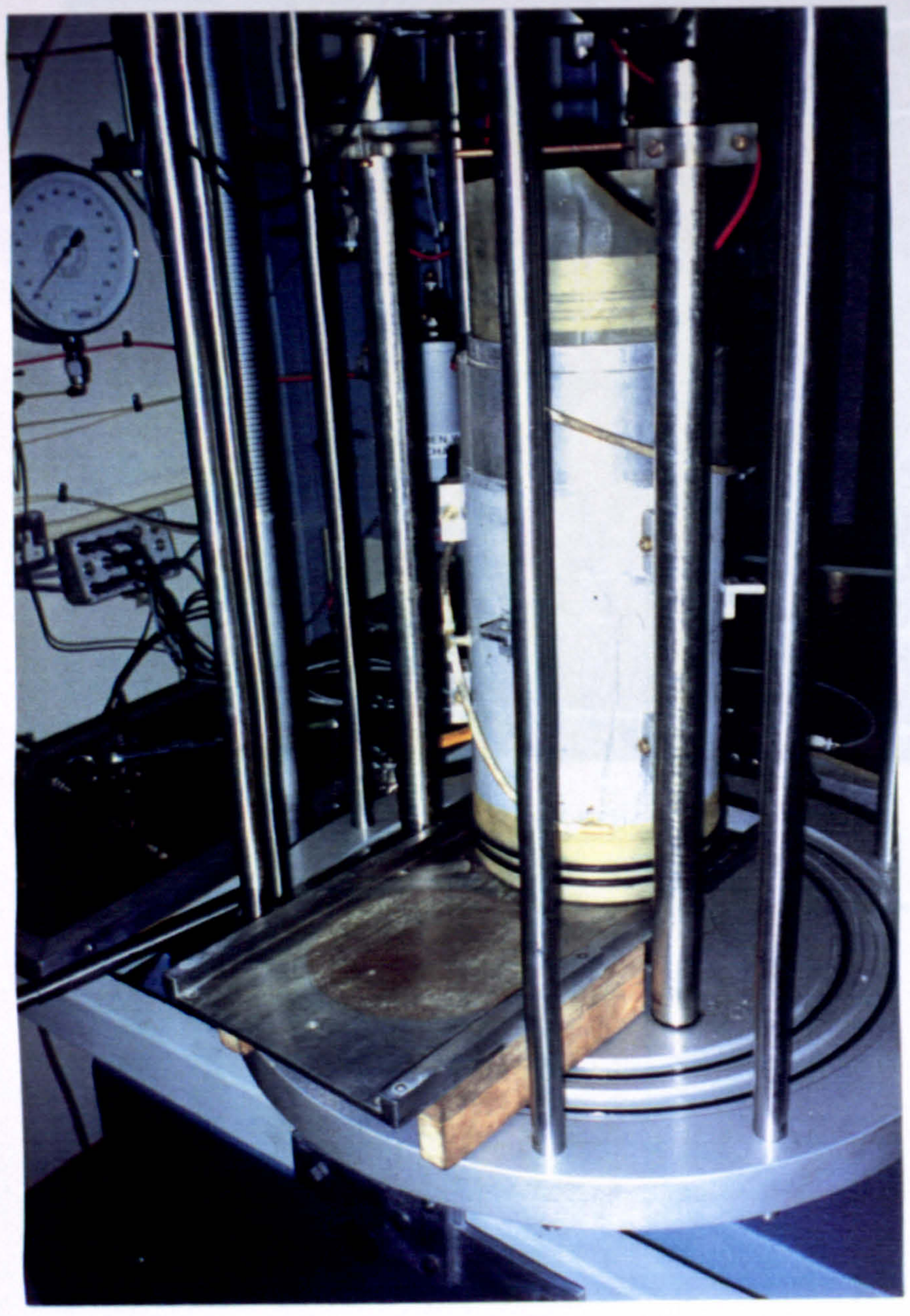

Plate 6.8 (Left)- Mould with specimen pushed across its base to the base pedestal

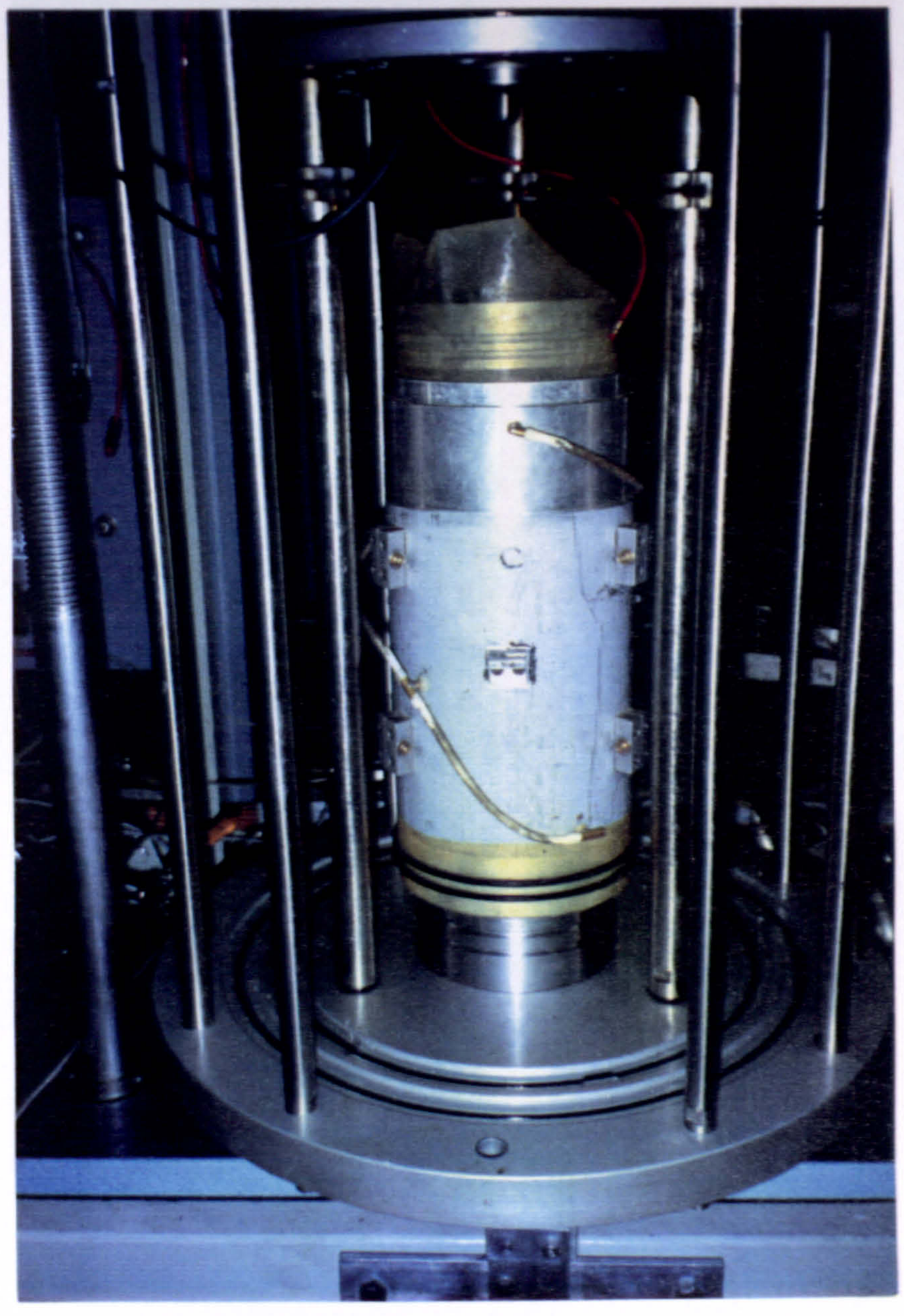

Plate 6.9 (Right)- The mould after the base and wooden block were removed

Plate 6.10 (Top)- Metal ring was used to insert the second membrane around the specimen

Plate 6.11 (Left)- Inserting the second membrane around specimen

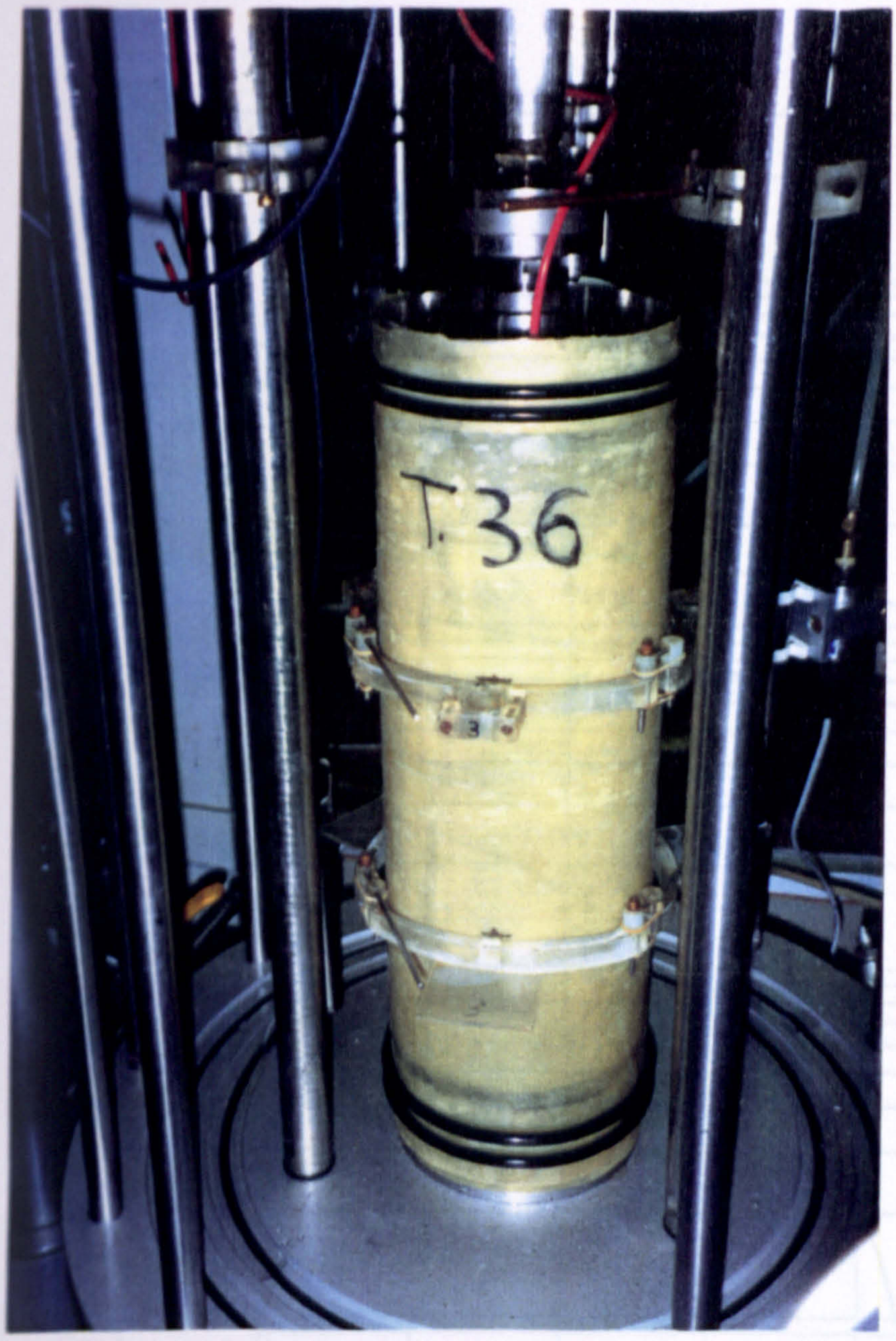

Plate 6.12 (Left)- The specimen after fixing the mounting system of the axial LVDTs

Plate 6.13 (Bottom)- The double-wall triaxial cell after placing the axial and lateral LVDTs

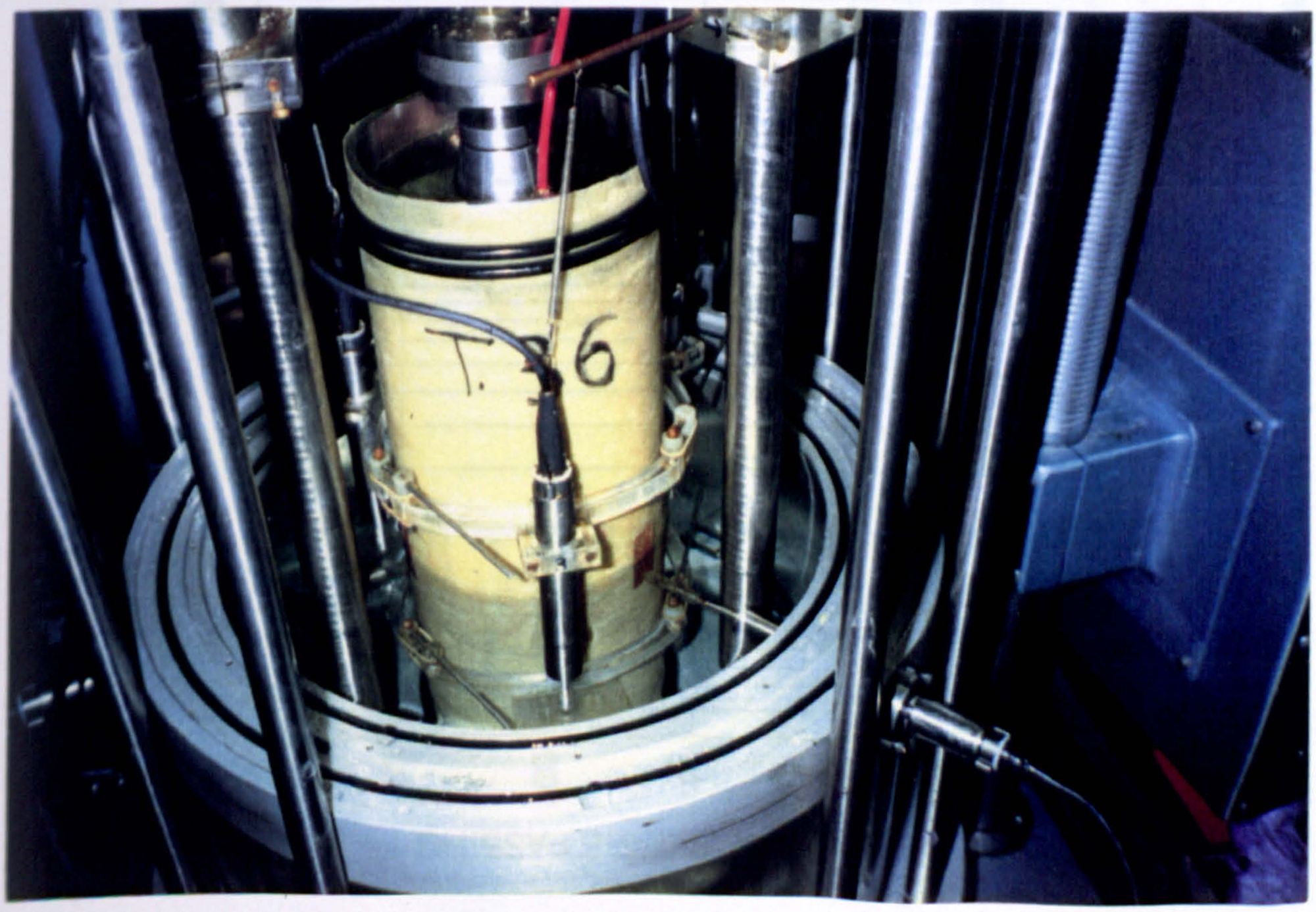

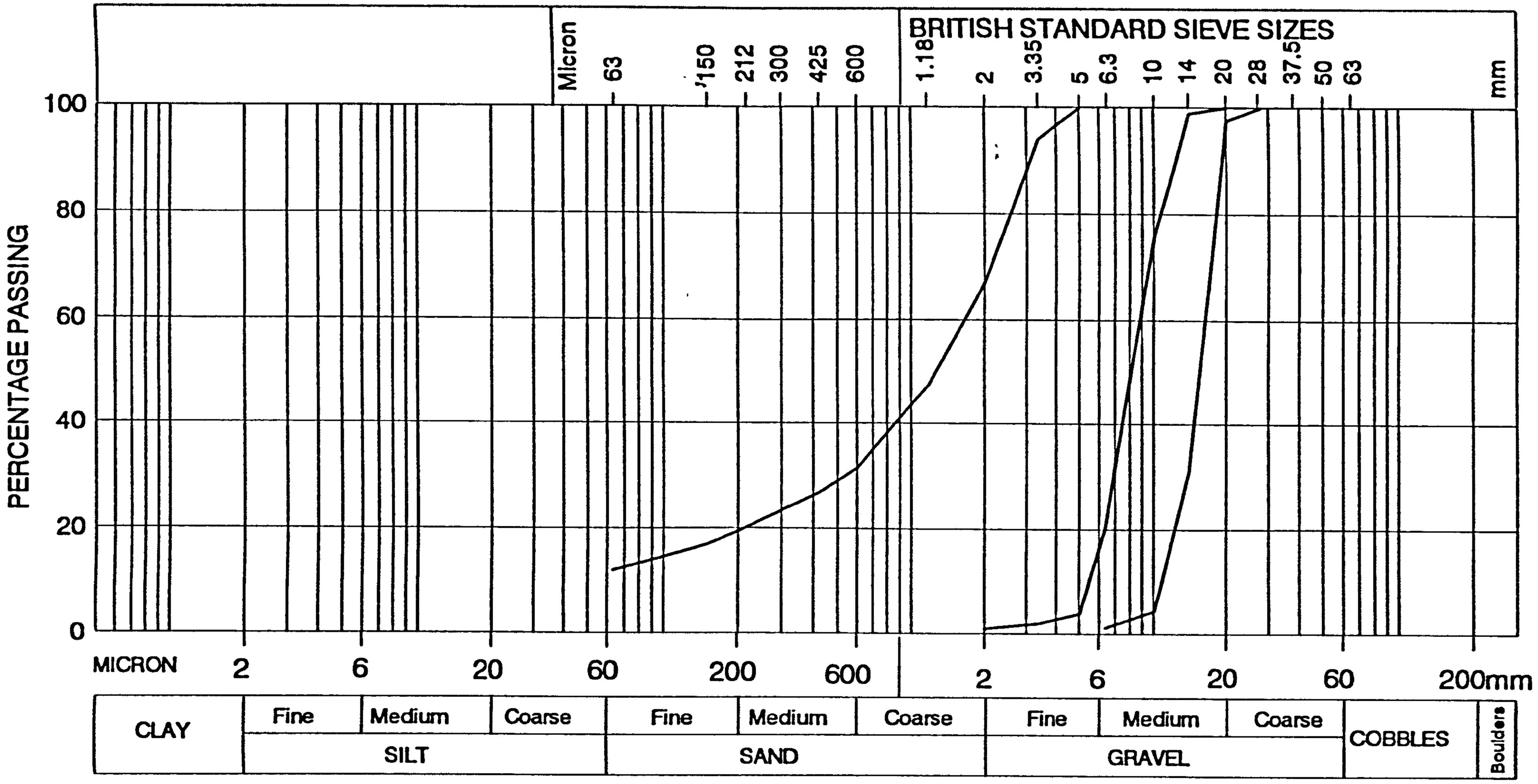

Fig. 6.1- Grading curves for the supplied limestone aggregate (after Goodwin, 1991).

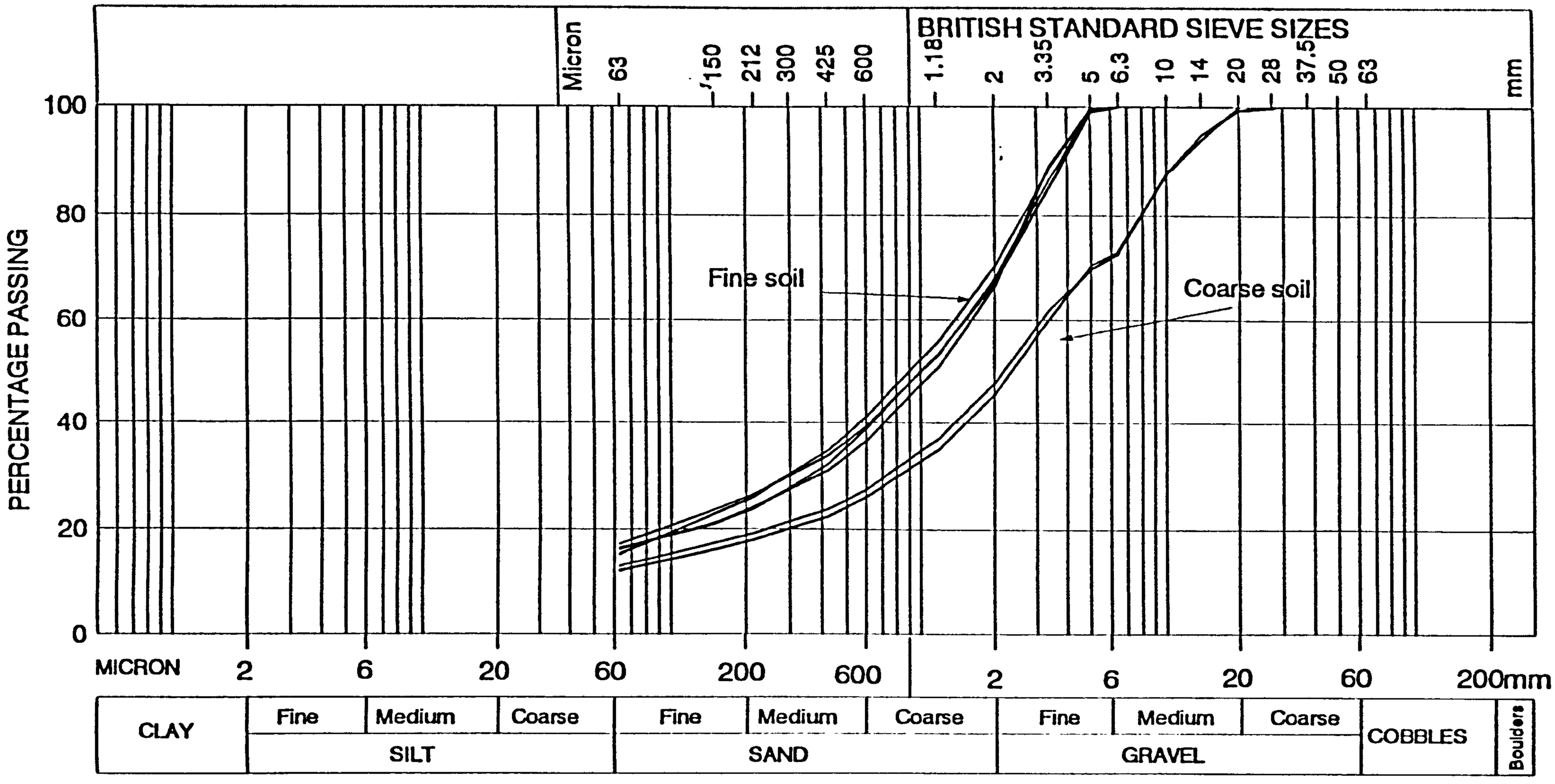

Fig. 6.2- Grading analysis for the fine and coarse grading soils.

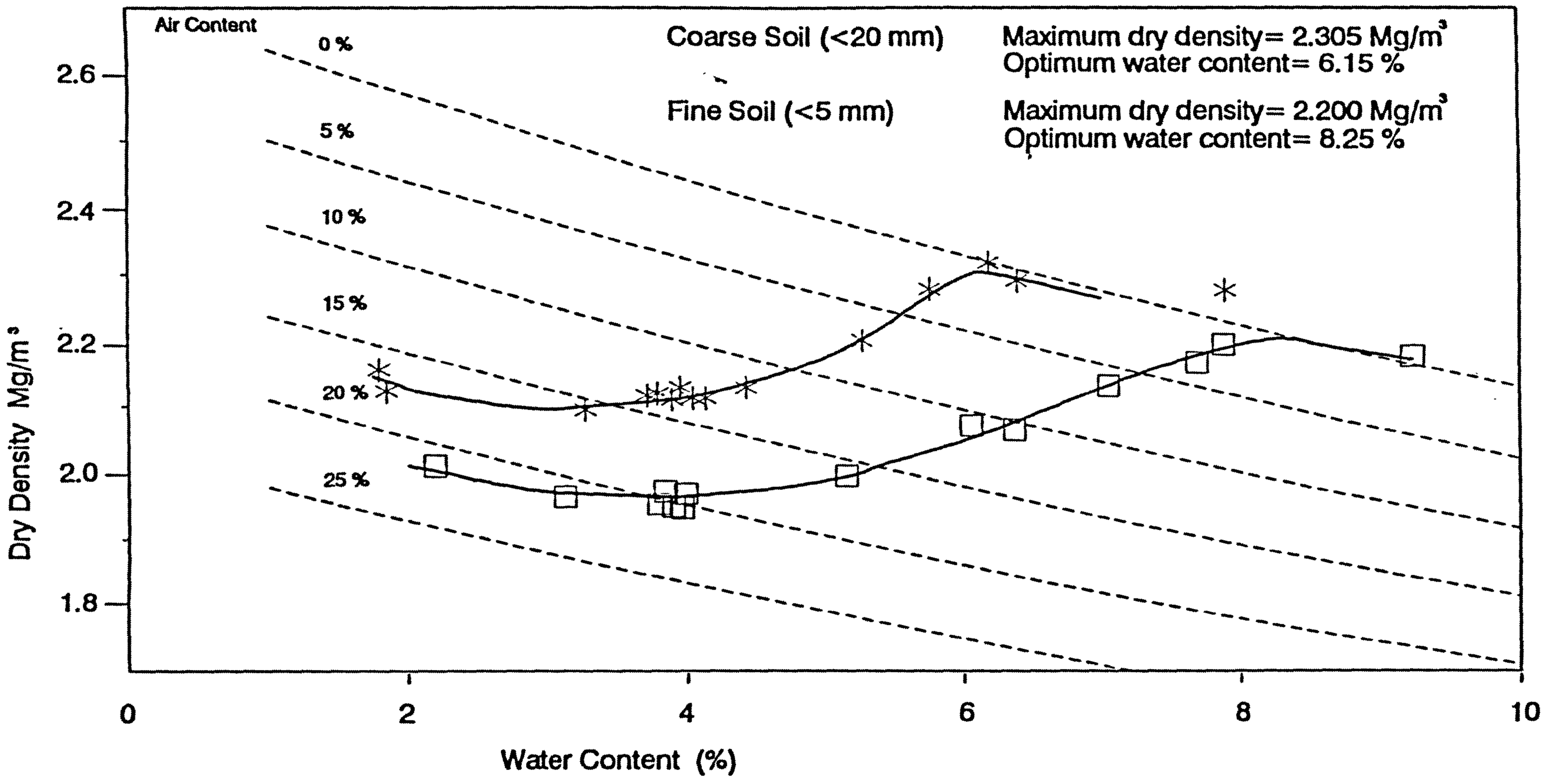

Fig. 6.3- Compaction test curves for the fine and coarse gading soils.

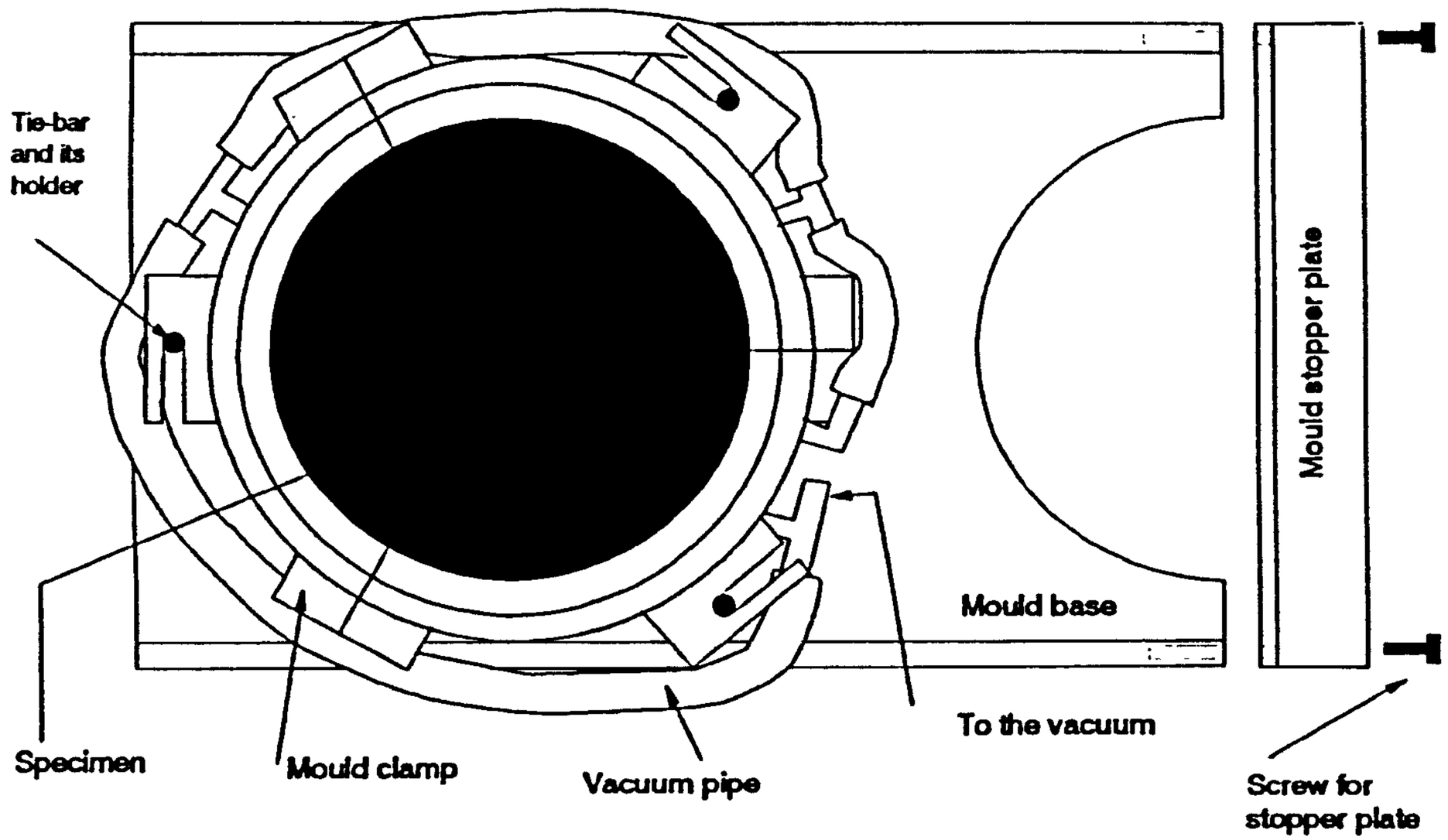

Top face

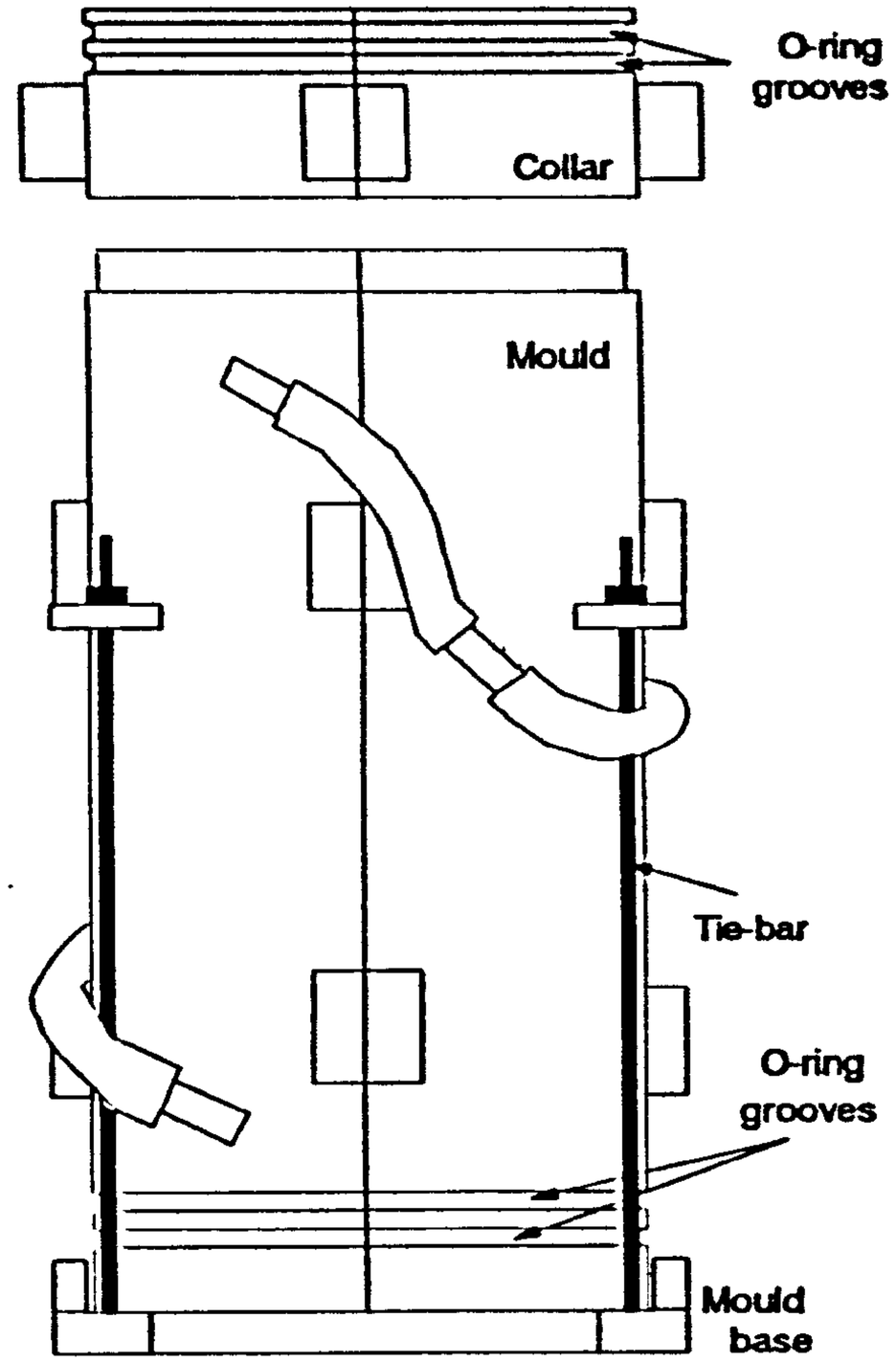

Front face

Fig. 6.4- Specimen compaction mould

Chapter 7

Test Results

7.1 Introduction

In this Chapter all test results, together with the initial interpretation and discussion of the behaviour of the soil, will be given. The results will be discussed in more detail in Chapter 8. It should be noted that all of the specimens, i.e. both fine and coarse grading were compacted at the same total water content (4%) and with the same compactive effort, to keep the initial soil fabric approximately the same for each soil grading.

In Section 5.3 a number of corrections which are made to the test results were described. However, some other errors which it is very difficult or impossible to make corrections for may occur. Before presenting the test results, and to make the interpretation of the results clearer, these errors are described and discussed in the following Section together the performance of the new double-wall triaxial cell.

7.2 Performance of the New Double-Wall Triaxial Cell

The performance of the new cell was good, in that the methods and techniques used in the cell design have been shown to be workable. Such methods and techniques include the double-wall cell, axis translation technique (Section 3.2), spiral groove (Section 4.2.1E) etc. There were some errors which occurred during specimen testing, which could not be

calibrated to correct the test results because they were variable and unpredictable. These errors are as follows:

1. Membrane buckling. It was observed during specimen compression, that the membrane started to buckle (wrinkle) at internal axial strains above about 0.3%. If the buckling occurs beneath the lateral LVDT target, as shown in Fig. 7.1, the internal lateral strain measurements will be affected, which in turn affect the calculation of the specimen volumetric strain calculated using the internal strain measurements.

2. Water leakage through the rubber membrane. Water can leak through the membrane at a rate of 1.7 cc per 100 kPa per week per single ungreased membrane (Section 3.4). Although a silicone grease was used between the two membranes around the specimen in the current research (Section 6.3.3) to prevent water leakage, water may still enter the specimen through holes in the inner membrane which were developed during specimen compaction. This leakage could cause maximum errors of 0.004 % and 0.002% per week in the measurements of the specimen volumetric strain (measured using the volume change unit) and water content change respectively. This type of water leakage is variable and depends on whether or not there are holes in the rubber membrane, but the maximum errors were considered to be insignificant when compared to the maximum volumetric strains and water content changes.

3. Axial LVDT tilting. The internal axial LVDTs used in the double-wall triaxial cell (Figs. 4.4 and 4.5) may tilt either due to specimen bulging during shearing process, or due to the pull force of the springs holding the LVDTs. The verticality of each internal axial LVDT was checked at the start of the test. It was observed that specimen bulging did not occur before the failure deviator stress was reached, which means that tilting errors due to specimen bulging were insignificant prior to failure. Errors due to the spring pull may also be insignificant, because the specimen lateral displacement at failure was about 0.4 mm (0.53% lateral strain). Knowing that the spring was very light (1 mm extension per 3.4 grams), it may be concluded that the force applied by the spring to the LVDT at failure

will be approximately 0.014 N. This is a very small force, and even if it tilted the LVDT, it would be tilted at a very small angle and will give an insignificant error.

4. Spring snapping. The spring carrying the internal axial LVDT, used in the double-wall triaxial cell (Fig. 4.4) snapped during tests FU-A7 and FU-A11 (Table 6.4) probably due to corrosion. When the spring snapped the weight of the LVDT was carried by the perspex curve holder of the mounting system of the axial LVDTs (Fig. 4.5) which may have caused smaller axial strain than expected to be recorded.

5. Specimen tilting. Fig. 7.2 shows a typical graph for three lateral LVDT readings during specimen shearing stage of test FU-A8 (Table 6.4). Point A in this figure indicates the time when readings in the load cell showed an increase in the applied load, i.e. shearing of the specimen was commencing. The readings of LVDT numbers 1 and 2 between time zero and point A show an almost linear lateral displacement, while LVDT number 3 shows zero readings. It can also be seen that LVDT number 1 indicates slightly more movement than LVDT number 2. The average of the three LVDT readings showed that there was some apparent straining before applying any load. The reason for this behaviour may be attributed to slight misalignment between the piston and the top cap. The piston at the start of the test may not have been at the top cap centre. It had to push the specimen sideways to centre itself. During this time the load cell recorded a constant and very small load, about 7N, which corresponds to a 0.3 kPa deviator stress. This load was the load that the piston needed to move the specimen. When the piston has reached the top cap centre, the load cell started to record an increase in the applied load, and no further translation of the specimen occurred. This may be seen in Fig. 7.2, as the change in the behaviour when the time reached point A, indicating that the piston was on, or close to, the top cap centre. This specimen movement affected the calculation of the specimen volumetric strain and Poisson's ratio. The maximum error in the specimen volumetric strain could be 0.01%, while the error in the calculation of Poisson's ratio could be significant below an internal axial strain of 0.3%, and could be as big as 0.15 at 0.1% internal axial strain.

6. Bedding error. Bedding error due to an irregular top surface of the specimen can occur because of the difficulty of getting an even surface between the top cap and top surface of the specimen particularly with granular soils. If one particle is trapped between the top cap and specimen it can cause large bedding errors. Bedding error affects the measurements of the external axial strain as was shown in Section 3.6. Also it can cause errors in the specimen volume change measured using the volume change unit by showing an apparent specimen contraction. In the current research an average error of about 0.02% of the specimen volumetric strain was found.

7.3 Results of Test Series A

In this series, drained tests were carried out on fine grading soil specimens at different net cell pressures and suctions (Table 6.4). The equalisation and consolidation stages were combined for all tests except tests FU-A3 and FU-A12 (Section 6.2.2). The results of this series are shown in Tables 7.1 and 7.2.

7.3.1 Equalisation and Consolidation Stages Results

The changes in the volume and water content were recorded during the equalisation (during which the specimen was left under very low net cell pressure, 10 kPa, for suction to equalise along the specimen) and consolidation stages or the combined equalisation and consolidation stage

7.3.1.1 Specimen Volume

Figs. 7.3a, 7.3b, 7.4a and 7.4b show the specimen volumetric strain and specific volume *(1+Void Ratio)* for tests FU-A3 and FU-A12 (Table 6.4) during the equalisation and consolidation stages respectively, while Figs. 7.5a, to 7.7b show the specimen volumetric strain and specific volume for the combined equalisation and consolidation stage of the

other tests in the series (Table 6.4) carried out under 75, 50 and 25 kPa suctions respectively. The specimen volumetric strain was calculated by dividing the change in its volume to its volume at the start of each stage.

Two curves of the specimen volumetric strain for each test are shown in Figs. 7.3a, 7.4a, 7.5a, 7.6a and 7.7a, one determined from the 1000 cc volume change unit (Section 5.2.2) readings which is called MVS. The other, which is called CVS, was determined using the internal axial and lateral strain measurements, and was calculated according to Equation 7.1;

$$\varepsilon_v = \varepsilon_1 + 2\,\varepsilon_3 \qquad (7.1)$$

where ε_v , ε_1 and ε_3 are the specimen volumetric, axial and lateral strains respectively. It should be noted that the net cell pressure, $(\sigma_3 - u_a)$, of test FU-A13 (Fig. 7.7) was increased after one day from 70 kPa to 92.6 kPa.

There was a maximum difference of about 0.55% between the values of MVS and CVS during the equalisation stage (Fig. 7.3a), while the difference became less during the consolidation stage (Fig. 7.4a), about 0.15%. A maximum difference of about 0.7% between the MVS and CVS can be seen during the combined equalisation and consolidation stage, as shown in Figs. 7.5a, 7.6a and 7.7a. This difference may be due to bedding errors (Section 7.2) and the compression of the two specimen membranes and compression of the grease and any trapped air between the two rubber membranes, due to the increase in the cell and air pressures. A change of 0.05 mm, for example, in the thickness of both membranes (0.5 mm thick each) can produce an error in the MVS of about 0.26% (if the membrane Young's modulus times its thickness (Fig. 5.7) is assumed to be 1 kN/mm, a 100 kPa pressure on each side of the membrane can produce a compression of about 0.05 mm to the membrane). Also a bedding error can show an

apparent reduction in specimen volume, as water was drawn into the inner cell when top cap moved down during bedding (Section 7.2).

The reason why the difference between MVS and CVS was higher during the equalisation stage than that during the consolidation stage may be due to the compression of the trapped air between the membranes having not occurred during the consolidation stage, because all trapped air was compressed and passed through the membrane, either to the specimen or the cell water, during the equalisation stage.

During the equalisation stage, both curves of MVS and CVS (Fig. 7.3a) showed approximately similar behaviour, as the net cell pressure $(\sigma_3 - u_a)$ and suction $(u_a - u_w)$ were applied. The CVS first decreased and then increased with time until the change became very small. Similar behaviour can also be seen during the combined equalisation and consolidation stage (Figs. 7.5a 7.6a and 7.7a). The CVS did not increase during the consolidation stage (Fig. 7.4a) when the net cell pressure was increased, during which the specimen volume decreased until the change became very small.

It may be seen that for some tests the MVS curve shows a continuous change at the end of the test of less than 0.025% per day, while the CVS showed zero or very small change at the end of the test. This may be due to the fact that the formula used to correct for the cell water leakage (Section 5.3.2) may give an error of about ±0.009% per day, or it may be due to downward movement of the piston due to improper contact between piston and top cap, as the piston was not clamped, and this movement displaced water from the inner cell.

There is another difference between the MVS and CVS curves which may only be seen during the equalisation stage (Fig. 7.3a) and the combined stage (Figs. 7.5a, 7.6a and 7.7a). The figures show that the CVS curve shows that the specimen volume started to

increase soon after the specimen volume first decreased. The MVS curve shows that the specimen volume starting to increase at a later time after its volume had first decreased. This may be due to air trapped between the two membranes taking some time to pass through the membrane to either the specimen or the cell water. This leakage of trapped air will only be detected when measuring the change in the inner cell water volume.

It may be concluded that the main discrepancy between the measurements of CVS and MVS arises during the application of step changes of cell pressure, which affects the measurements of specimen volume change using the volume change unit during the equalisation, consolidation or combined stages. This leaves the use of the internal strain measurements method to calculate the specimen volume change as the most preferable method during these stages, this is because increasing the cell pressure did not affect the measurements of the specimen internal strains. Further discussion about the difference between CVS and MVS will be given in Section 7.3.2.2.

From the above discussion, the specific volume of all unsaturated specimens during the equalisation, consolidation and combined stages (Figs. 7.3b, 7.4b, 7.5b, 7.6b and 7.7b), was calculated using measurements of the internal strains to avoid errors due to the step changes of the cell pressure.

7.3.1.2 Specimen Water Content

Figs. 7.8 and 7.9 show graphs of the change in the specimen water content during equalisation and consolidation stages respectively, plotted against square root of time for tests FU-A3 and FU-A12. Figs. 7.10 to 7.12 shows graphs of the specimen water content change during the combined equalisation and consolidation stage plotted against square

root of time for the other tests in the series (Table 6.4) carried out at 75, 50 and 25 kPa suctions respectively.

It can be seen that water was draining out of the specimen for all tests, which may indicate that the specimens had an initial suction, after compaction, less than 25 kPa. The tests showed a similar behaviour in that as the net cell pressure was increased the specimen water started to drained until the change in the specimen water content was very small, which indicated that the specimen had reached the applied suction. Fig. 7.10 shows that the specimen water content at the end of the combined equalisation and consolidation stage for some tests appears to continue to change, although they were left for long time. This was assumed to be due to a small amount of water leakage through the rubber membrane (Section 7.2).

Figs. 7.8 to 7.12 show that the time at which the change in specimen water content became very small, increased as the net cell pressure and suction increased. This is because as the suction increased the specimen water content decreased, i.e. more water should be expelled out of the specimen to increase the specimen suction. Also, as the net cell pressure increases, the specimen volume decreases, i.e. the degree of saturation increases, so some water should be expelled out of the specimen to reduce the degree of saturation and increase suction. Figs. 7.8 to 7.12 shows that the curves show a linear variation of specimen water content change with the square root of time.

These Figures also show that the initial water content differs from specimen to specimen, this may be due to the loss of water during the preparation of the specimen, as will be discussed in section 8.3.

7.3.2 Shearing Stage Results

7.3.2.1 Stress-Strain Behaviour

Figs. 7.13 to 7.15 show curves of the deviator stress plotted against the average internal axial strain measured from the three axial LVDT (Fig. 4.4) for all series A tests carried out under 75, 50 and 25 kPa suctions respectively, and sheared at a rate of strain of 0.00011 %/min. It should be noted that one of the springs carrying a vertical LVDT (Fig. 4.4) snapped during tests FU-A7 and FU-A11, which caused smaller readings of the internal axial strain.

All tests were stopped one to two days after the failure stress for the specimens had been reached. As can be seen from the Figures, there is a similar behaviour in all of the tests. The Figures show that the initial part of each curve (below about 0.3% internal axial strain) appears to be linear (elastic section) , and this linear portion is followed by a non-linear part (plastic section) until the failure (peak) stress is reached, then the deviator stress starts to decrease. To show these two parts of the curve, values of secant Young's modulus (deviator stress / internal axial strain) are plotted against the internal axial strain in Figs. 7.16 to 7.18 for test series A. Values of the Young's modulus below about 0.05% internal axial strain is not considered, because the accuracy of the LVDTs measuring the internal axial strain was about 0.05% internal axial strain (Section 5.2.1).

Figures 7.16 to 7.18 show that the Young's modulus is high for axial strains below about 0.1% internal axial strain, and then it decreases until it becomes constant or almost a constant between internal axial strains of about 0.1% to 0.3% thereafter it decreases non linearly. The increase in soil stiffness as axial strain decreases was also reported by Jardaine et al. (1982) for London clay. The Figures also show that the strain range over which the value of Young's modulus becomes constant or almost constant, become shorter as the net cell pressure increases.

The stress-strain behaviour of the unsaturated specimens, shown in Figs. 7.13 to 7.15, is similar to that seen in saturated dense granular soils or overconsolidated clay soils. In those soils the deviator stress starts to decrease after a peak stress is reached. This behaviour, as was discussed by may authors such as Atkinson and Bransby (1978), is due to the effect of particle interlocking.

Fig. 7.19 shows a typical comparison between the secant Young's modulus calculated using the internal and external axial strains. It can be seen that the external axial strain measurements can give lower values of the Young's modulus than the internal axial strain measurements. Both curves show approximately similar behaviour above about 0.15% axial strain. The part where the Young's modulus becomes constant or close to constant is better seen when it is calculated using the internal axial strain measurements. The difference between the two curves may be attributed to the effect of bedding errors and end friction as was discussed in Sections 3.3.2 and 3.6.

7.3.2.2 Specimen Volume

Figs. 7.20 to 7.22 show the specimen volumetric strains and specific volume measured using the volume change unit, MVS (Section 5.2.2) plotted against the internal axial strain for all specimens in test series A. The specific volume just before starting the shearing stage is taking from the measurements of the internal strain at the end of the consolidation or the equalisation and consolidation combined stage. Figs. 7.23 to 7.25 show the specimen volumetric strain measured using the volume change unit, MVS, and the specimen volumetric strain calculated using the internal axial and lateral strain measurements, CVS (Equation 7.1) for tests sheared at 75, 50 and 25 kPa suctions respectively.

Figs. 7.23 to 7.25 show that the CVS curves are in many cases similar values to the MVS curves, but for some tests above an internal axial strain of about 0.3%, the curves diverge. This may be due to the effect of the rubber membrane buckling during shearing and the change in specimen shape due to non-uniform deformation, such as bulging, which affected the lateral strain measurements, as was discussed in Section 7.2. This, in turn, affected the calculation of CVS. For this reason the specific volume for all tests during shearing stage, see Figs. 7.20a, 7.21a and 7.22a, are calculated from measurements of the volume change unit. It was discussed in section 7.3.1.1 that errors due to step changes of cell pressure were introduced in the measurements of the volume change using the volume change unit during the equalisation, consolidation and combined stages. The cell pressure was not changed during the shearing stage, which means that errors due to step changes of cell pressure were not introduced during shearing.

These figures show that all of the tests exhibit similar behaviour during shearing which is similar to what be observed for conventional saturated drained triaxial tests on dense granular or overconsolidated clay soils. The specimen volume first decreased or compressed which corresponds to the elastic behaviour of the stress path and then increased, dilates, before the failure strain (about 1% internal axial strain) was reached and continued to increase after failure, which corresponds to the plastic behaviour after yielding. The lower the net cell pressure (or the higher the overconsolidation ratio as with the overconsolidated soils) the higher the amount of dilation. The behaviour of dilation and the peak stress shown in Figs. 7.13 to 7.15, is due to the effect of interlocking. Before a complete shear failure can take place, this interlocking must be overcome in addition to the frictional resistance and tensile forces due to the menisci at the points of contact. After a peak stress is reached the degree of interlocking decreases and the shear stress necessary to continue shear displacement is correspondingly reduced. The decrease in the degree of interlocking produces an increase in the specimen volume (dilation) during shear.

It should be noted that due to the effect of end restraint (Section 3.3.2), part of the specimen (usually the middle part) reaches the peak strength and has higher dilation than the rest of the specimen, as shown in Fig. 3.2. This means that the measured specimen volume change using the volume change unit is the average volume change of the specimen.

7.3.2.3 Specimen Water Content

Figs. 7.26 to 7.28 show the specimen water content during the shearing stage, plotted against the internal axial strain for all tests in series A carried out at 75, 50 and 25 kPa suctions respectively.

The figures show a similar behaviour for all tests with the water initially forced out of the specimen and then drawn back into the specimen. By comparing these figures with those of the specimen volumetric strain, shown in Figs. 7.20 to 7.22, it can be seen that as the specimen volume was decreasing, specimen water was expelled out of the specimen, and it was drawn back into the specimen when the specimen volume was increasing. In drained tests, during which the suction was kept constant, a reduction in the specimen volume led to a reduction in the void ratio, and this in turn led to an increase in the degree of saturation. This caused a reduction in the soil suction, because suction depends on the amount of water exists in the soil voids (Section 2.4). So some water had to be removed from the specimen to return the specimen suction back to the value it had before the reduction of the specimen volume occurred. The opposite behaviour occurred when the specimen volume increased.

7.3.2.4 Specimen Water Content at the End of Test

At the end of each test when the specimen was removed from the triaxial cell, four samples, each of about 2 kg mass, were taken at different heights along the tested specimen (Section 6.3.3) to determine the distribution of the water content along the tested specimen. Although maximum care was taken, it is possible that some water may have been lost during cutting and handling of the samples. A 0.5 cc water loss from each sample may cause an error of about 0.05% in the calculated water content.

Table 7.3 shows values of the water content along the height of some of the tested specimens at the end of the tests. The water content at the end of test for other specimens was not determined because some water had entered the tested specimen when the triaxial cell was dismantled and specimen removed. This changed the specimen water content.

The Table shows that the water content of the specimen at the end of the test was nearly uniform with a maximum variation of about 0.05%, which may be due to water loss during cutting and handling the specimens.

7.4 Results of Test Series B

In this series, two tests were carried out, FU-B1 and FU-B2. The equalisation and consolidation stages, were combined only for test FU-B1. The results of this series are presented in Tables 7.4 and 7.5. For both tests a suction of 25 kPa was applied during the equalisation and consolidation stages for test FU-B1 and the combined equalisation and consolidation stage of test FU-B2, by allowing some water to drain out of the specimen (drained test). The specimens were then sheared with no further specimen water drainage

was allowed, (constant water content tests), at rate of strain 0.00011 %/min (Section 6.2.3 and Table 6.5).

The specimen volumetric strain, specific volume and water content during equalisation stage of test FU-B2 are shown in Figs. 7.3a, 7.3b and 7.8 respectively. And those during the consolidation stage of this test are shown in Figs. 7.4a, 7.4b and 7.9 respectively. The specimen volumetric strain, specific volume and water content during the combined equalisation and consolidation stage of test FU-B1 are shown in Figs. 7.7a, 7.7b and 7.12 respectively. For both tests the behaviour of the specimen volumetric strain and water content change before shearing is similar to that shown for test series A (Section 7.3.1).

The shearing stage results for both tests are shown in Figs. 7.29, 7.30, 7.31a and 7.31b respectively, with deviator stress, Young's modulus, specimen volumetric strain and specific volume plotted against the internal axial strain. The Figures show similar behaviour to that shown in Section 7.3.2 for test series A. Fig. 7.32 shows the suction change plotted against the internal axial strain during the shearing stage of both tests. It may be seen when studying the change in specimen suction and the change in specimen volume (Fig. 7.31) during the shearing stage, that when the specimen volume decreased, the suction decreased, and the suction increased when the specimen volume increased. This was due to the change in degree of saturation as was discussed in Section 7.3.2.3. This behaviour of suction (Pore Water Pressure) and volume during shearing stage is similar to what would be observed for undrained saturated dense granular and overconsolidated clay soils

7.5 Results of Test Series C

In this test series two specimens were tested under different net cell pressures (Table 6.6) and at a different rate of strain to earlier tests. The equalisation and consolidation stages for both tests were separate. The initial water content (after compaction) was not allowed to change during the tests (i.e. constant water content test). Tables 7.6 and 7.7 show the results for both tests. It should be noted that test FU-C2 had a higher dry density ($2.047\,Mg/m^3$) than that of test FU-C1 ($1.958\ Mg/m^3$). This may have been due to the compactive effort being slightly higher in test FU-C2. Both specimens were sheared at rate of strain 0.00093 %/min, which was faster than that for test series A and B (0.00011 %/min).

Figs. 7.33a, 7.33b and 7.34 show the specimen volumetric strain, specific volume and suction respectively during the equalisation stage for both tests. The volumetric strain and specific volume have similar behaviour to that described for drained series A tests (Section 7.3.1.1). Specimen FU-C1 showed a higher values of specific volume than specimen FU-C2, which may be due the fact that specimen FU-C2 had higher dry density than that for specimen FU-C1 (Table 6.6). This difference in dry density has also slightly affected the suction change as shown in Fig. 7.34.

The specimen volumetric strain and specific volume during the consolidation stage for both tests is shown in Fig. 7.35a and 7.35b respectively. The figure shows similar behaviour to that shown for drained tests in series A (Fig. 7.4), but the time for 100% consolidation of series C tests (constant water content test) was shorter than that for the drained tests. A possible explanation for this is that in drained tests the water moves through narrow channels within the specimen from the specimen top to its bottom, while in the constant water content tests the specimen water may only move short distances where there is a suction gradient.

The pore water pressure change during consolidation for both tests is shown plotted against the logarithm of time in Fig. 7.36. As can be seen that for test FU-C2 when the net cell pressure was increased for each test the pore water pressure increased. then the pore water pressure dissipated until the change was very small. It may also be seen that for test FU-C1 the pore water pressure continued to drop (about 1 kPa per day), which may have been due to a slight leak in the fittings of the pore water pressure measurement system.

Figs. 7.37, 7.38, 7.39a, 7.39b and 7.40 show the results for the deviator stress, Young's modulus, volumetric strain, specific volume and suction respectively during the shearing stage of both tests. The behaviour of both specimens during shearing was similar to that discussed in Section 7.4 for test series B.

7.6 Results of Test Series D

Three constant water content tests were carried out on unsaturated coarse grading specimens (Table 6.7). The equalisation and consolidation stages were kept separate for these tests, and the water content was not allowed to change at any stage of the test. Tables 7.8 and 7.9 show the test results for all test stages. The specimens were sheared at rate of strain 0.00093 %/min, which was similar to that used for test series C.

Figs. 7.41 to 7.48 show the results for the equalisation, consolidation and shearing stages for these three tests. The behaviour is similar to that discussed in Section 7.5 for tests series C. It should be noted that, by mistake, specimen test CU-D2 was quickly loaded

and unloaded at the end of the consolidation stage. This may have affected the test results during the shearing stage.

7.7 Test Results of Series E

Drained tests were carried out on fine grading saturated specimens (Table 6.8), which were compacted at the same water content and compactive effort as those in the other series A to D. After the specimens were saturated, they were consolidated at different effective cell pressures, then sheared at the same rate of strain as that used to shear the unsaturated specimens in series A and B (0.00011 %/min). Tables 7.10 and 7.11 show the test results of this series.

The volume of water that entered the specimen air voids was measured during the saturation process (Section 6.3.4), so as to be compared with that calculated volume of the air voids, so that any volume change that occurred to the specimen during saturation could be determined by taking the difference between them. However, this method may not be reliable due to the following factors:

(a) The calculation of the volume of air voids may not be accurate due to the compression of the rubber membrane (0.5 mm thickness) that contains the specimen during compaction by the soil particles. For example, a compression of 0.1 mm in the membrane may cause an error of about 70 cc.

(b) The measured volume of water that enters the air voids during the saturation process may not be accurate due to the compression of the two rubber membranes and any air that is trapped between them during application of the cell and back pressures, in similar way to that discussed for unsaturated specimens in Section 7.3.1.1. It was shown in Section 7.3.1.1 that an error of about 0.55% (23 cc) can be caused to the unsaturated specimen volume due to such compression. A larger error may be

expected for the saturated specimens because higher cell and back pressures were used for the saturated specimen (550 kPa and 540 kPa) than for the unsaturated specimens (100 kPa and 90 kPa).

(c) A gap may be formed between the top cap and top of the specimen, if soil particles are trapped between them. This gap is filled with water during saturation process causing an error in the measurement of the volume of water entering the specimen during saturation.

For the above reasons, the measurements of the specimen volume change during saturation will not be used. The specimen volume before consolidation was assumed to be unchanged during the saturation stage. This assumption may cause a very small error in the calculation of the specimen volumetric strain. For example if, after saturation, the specimen volume was 100 cc less than the initial volume, a maximum error of about 0.009% may be caused at 40 cc volume change during consolidation stage.

Fig. 7.49a and 7.49b show curves of the specimen volumetric strain and specific volume during the consolidation stage respectively, plotted against the square root of time, for all of the saturated specimens. As can be seen that the specimen volume decreases after the application of the effective cell pressure and reaches a steady state at a time shorter than that for the unsaturated drained specimen test series A.

Figs. 7.50, 7.51, 7.52a and 7.52b show the shearing stage results for the deviator stress, Young's modulus, volumetric strain and specific volume respectively, plotted against the external axial strain (no internal strain measurements were carried out) for all saturated specimens. The Young's modulus was calculated using the external axial strain. It may be seen from Fig. 7.50 and 7.51, that test FS-E2 shows a lower stiffness than expected (it was expected to be between tests FS-E1 and FS-E3). This may have been due to

improper clamping of the LVDT that was measuring the external axial strain, which in turn led to the downward movement of the LVDT during shearing.

Test FS-E3 was left under compression for a longer time than the other tests, (usually the specimen compression was stopped one to two days after the specimen reached the failure stress). It was observed during this test that the specimen first bulged then was sheared along a single plane at an external axial strain of about 2.1%, which was beyond the strain at which failure stress was reached. It may be seen that constant strength of this specimen was reached at about 1% external axial strain (Fig. 7.50), and in Fig. 7.52 constant volume behaviour (no volume change) was also reached, which may indicate that the critical state was approached. Researchers such as Chu and Lo (1993) stated that the critical state of a drained or undrained test of dense granular specimen can not be reached due to the non-uniform deformation that occurs before the critical state is reached.

It was shown in Section 7.3.2.1 that the calculation of Young's modulus using the external axial strain measurements, may give lower values of Young's modulus than those calculated using the internal axial strain measurements, but it can give approximately similar behaviour above axial stains of about 0.15% (Fig. 7.19). This may be helpful when interpreting the Young's modulus behaviour of the saturated specimens. As can be seen in Fig. 7.51, that there is some evidence that the stress-strain curve of the saturated specimens may be non-linear. This is different to the stress-strain behaviour of the unsaturated fine grading specimens (Section 7.3.2.1), which was shown to consist of a linear part between 0.1% to 0.3% internal axial strains. Further tests on saturated specimens are required using the internal strain measurements to examine this point.

Fig. 7.52a and 7.52b show that the saturated specimen volumetric strain and specific volume has similar behaviour to that of unsaturated specimen drained tests (Figs. 7.20 to

7.22) which what would be expected from saturated drained dense granular specimen test, the specimen volume first decreased then, before the failure stress was reached, it increased. Fig. 7.52 also indicates, apart from test FS-E1, that the specimens reached the state where their volume became constant at about 0.4% axial strain after the failure strain. The unsaturated specimens (Figs. 7.20 to 7.22) did not show this behaviour.

Test No.	Equalisation Stage			Consolidation Stage +		
	Specimen Specific Volume • at the end of this stage %	Specimen Water Content %	Specimen Suction ** $(u_a - u_w)$ kPa	Specimen Specific Volume • at the end of this stage %	Specimen Water Content %	Specimen Suction ** $(u_a - u_w)$ kPa
FU-A3	1.381	3.91	75	1.378	3.87	75
FU-A12	1.396	3.92	25	1.392	3.90	25

	Combined Equalisation and consolidation Stage +		
FU-A1	1.412	3.62	75
FU-A2	1.402	3.54	75
FU-A4	1.372	3.78	75
FU-A5	1.372	3.66	75
FU-A6	1.373	3.91	50
FU-A7	1.371	3.94	50
FU-A8	1.384	3.74	50
FU-A9	1.381	3.80	50
FU-A10	1.394	4.07	25
FU-A11	1.383	4.05	25
FU-A13	1.363	3.78	25
FU-A14	1.372	3.84	25

+ Net cell pressure values for the consolidation or combined stage are same as those in the shearing stage (Table 7.2).

• Values of Specific Volume are calculated from measurements of internal strains.

** $u_a = 90$ kPa

Table 7.1- Results of the equalisation, consolidation and combined equalisation and consolidation stages for test series A, for the unsaturated fine grading specimens.

Test No.	Suction ** $(u_a - u_w)$ kPa	Net Cell Pressure ** $(\sigma_3 - u_a)$ kPa	Deviator Stress $(\sigma_1 - \sigma_3)_f$ at Failure kPa		Axial Strain at Failure %		Internal Lateral Strain at Failure %	Specimen Specific Volume * at Failure %	Specimen Water Content at Failure %
			Calculated using						
			IAS +	EAS +	Internal	External			
FU-A1	75	36.8	449.2	448.4	0.565	0.747	0.558	1.419	3.62
FU-A2	75	62.9	592.4	591.7	0.809	0.916	0.461	1.405	3.52
FU-A3	75	78.4	669.3	665.8	0.638	1.161	0.363	1.379	3.82
FU-A4	75	91.3	730.9	729.3	0.883	1.099	0.618	1.377	3.75
FU-A5	75	91.6	751.0	748.3	0.997	1.351	0.471	1.377	3.63
FU-A6	50	31.7	394.1	394.0	0.644	0.645	0.554	1.380	3.90
FU-A7	50	57.7	509.4	506.8	0.530	1.041	0.342	1.377	3.94
FU-A8	50	81.2	607.4	606.1	0.631	0.850	0.392	1.386	3.72
FU-A9	50	115.1	757.1	755.4	0.973	1.192	0.571	1.382	3.78
FU-A10	25	35.8	309.0	308.5	0.554	0.705	0.296	1.401	4.08
FU-A11	25	61.4	426.4	424.9	0.483	0.836	0.264	1.385	4.03
FU-A12	25	80.3	543.7	542.7	0.747	0.927	0.393	1.394	3.90
FU-A13	25	92.6	703.0	701.7	0.928	1.111	0.484	1.366	3.76
FU-A14	25	114.2	730.8	730.3	0.965	1.037	0.457	1.375	3.84

+ IAS and EAS = deviator stress calculated using the Internal and External Axial Strain measurements respectively.

* Values of Specific Volume are calculated from measurements of volume change unit.

** u_a = 90 kPa

Table 7.2- Results of the drained shearing tests for test of series A, for the unsaturated fine grading specimens.

Test No.	Water Content (%) at different locations in the tested specimen Top → Bottom			
FU-A2	3.59	3.60	3.61	3.61
FU-A3	3.74	3.87	3.75	3.76
FU-A7	3.88	3.80	3.82	3.90
FU-A8	3.85	3.91	3.79	3.75
FU-A9	3.66	3.69	3.71	3.69
FU-A10	4.05	3.99	4.05	4.02
FU-A13	3.80	3.84	3.81	3.77
FU-A14	3.83	3.84	3.84	3.83
FU-B1	3.84	3.91	3.89	3.86
FU-C1	4.03	3.98	3.97	3.92
FU-C2	3.99	3.91	3.97	3.99
CU-D1	3.98	3.98	3.96	3.99
CU-D3	4.09	4.13	4.12	4.11

Table 7.3- Values of the water content of the tested specimens, taken at the end of the test, at different heights in the specimen

Test No.	Equalisation Stage			Consolidation Stage +		
	Specimen Specific Volume * at the end of this stage %	Specimen Water Content %	Specimen Suction ** (u_a-u_w) kPa	Specimen Specific Volume * at the end of this stage %	Specimen Water Content %	Specimen Suction ** (u_a-u_w) kPa
FU-B2	1.392	3.93	25	1.389	3.91	25

	Combined Equalisation and consolidation Stage +		
FU-B1	1.373	4.00	25

+ Net cell pressure values for the consolidation or combined stage are same as those in the shearing stage (Table 7.5).

* Values of Specific Volume are calculated from measurements of internal strains.

** u_a = 90 kPa

Table 7.4- Results of the equalisation, consolidation and combined equalisation and consolidation stages for test series B, for the unsaturated fine grading specimens.

Test No.	Suction ** (u_a-u_w) at Failure kPa	Net Cell Pressure ** (σ_3-u_a) kPa	Deviator Stress $(\sigma_1-\sigma_3)_f$ at Failure kPa		Axial Strain at Failure %		Internal Lateral Strain at Failure %	Specimen Specific Volume * at Failure %
			Calculated using					
			IAS +	EAS +	Internal	External		
FU-B1	34.7	93.6	696.0	693.0	1.0336	1.459	0.729	1.376
FU-B2	34.5	93.9	658.3	652.9	0.963	1.786	0.445	1.392

+ IAS and EAS = deviator stress calculated using the Internal and External Axial Strain measurements respectively.

* Values of Specific Volume are calculated from measurements of volume change unit.

** u_a = 90 kPa

Table 7.5- Results of the constant water content shearing tests for test series B, for the fine grading specimens.

Test No.	Equalisation Stage		Consolidation Stage +	
	Specimen Specific Volume • at the end of this stage %	Specimen Suction •• at the end of this stage $(u_a - u_w)$ kPa	Specimen Specific Volume • at the end of this stage %	Specimen Suction •• at the end of this stage $(u_a - u_w)$ kPa
FU-C1	1.386	31.2	1.386	32.7
FU-C2	1.327	37.4	1.326	34.7

+ Net cell pressure values for the consolidation stage are same as those in the shearing stage (Table 7.7).

• Values of Specific Volume are calculated from measurements of internal strains.

•• u_a = 60 kPa

Table 7.6- Results of the equalisation and consolidation stages of test series C, for the unsaturated fine grading specimens.

Test No.	Suction •• $(u_a - u_w)$ at Failure kPa	Net Cell Pressure •• $(\sigma_3 - u_a)$ kPa	Deviator Stress $(\sigma_1 - \sigma_3)_f$ at Failure kPa		Axial Strain at Failure %		Internal Lateral Strain at Failure %	Specimen Specific Volume • at Failure %
			Calculated using					
			IAS +	EAS +	Internal	External		
FU-C1	28.1	64.9	493.9	492.5	0.638	0.913	0.401	1.390
FU-C2	31.2	84.6	741.3	738.9	0.722	1.042	0.390	1.331

+ IAS and EAS = deviator stress calculated using the Internal and External Axial Strain measurements respectively.

• Values of Specific Volume are calculated from measurements of volume change unit.

•• u_a = 60 kPa

Table 7.7- Results of the constant water content shearing tests for test series C, for the unsaturated fine grading specimens.

Test No.	Equalisation Stage		Consolidation Stage +	
	Specimen Specific Volume * at the end of this stage %	Specimen Suction ** at the end of this stage $(u_a - u_w)$ kPa	Specimen Specific Volume * at the end of this stage %	Specimen Suction ** at the end of this stage $(u_a - u_w)$ kPa
CU-D1	1.286	12.2	1.286	12.7
CU-D2	1.272	11.8	1.270	12.8
CU-D3	1.280	9.7	1.277	10.2

+ Net cell pressure values for the consolidation stage are same as those in the shearing stage (Table 7.9).

* Values of Specific Volume are calculated from measurements of internal strains.

** u_a = 60 kPa

Table 7.8- Results of the equalisation and consolidation stages for test series D, for the unsaturated coarse grading specimens.

Test No.	Suction ** $(u_a - u_w)$ at Failure kPa	Net Cell Pressure ** $(\sigma_3 - u_a)$ kPa	Deviator Stress $(\sigma_1 - \sigma_3)_f$ at Failure kPa		Axial Strain at Failure %		Internal Lateral Strain at Failure %	Specimen Specific Volume * at Failure %
			Calculated using					
			IAS +	EAS +	Internal	External		
CU-D1	10.1	40.8	492.1	491.1	0.770	0.985	0.807	1.296
CU-D2	11.3	64.2	625.0	623.8	0.545	0.744	0.862	1.278
CU-D3	8.3	87.8	677.0	674.6	0.729	1.091	0.440	1.284

+ IAS and EAS = deviator stress calculated using the Internal and External Axial Strain measurements respectively.

* Values of Specific Volume are calculated from measurements of volume change unit.

** u_a = 60 kPa

Table 7.9- Results of the constant water content shearing tests for test series D, for the unsaturated coarse grading specimens.

Test No.	Specimen Specific Volume • at the end of the consolidation stage %
FS-E1	1.399
FS-E2	1.388
FS-E3	1.391
FS-E4	1.395
FS-E5	1.382

Effective cell pressure values for the consolidation stage are same as those in the shearing stage (Table 7.11).

• Values of Specific Volume are calculated from measurements of volume change unit.

u_w = 540 kPa

Table 7.10- Results of the consolidation stage of test series D, for the saturated fine grading specimens.

Test No.	Effective Cell Pressure •• $(\sigma_3 - u_w)$ kPa	Deviator Stress $(\sigma_1 - \sigma_3)_f$ at Failure kPa	External Axial Strain at Failure %	Specimen Specific Volume • at Failure %
FS-E1	25.7	252.6	0.556	1.403
FS-E2	50.7	335.6	1.069	1.385
FS-E3	75.7	433.5	0.702	1.389
FS-E4	100.7	497.0	0.678	1.395
FS-E5	125.7	608.2	0.745	1.382

• Values of Specific Volume are calculated from measurements of volume change unit.

•• u_w = 540 kPa

Table 7.11- Results of the drained shearing tests for test series E, for the saturated fine grading specimens.

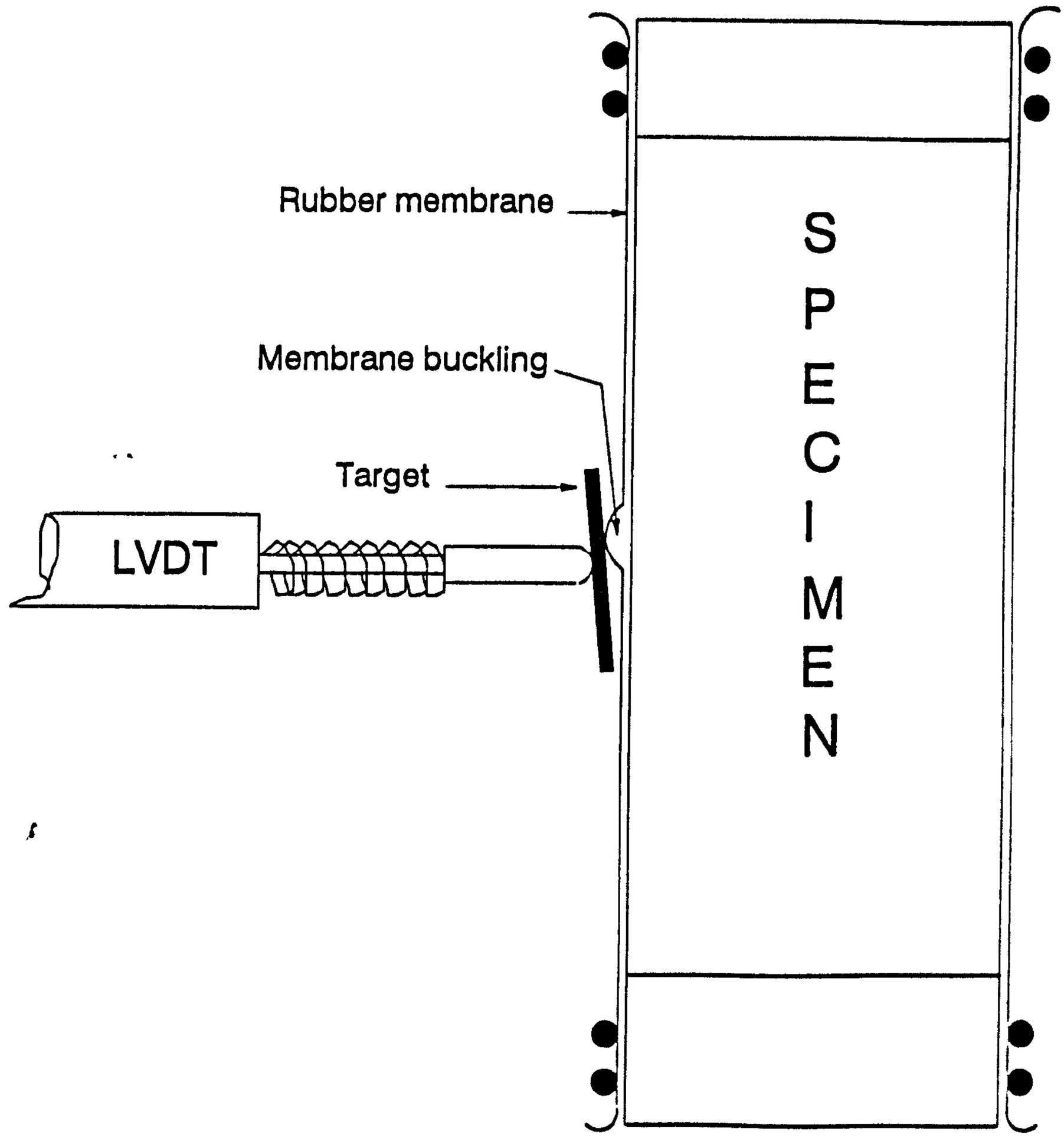

Fig. 7.1- Effect of the membrane buckling on lateral strain measurements

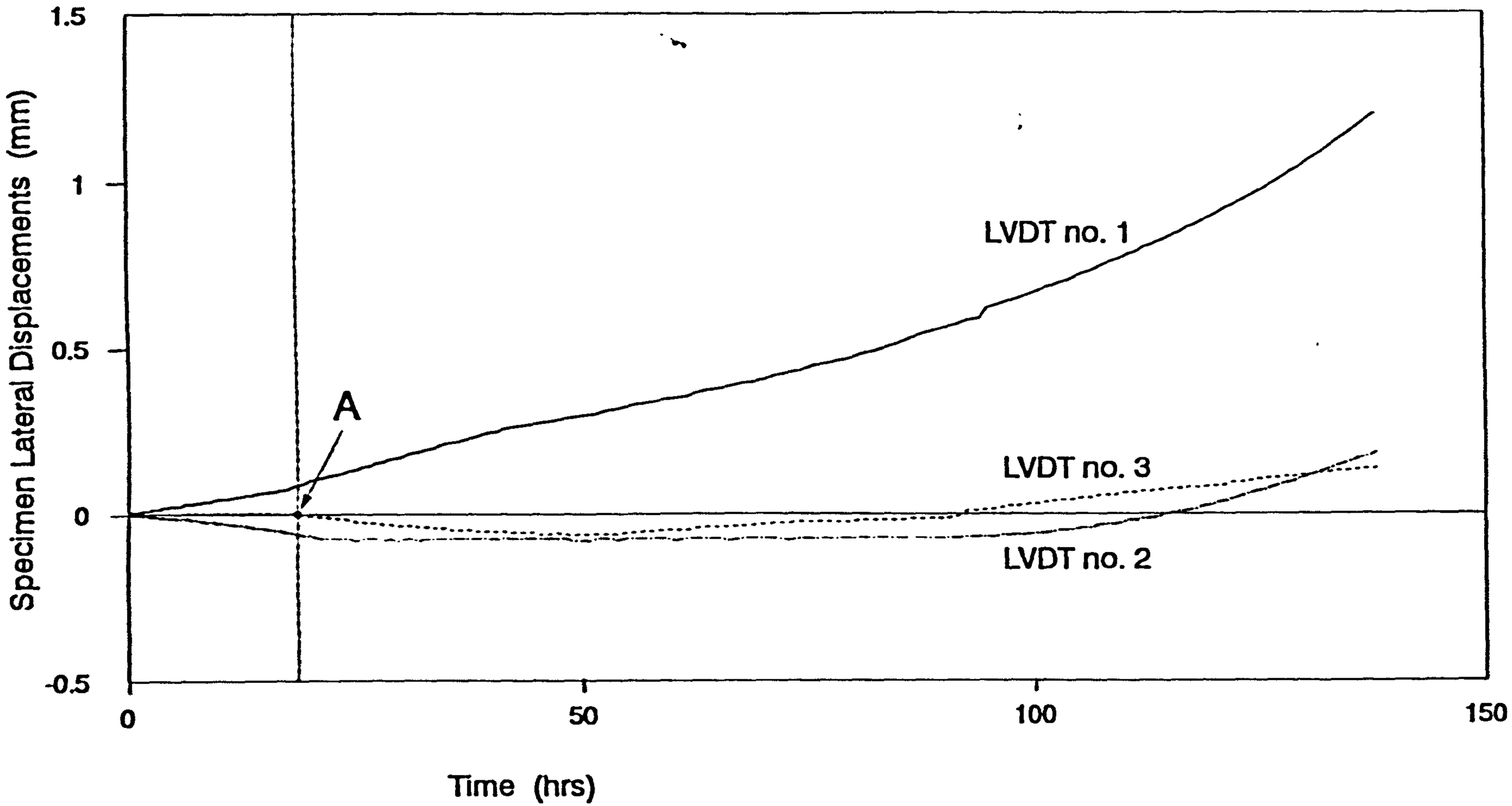

Fig. 7.2- Readings of the three lateral LVDTs during shearing process of test FU-A8.

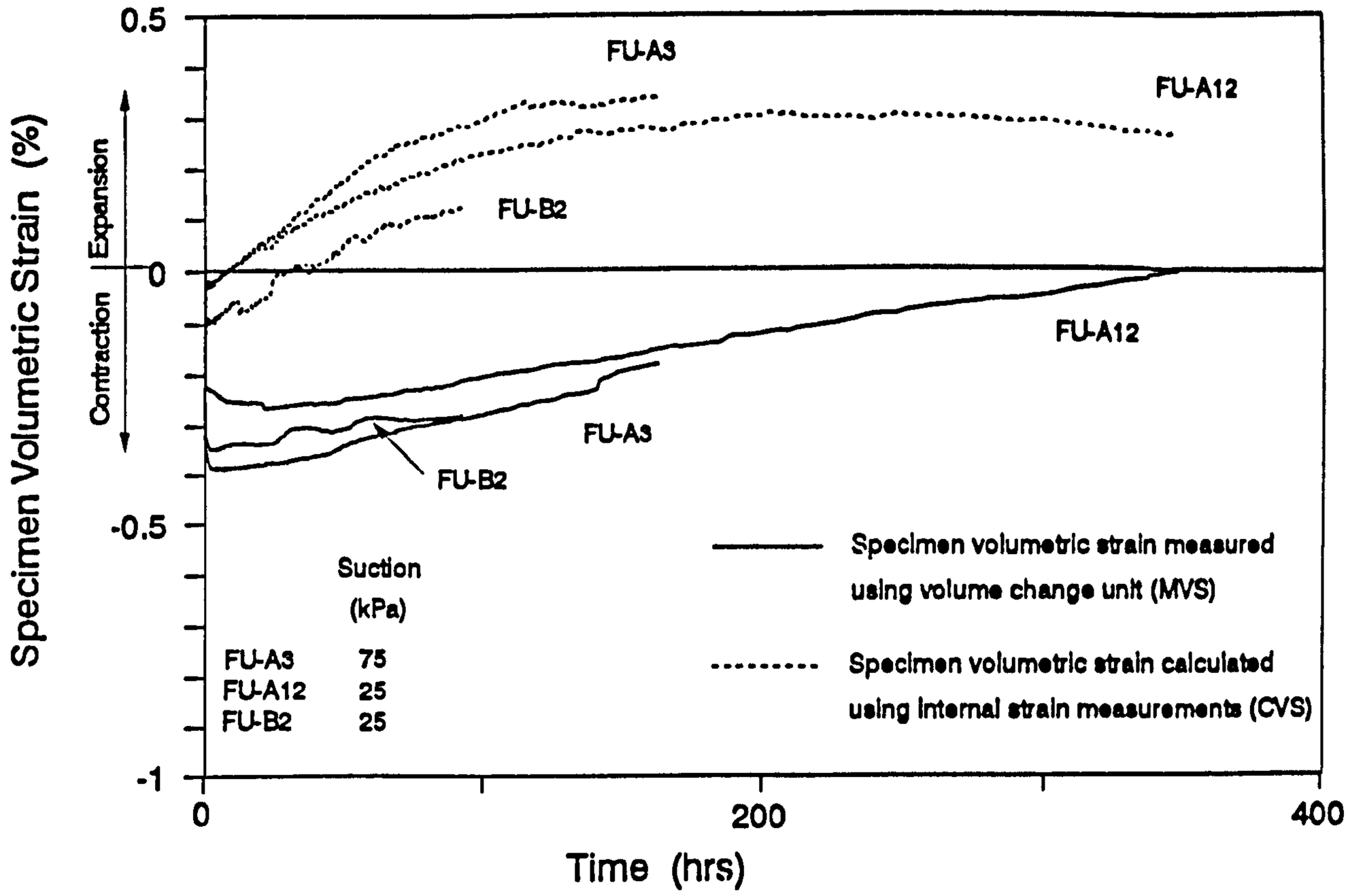

Fig. 7.3a- Specimen volumetric strain during the equalisation stage of tests FU-A3, FU-A13 and FU-B2

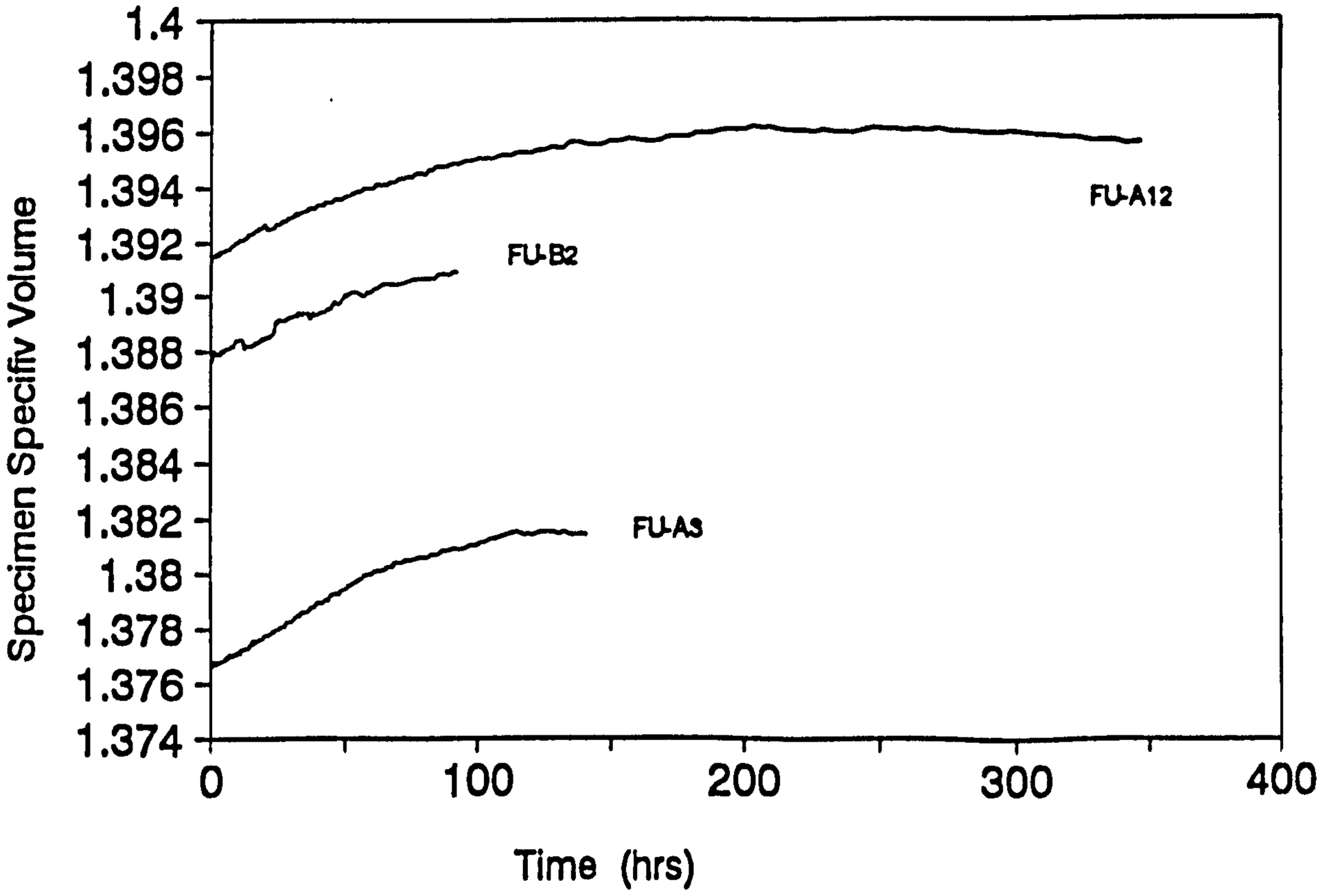

Fig. 7.3b- Specimen Specific Volume during the equalisation stage of tests FU-A3, FU-A13 AND FU-B2

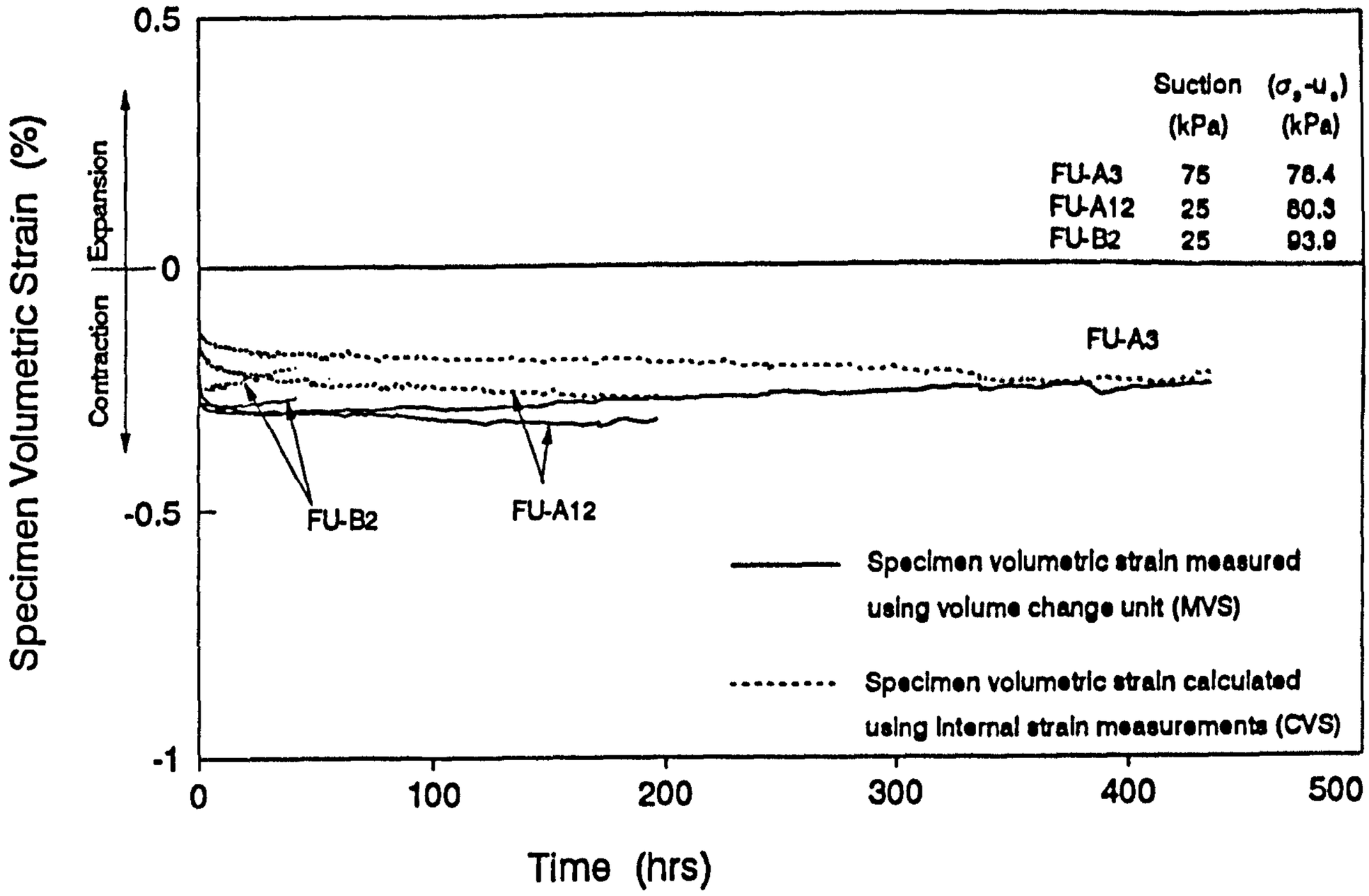

Fig. 7.4a- Specimen volumetric strain during the consolidation stage of tests FU-A3, FU-A13 and FU-B2

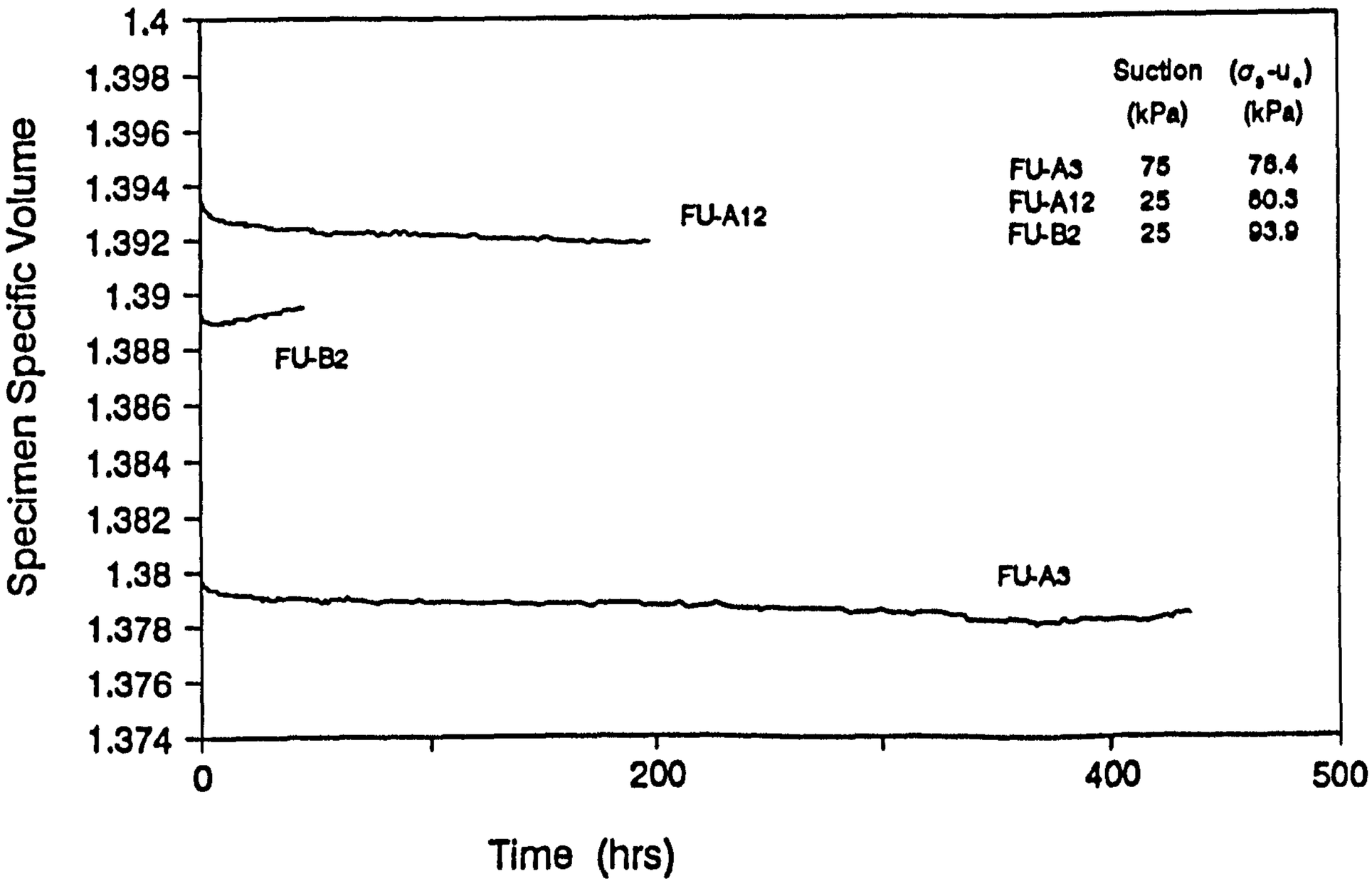

Fig. 7.4b- Specimen Specific Volume during the consolidation stage of tests FU-A3, FU-A13 AND FU-B2

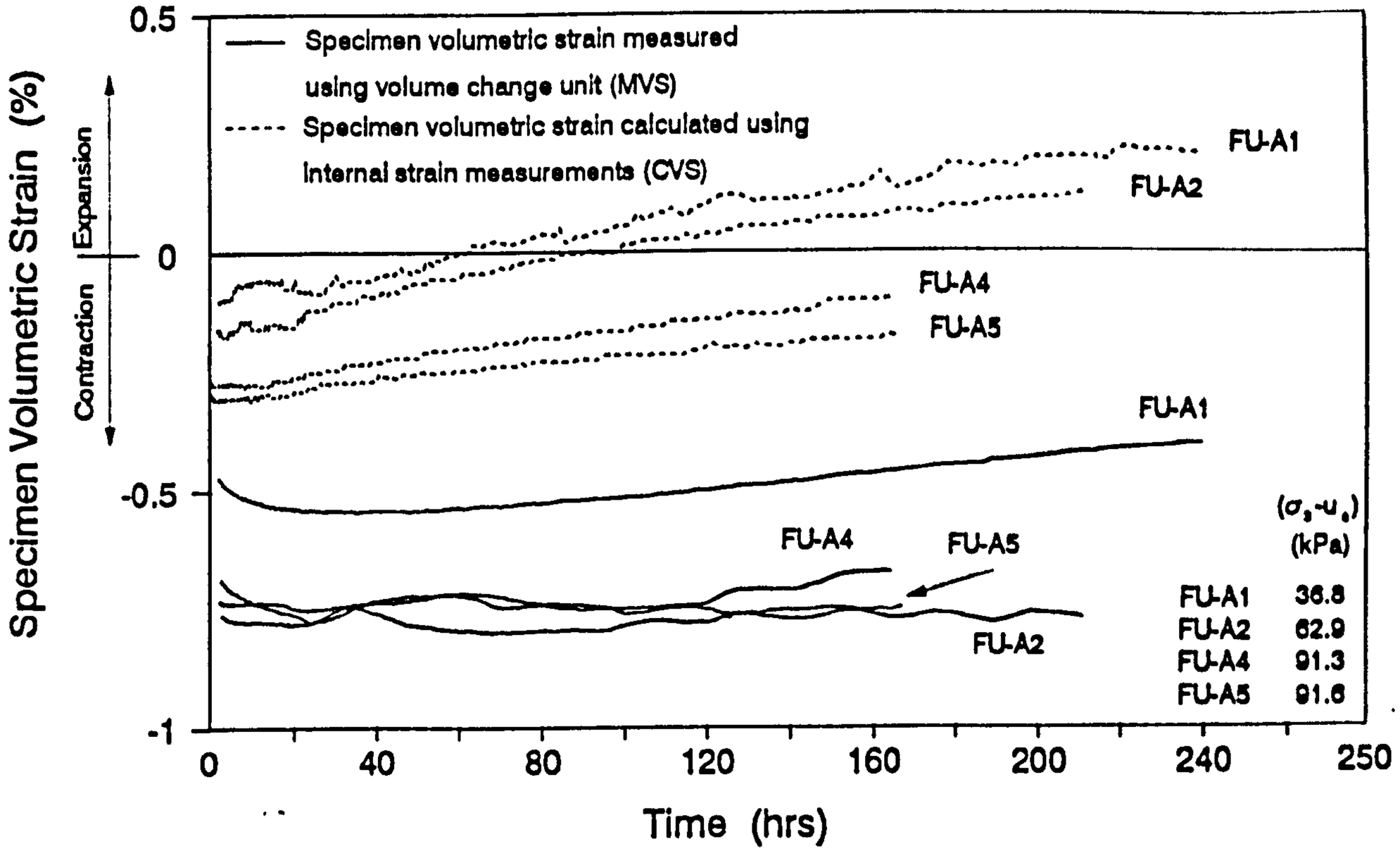

Fig. 7.5a- Specimen volumetric strain during the combined equalisation and consolidation stage, at suction 75 kPa.

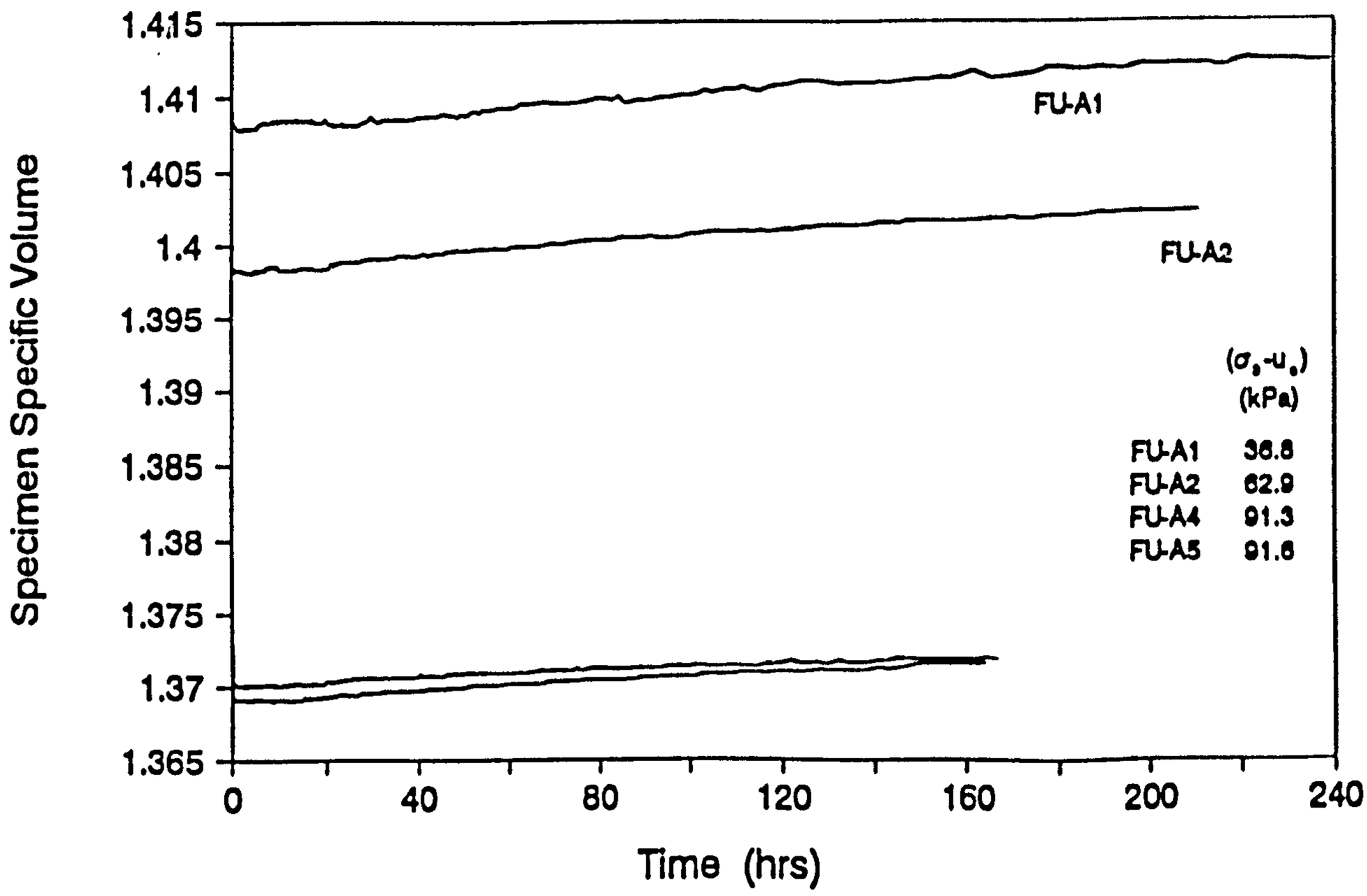

Fig. 7.5b- Specimen specific volume during the combined equalisation and consolidation stage, at suction 75 kPa.

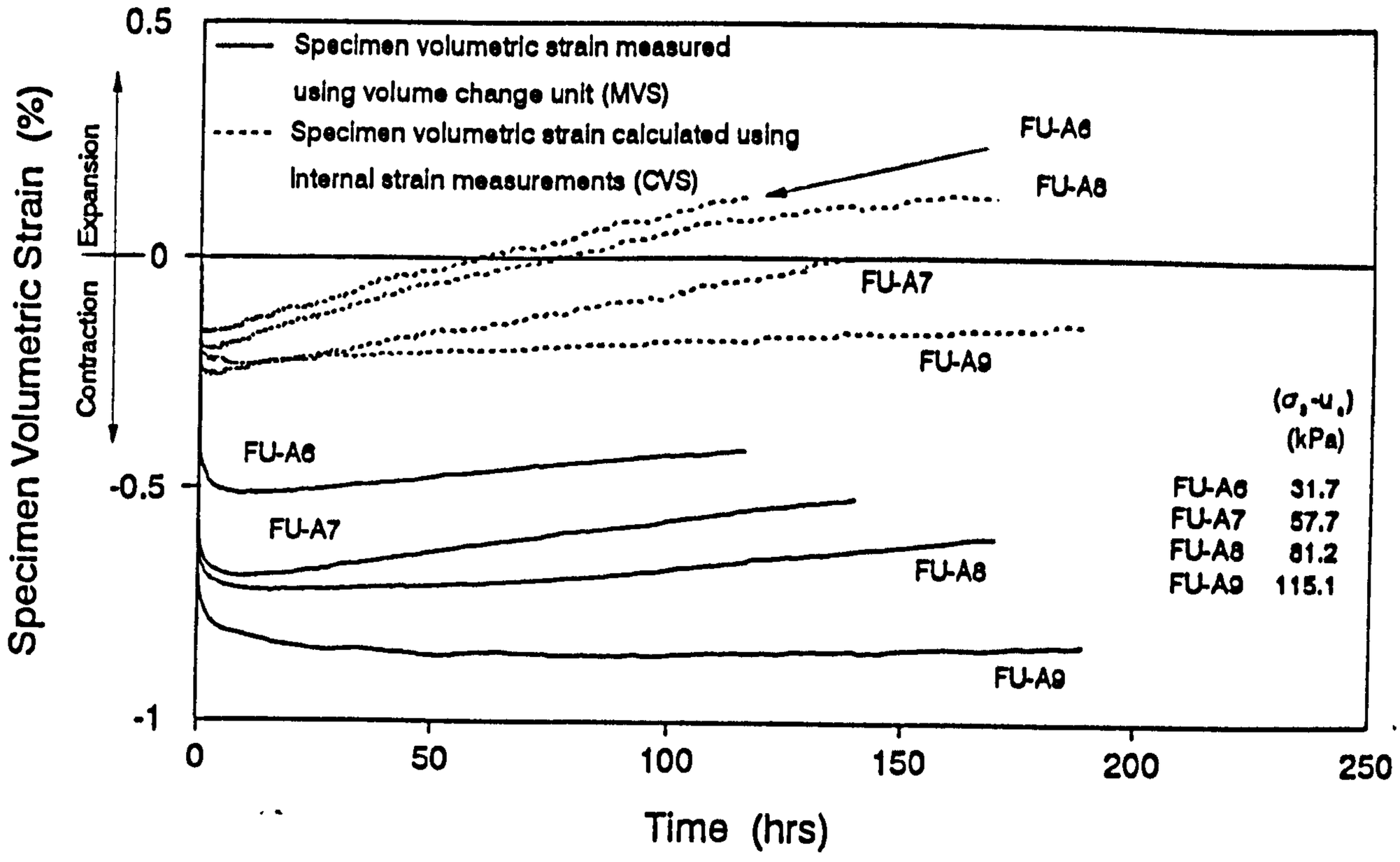

Fig. 7.6a- Specimen volumetric strain during the combined equalisation and consolidation stage, at suction 50 kPa.

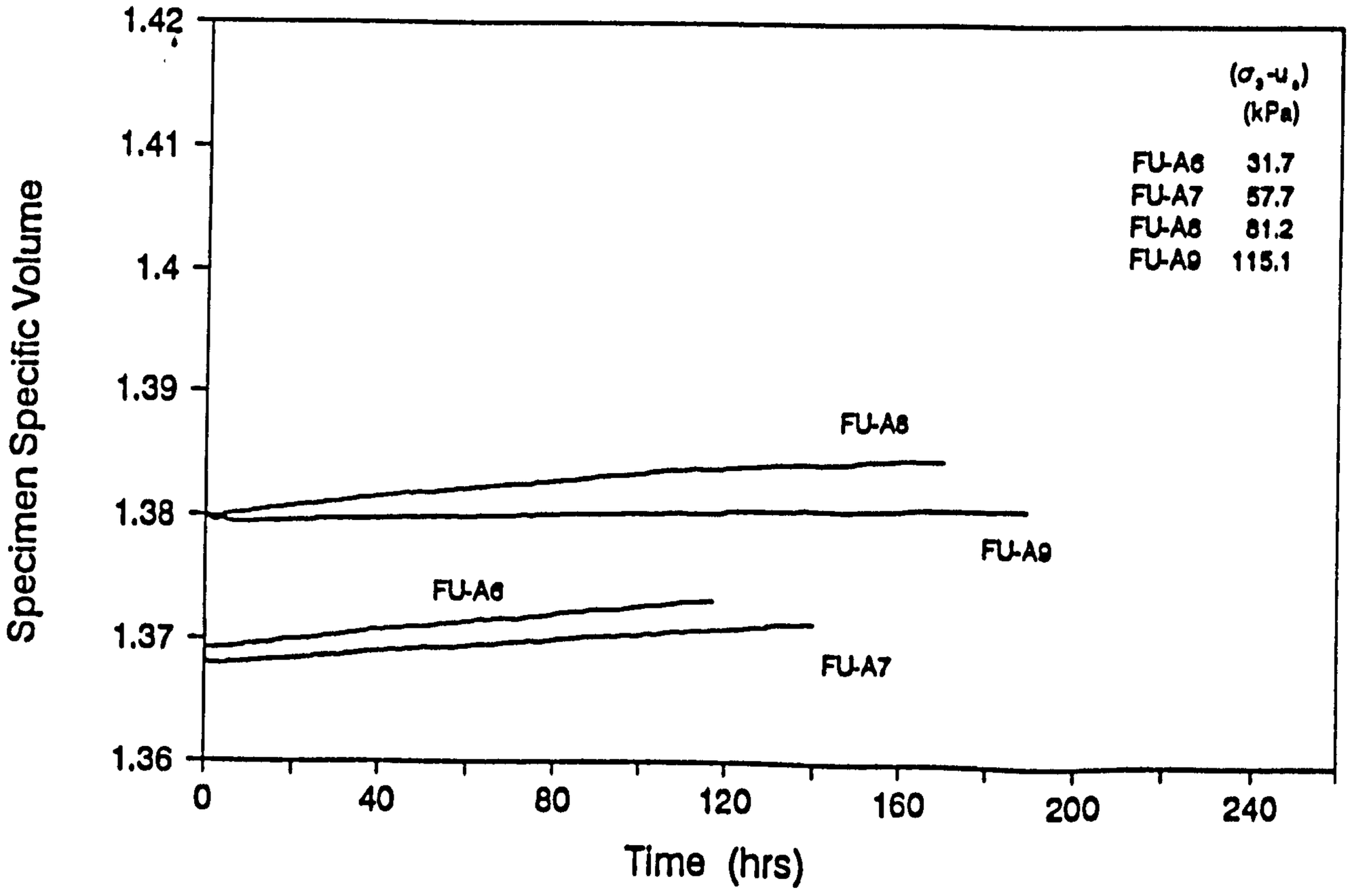

Fig. 7.6b- Specimen specific volume during the combined equalisation and consolidation stage, at suction 50 kPa.

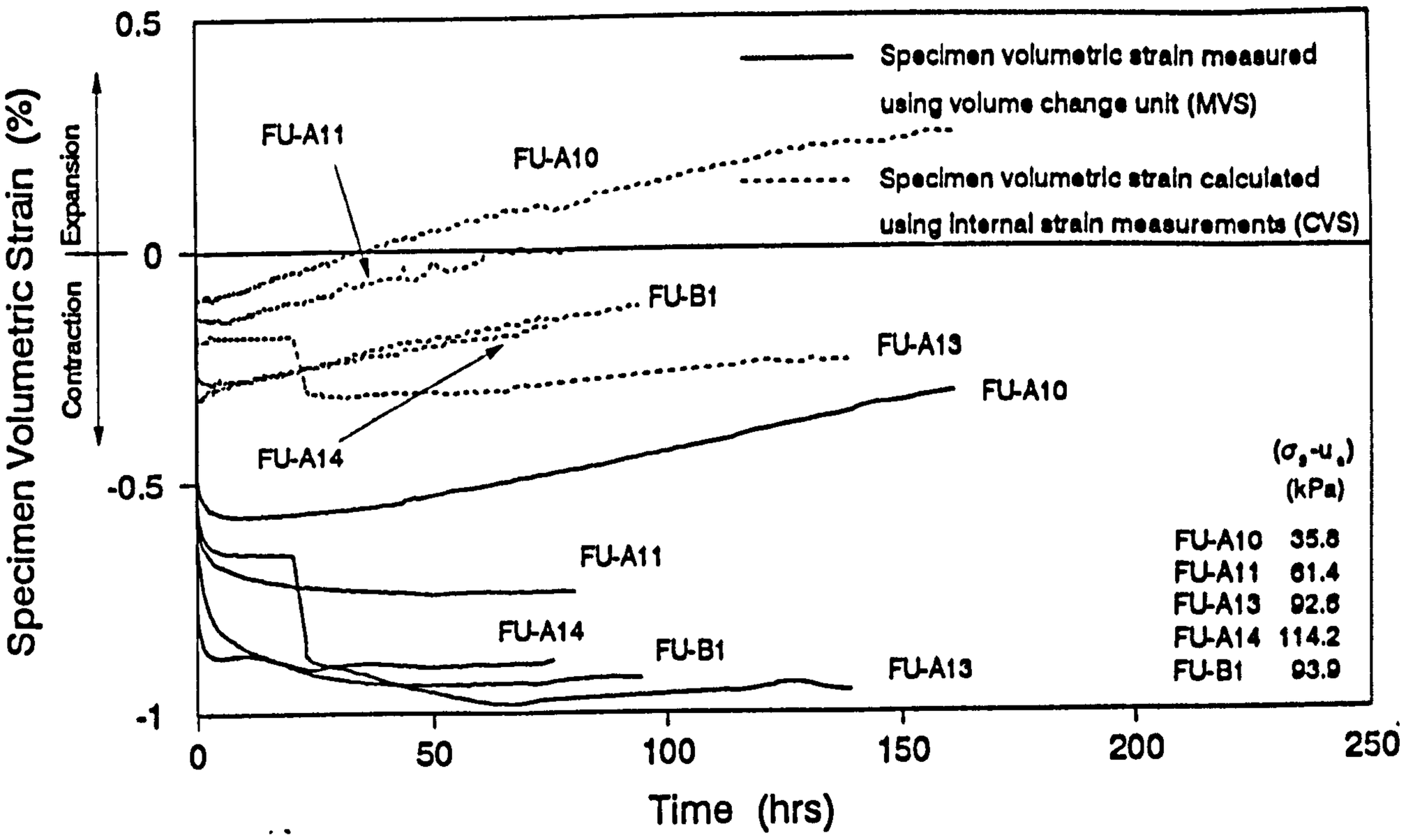

Fig. 7.7a- Specimen volumetric strain during the combined equalisation and consolidation stage, at suction 25 kPa

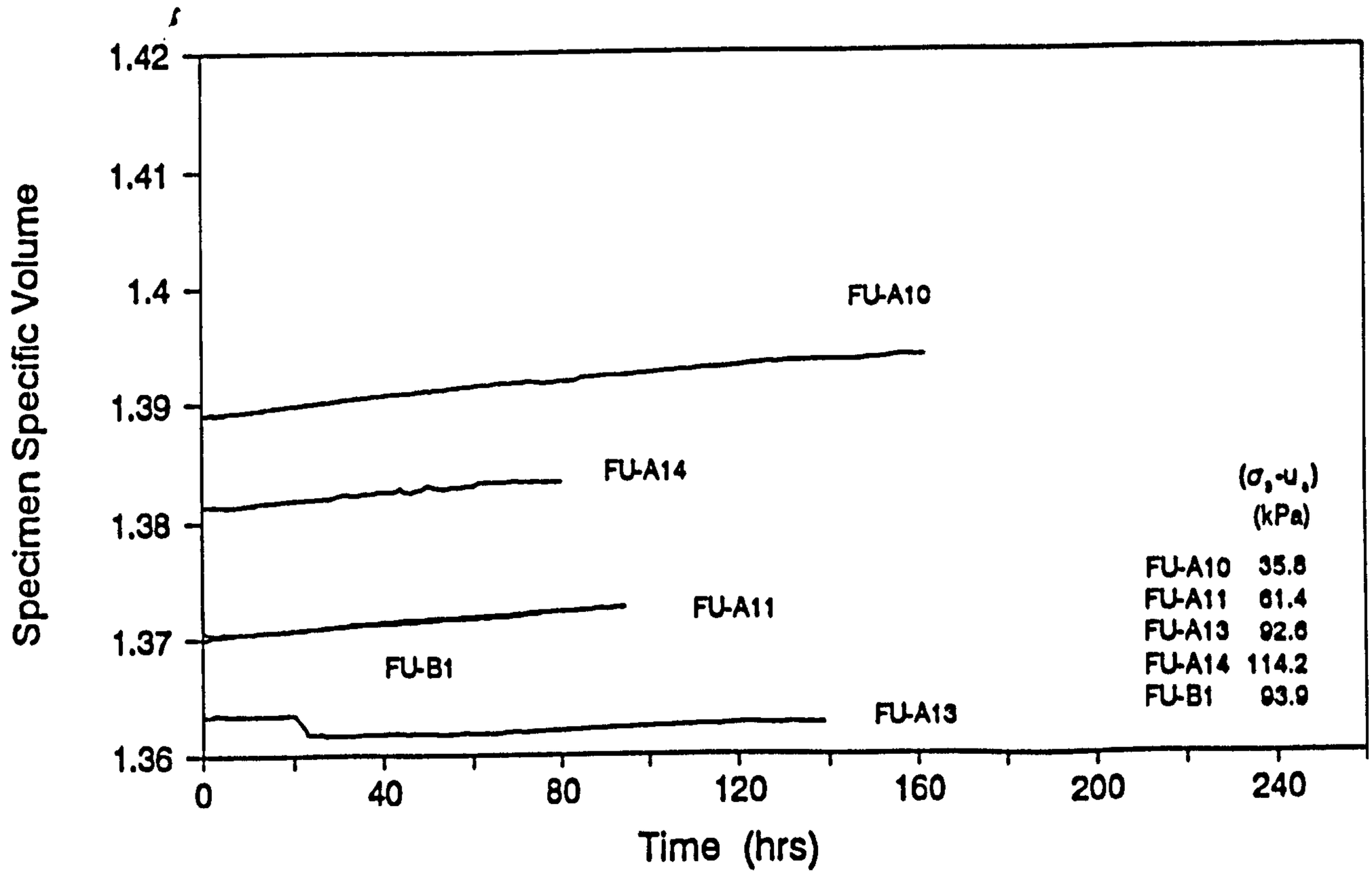

Fig. 7.7b- Specimen specific volume during the combined equalisation and consolidation stage, at suction 25 kPa

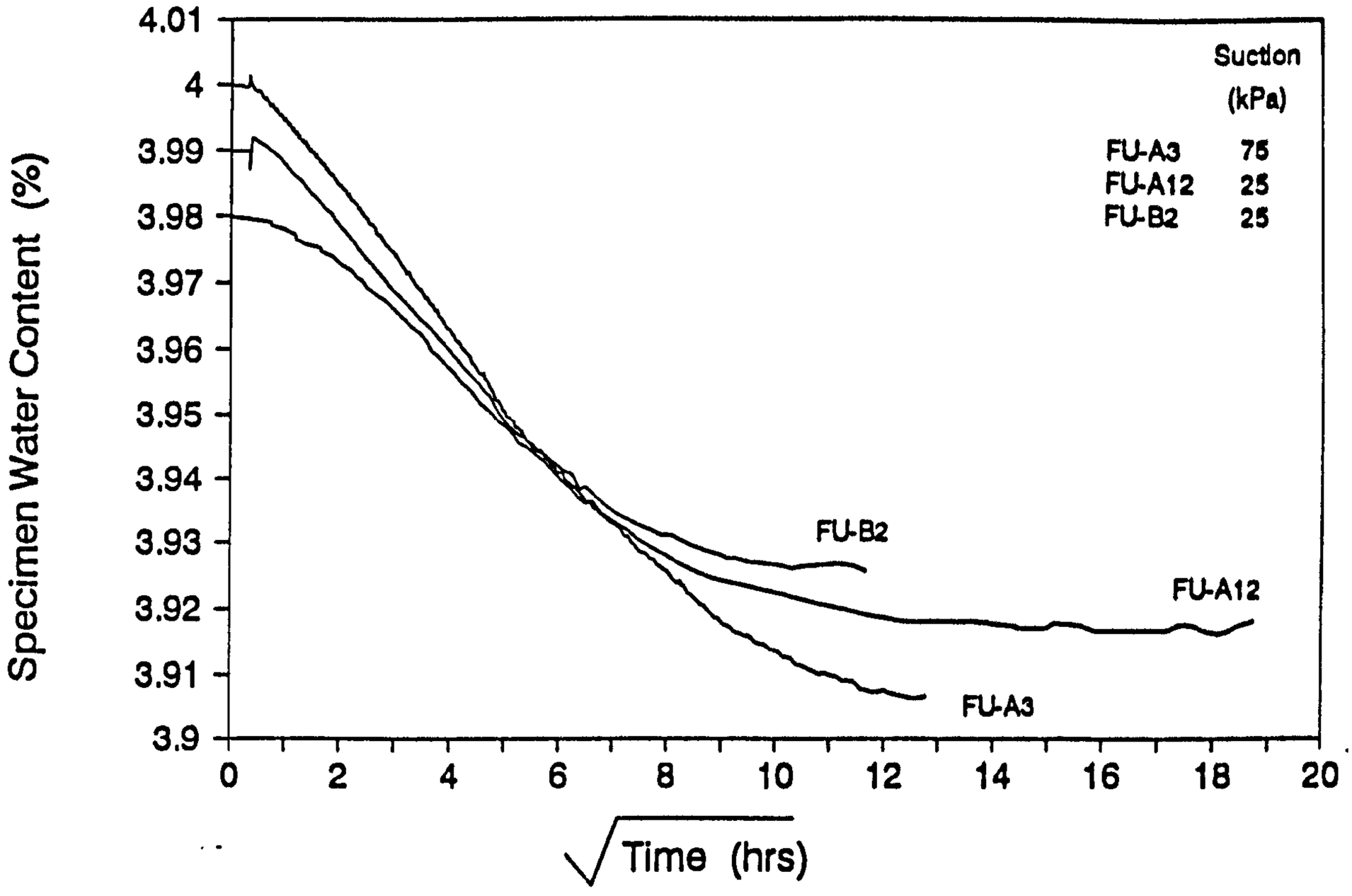

Fig. 7.8- Specimen water content during the equalisation stage of the fine grading specimen tests FU-A3, FU-A13 and FU-B2.

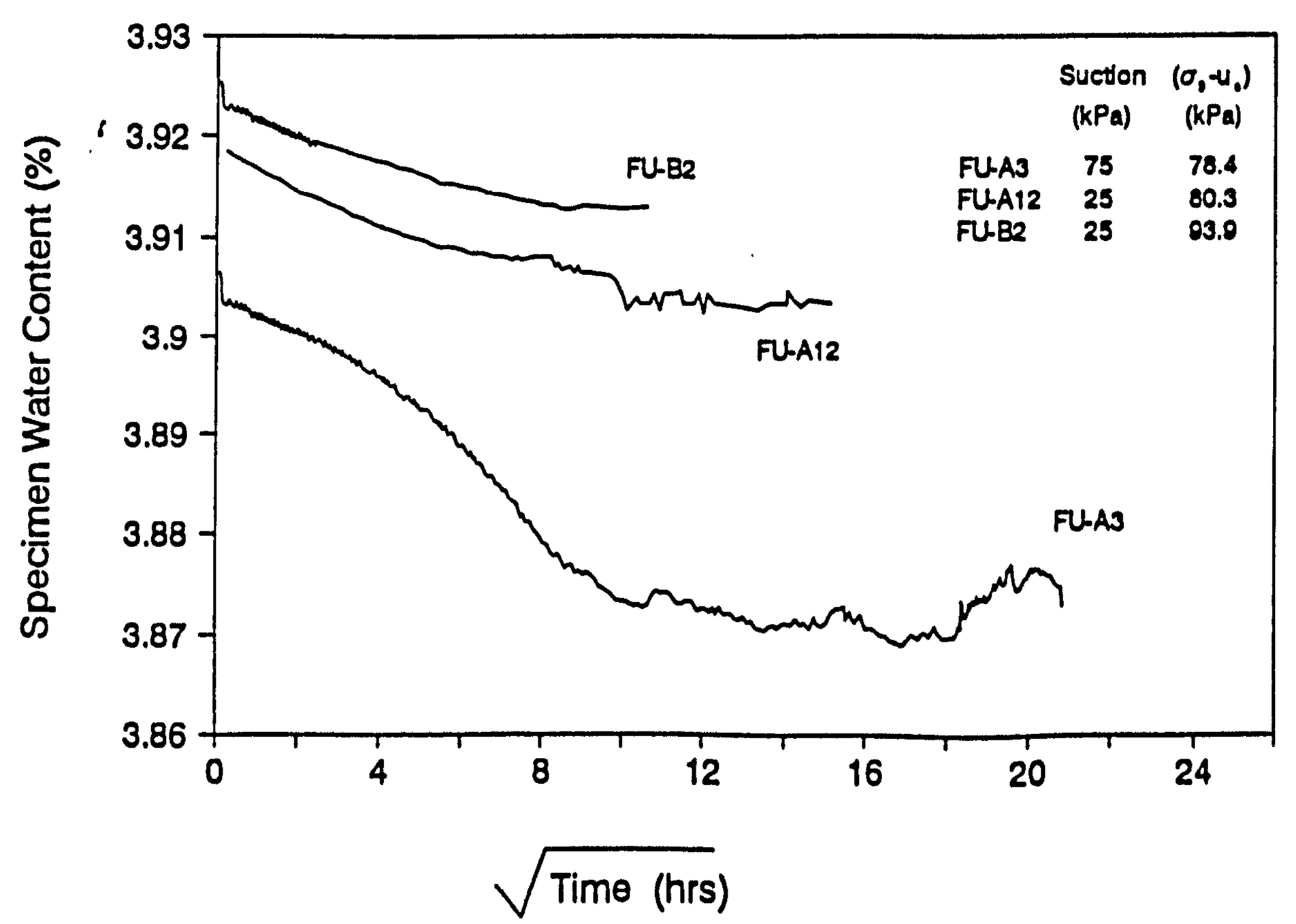

Fig. 7.9- Specimen water content during the consolidation stage of the fine grading specimen tests FU-A3, FU-A13 and FU-B2.

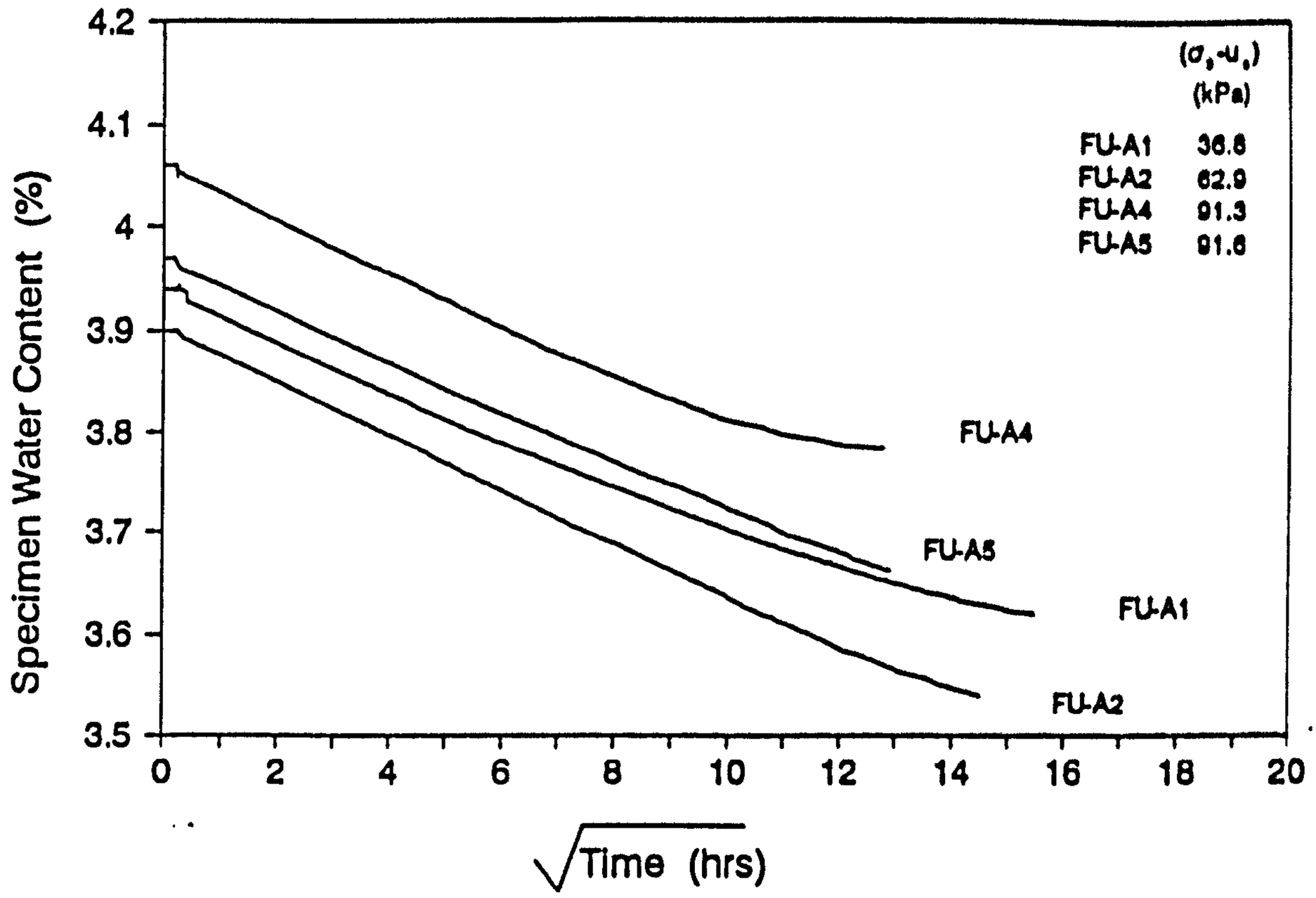

Fig. 7.10- Specimen water content during the combined equalisation and consolidation stage at suction 75 kPa for the fine grading specimens

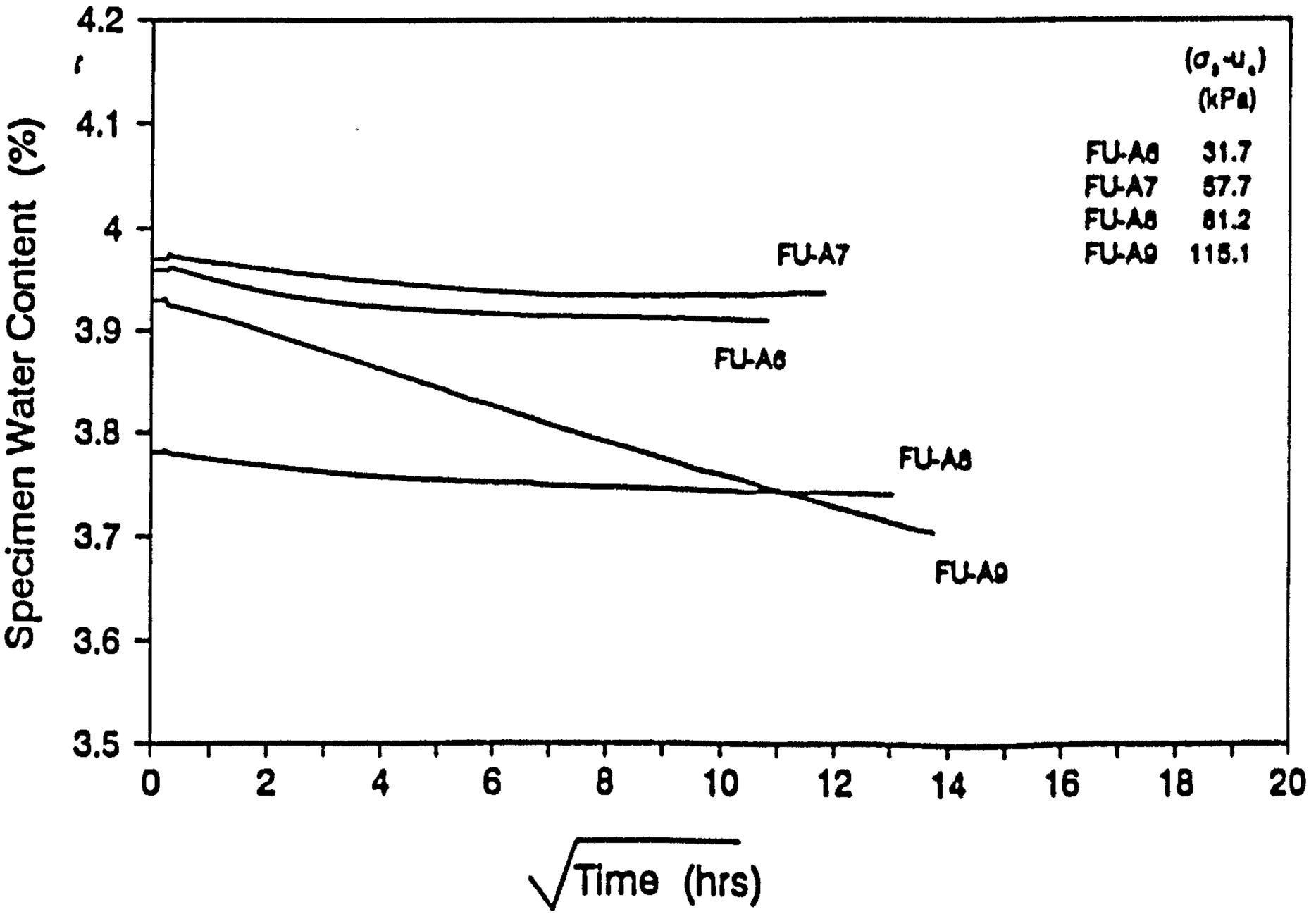

Fig. 7.11- Specimen water content during the combined equalisation and consolidation stage at suction 50 kPa for the fine grading specimens

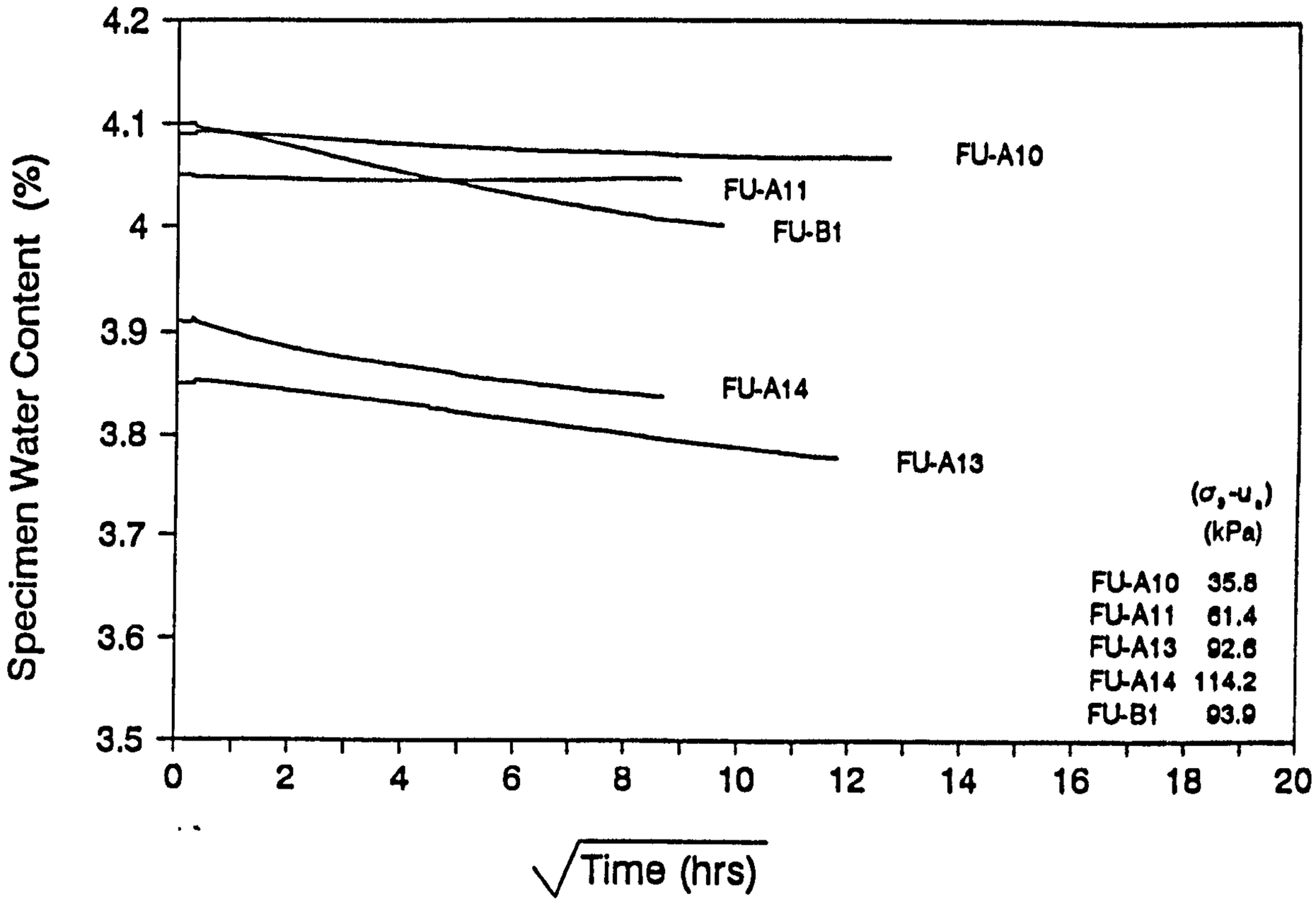

Fig. 7.12- Specimen water content during the combined equalisation and consolidation stage at suction 25 kPa, for the fine grading specimens.

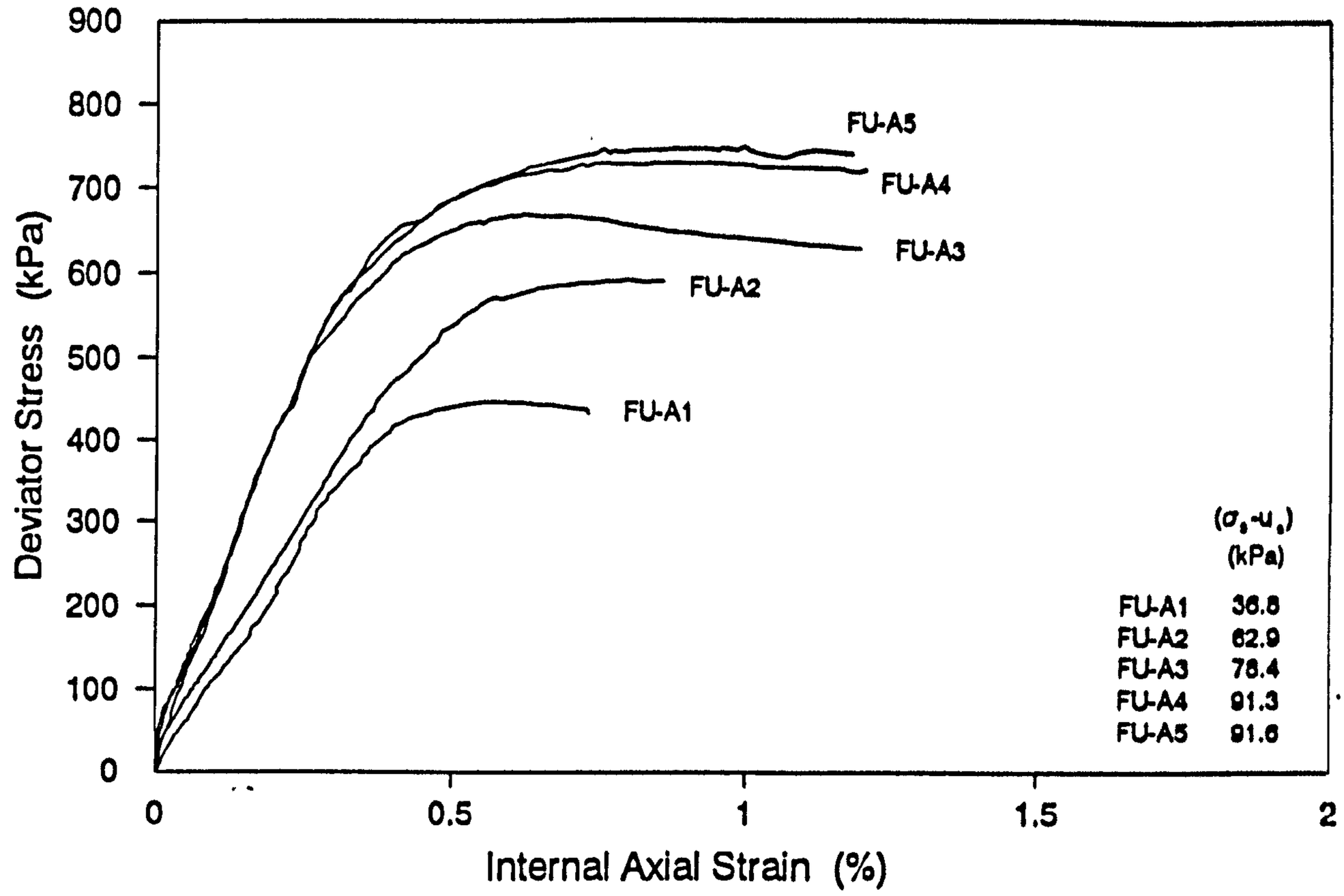

Fig. 7.13 -Deviator stress-strain curves for test series A (Suction =75 kPa)

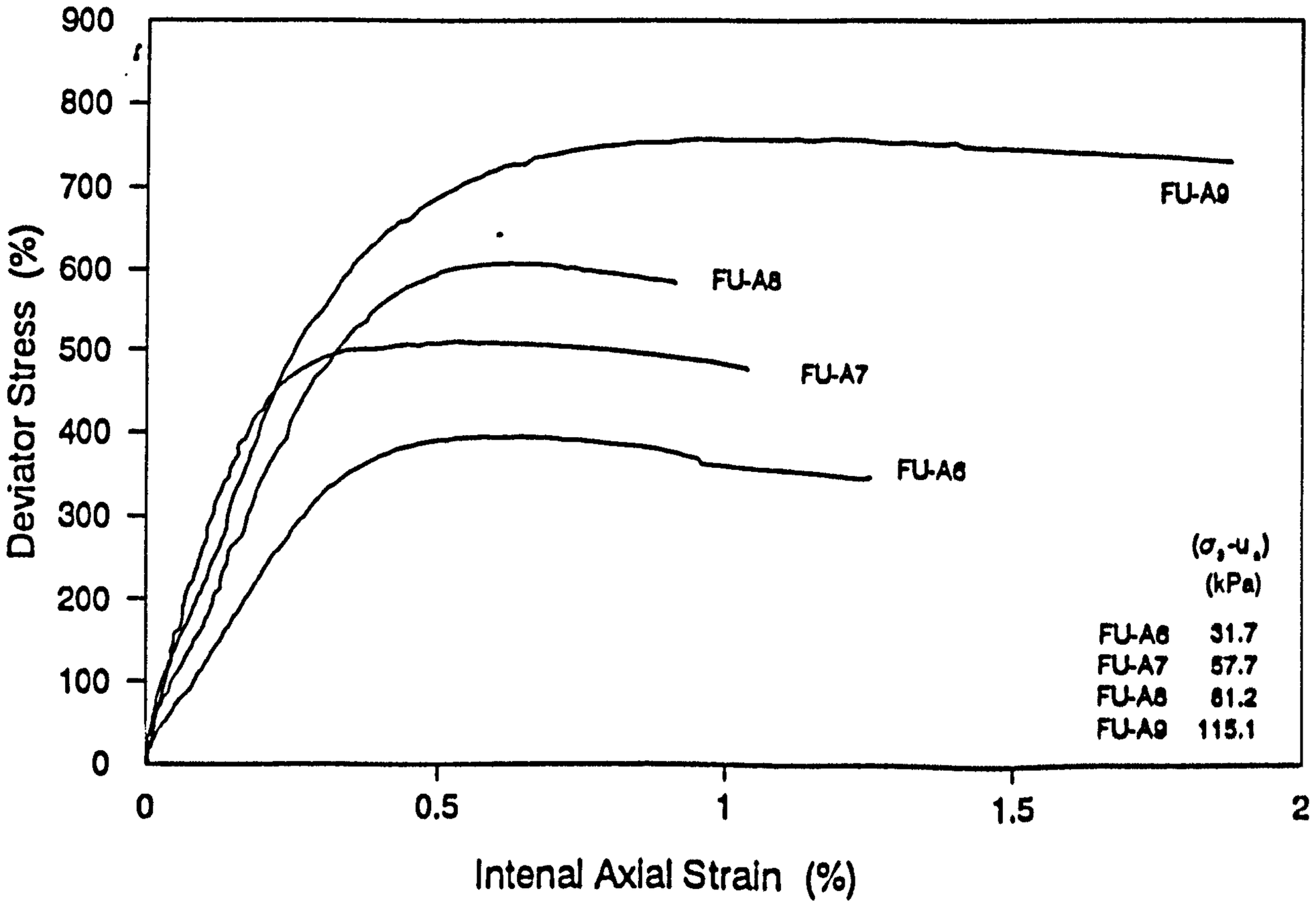

Fig. 7.14 -Deviator stress-strain curves for test series A (Suction =50 kPa)

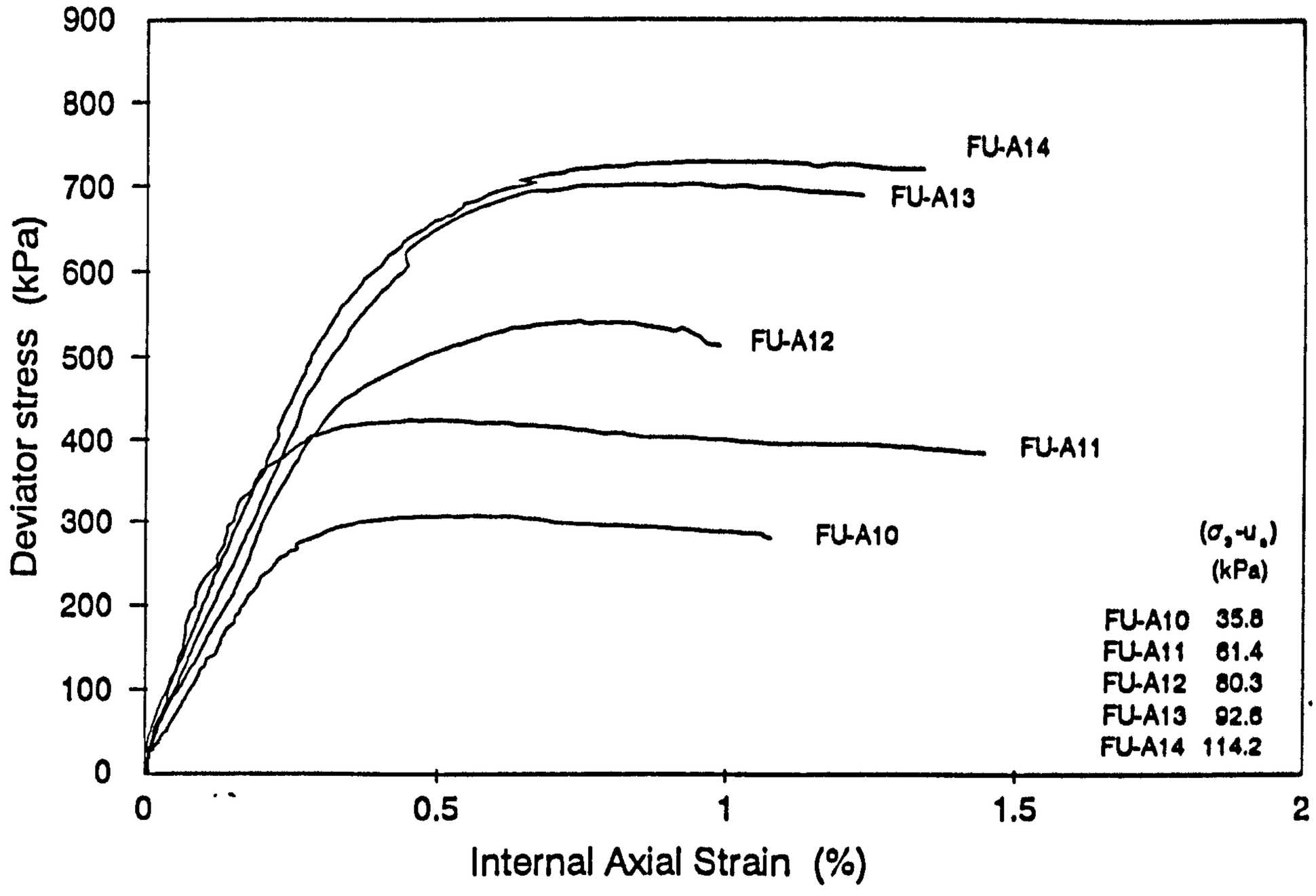

Fig. 7.15 -Deviator stress-strain curves for test series A (Suction =25 kPa)

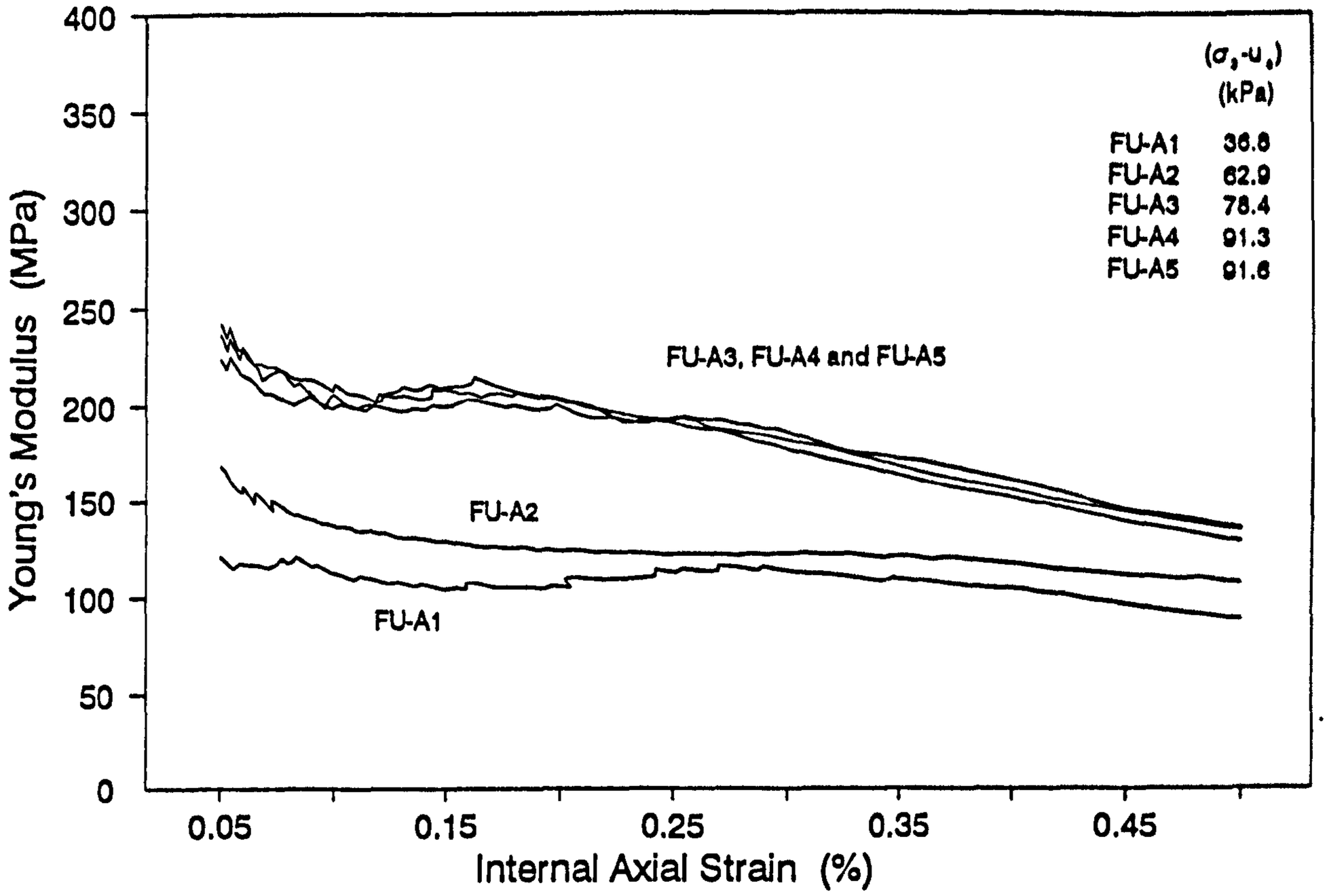

Fig. 7.16- Young's modulus plotted against internal axial strain for test series A (Suction =75 kPa)

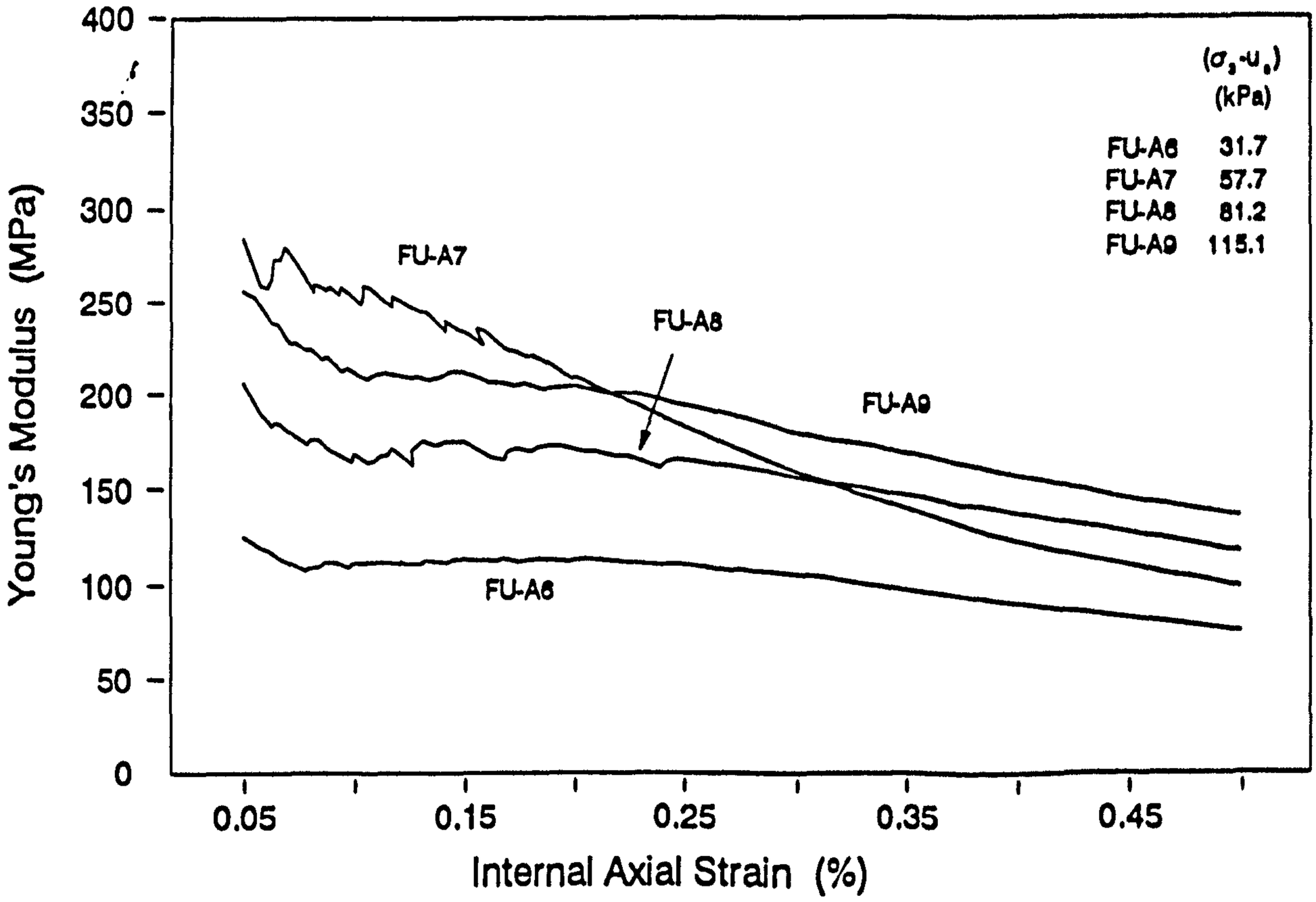

Fig. 7.17- Young's modulus plotted against internal axial strain for test series A (Suction =50 kPa)

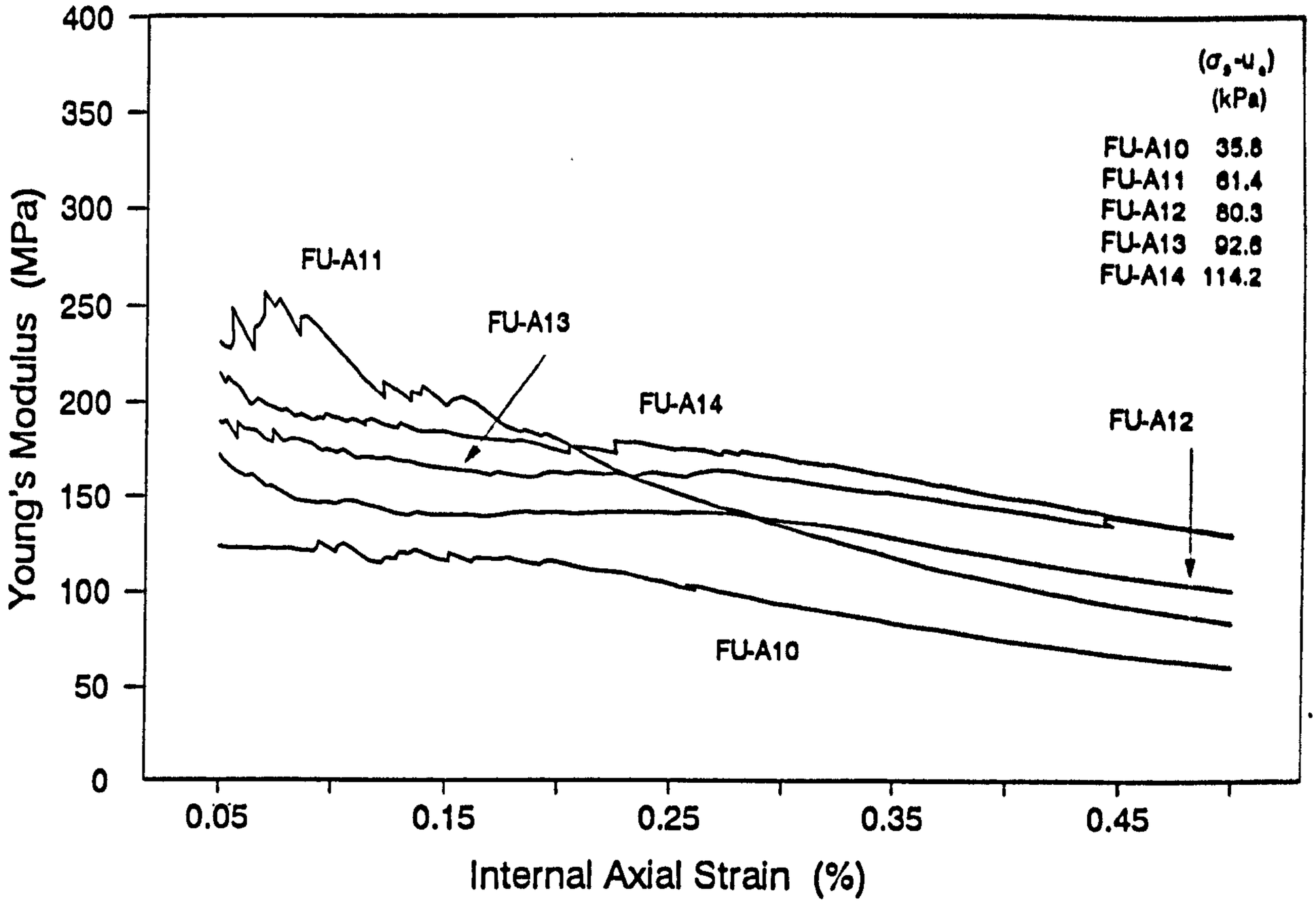

Fig. 7.18- Young's modulus plotted against internal axial strain for test series A (Suction =25 kPa)

Fig. 7.19- Comparison between the Young's modulus calculated using the internal and external axial strains.

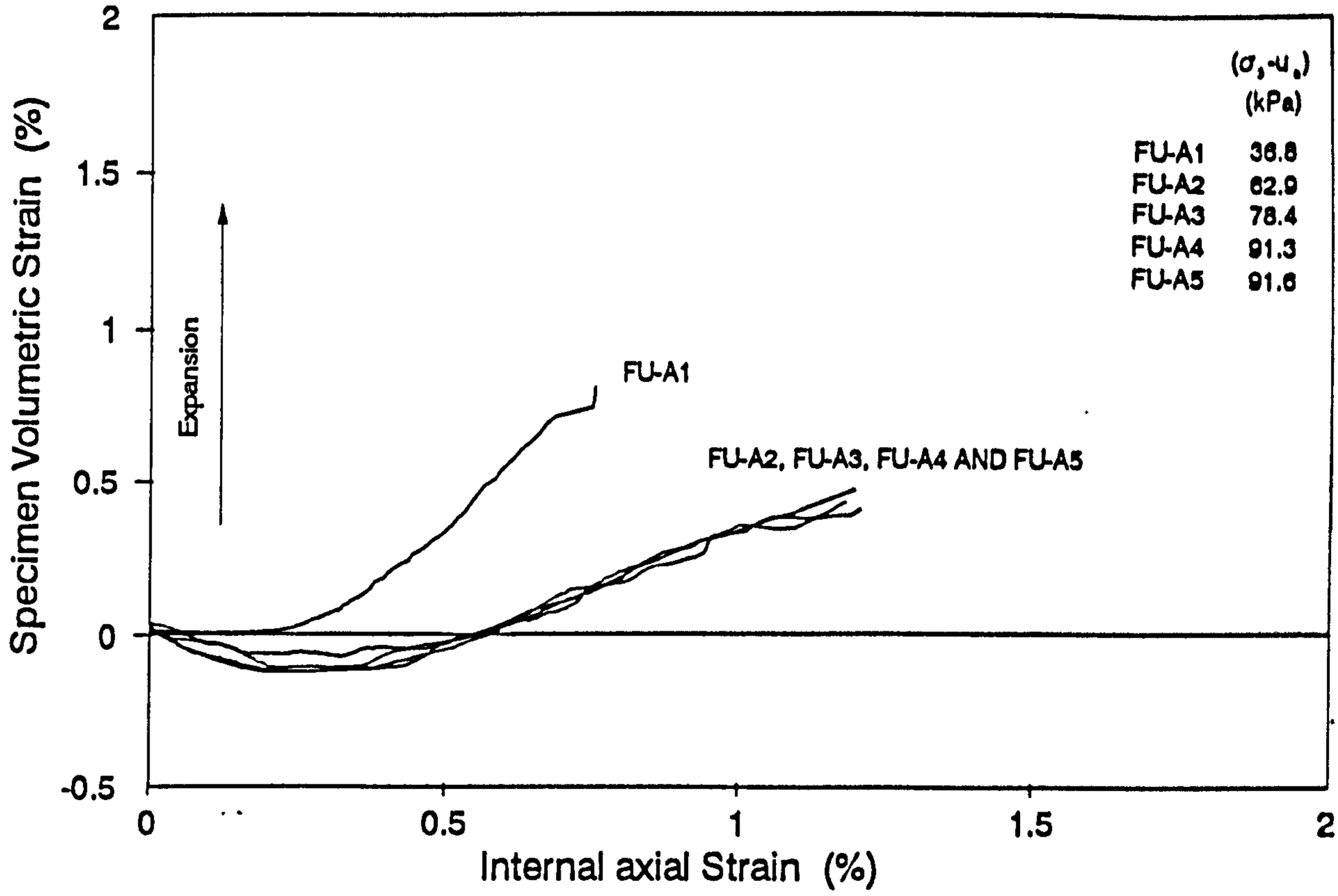

Fig. 7.20a- Specimen volumetric strain measured using the volume change unit during the shearing stage for test series A (Suction =75 kPa)

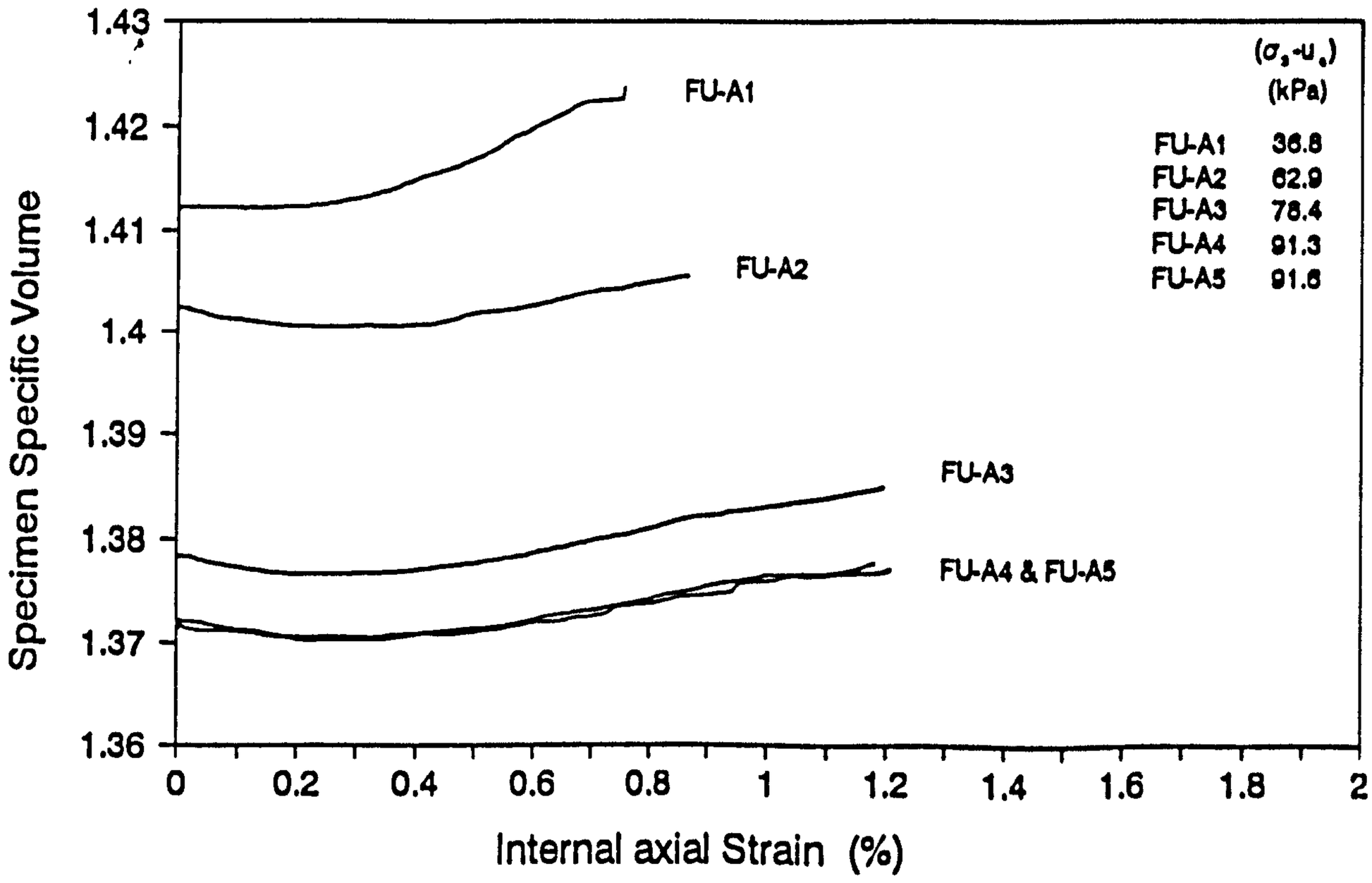

Fig. 7.20b- Specimen specific volume measured using the volume change unit during the shearing stage for test series A (Suction =75 kPa)

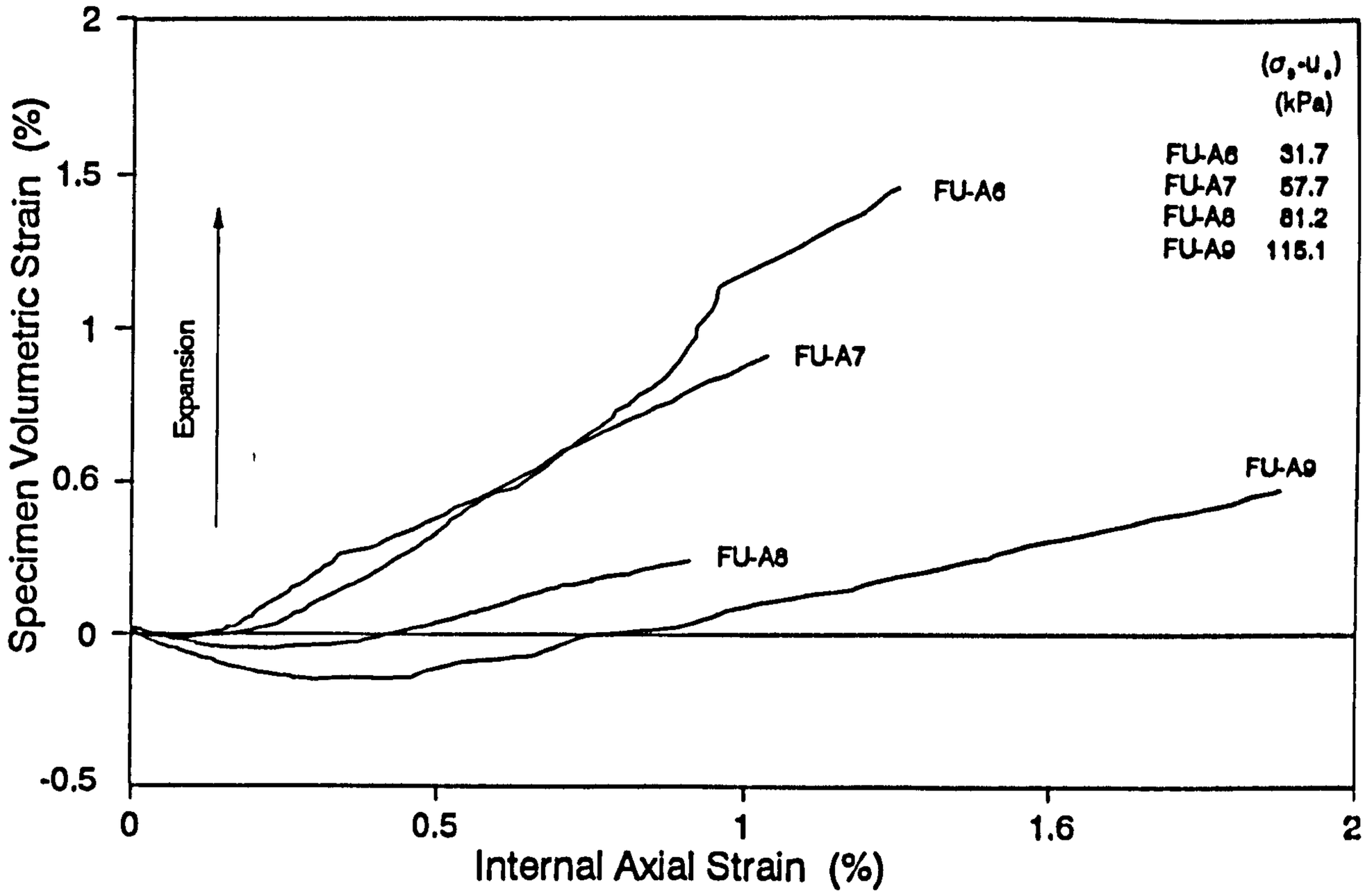

Fig. 7.21a- Specimen volumetric strain measured using the volume change unit during the shearing stage for test series A (Suction =50 kPa)

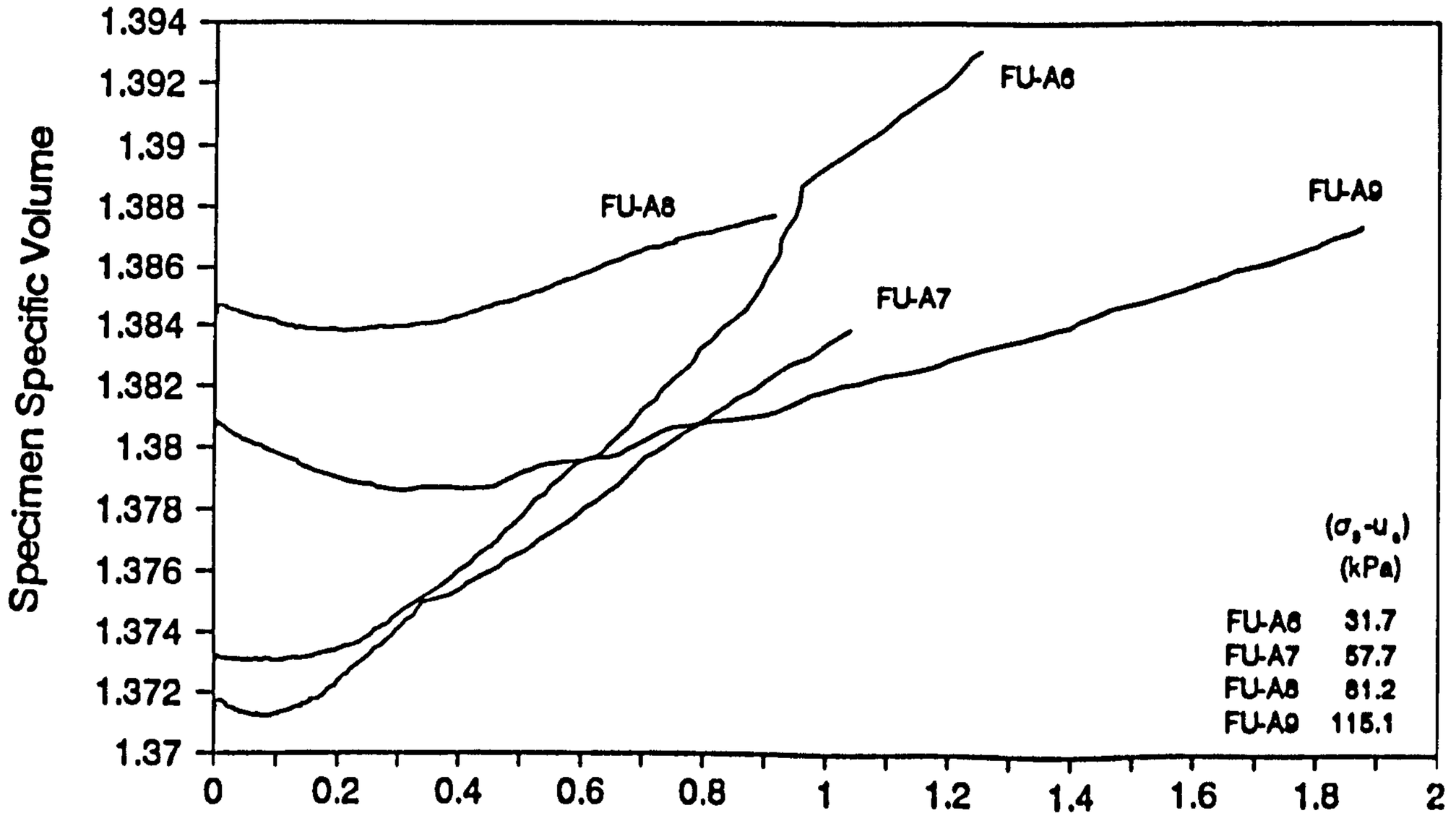

Fig. 7.21b- Specimen specific volume measured using the volume change unit during the shearing stage for test series A (Suction =50 kPa)

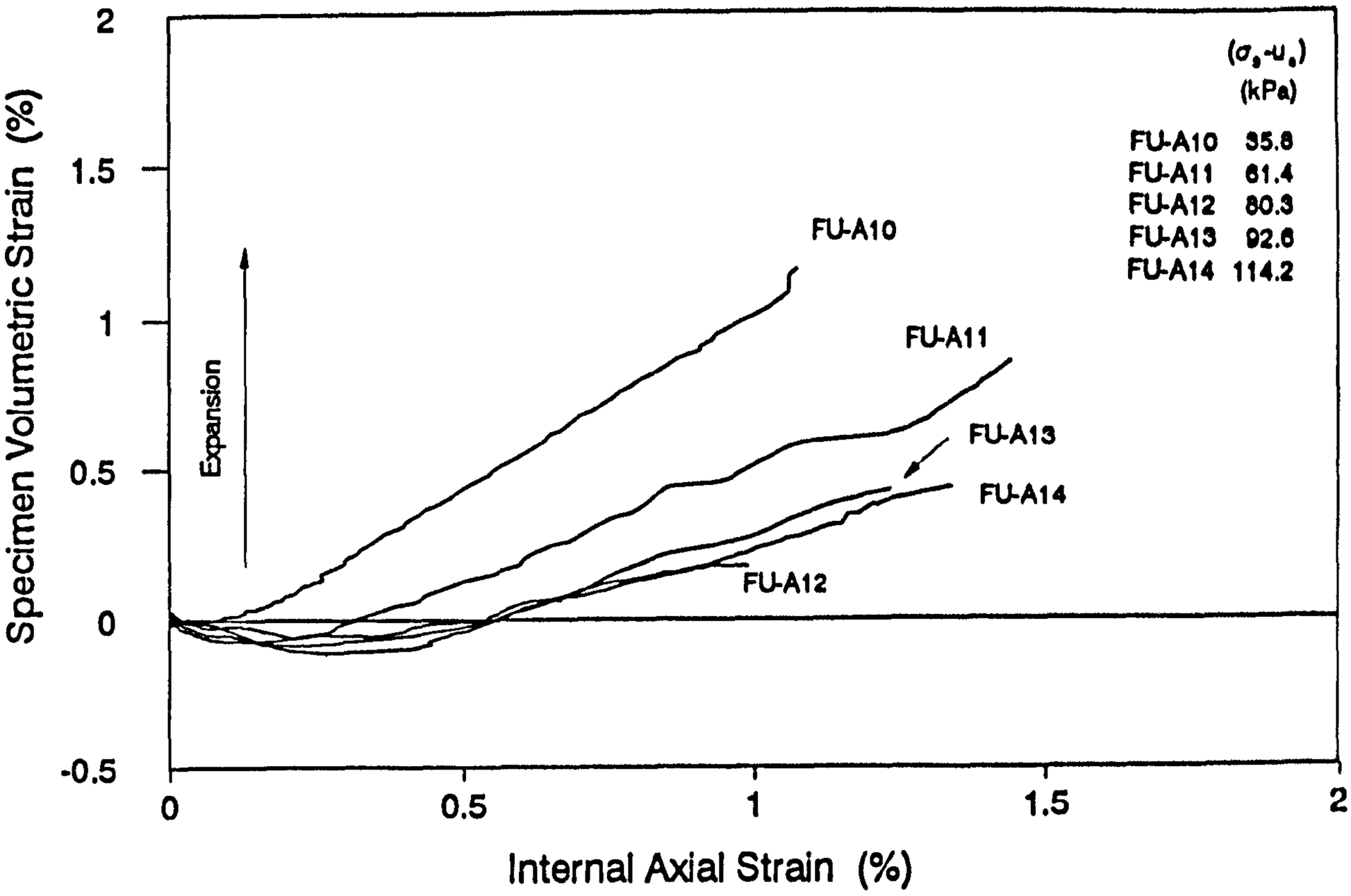

Fig. 7.22a- Specimen volumetric strain measured using the volume change unit during the shearing stage for test series A (Suction =25 kPa)

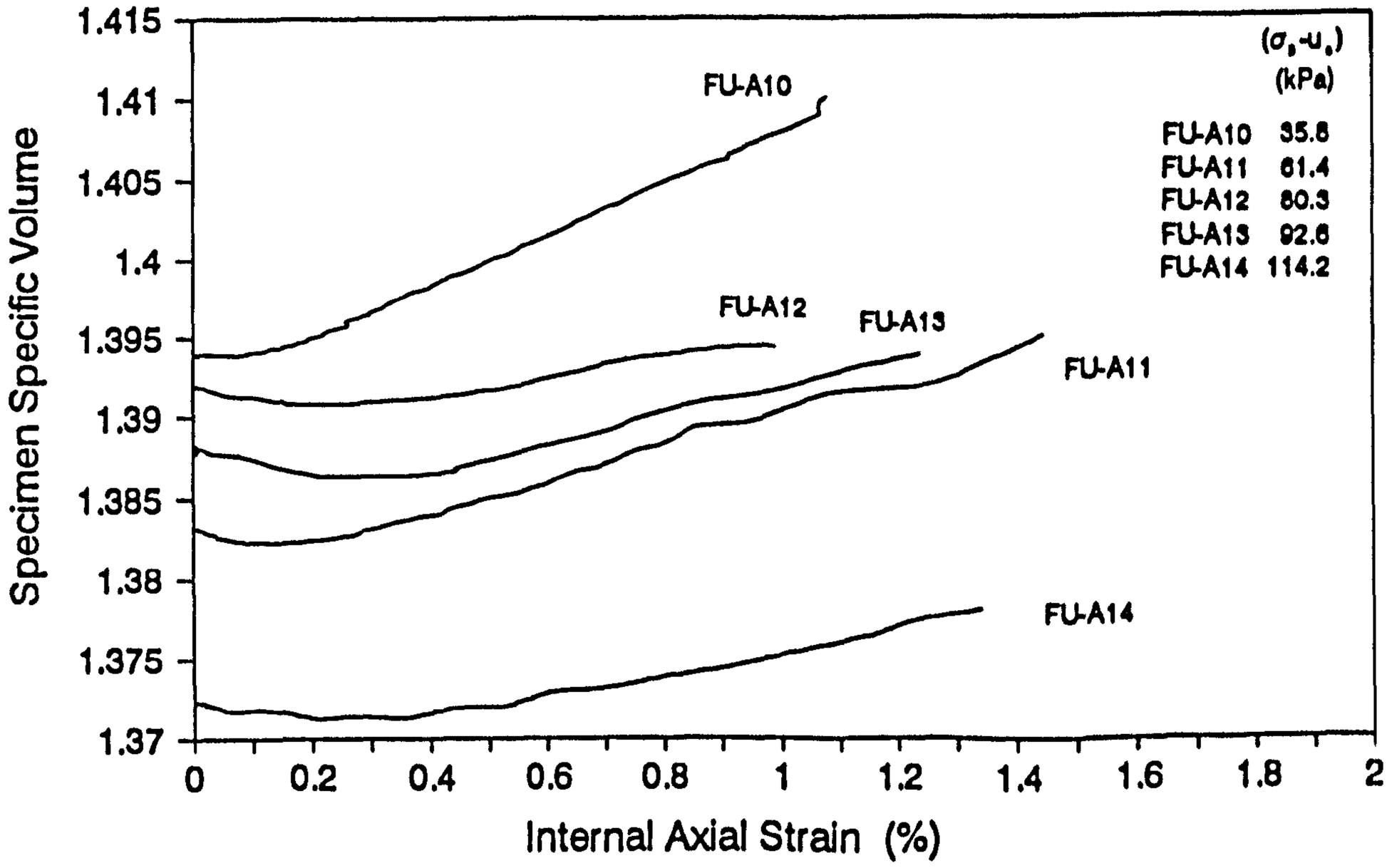

Fig. 7.22b- Specimen specific volume measured using the volume change unit during the shearing stage for test series A (Suction =25 kPa)

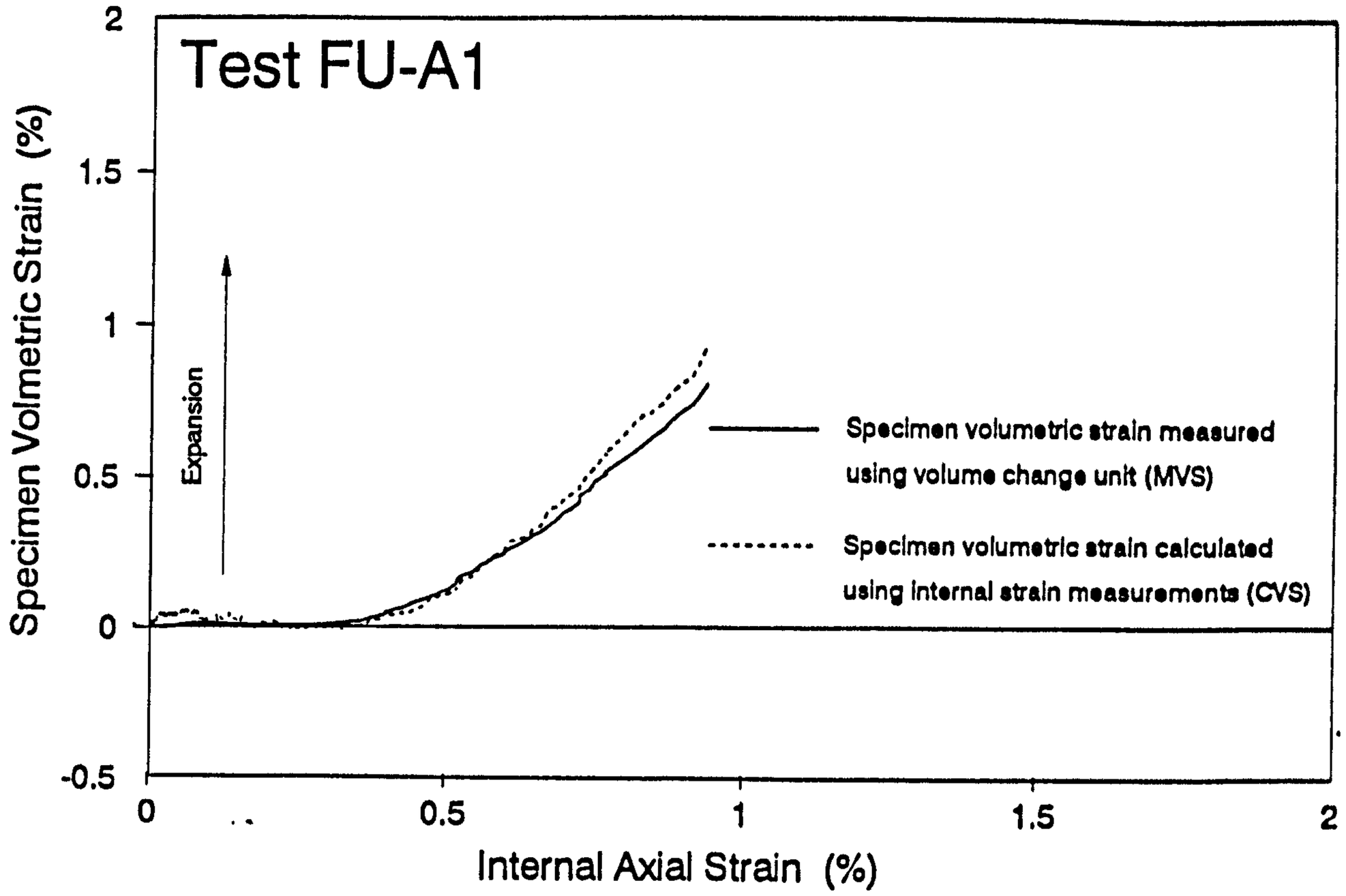

Fig. 7.23A- Specimen volumetric strain during the shearing stage of test FU-A1 (suction= 75 kPa)

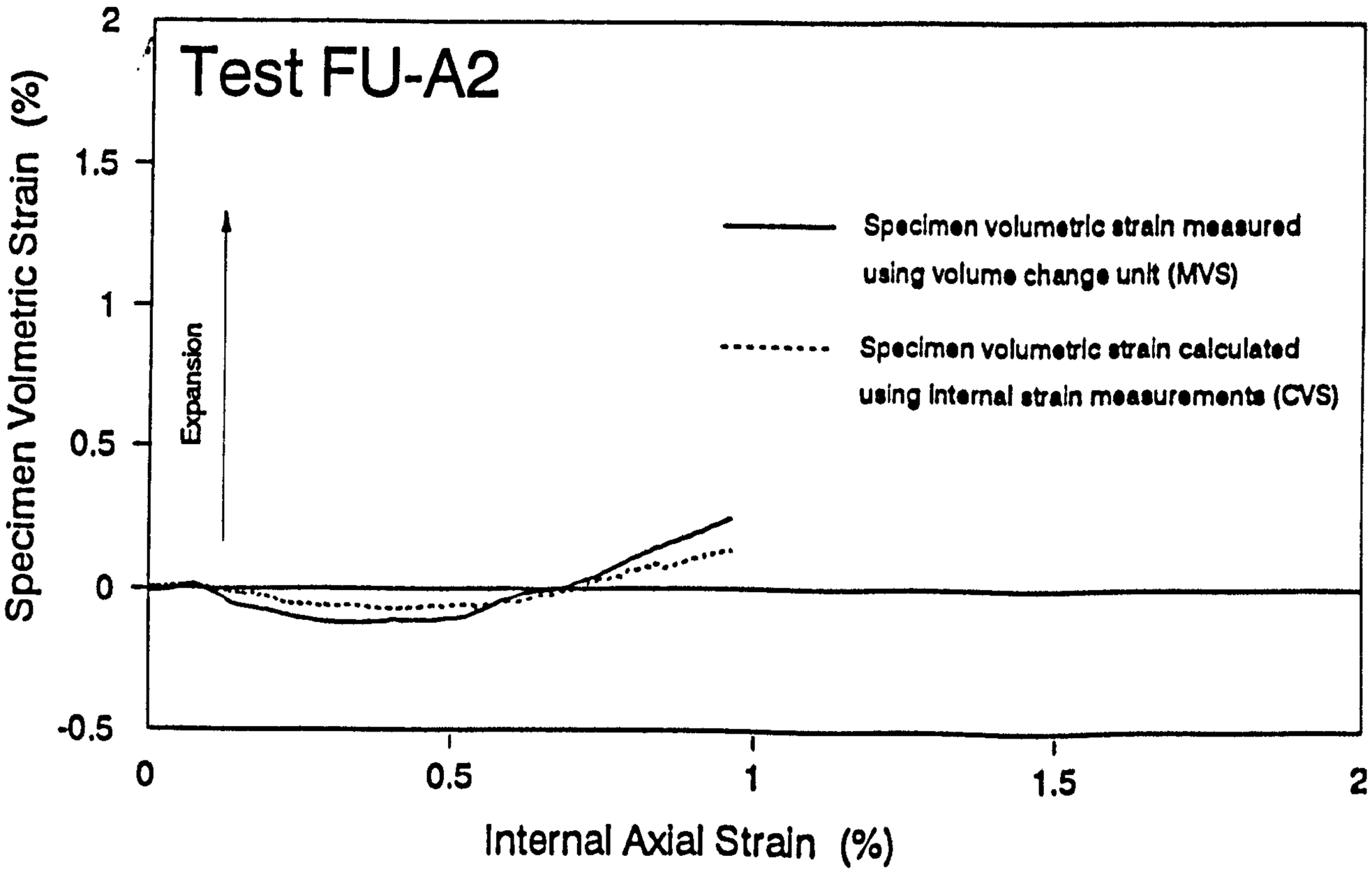

Fig. 7.23B- Specimen volumetric strain during the shearing stage of test FU-A2 (suction= 75 kPa)

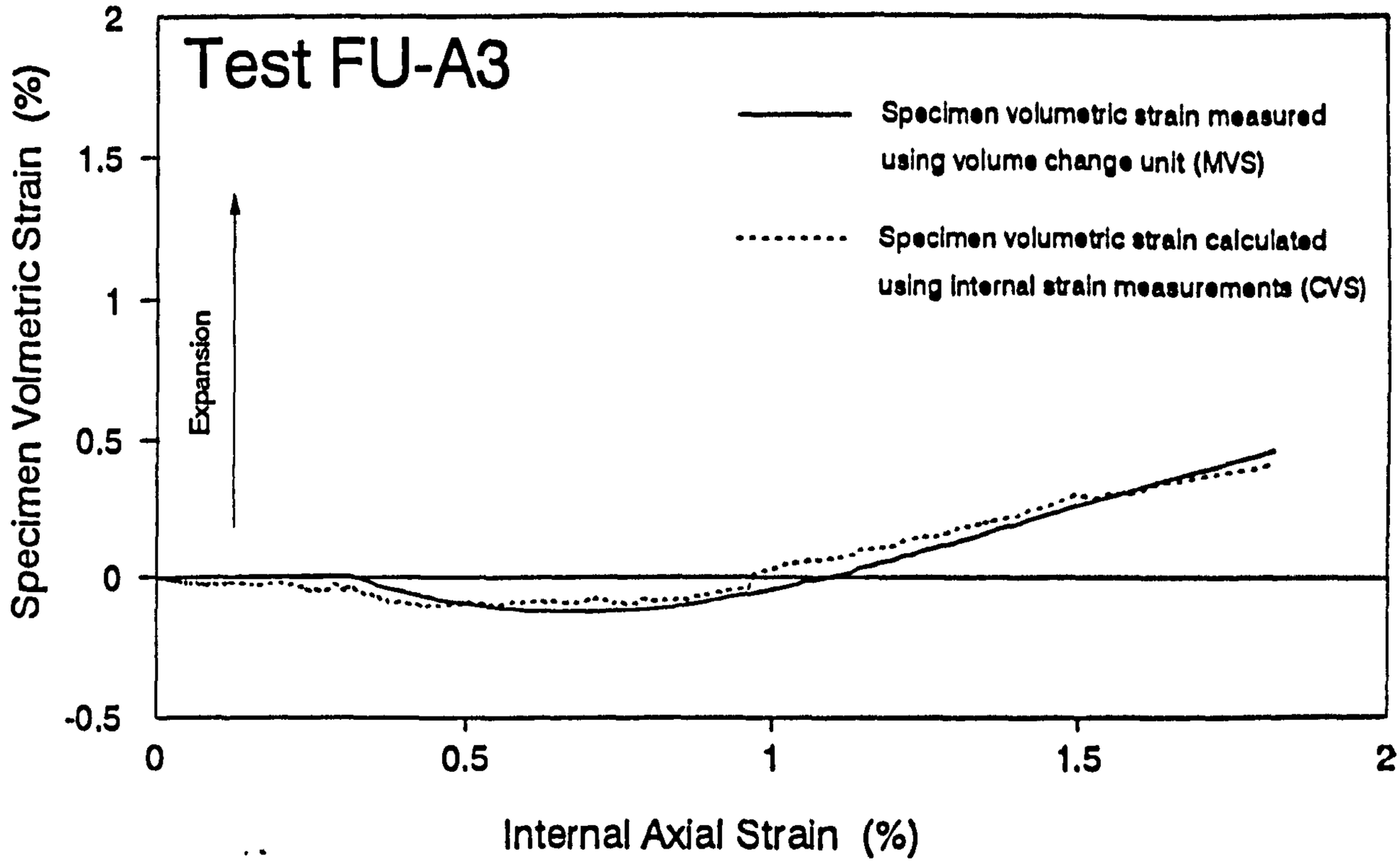

Fig. 7.23C- Specimen volumetric strain during the shearing stage of test FU-A3 (suction= 75 kPa)

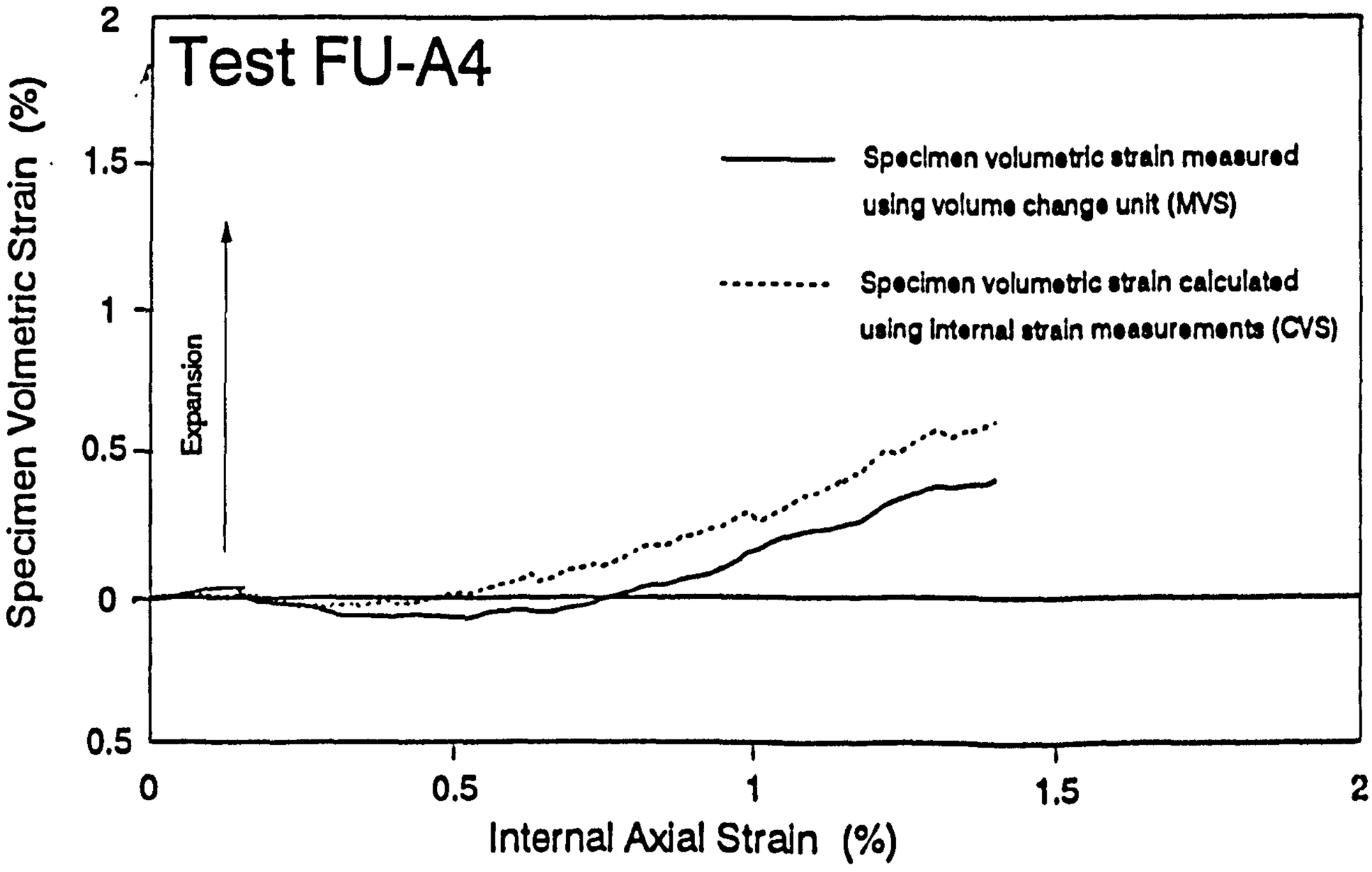

Fig. 7.23D- Specimen volumetric strain during the shearing stage of test FU-A4 (suction= 75 kPa)

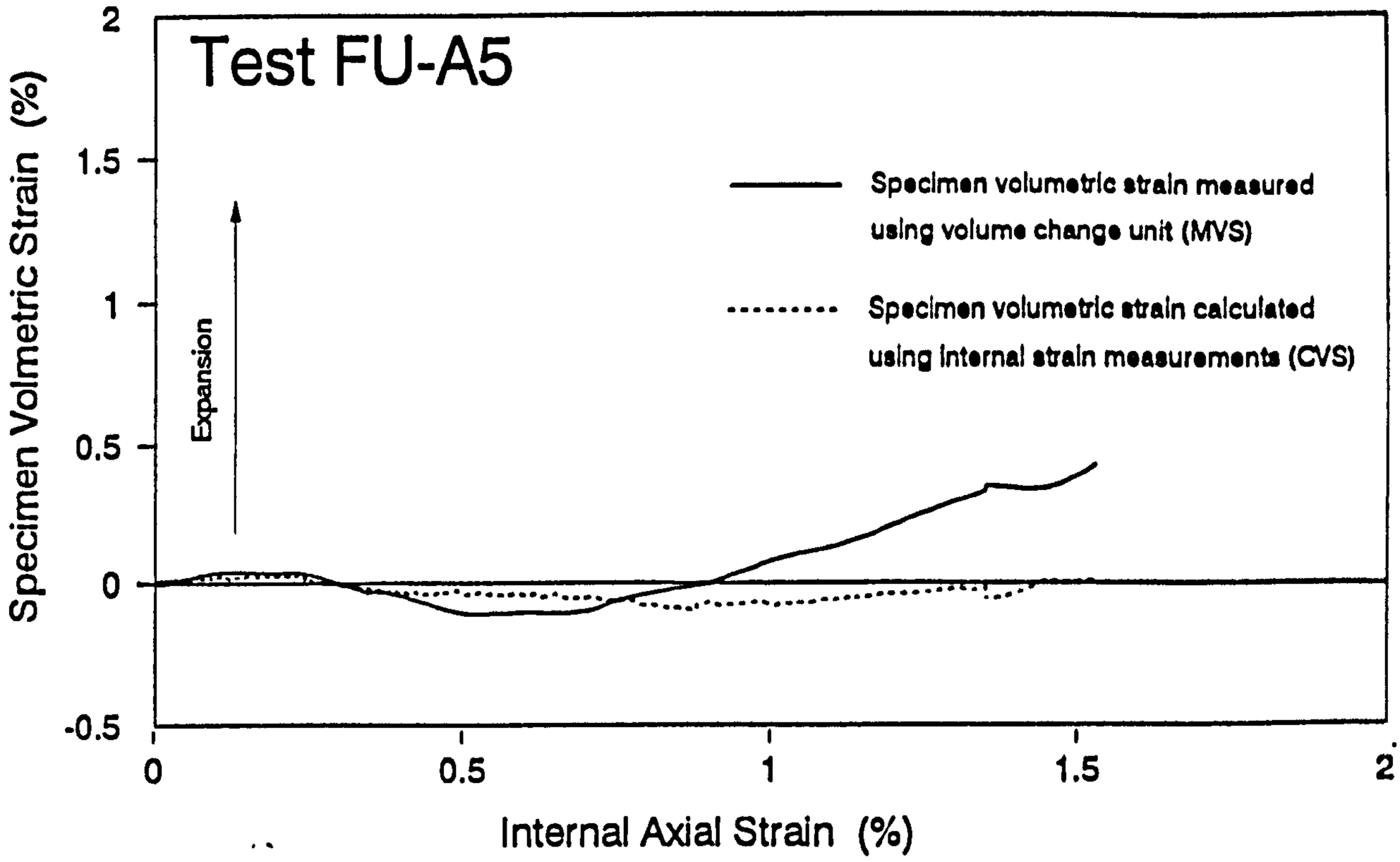

Fig. 7.23E- Specimen volumetric strain during the shearing stage of test FU-A5 (suction= 75 kPa)

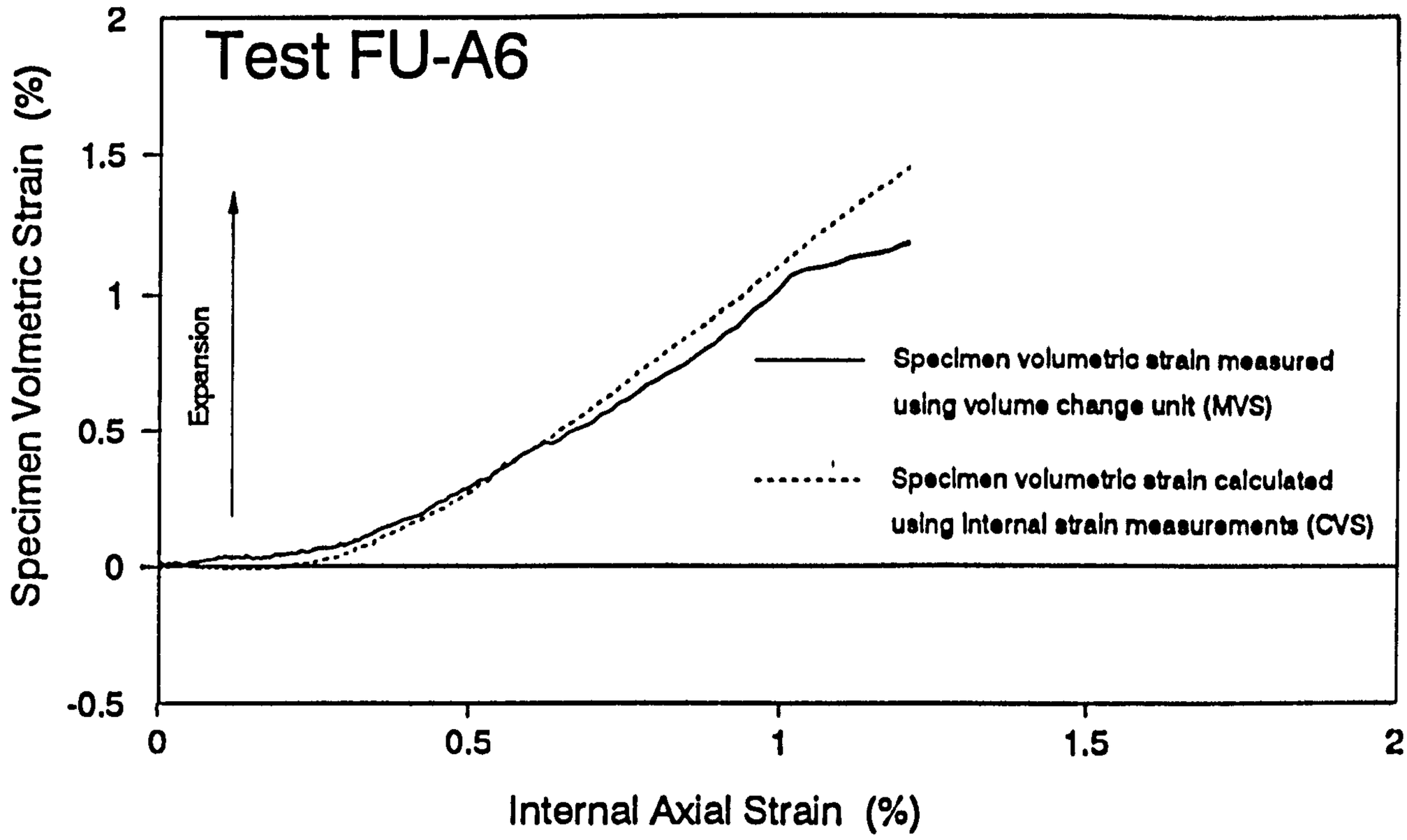

Fig. 7.24A- Specimen volumetric strain during the shearing stage of test FU-A6 (suction= 50 kPa)

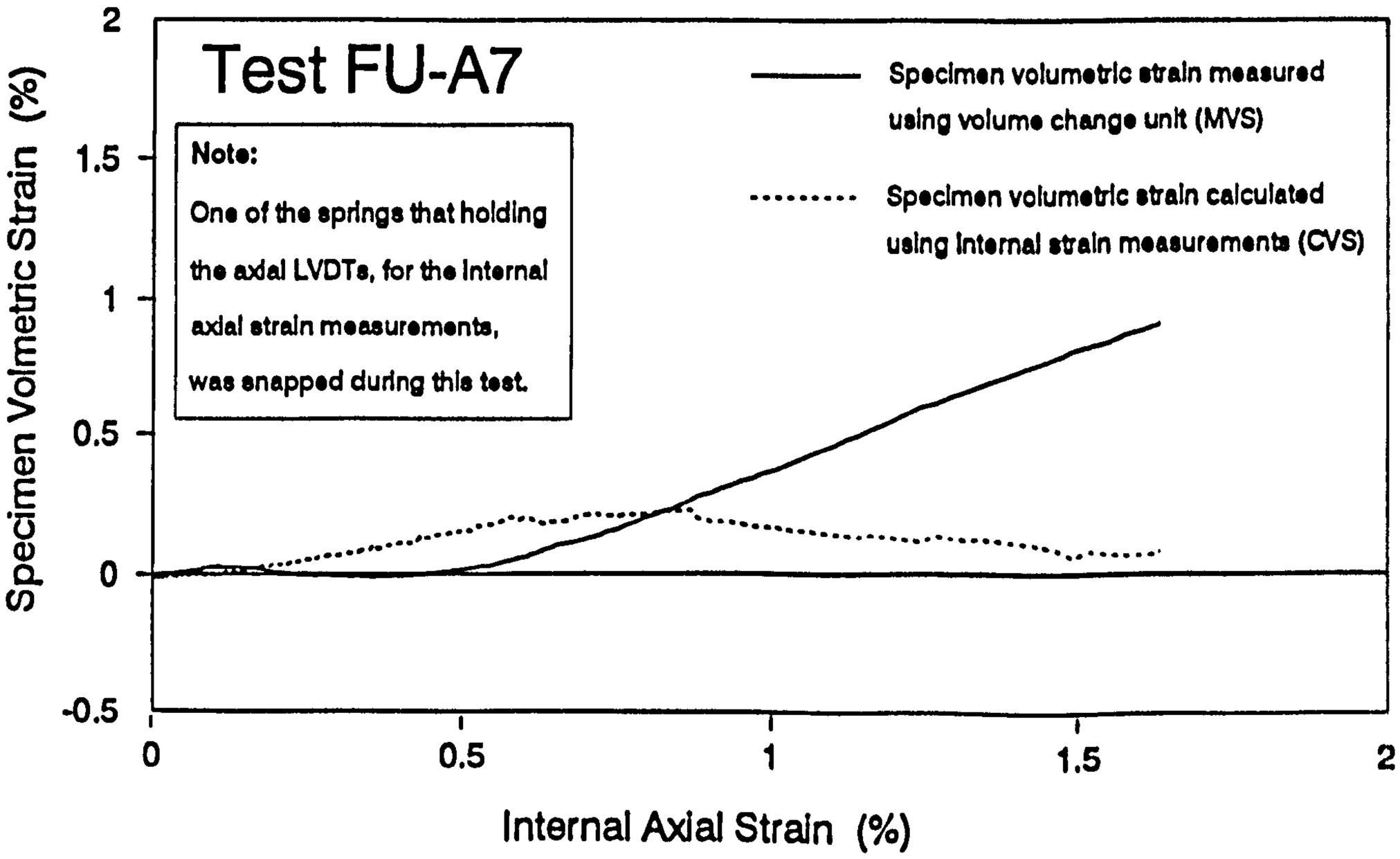

Fig. 7.24B- Specimen volumetric strain during the shearing stage of test FU-A7 (suction= 50 kPa)

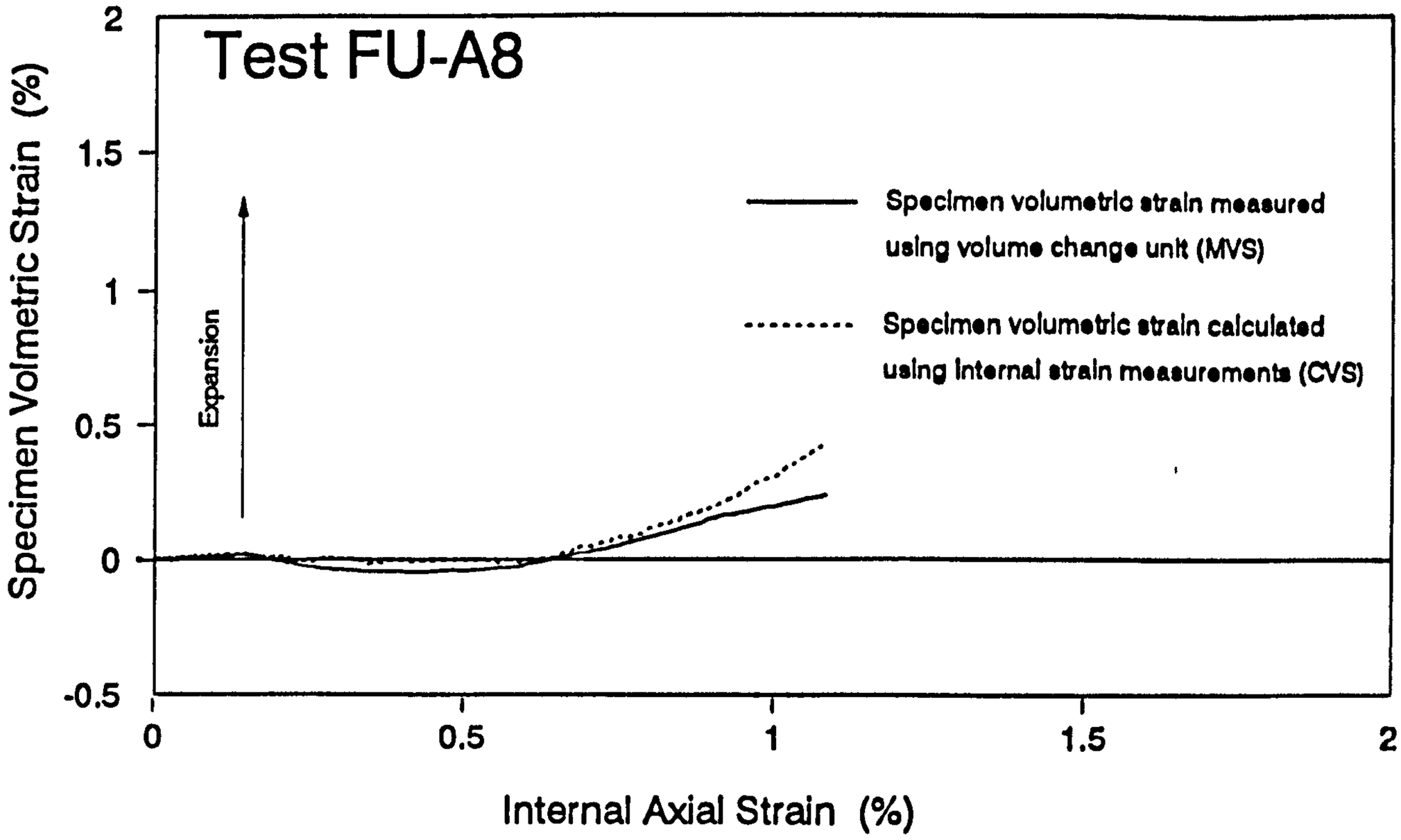

Fig. 7.24C- Specimen volumetric strain during the shearing stage of test FU-A8 (suction= 50 kPa)

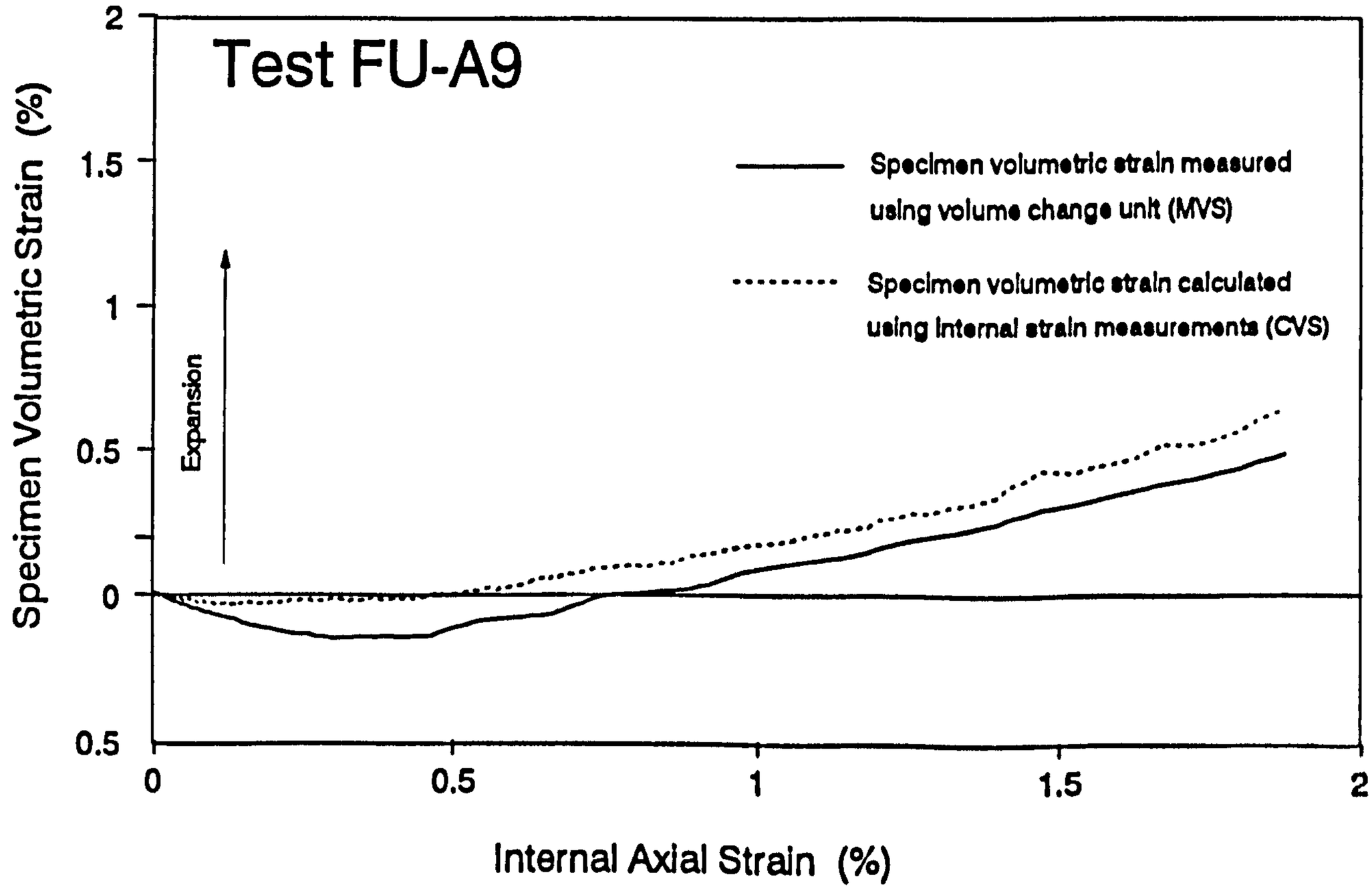

Fig. 7.24D- Specimen volumetric strain during the shearing stage of test FU-A9 (suction= 50 kPa)

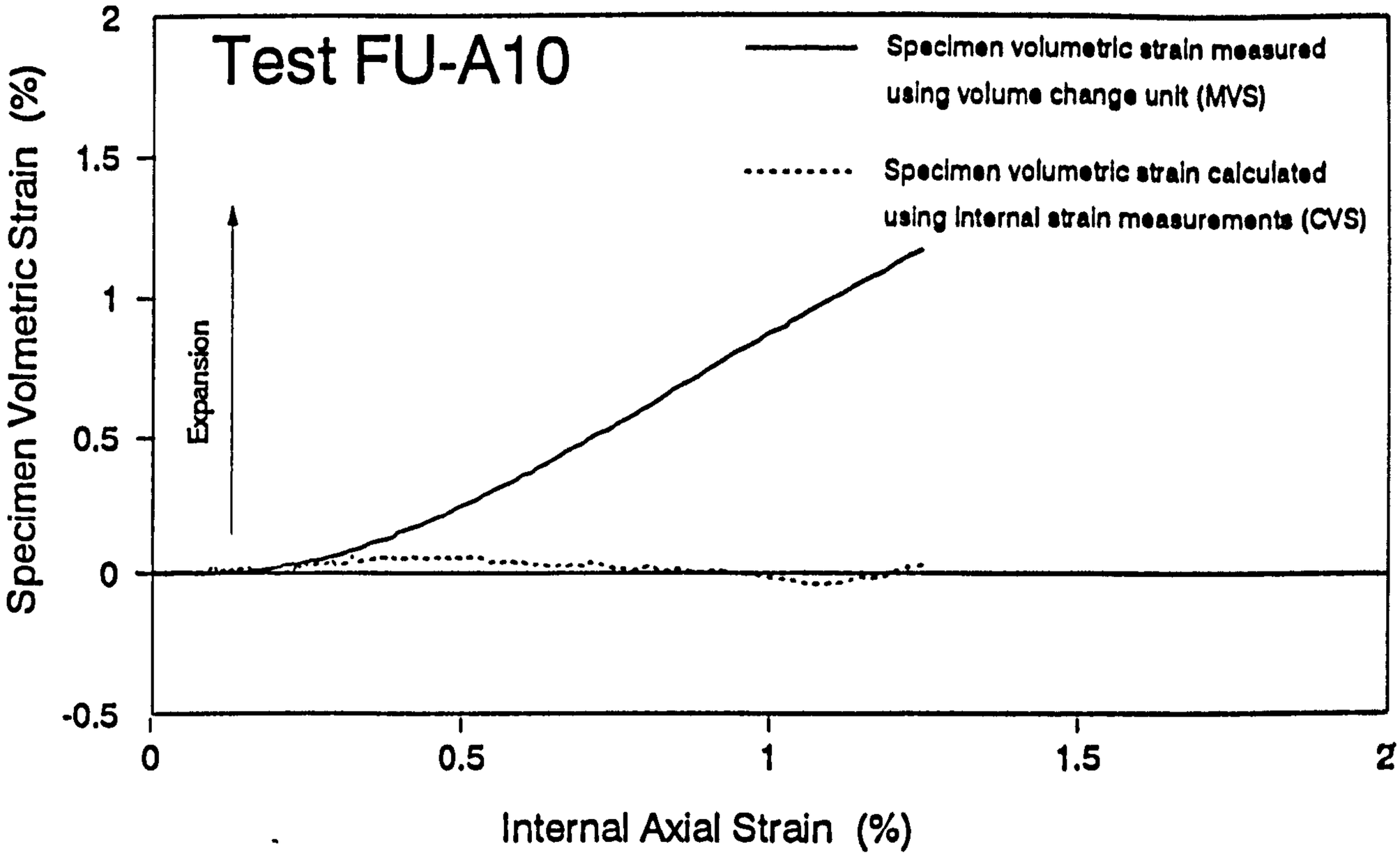

Fig. 7.25A- Specimen volumetric strain during the shearing stage of test FU-A10 (suction= 25 kPa)

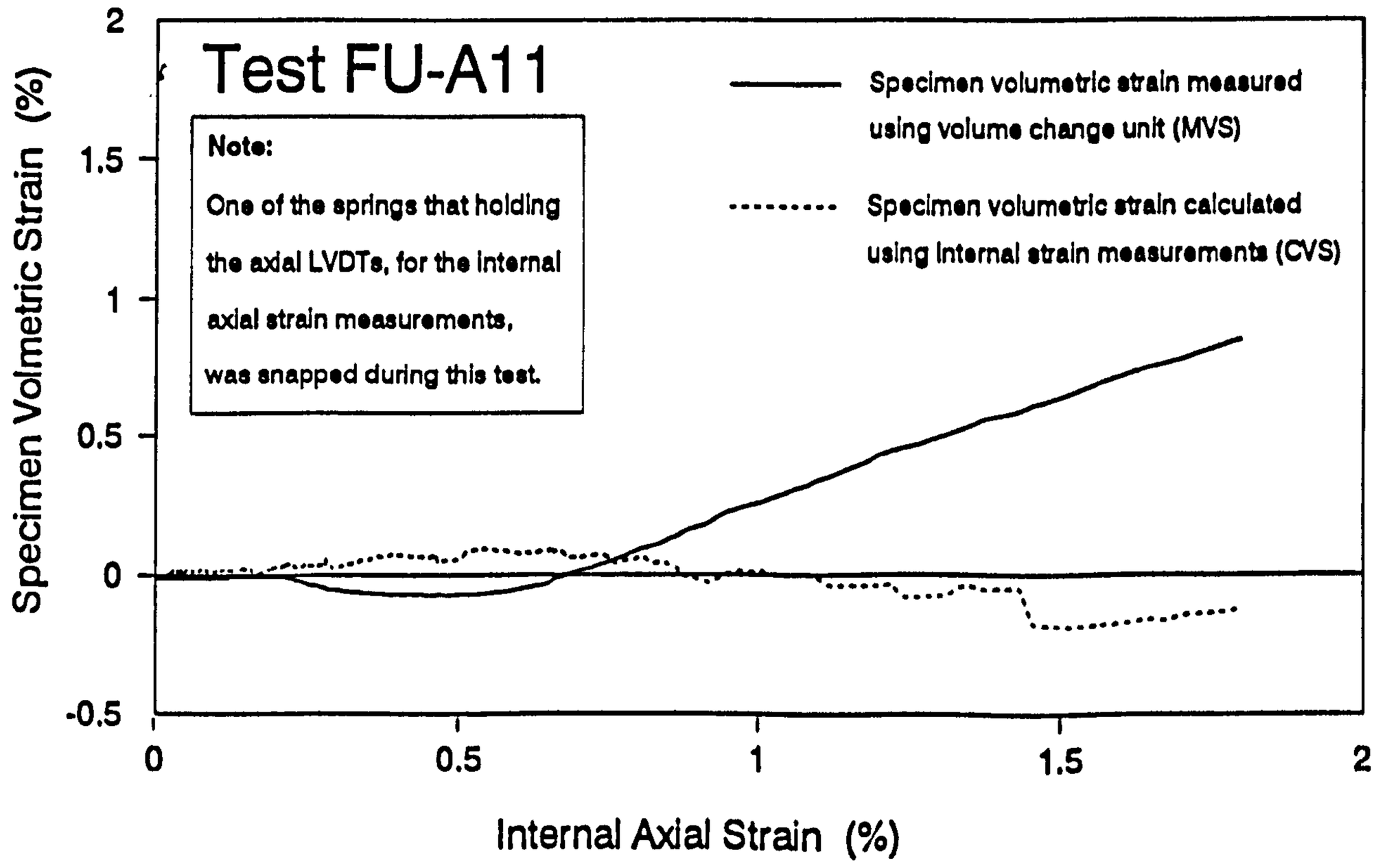

Fig. 7.25B- Specimen volumetric strain during the shearing stage of test FU-A11 (suction= 25 kPa)

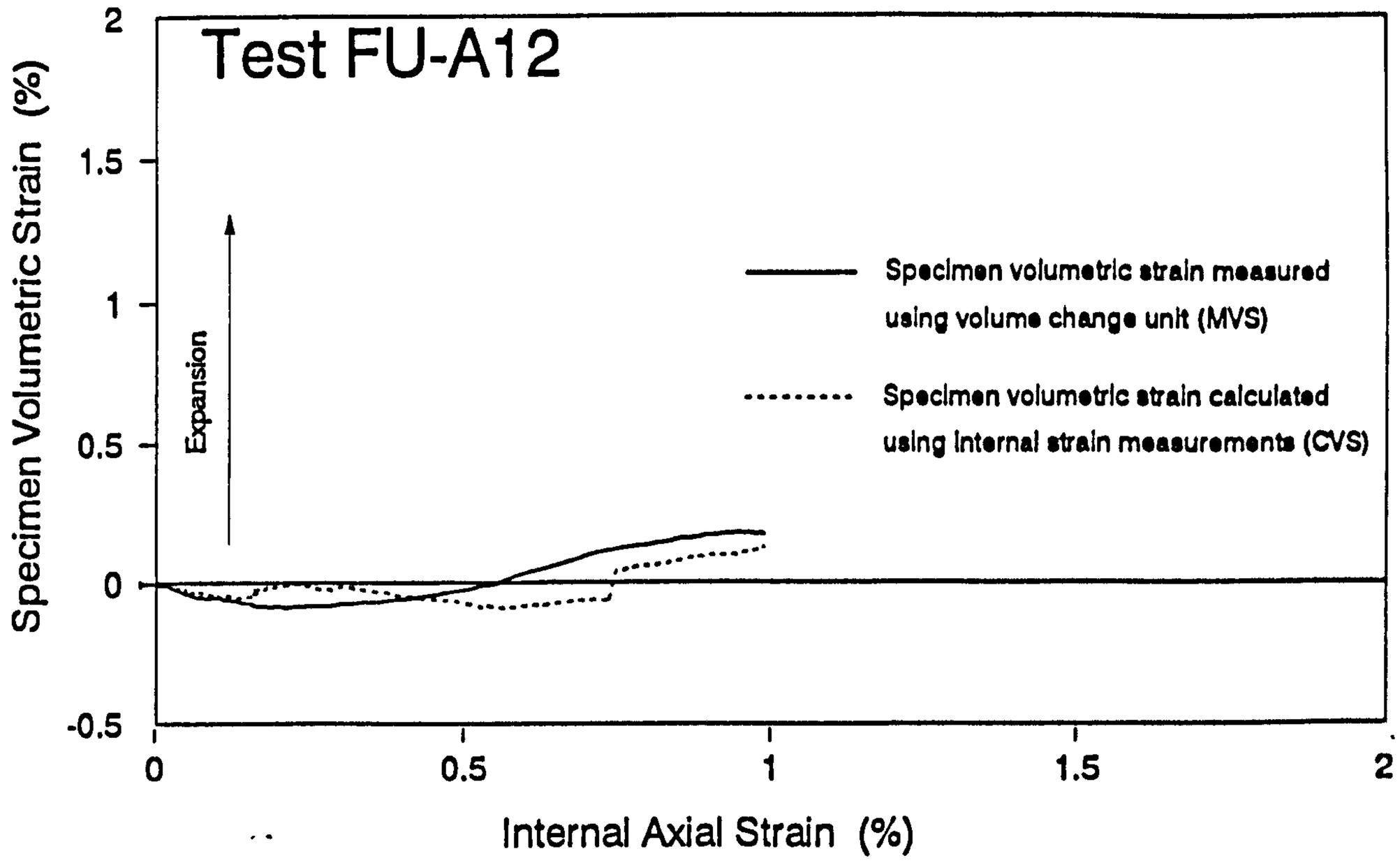

Fig. 7.25C- Specimen volumetric strain during the shearing stage of test FU-A12 (suction= 25 kPa)

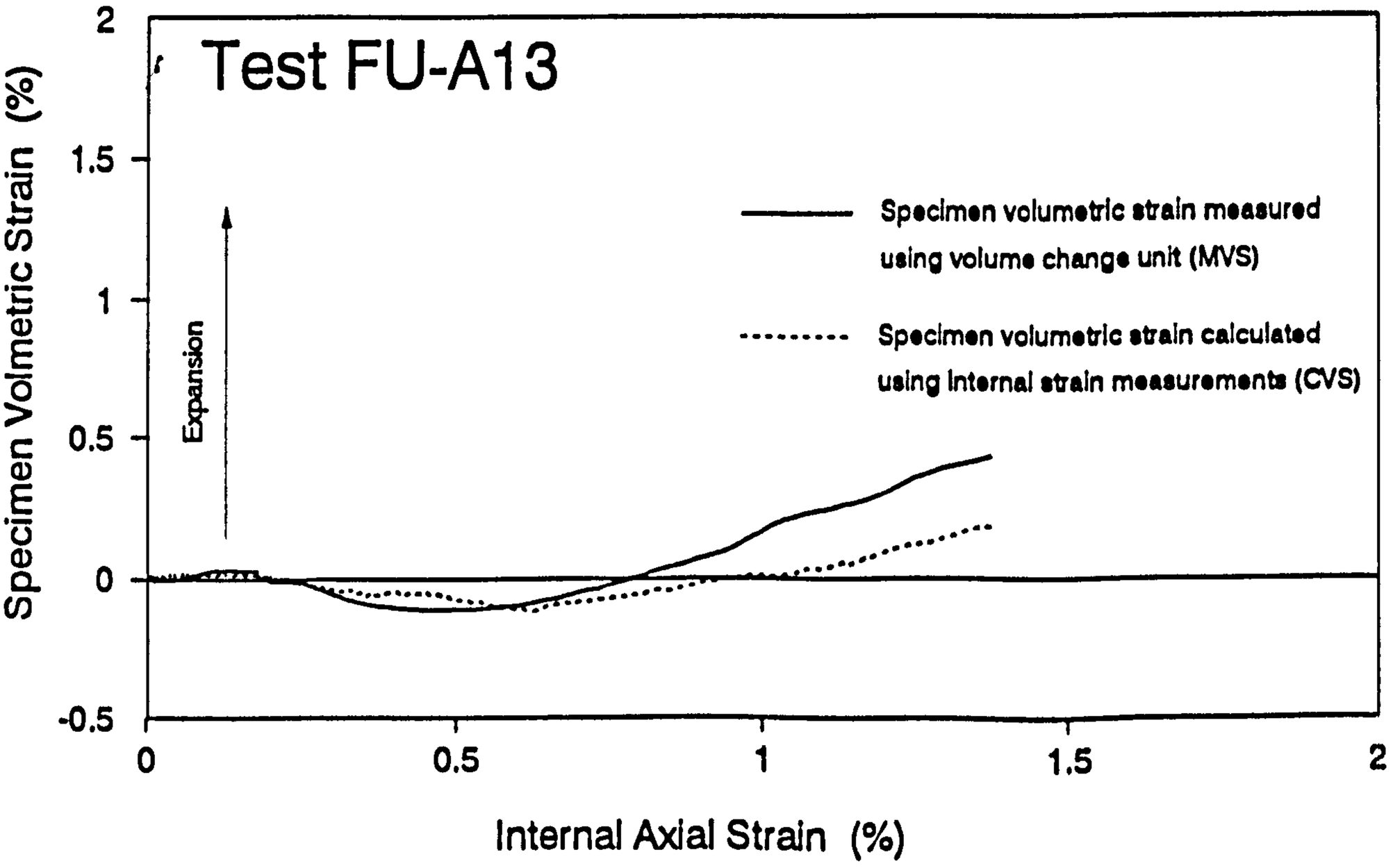

Fig. 7.25D- Specimen volumetric strain during the shearing stage of test FU-A13 (suction= 25 kPa)

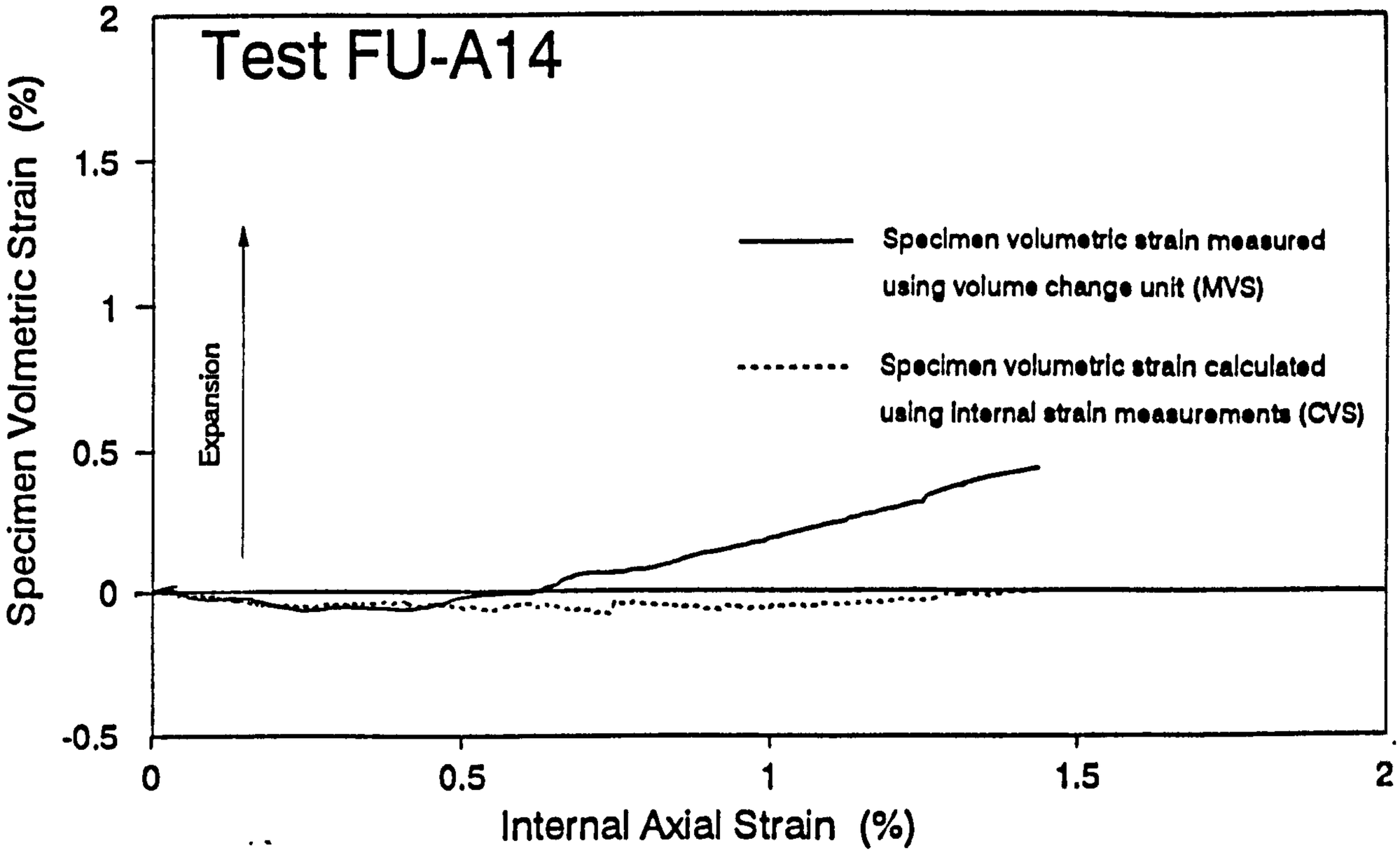

Fig. 7.25E- Specimen volumetric strain during the shearing stage of test FU-A14 (suction= 25 kPa)

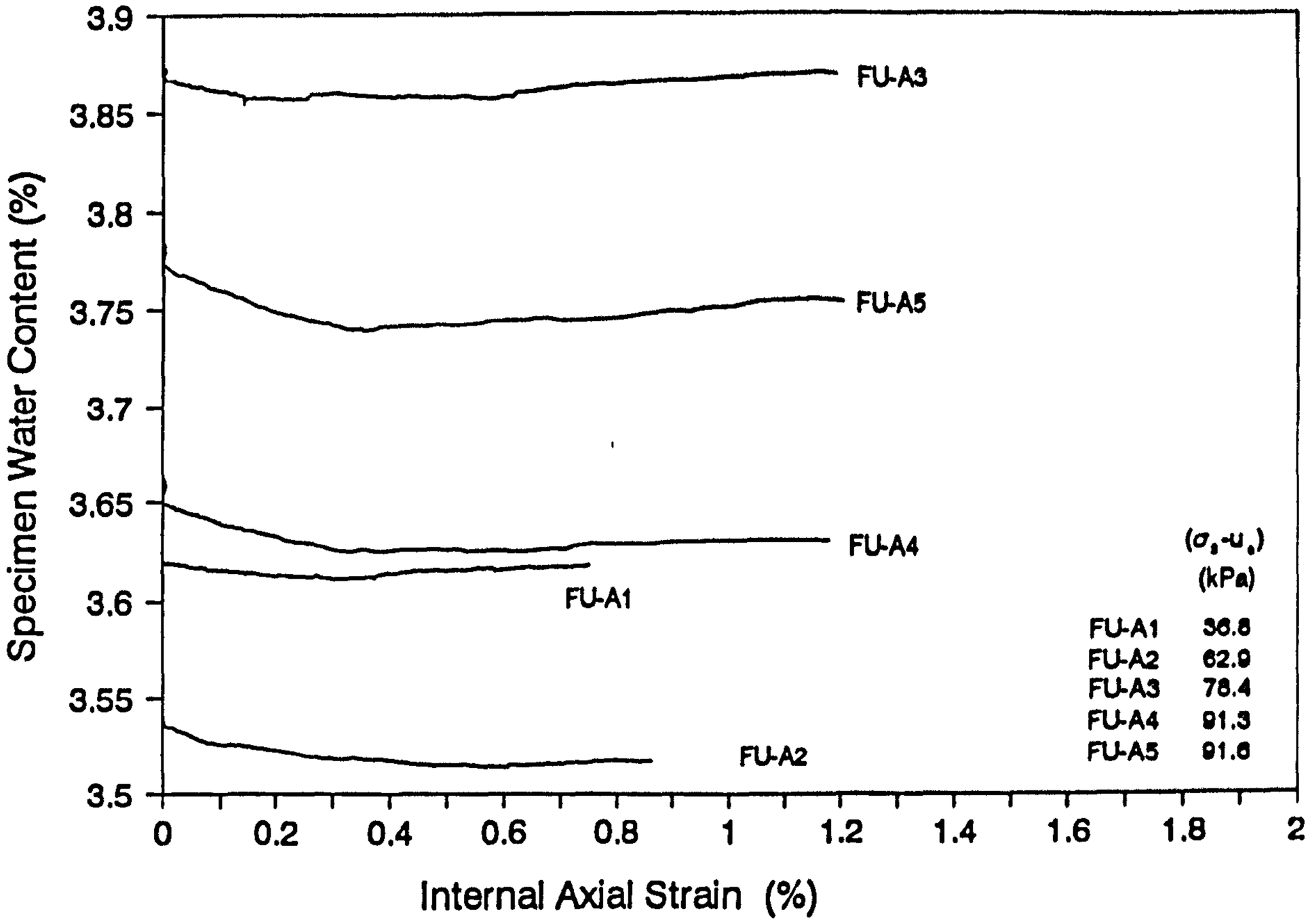

Fig. 7.26- Specimen water content during shearing in test series A (suction=75 kPa)

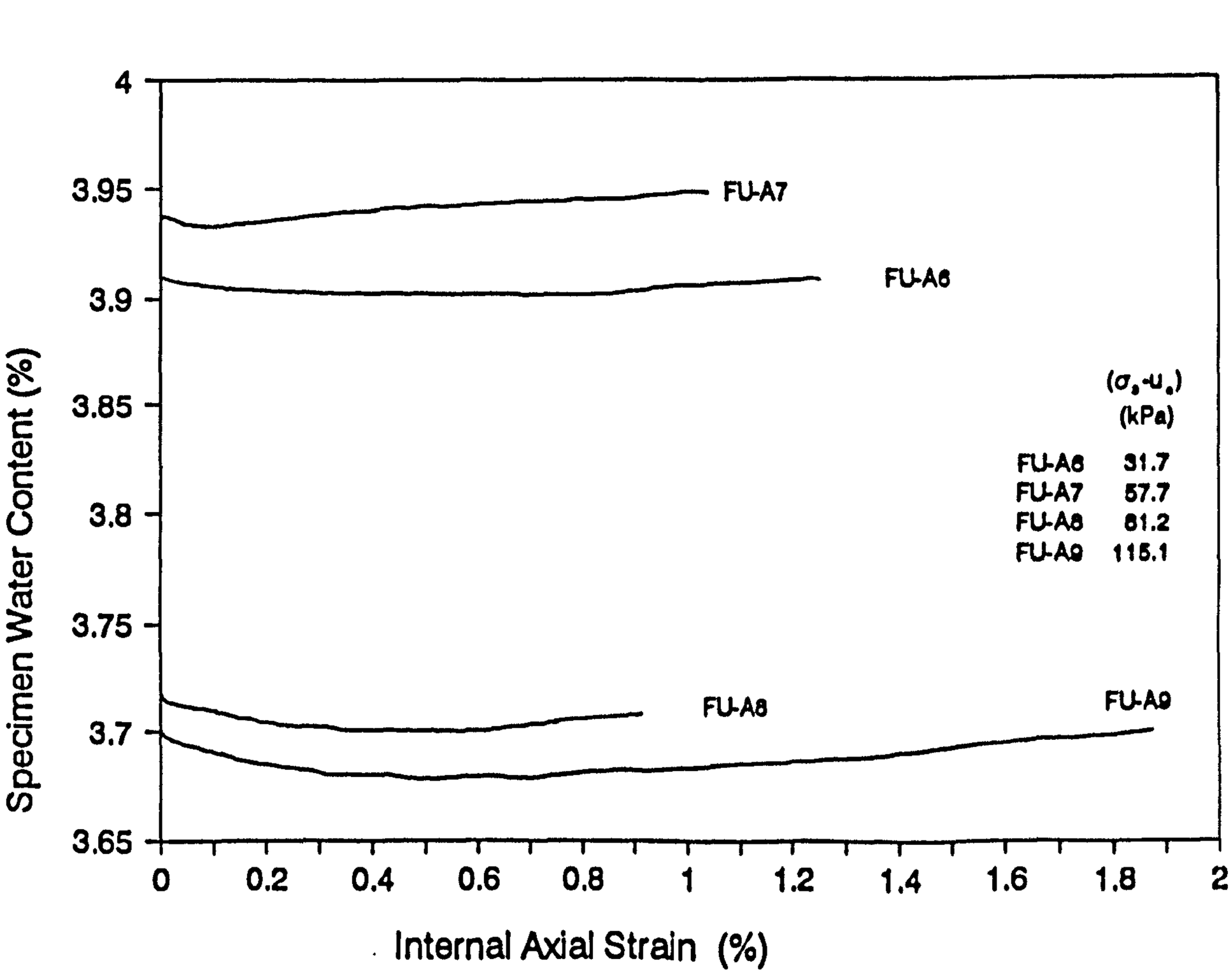

Fig. 7.27- Specimen water content during shearing in test series A (suction=50 kPa)

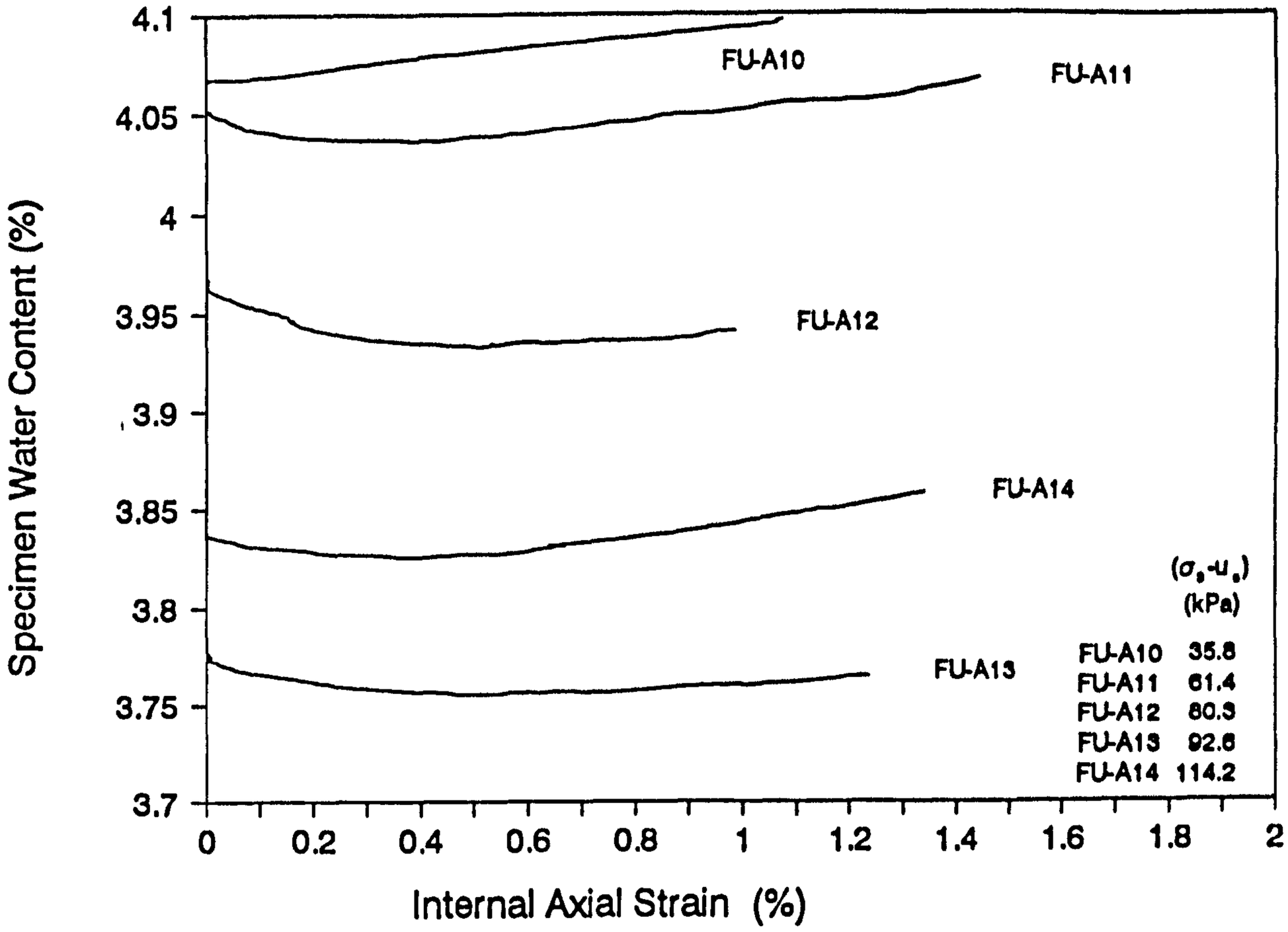

Fig. 7.28- Specimen water content during shearing in test series A (suction=25 kPa)

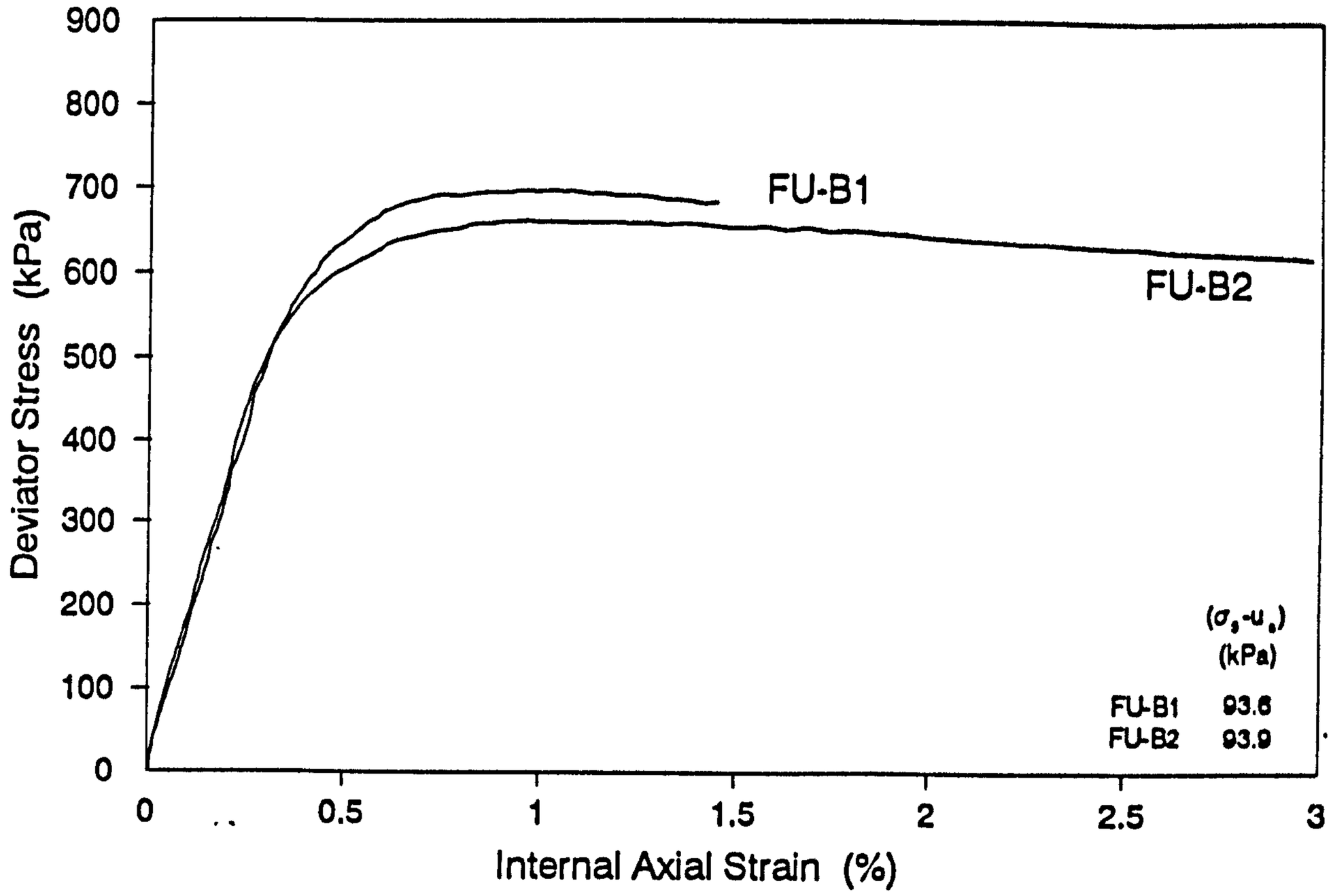

Fig. 7.29- Deviator stress-strain curves for test series B.

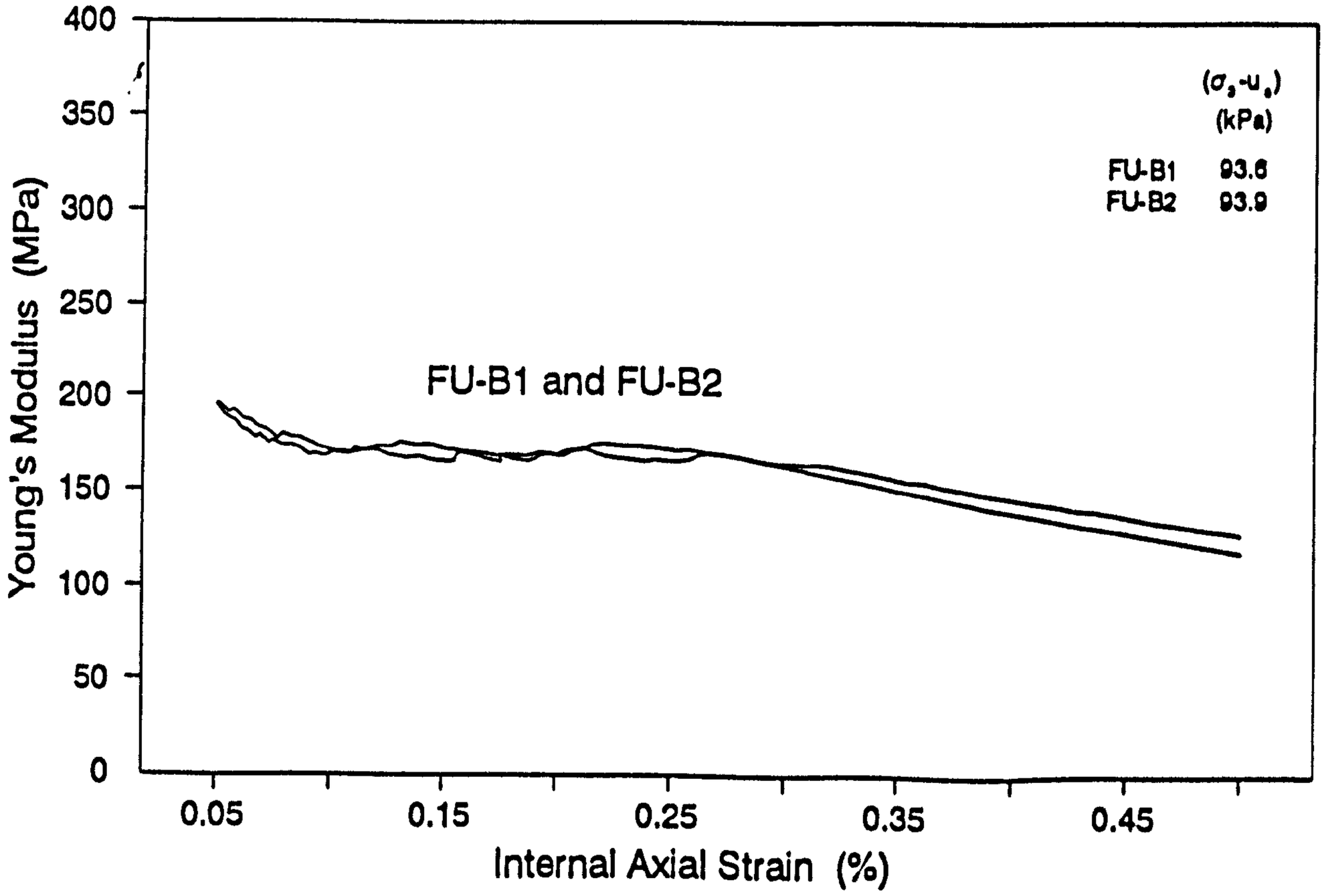

Fig. 7.30- Young's modulus plotted against internal axial strain for test series B.

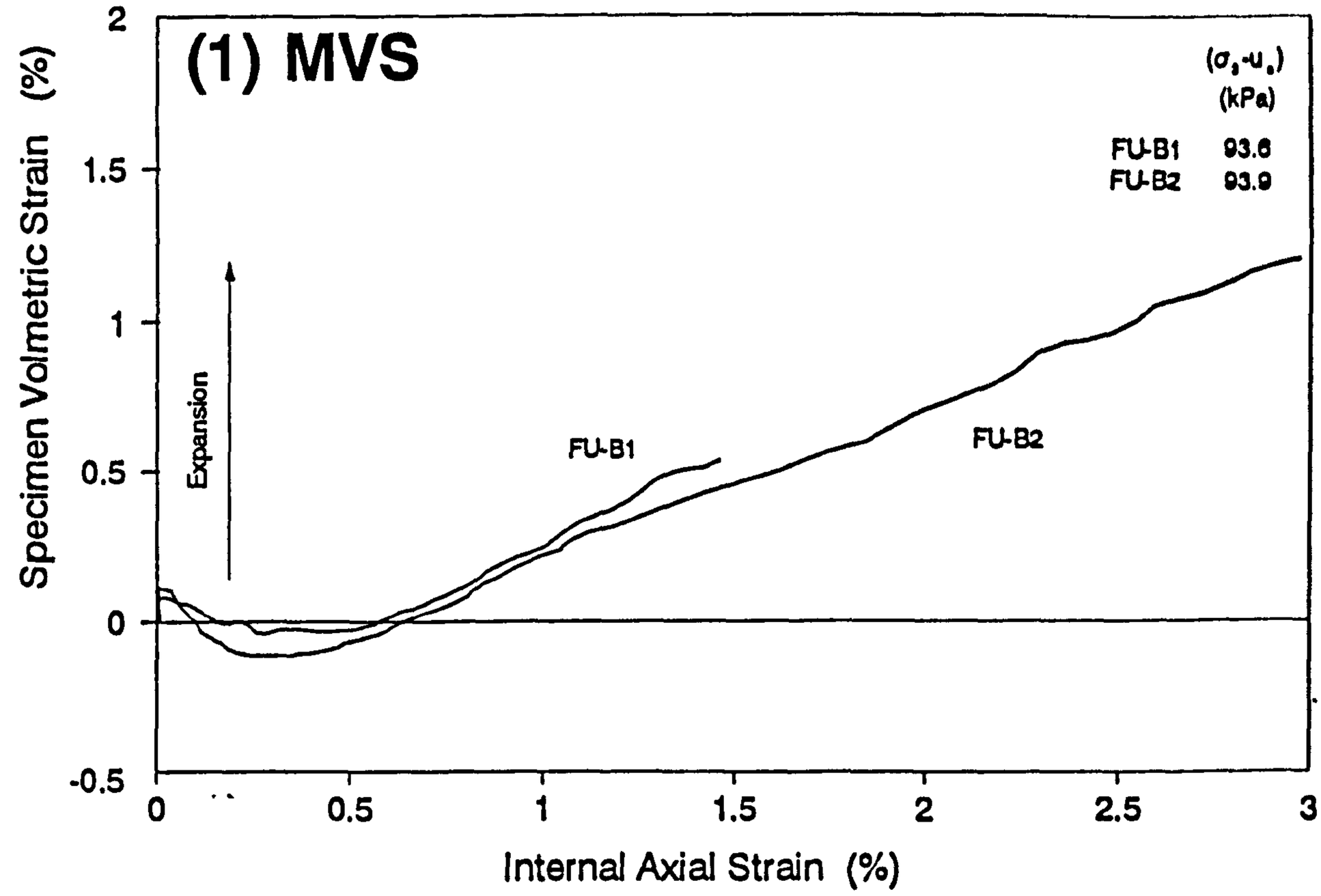

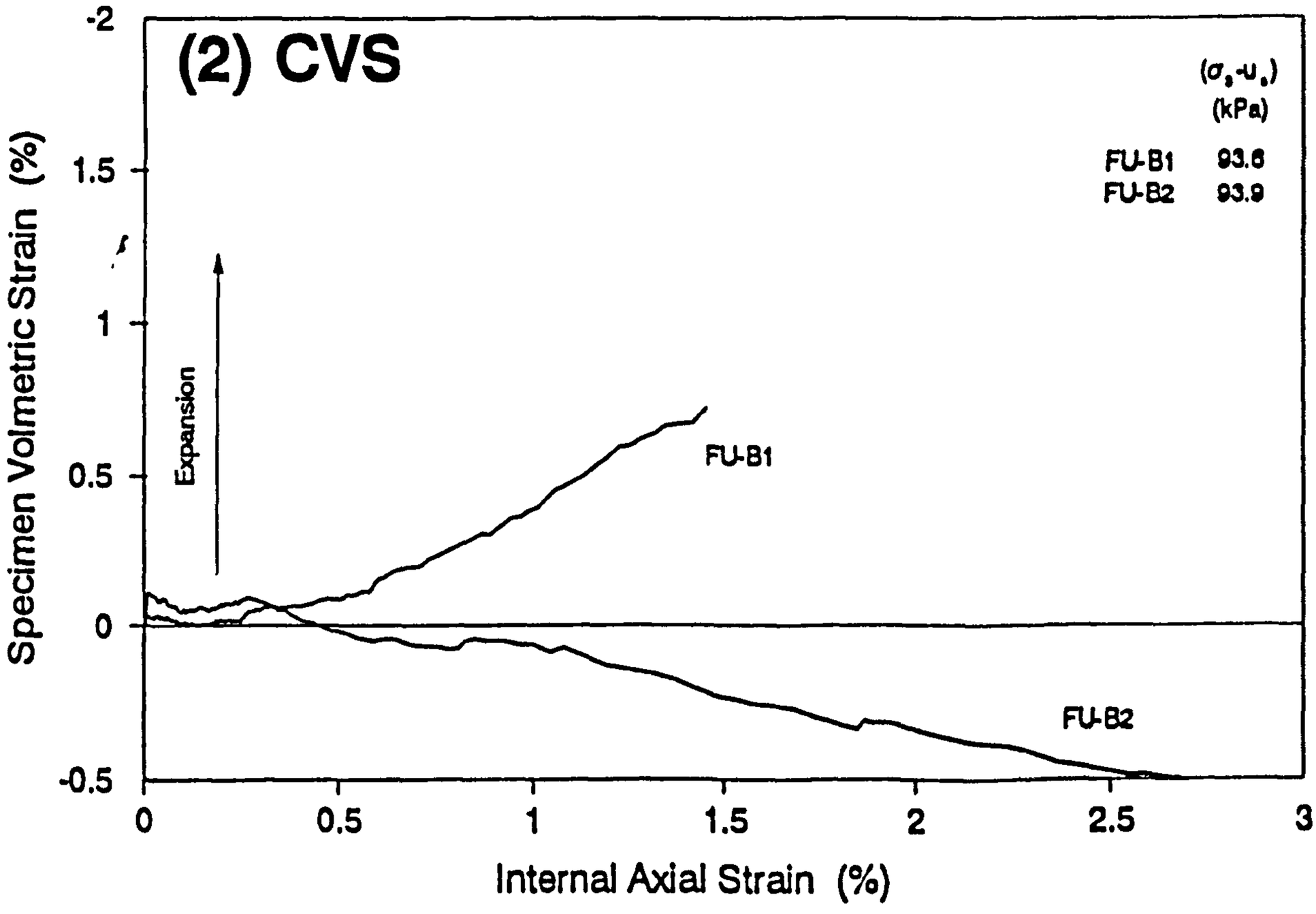

Fig. 7.31a- Specimen volumetric strain during the shearing stage of test series B, measured using the (1) volume change unit (MVS) and (2) internal strain measurements (CVS).

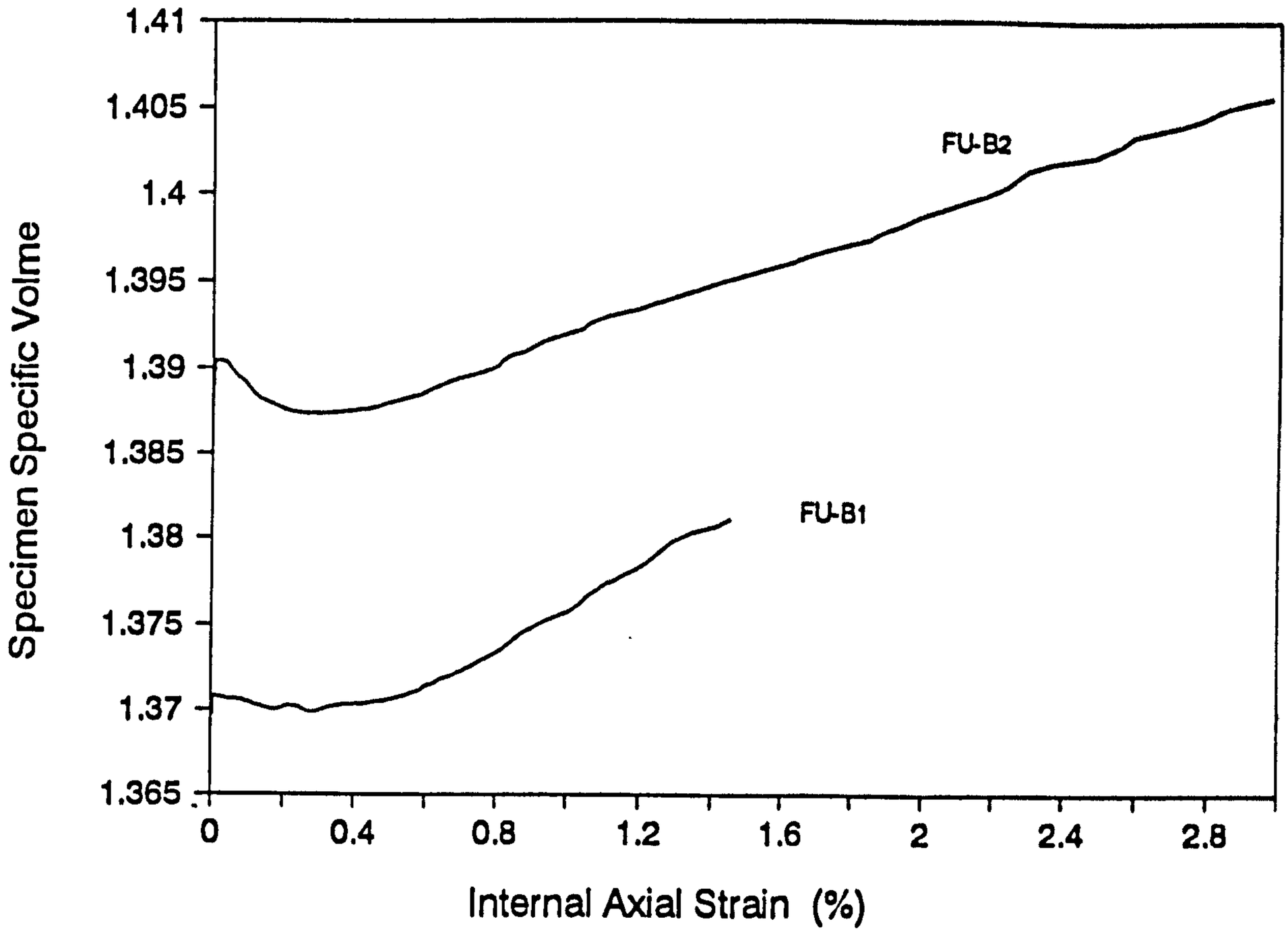

Fig. 7.31b- Specimen specific volume during the shearing stage of test series B, measured using the volume change unit

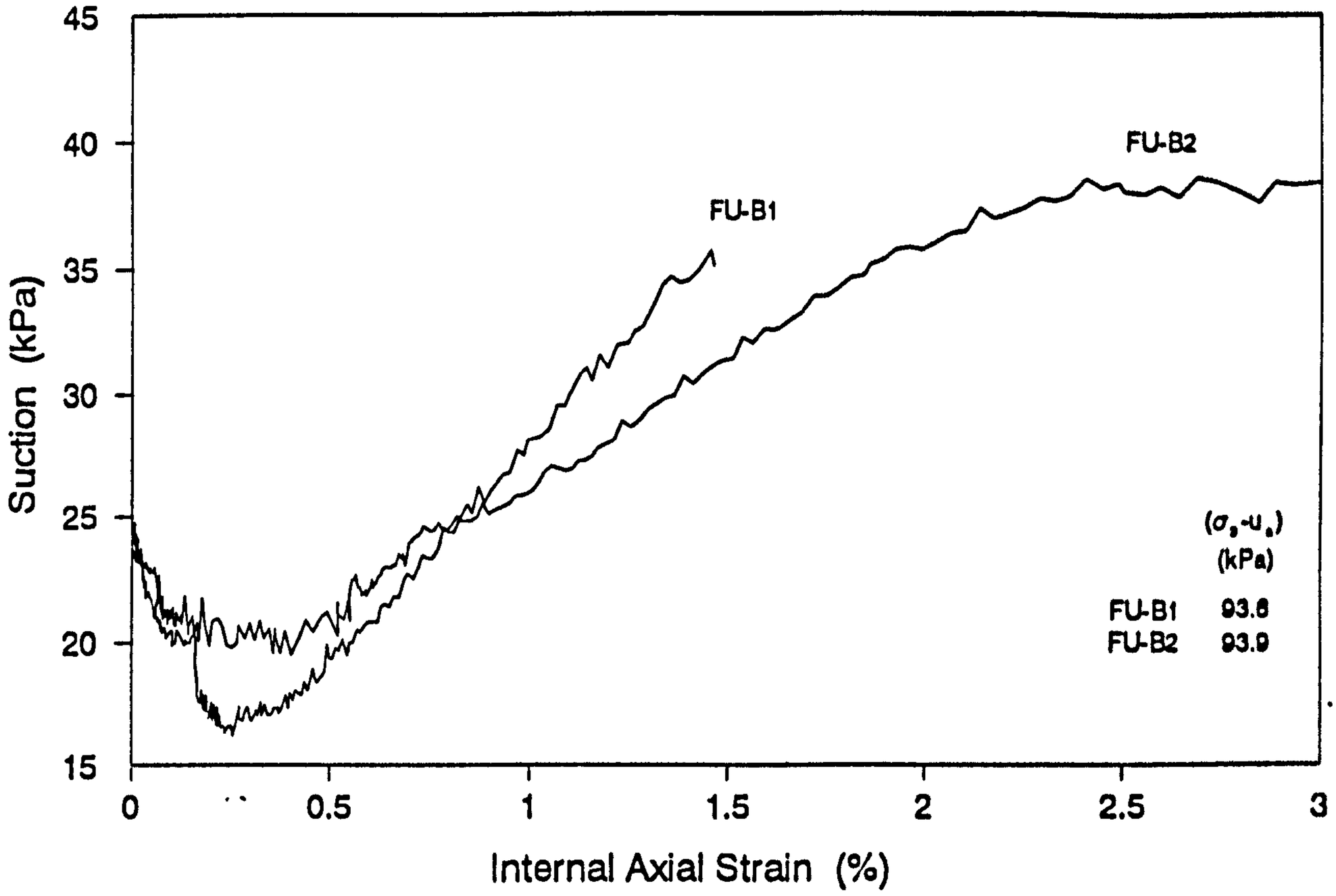

Fig. 7.32- Specimen suction change during the shearing of tests series B.

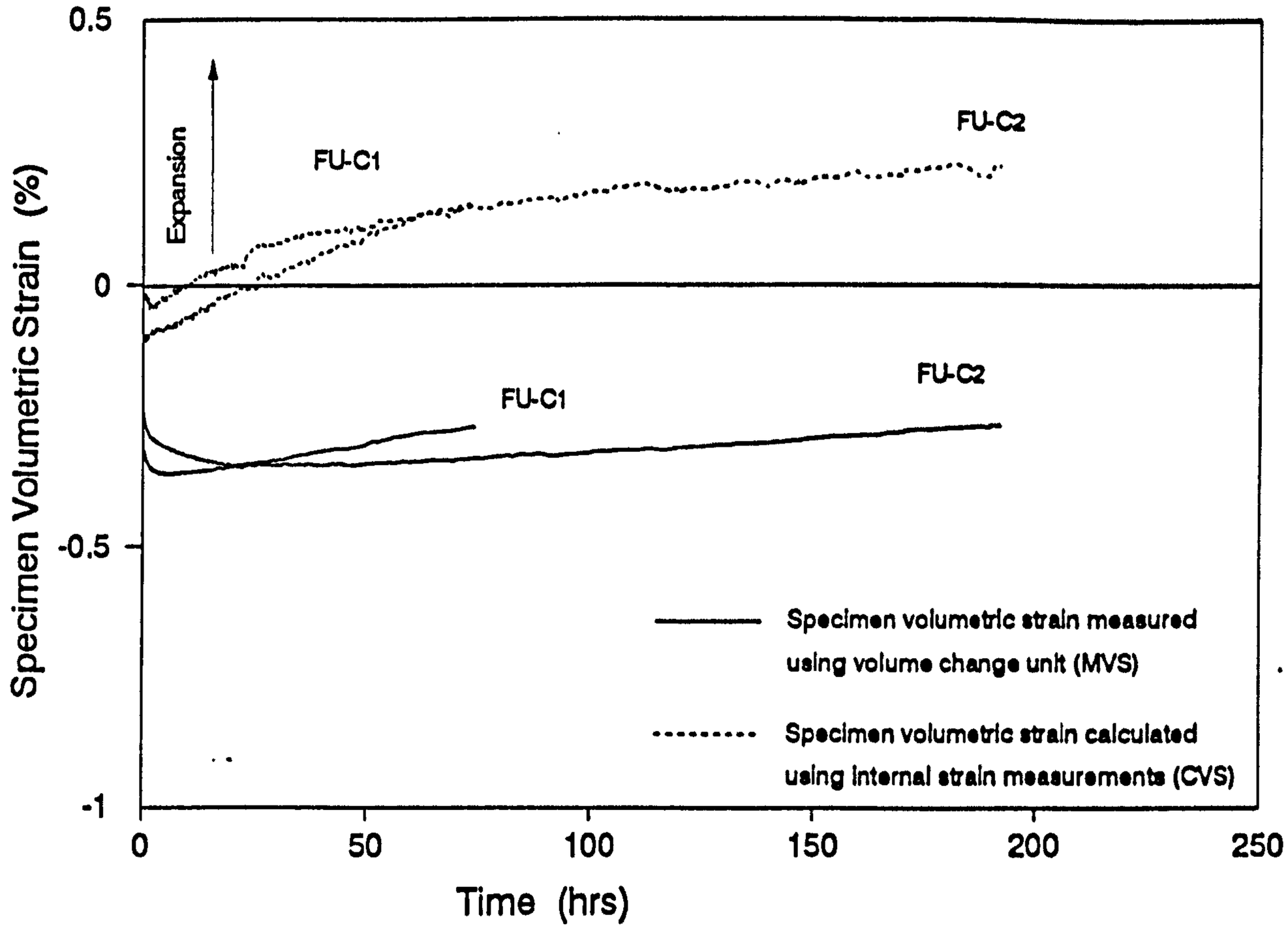

Fig. 7.33a- Specimen volumetric strain during the equalisation stage for test series C.

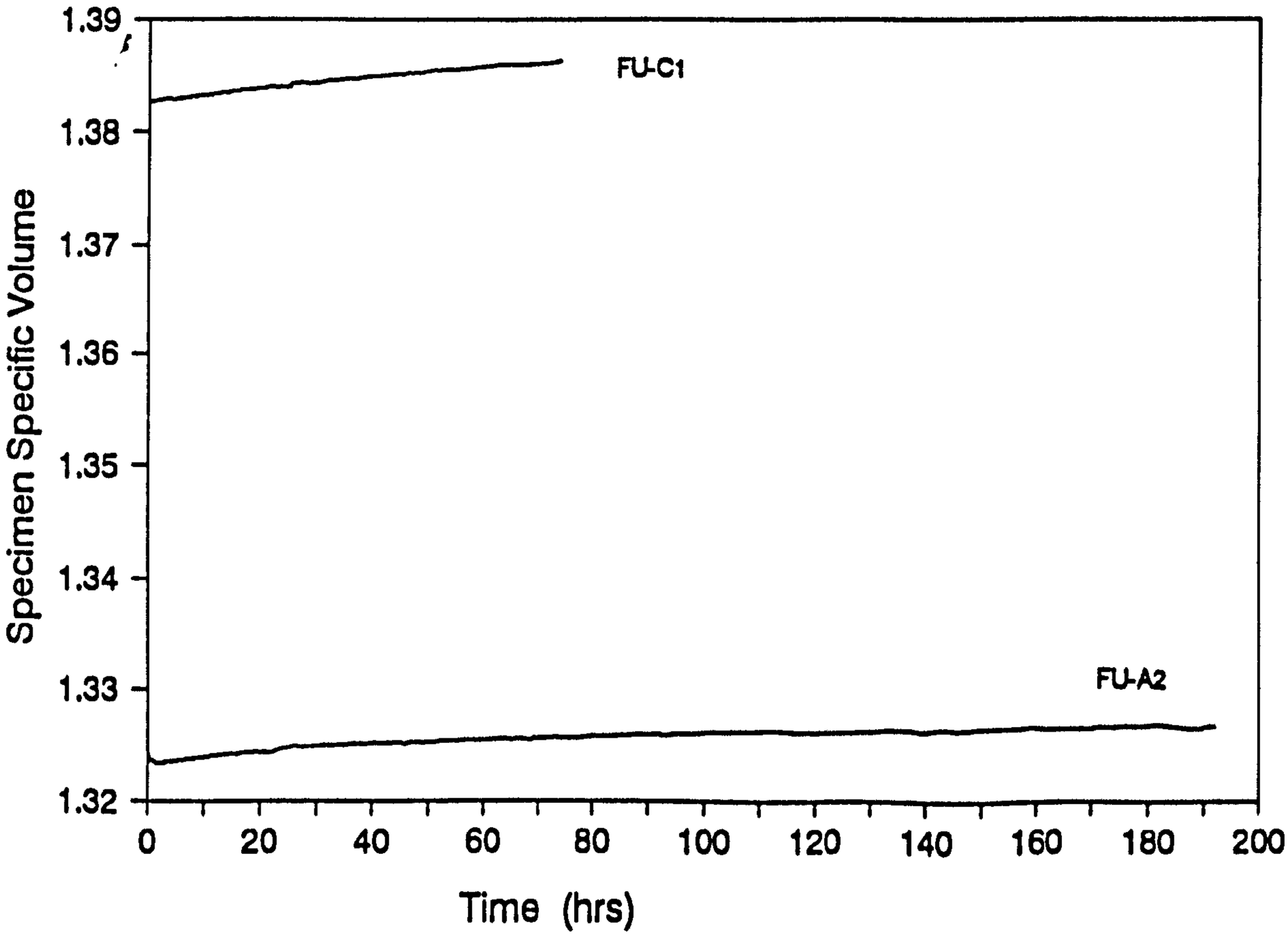

Fig. 7.33b- Specimen specific volume during the equalisation stage for test series C.

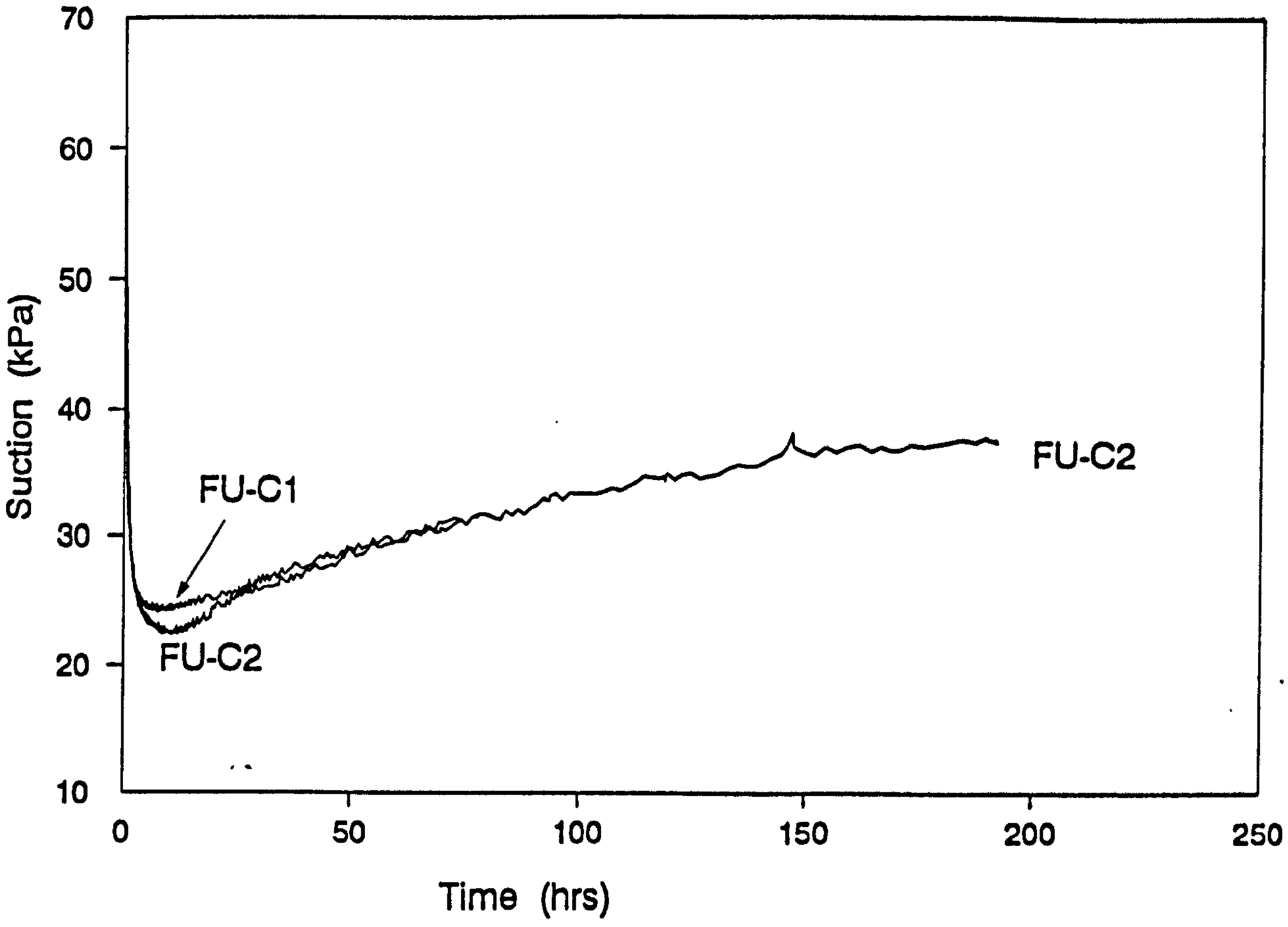

Fig. 7.34- Specimen suction during the equalisation stage for test series C.

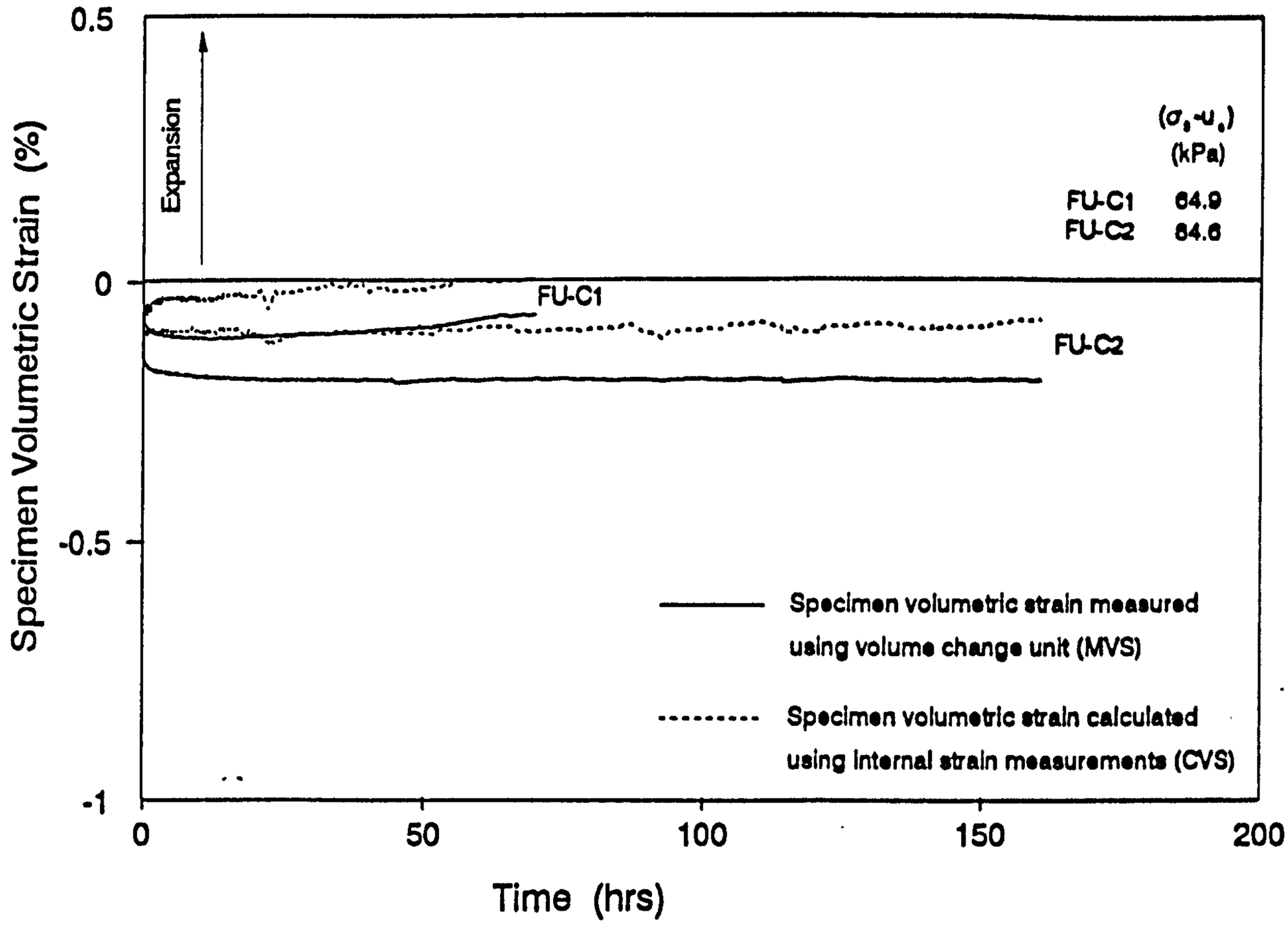

Fig. 7.35a- Specimen volumetric strain during the consolidation stage for test series C.

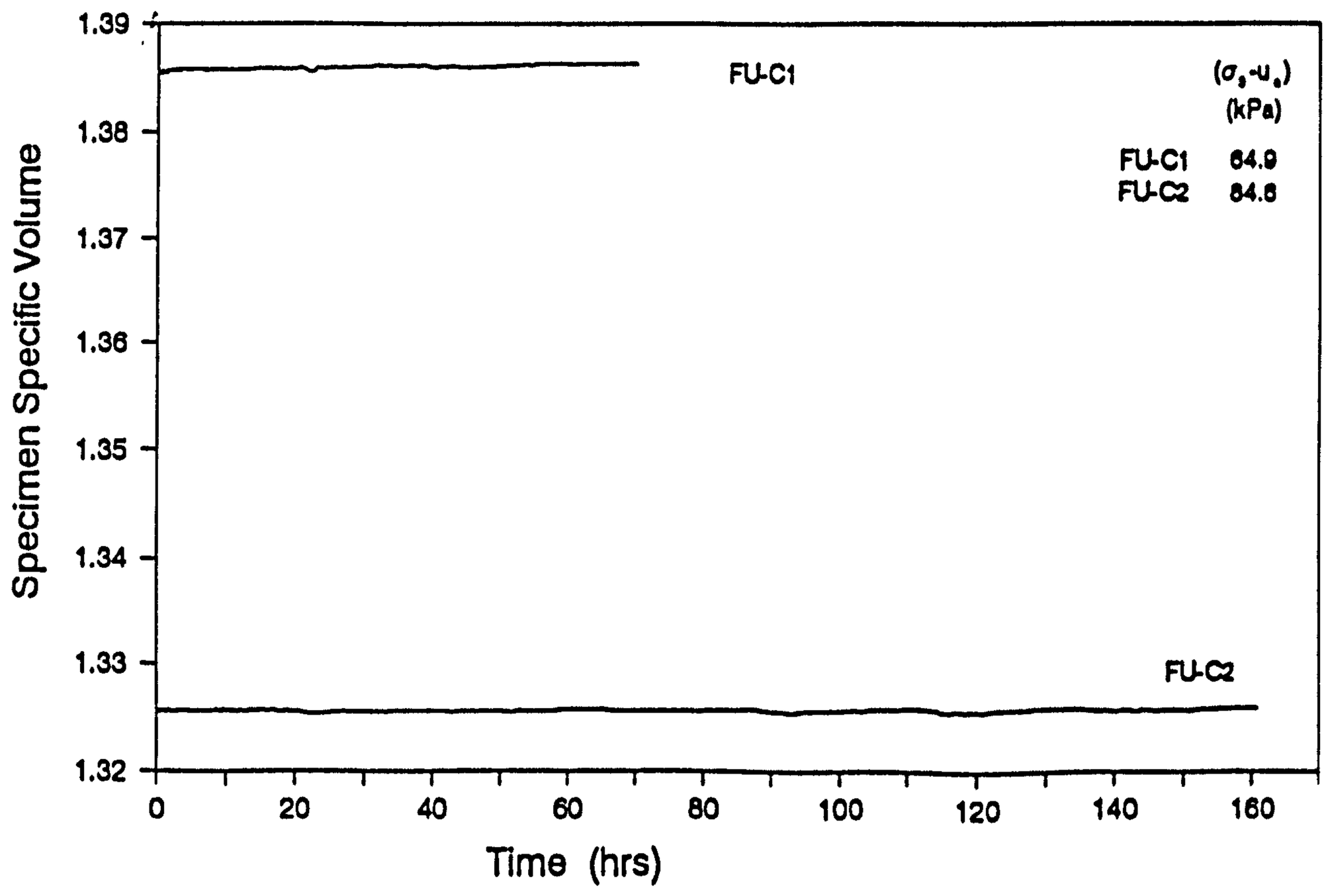

Fig. 7.35b- Specimen specific volume during the consolidation stage for test series C.

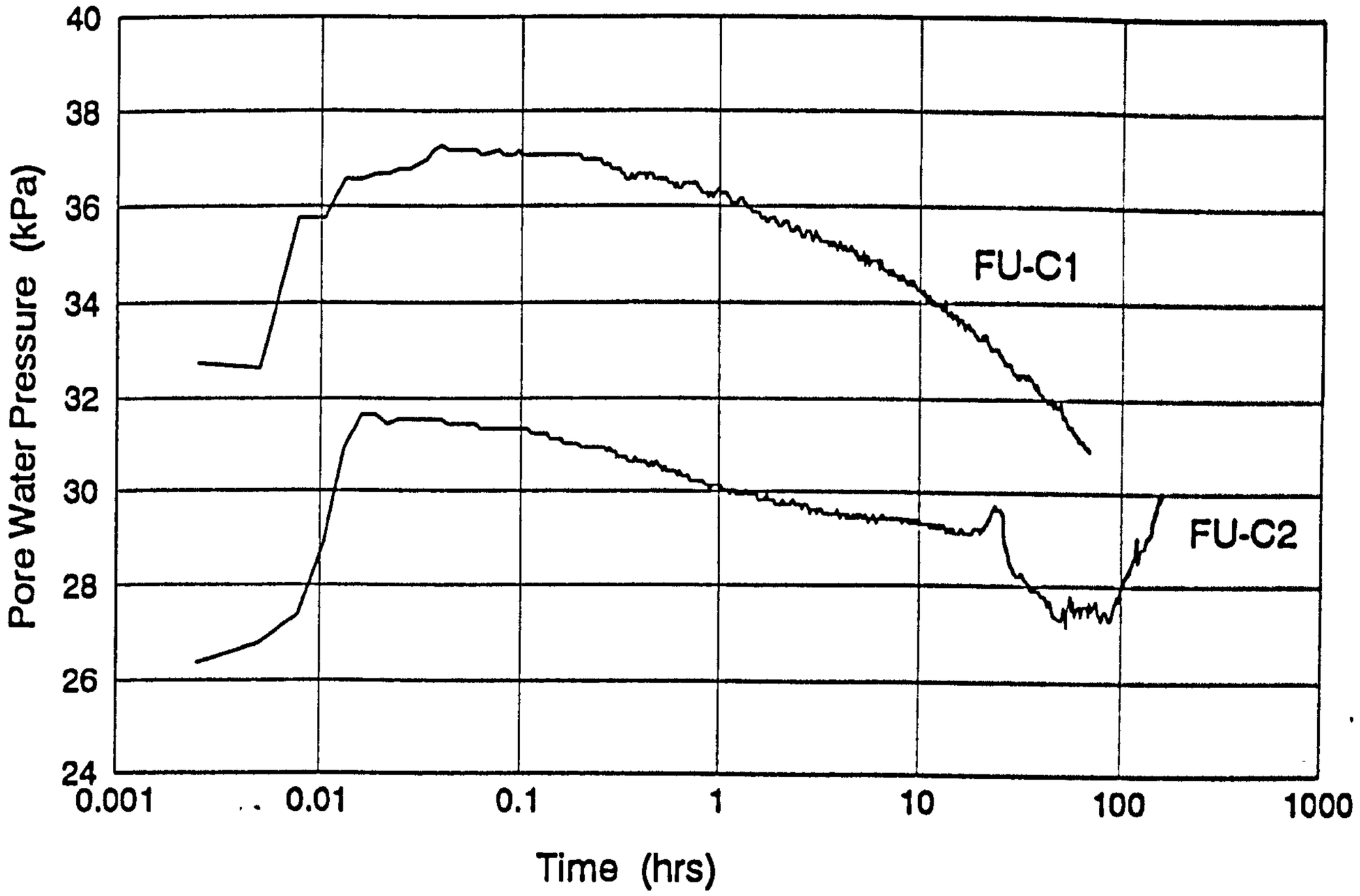

Fig. 7.36- Specimen pore water pressure measurements during the consolidation stage for test series C.

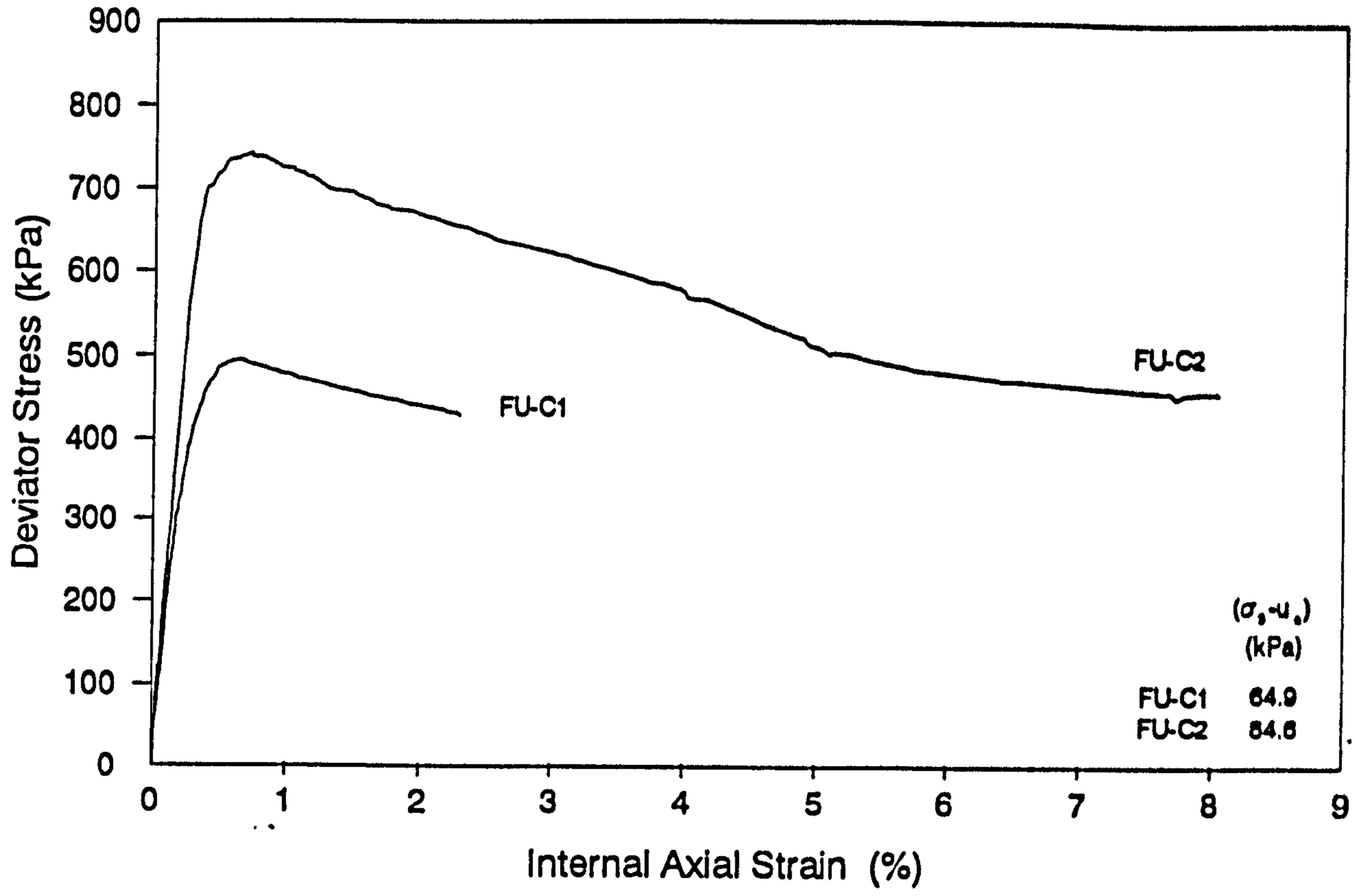

Fig. 7.37- Deviator stress-strain curves for test series C.

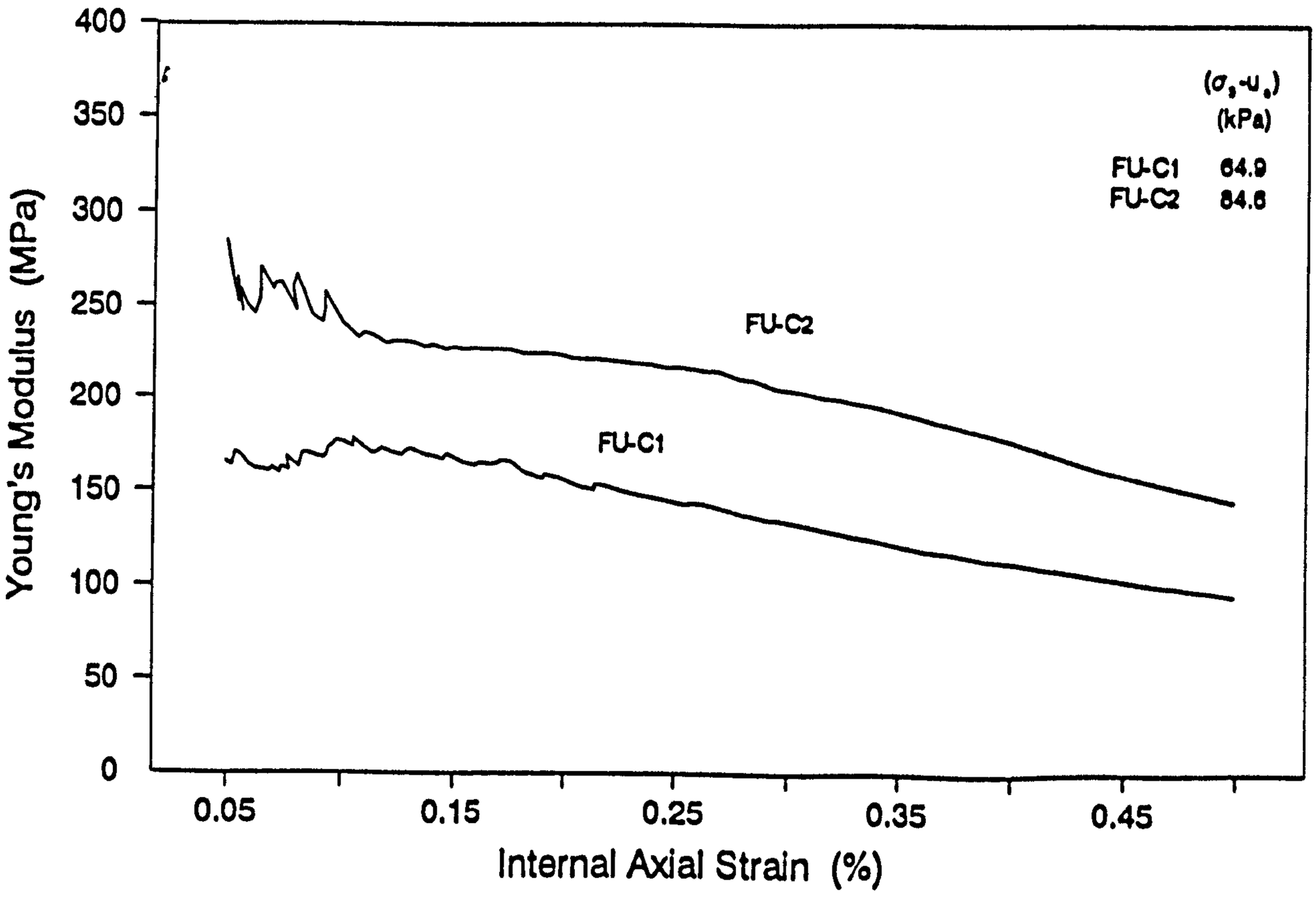

Fig. 7.38- Young's modulus plotted against internal axial strain for test series C.

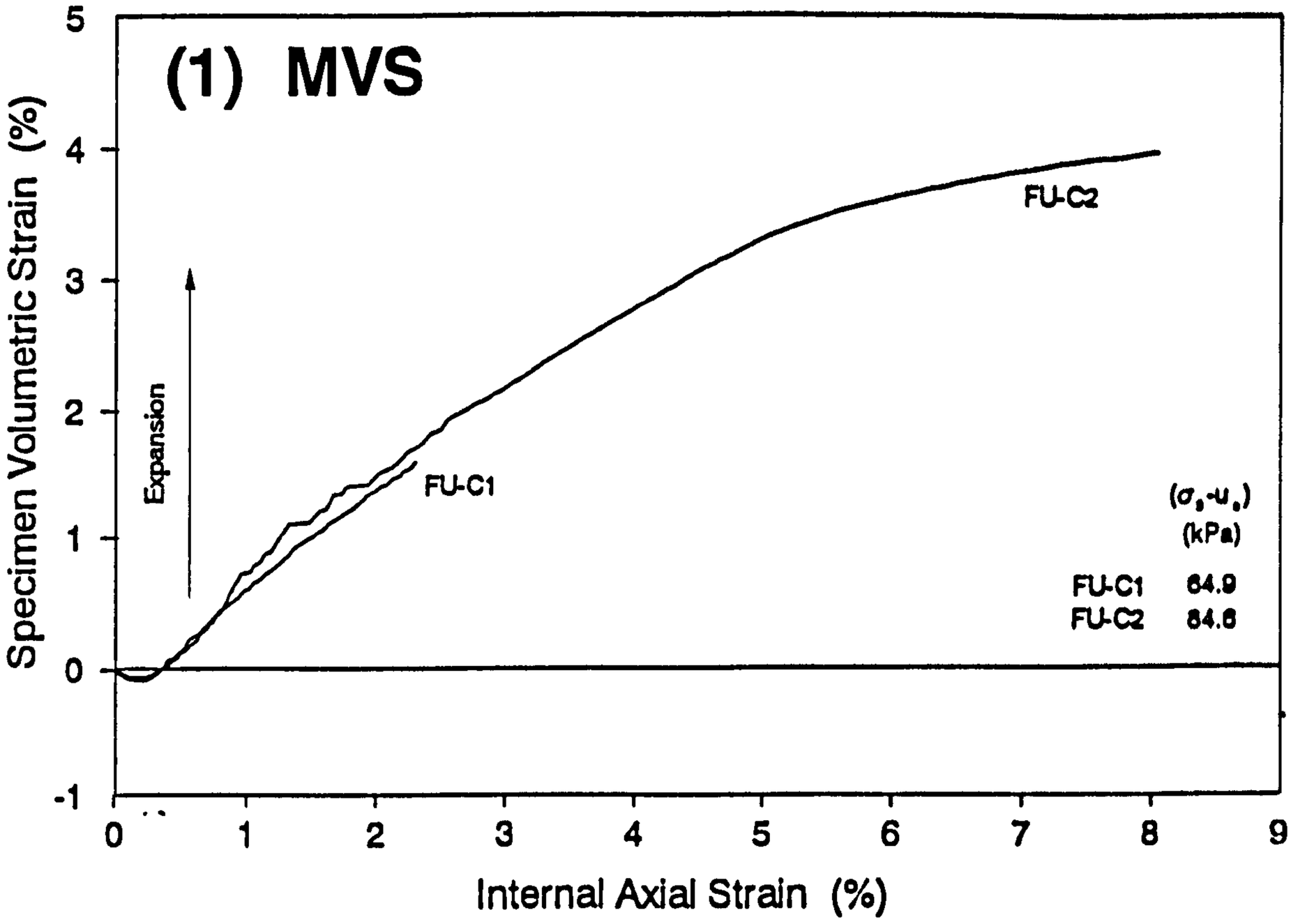

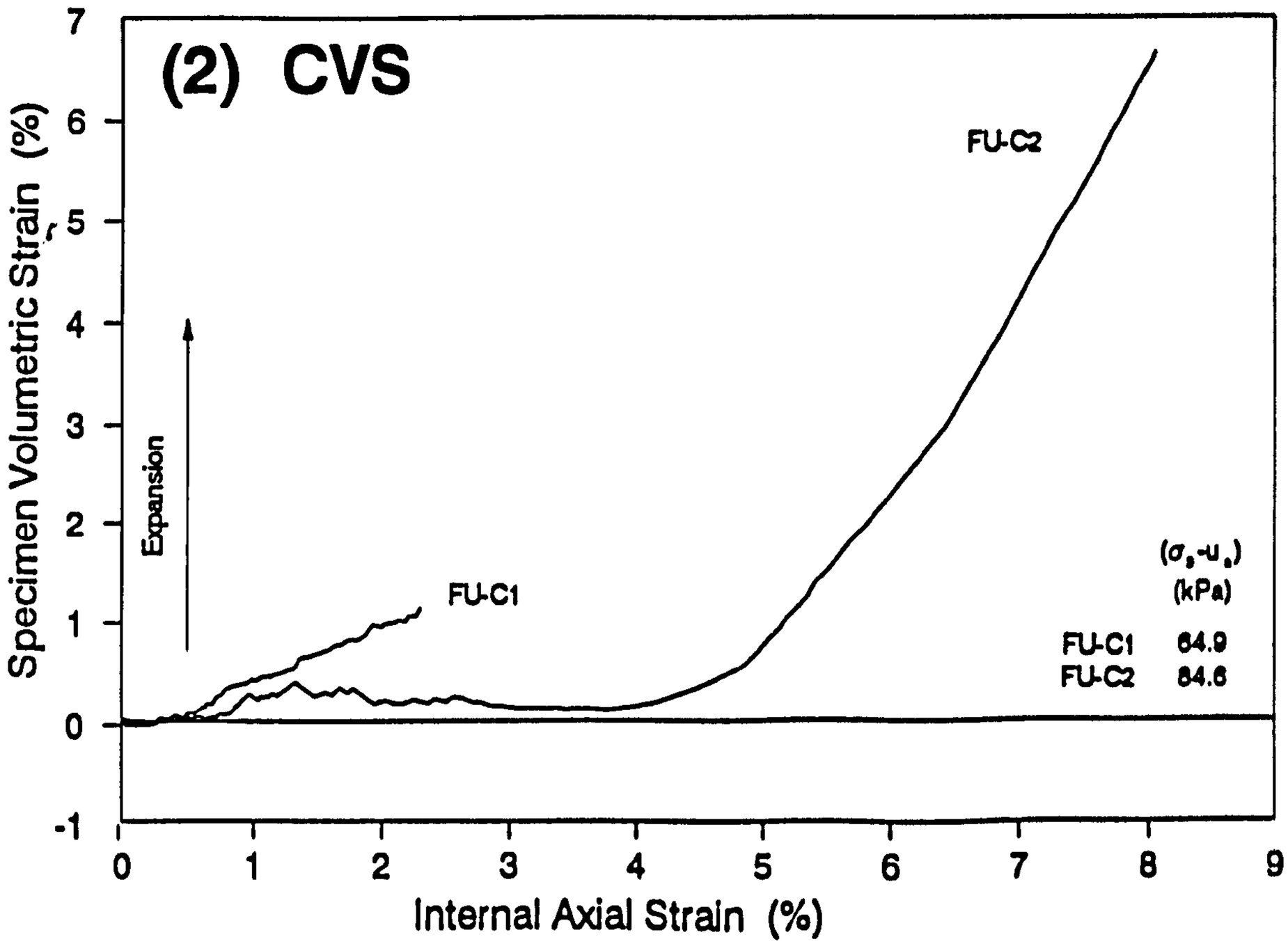

Fig. 7.39a- Specimen volumetric strain during the shearing stage of test series C, measured using (1) volume change unit (MVS) and (2) internal strain measurements (CVS).

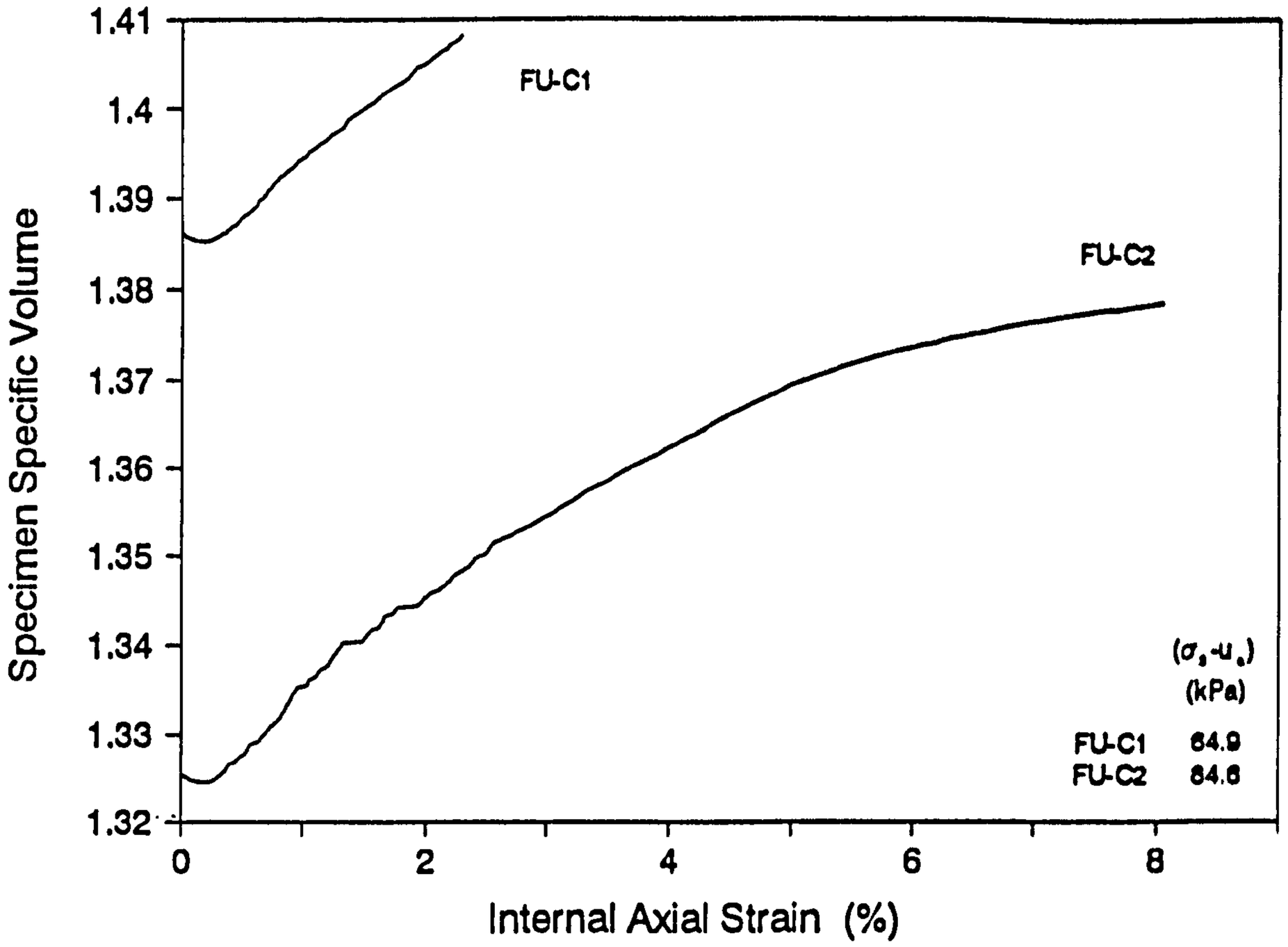

Fig. 7.39b- Specimen specific volume during the shearing stage of test series C, measured using the volume change unit

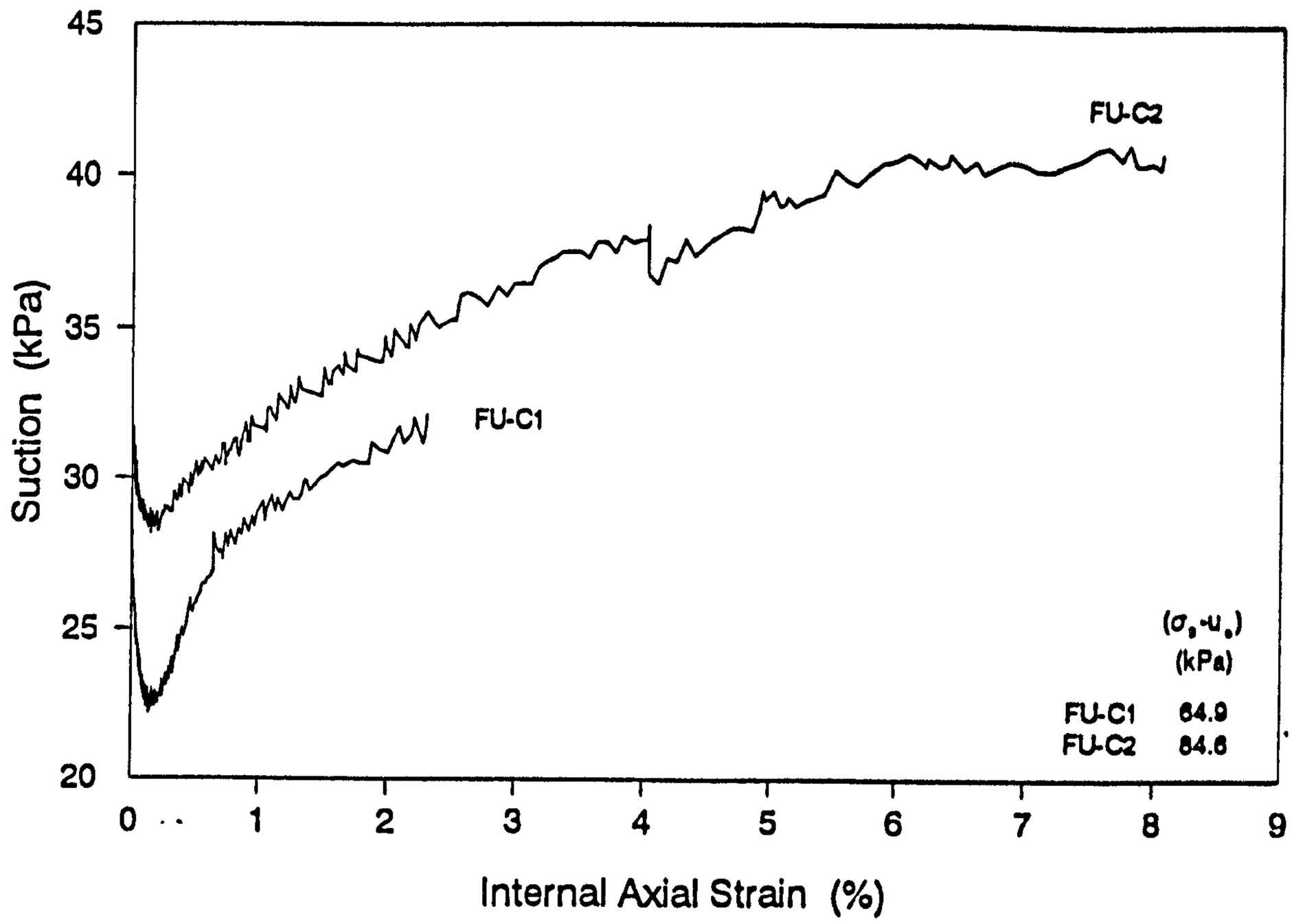

Fig. 7.40- Specimen suction change during the shearing stage of test series C.

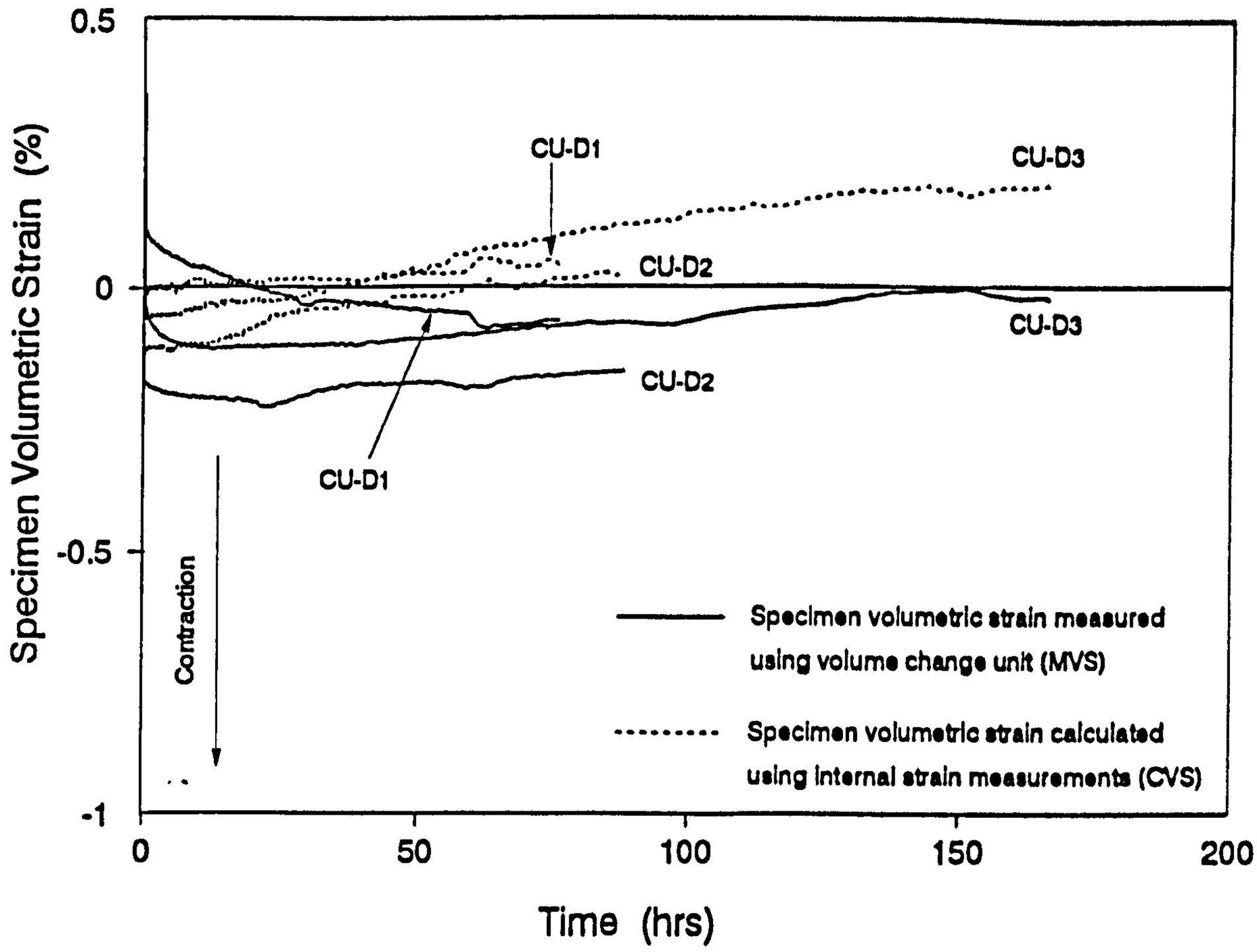

Fig. 7.41a- Specimen volumetric strain during the equalisation stage for test series D.

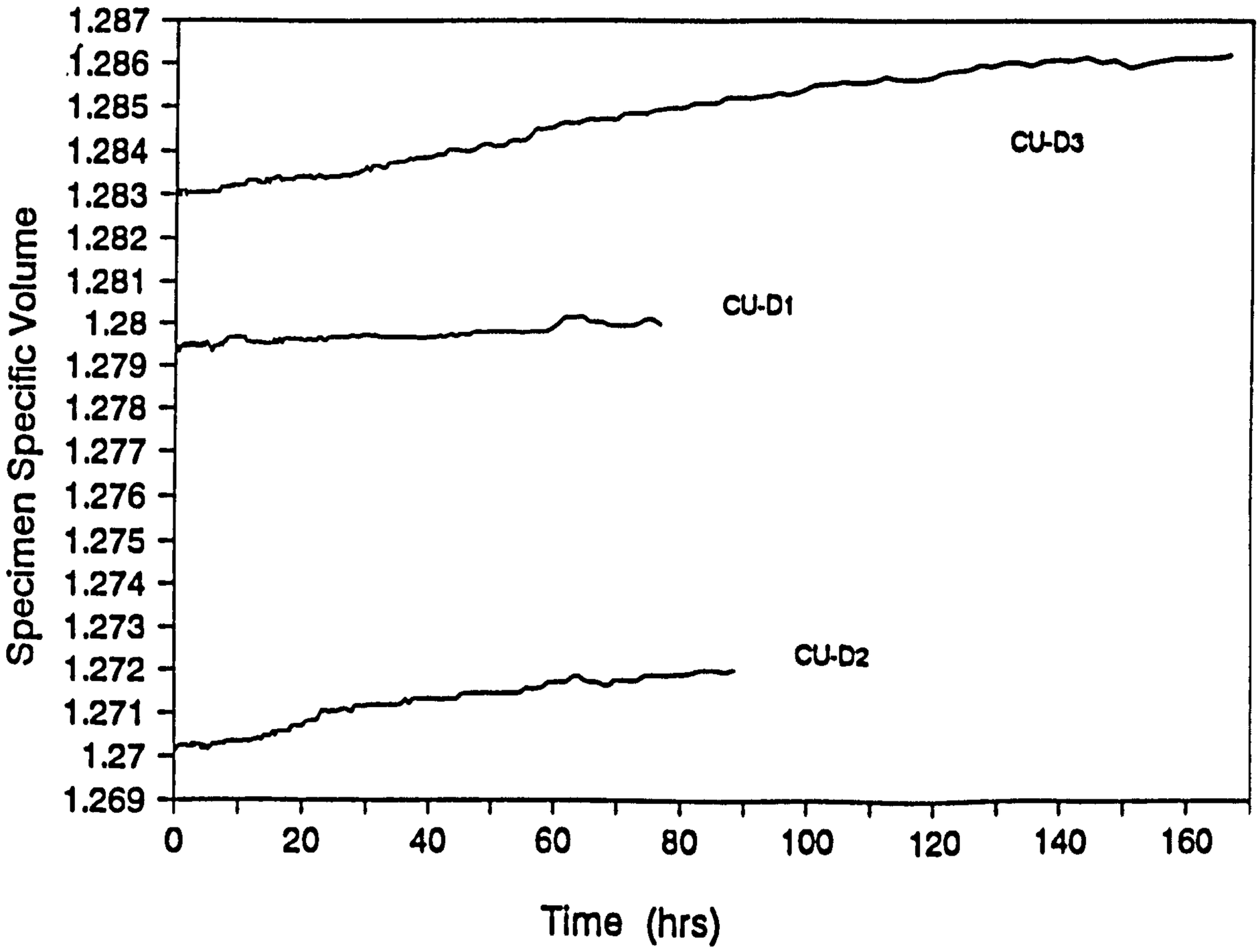

Fig. 7.41b- Specimen specific volume during the equalisation stage for test series D.

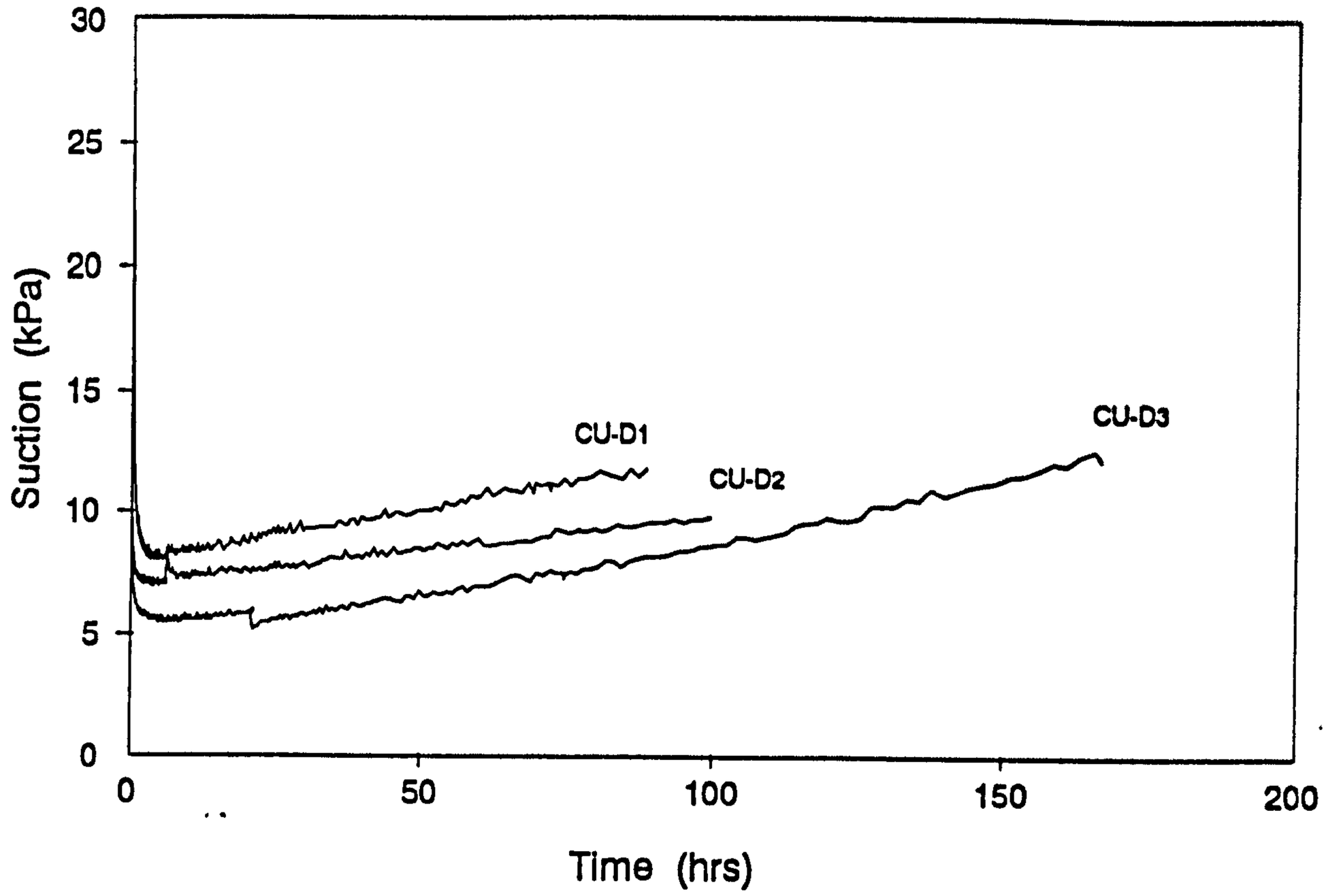

Fig. 7.42- Specimen suction during the equalisation stage for test series D.

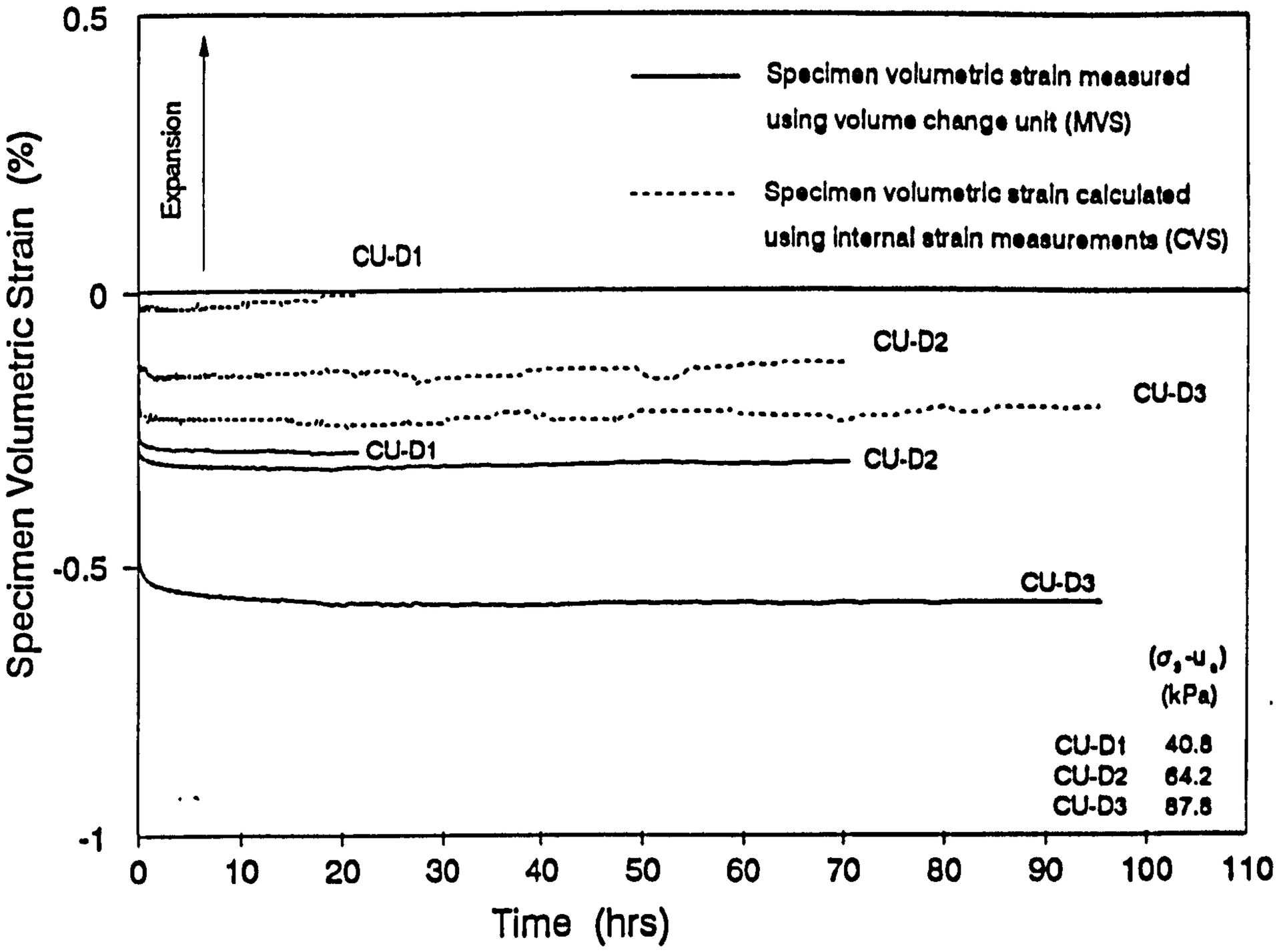

Fig. 7.43a- Specimen volumetric strain during the consolidation stage for test series D.

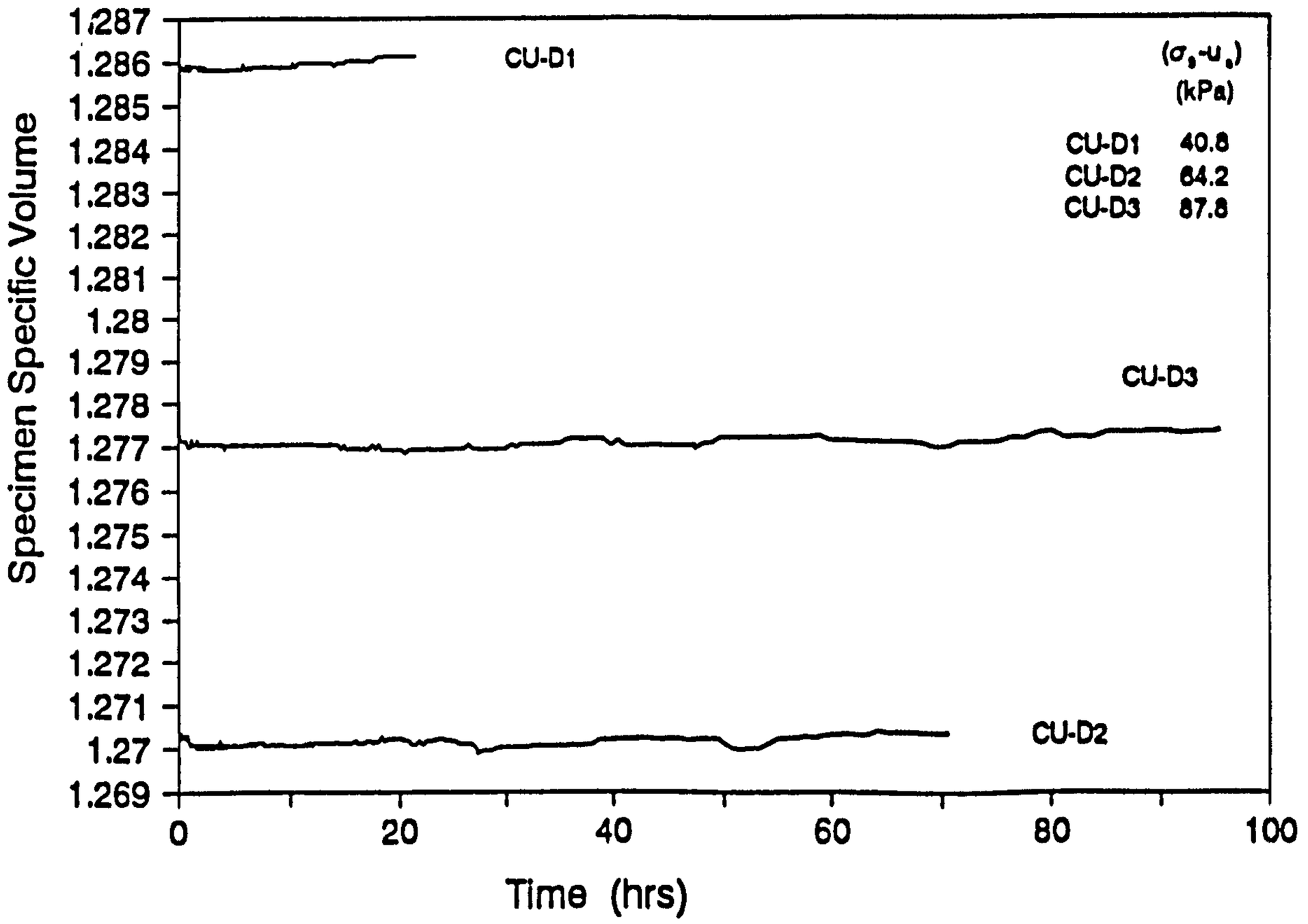

Fig. 7.43b- Specimen specific volume during the consolidation stage for test series D.

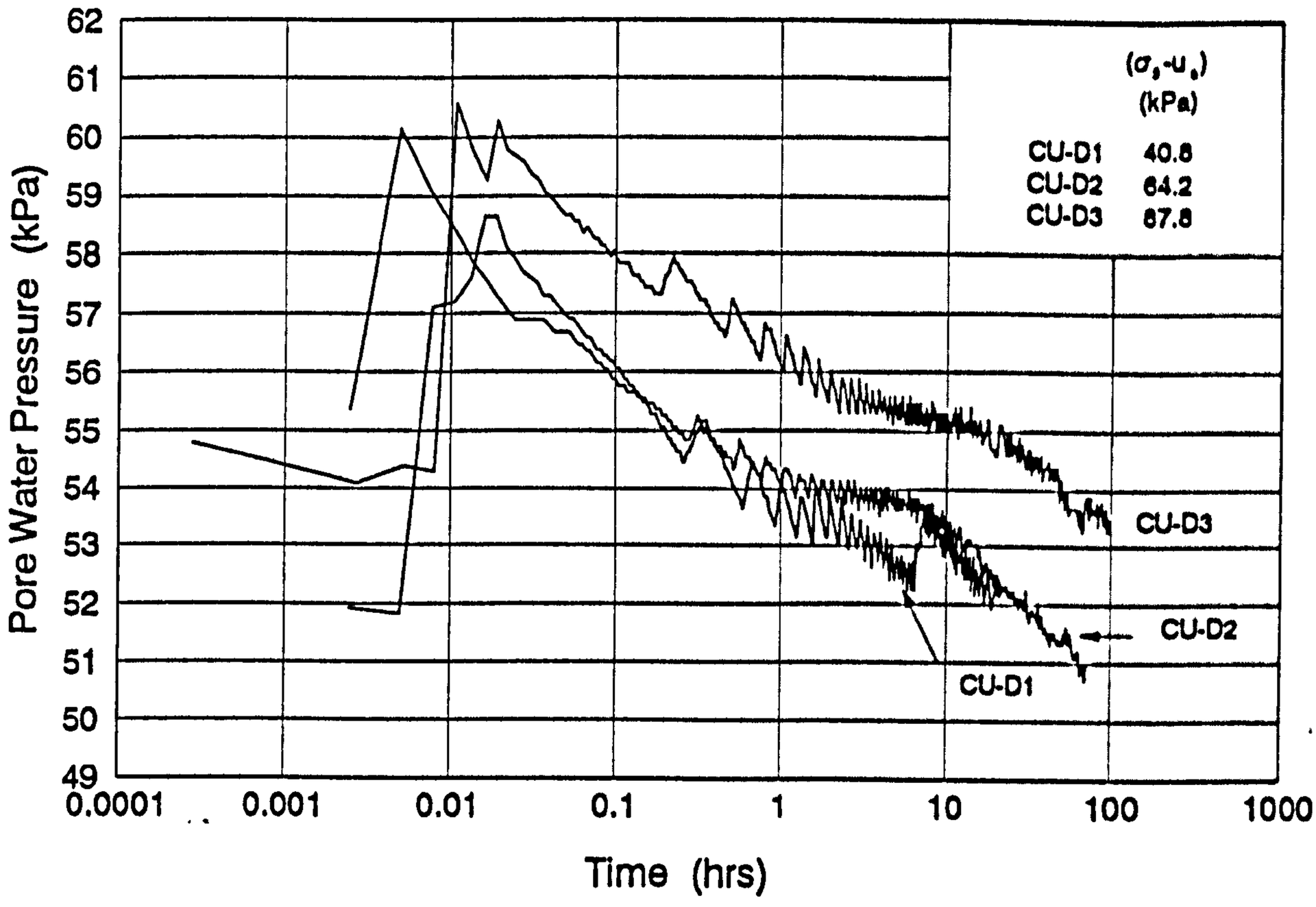

Fig. 7.44- Specimen pore water pressure measurements during the consolidation stage for test series D.

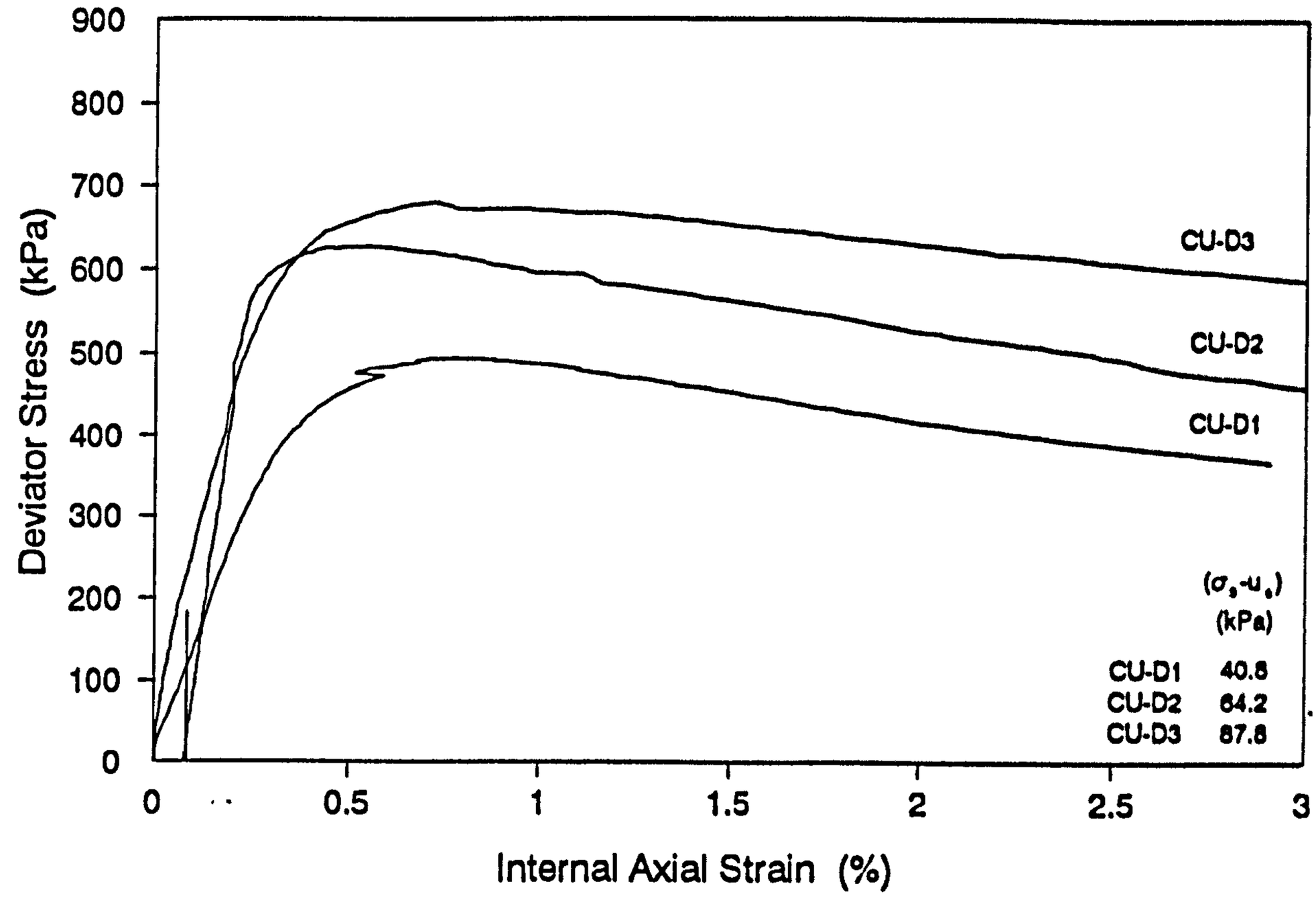

Fig. 7.45- Deviator stress-strain curves for test series D.

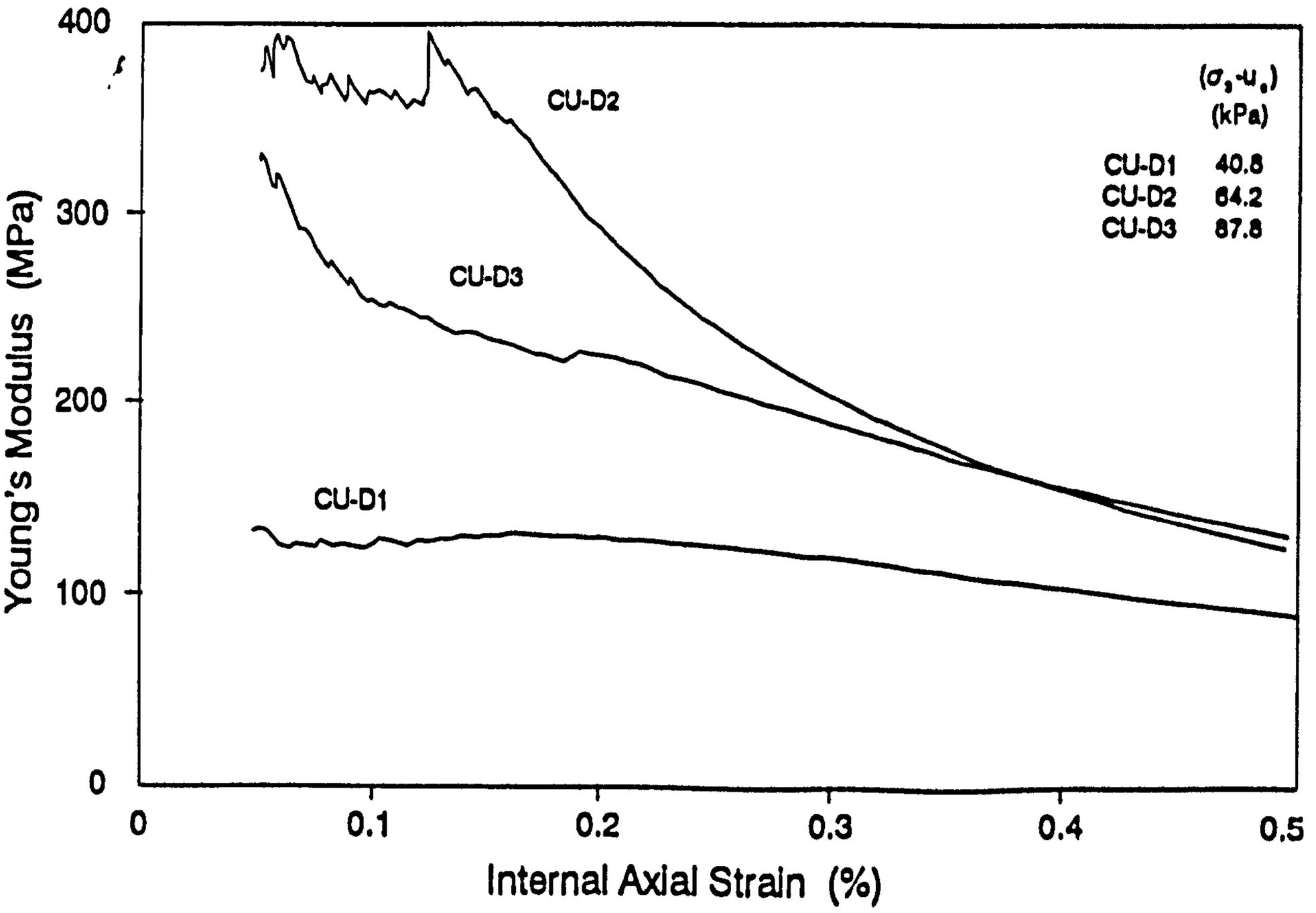

Fig. 7.46- Young's modulus plotted against internal axial strain for test series D.

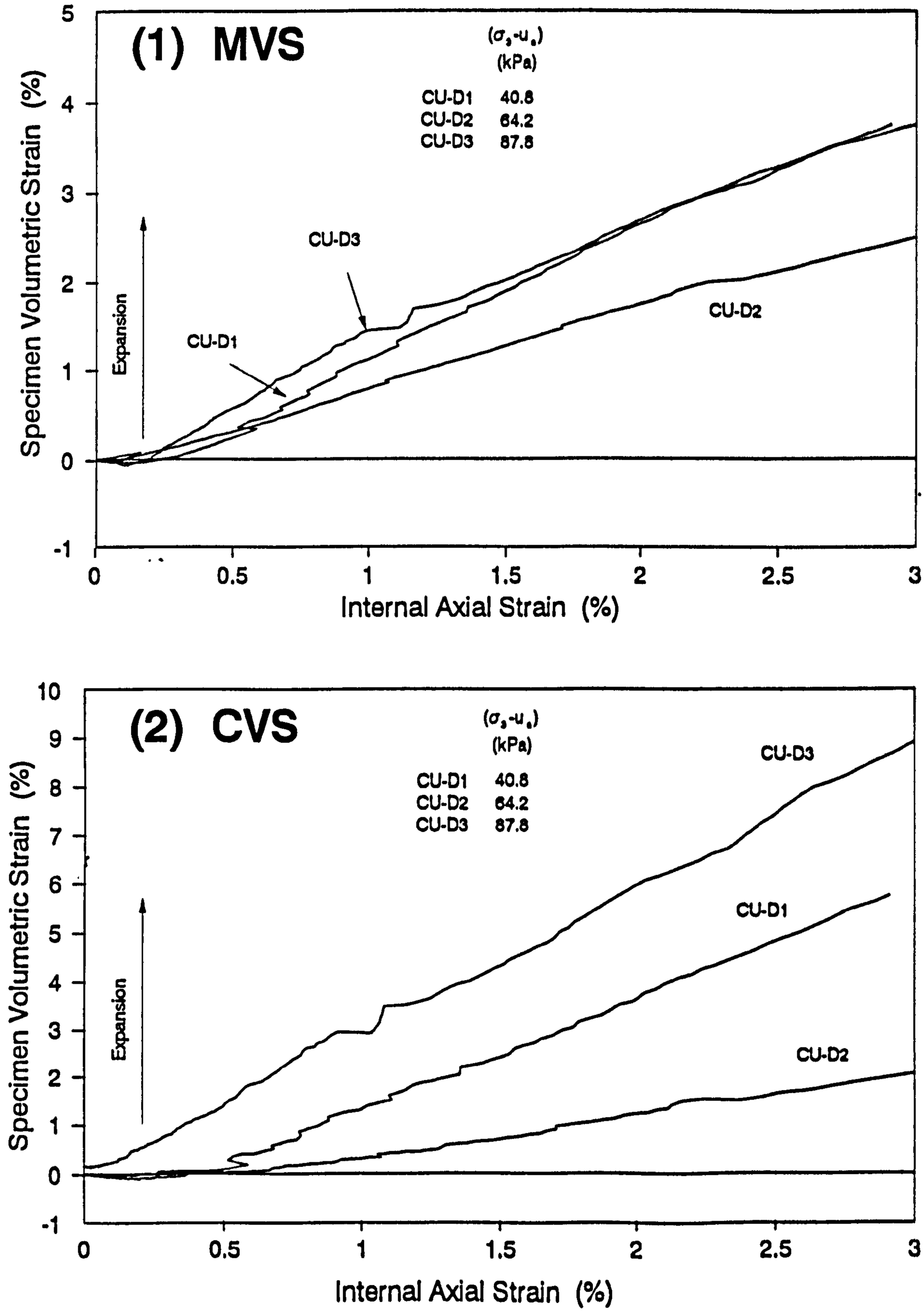

Fig. 7.47a- Specimen volumetric strain during the shearing stage of test series D, measured using the (1) volume change unit (MVS) and (2) internal strain measurements (CVS).

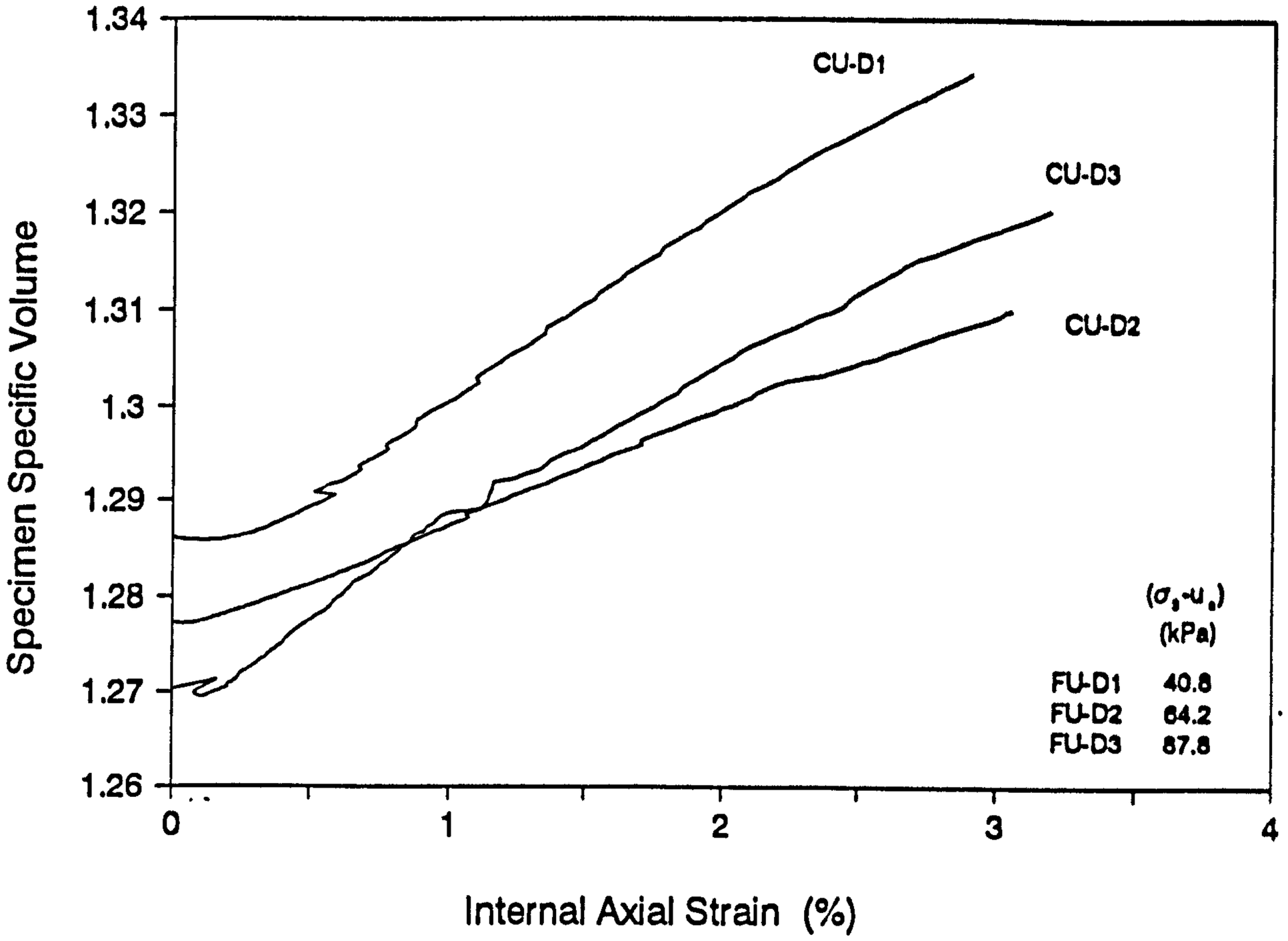

Fig. 7.47b- Specimen specific volume during the shearing stage of test series D, measured using the volume change unit

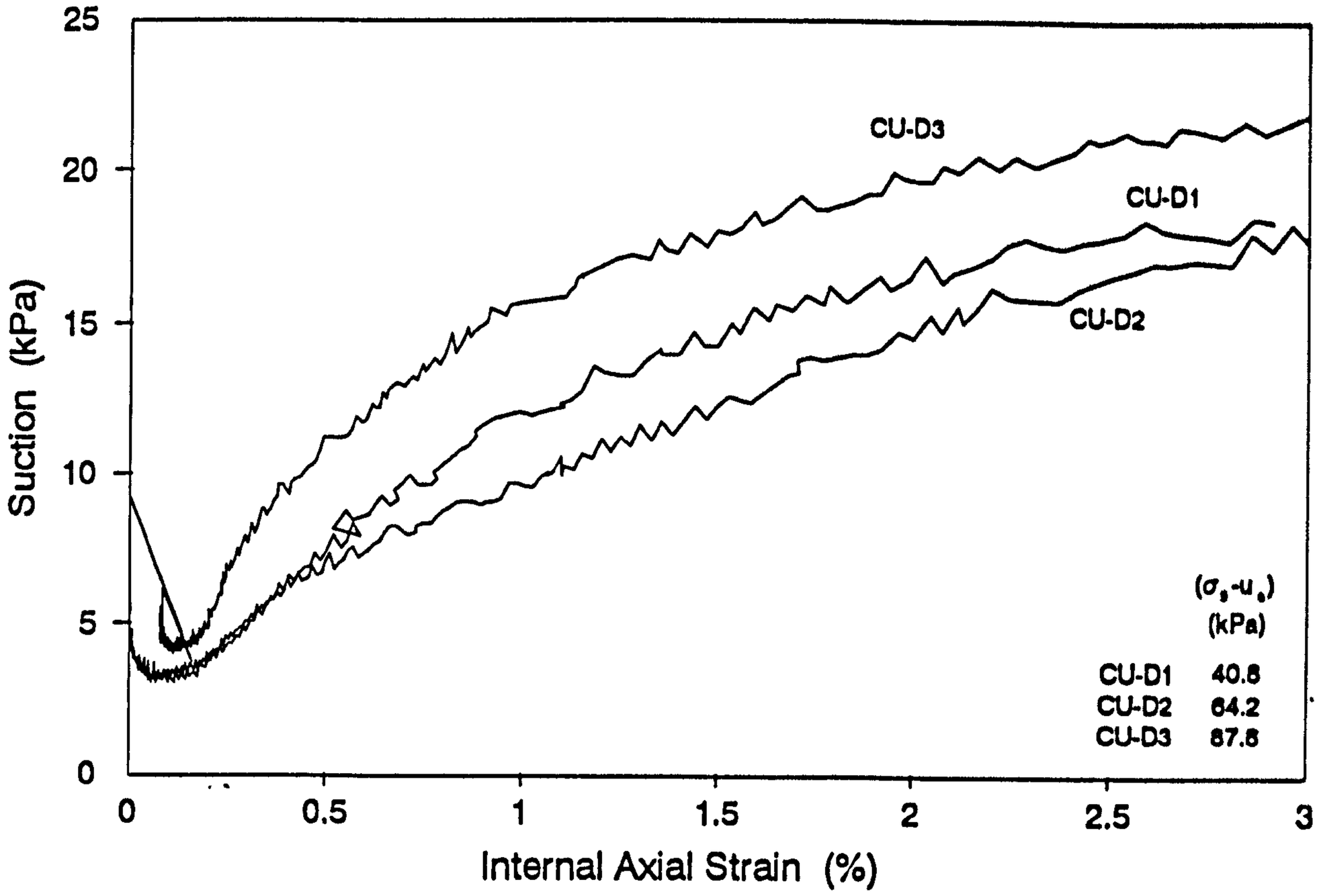

Fig. 7.48- Specimen suction change measured during the shearing stage of test series D.

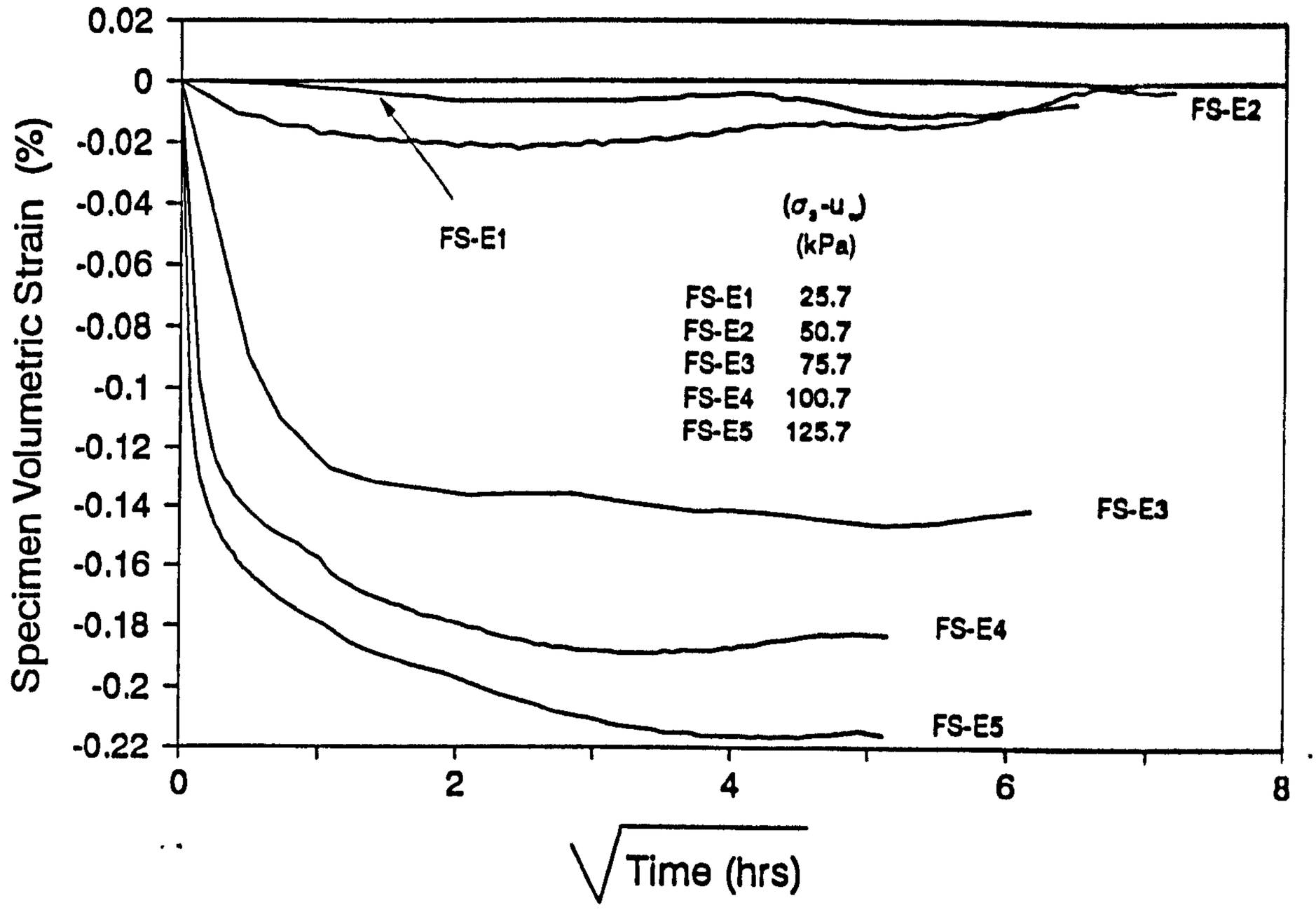

Fig. 7.49a- Saturated specimen volumetric strain measured using the volume change unit during the consolidation stage of test series E.

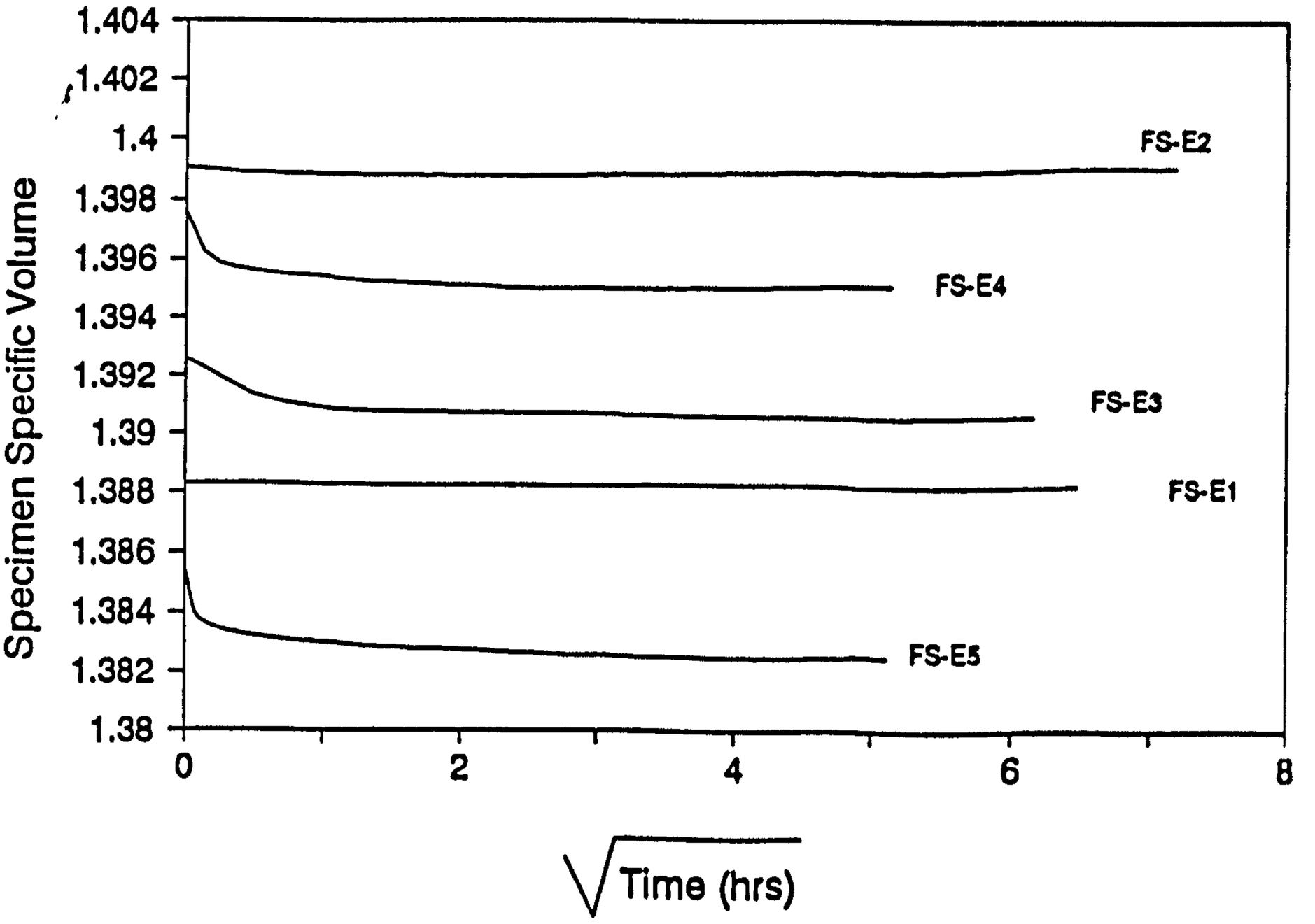

Fig. 7.49b- Saturated specimen specific volume measured using the volume change unit during the consolidation stage of test series E.

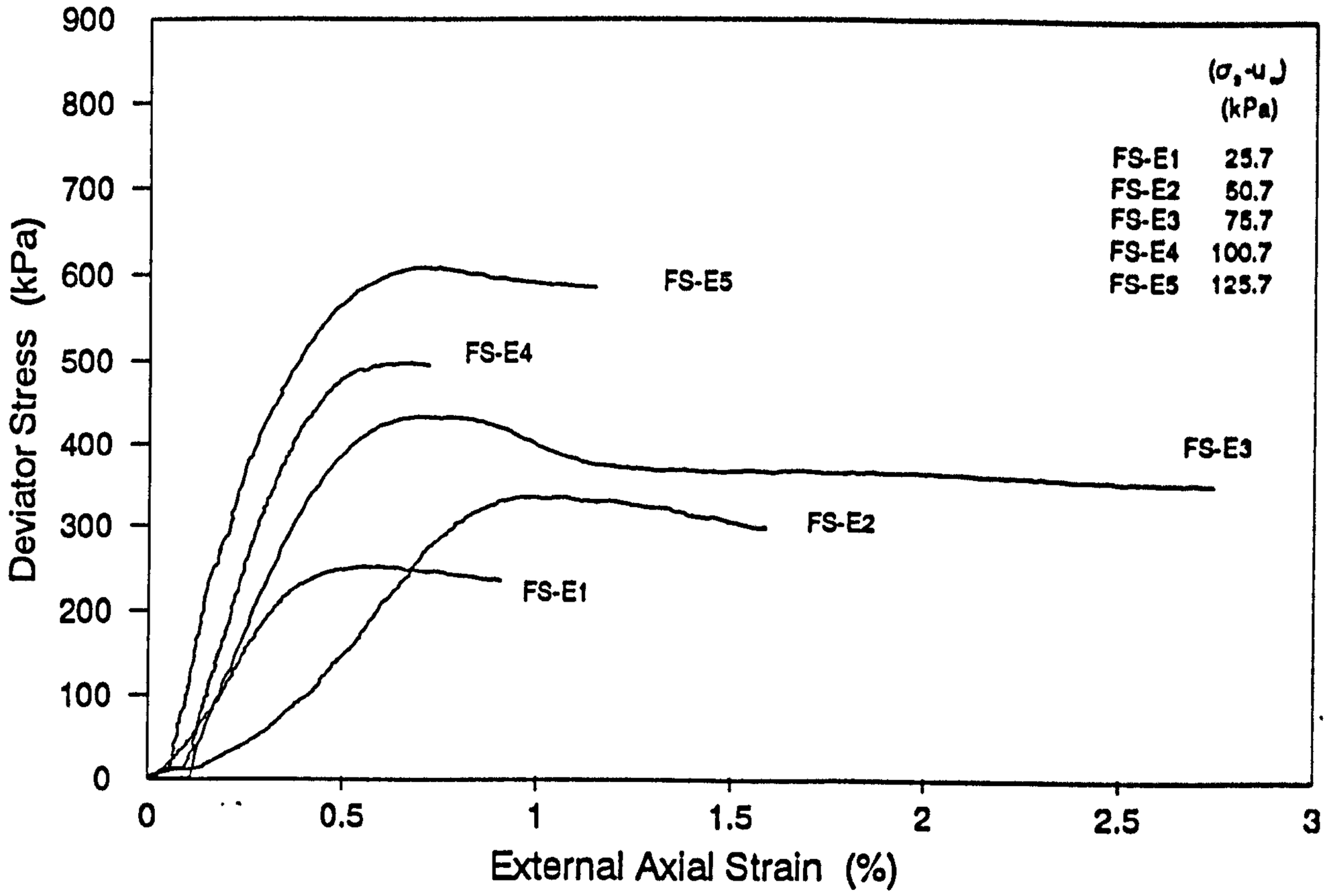

Fig. 7.50- Deviator stress-strain curves for test series E (saturated specimens).

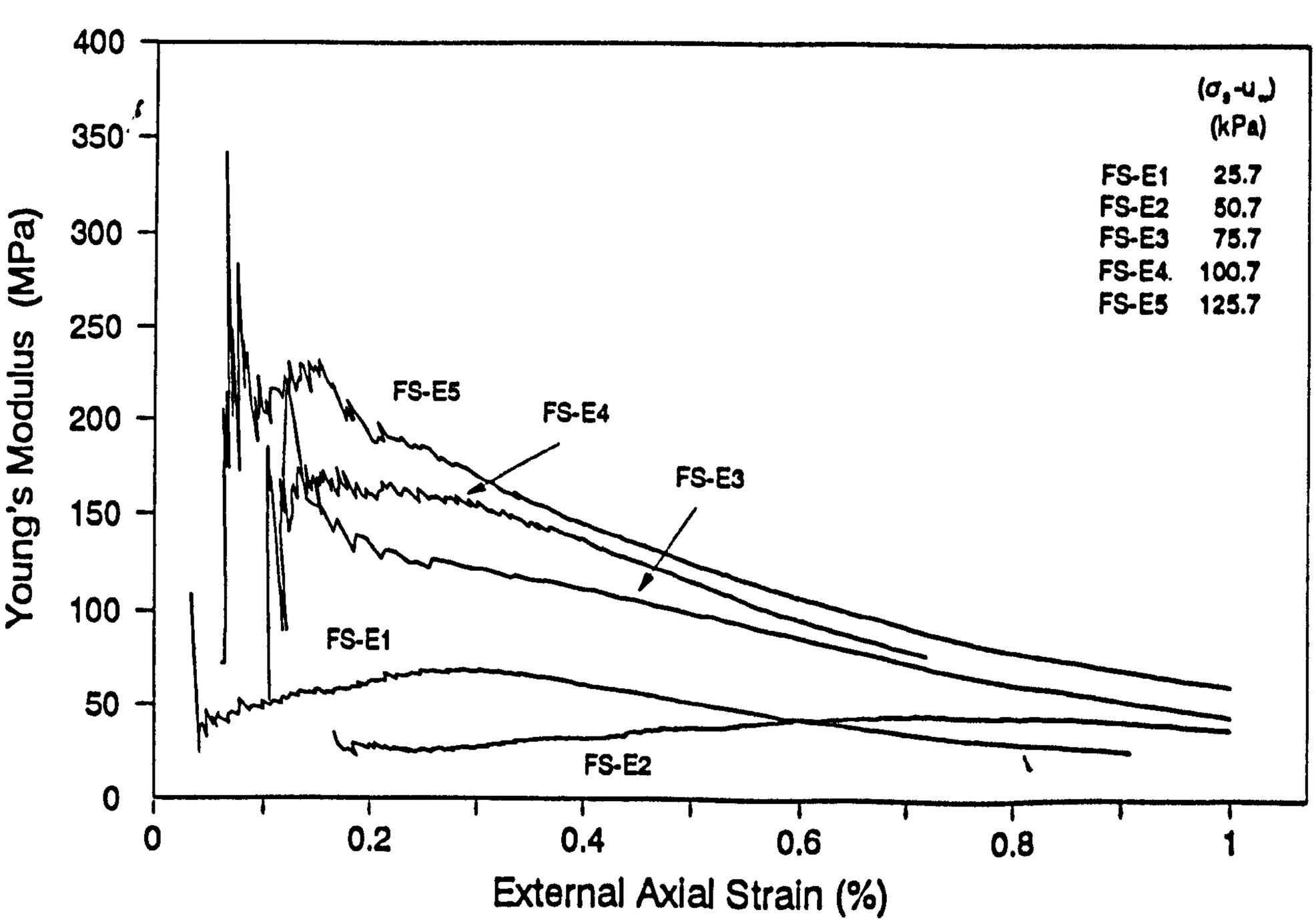

Fig. 7.51- Young's modulus plotted against external axial strain for test series E (saturated specimens).

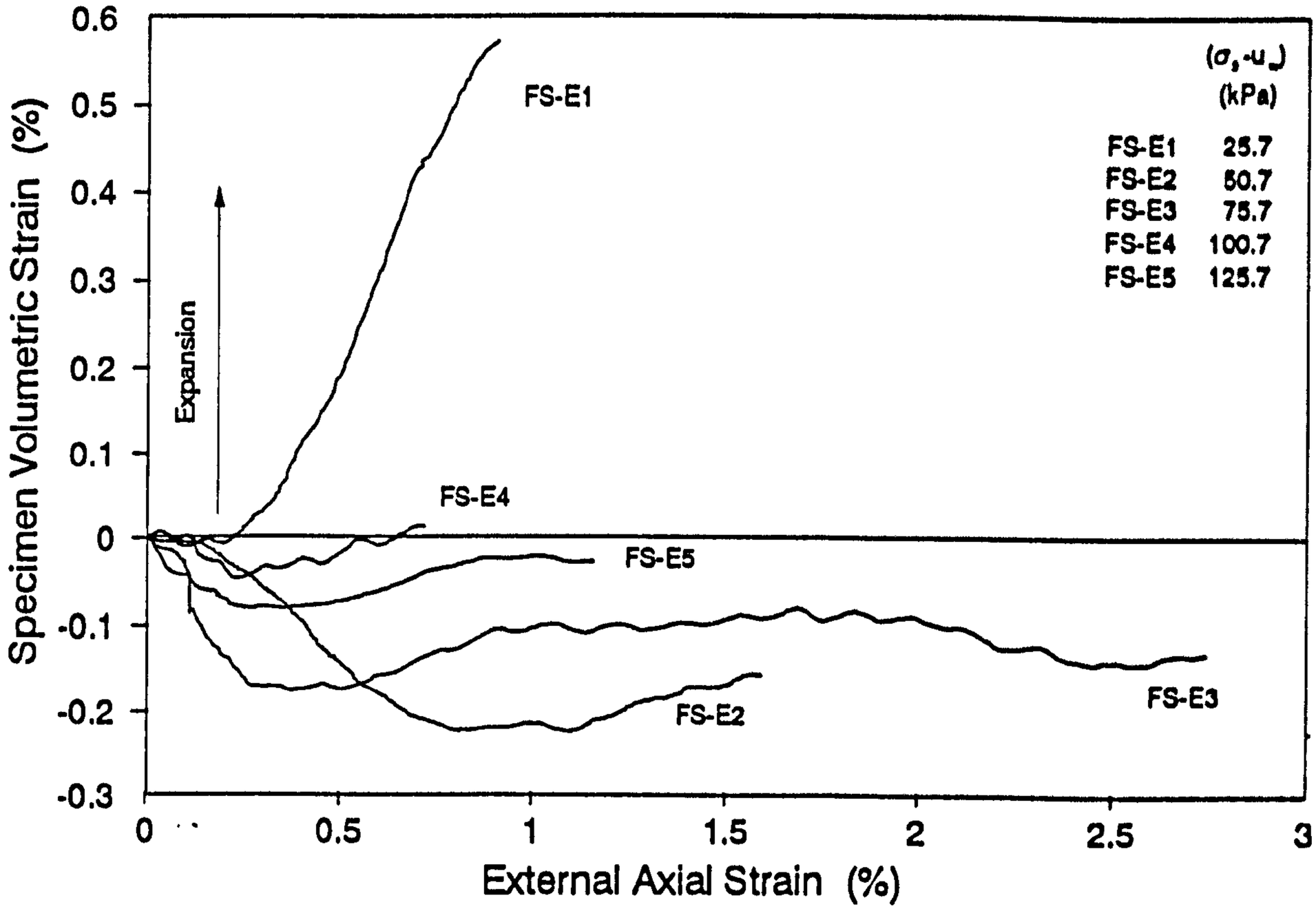

Fig. 7.52a- Saturated specimen volumetric strain during the shearing stage of test series E, measured using the volume change unit.

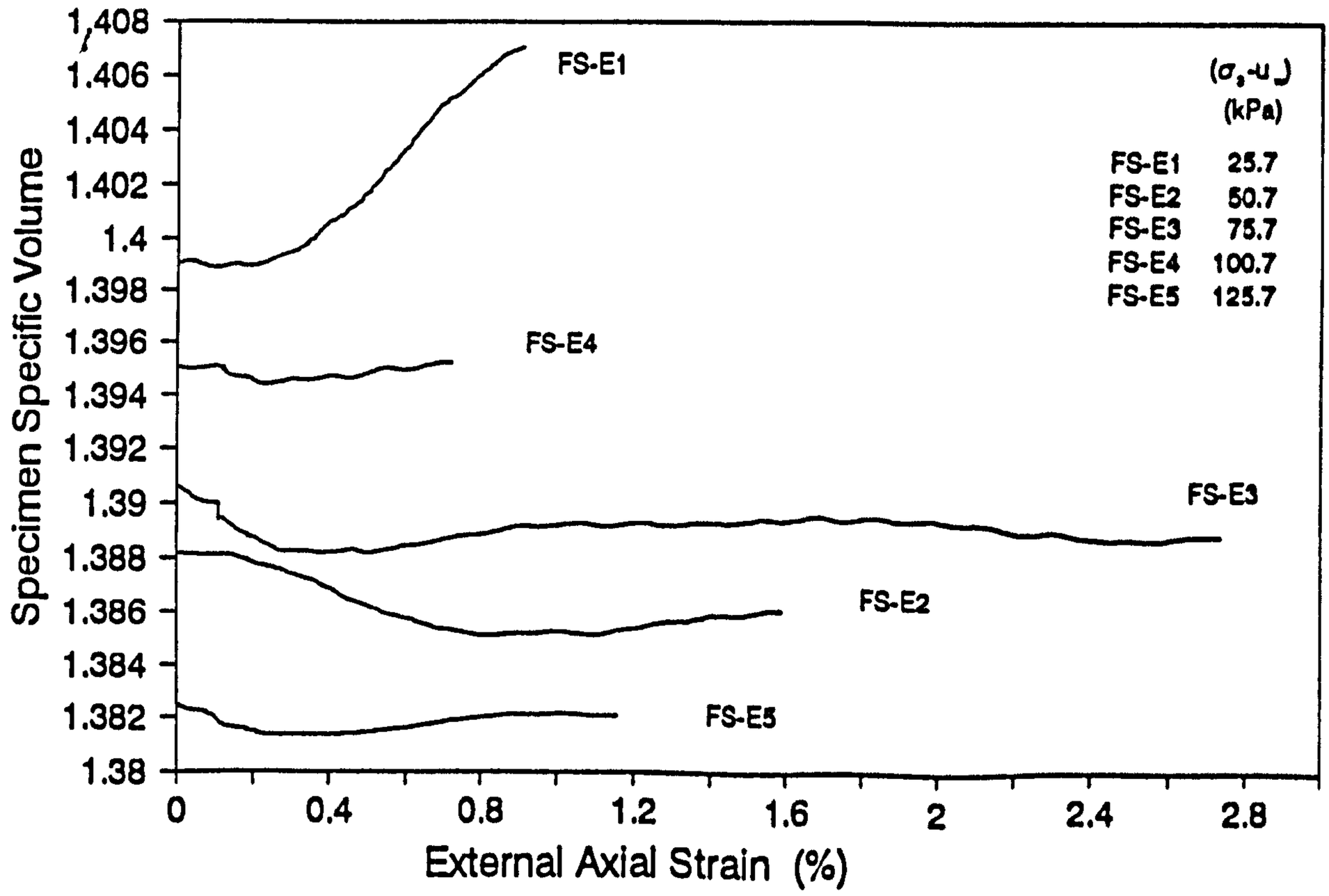

Fig. 7.52b- Saturated specimen specific volume during the shearing stage of test series E, measured using the volume change unit.

Chapter 8

Discussion

8.1 Introduction

Initial interpretation of the soil behaviour together with discussion on the performance of the new double-wall triaxial cell were given in Chapter 7, but more detailed discussion of the test results will be given in this chapter. The discussion will concentrate on the behaviour of the fine grading saturated and unsaturated soils, as most of the work in the current research was carried out on fine grading specimens. Comparison between the behaviour of the coarse and fine grading soils will be made in Section 8.16.

8.2 Suction Distribution within the Specimen

In the current research, pore water pressure was only measured at the specimen base (Section 4.2.1F) and therefore the values of the suction $(u_a - u_w)$ reported only apply strictly to the specimen base. It was reported in Section 2.4 that authors, such as Croney (1952), had found a relationship between suction and water content of a soil (Figs. 2.4 and 2.5). This relationship indicates that if there is a difference in water content at any two locations within a specimen, these two locations will have different values of suction, with the higher water content giving rise to a lower suction. This difference in suction induces a suction gradient, forcing water to migrate from the higher water content location to the lower one, until equilibrium is restored. Water migration can be either in the liquid or vapour phases, and can be upward when the suction difference at the two locations is higher then the gravitational stresses (Section 2.4)

From this discussion it can be concluded that for soils that contain only held water (Section 2.3), which is below the optimum water content, the difference in water content and suction between the top and bottom of a soil specimen can be very small. It may also be concluded that the difference in suction between the bottom and middle of the specimens used in this research (specimen height was 375 mm), was about 1.8 kPa, which was due to the gravitational stresses.

In this research, the water contents along the specimen were determined at the end of each test, as was described in Section 7.3.2.4, and Table 7.3 shows these results. It can be seen, within 0.05% accuracy, that the water contents were approximately uniform along the specimens. This may support the conclusion above that if a specimen contains held water, there will be a very small difference in suction between its top and bottom.

8.3 Variation in the Initial Conditions of the Tested Specimens

To study the behaviour of an unsaturated soil at different values of suction, the initial conditions of the tested specimens such as soil grading, compactive effort, dry density and water content, should be kept constant for all specimens. In the current research it was attempted to keep these factors constant. However, some variations were found and these may have had an effect on the test results.

A slight variation in the soil grading was found (Fig. 6.2) and the reasons for this were discussed in Section 6.1.1. The variation in initial water content was ±0.15% from the nominal value of 4.0%, as shown in Tables 6.4 to 6.8. This was due to the loss of water in

the trays where the soil was mixed, or in the plastic bags where the soil was stored after it was mixed with water.

For most of the fine grading specimens, the dry density varied between 1.947 Mg/m^3 to 1.976 Mg/m^3 with an average of 1.962 Mg/m^3. Four specimens showed significant deviations from this average dry density. Specimens FU-A1 and FU-A2 showed lower dry densities (1.923 Mg/m^3 and 1.935 Mg/m^3 respectively) than the average dry density (1.962 Mg/m^3), while specimens FU-A13 and FU-C2 showed higher dry densities (1.984 Mg/m^3 and 2.047 Mg/m^3 respectively) than the average dry density. The dry densities of the three coarse grading specimens varied from 2.118 Mg/m^3 to 2.131 Mg/m^3 (average of 2.121 Mg/m^3). It may be noted that fine grading specimen FU-C2 had a dry density (2.047 Mg/m^3) close to the average dry density for the coarse grading specimens.

This variation in dry density may be due to variations in the soil grading and variations in water content due to loss of water during specimen preparation and compaction. It may also due to friction between the compaction hammer and the mould's wall during compaction, which varied the compactive effort slightly. Where appropriate these variations will be referred to when discussing individual test results.

8.4 The Choice of the Rate of Strain

In the absence of a theoretical method for calculating the rate of strain for shearing unsaturated specimens, Bishop and Henkel's (1962) method for calculating the rate of strain for saturated specimens, was suggested by Donald (1961) as a way of calculating the rate of strain for unsaturated specimens. He used the specimen water content change vs. the square root of time graph of the consolidation stage to determine the time for 50% consolidation in similar method to that used for saturated specimens. In the current

research if this method was used the rate of strain would be extremely slow. For example consider test FU-A3 (Table 6.4) in which the equalisation and consolidation stages were not combined, and which was carried out with 75 kPa suction. If it is assumed that failure occurs at about 1 % axial strain, then the rate of strain is found to be 0.000025 mm/min, which means that the shearing process would takes at least 104 days to reach the failure stress, in addition to the time that the equalisation and consolidation stages take, which is 10 to 14 days. This rate of strain was not possible to apply because the lowest rate of strain that could be provided by the loading machine is 0.0001 mm/min. Also, a very slow rate of strain may introduce more errors in terms of water leakage through the rubber membrane (Section 7.2), which may increase with time as the rubber membrane deteriorates when left in water, and this would affect the specimen volume, water content and suction change measurements. Also, Bishop and Henkel's method ensures the equalisation or dissipation of the induced pore water and air pressures at the failure stress only, which implies that even slower rates of strain are required to ensure full equalisation or dissipation of the induced pore water and air pressures for the entire shearing process.

Satija and Gulhati (1979) carried out experiments on unsaturated soils at different rates of strain to find the best rate of strain that did not affect the changes in the suction (for constant water content tests) and specimen water content (for drained tests) during the shearing process. Also they compared these rates of strain to those calculated using Bishop and Henkel's method, which ensured equalisation or dissipation of the induced pore water and air pressures for the entire shearing process. They found from a number of drained tests, that choosing times to failure of 50 hours or more can give similar results, while the times to failure for these tests calculated using Bishop and Henkel's method were longer than 2262 hours, and were about 45 times slower than those found experimentally. They also found that the rate for strain for constant water content tests could be 5 times faster than that for drained tests.

Adopting the findings of Satija and Gulhati (1979), and being slightly conservative, a rate of strain of 0.0004 mm/min (0.00011 %/min) was chosen for the drained tests in this research. This was 16 times faster than that calculated according to Bishop and Henkel's method (0.000025 mm/min). A rate of strain of 0.0035 mm/min (0.00093 %/min) was chosen for the constant water content tests, which were carried out at lower values of suction (<30 kPa).

8.5 Repeatability Test

To check whether the specimen preparation and testing in the new double-wall triaxial cell with its associated measuring systems, can produce similar results if tests are repeated with similar test conditions, test FU-A5 was a repeat of test FU-A4 (Table 6.4). The results of both tests are shown in Tables 7.1 and 7.2

Figs. 7.5a, 7.5b and 7.10 show the specimen volumetric strain, specific volume and water content during the equalisation and consolidation combined stage for both tests. Both tests show similar behaviour during this stage, the small difference between both tests may be attributed to the slight variation in the initial conditions (Section 8.3) and some water leakage, may be through the membrane, as was discussed in Sections 7.2 and 7.3.2.3.

Fig. 8.1 shows a graph of the deviator stress against internal axial stress for both tests. It can be seen that there is a very good agreement between the two results, although test FU-A5 had a slightly higher peak strength than test FU-A4. This may be attributed to small variations in the soil grading and compactive effort (Section 8.3). The graphs also provide good evidence that the method adopted for measuring the internal axial stain was satisfactory as both curves show similar behaviour. The benefits of using internal strain measurement may be deduced from Fig. 8.2 which shows the deviator stress plotted

against external axial strain. Due to bedding errors, the external axial strain, where the deviator stress started to increase rapidly, was different for both tests and the curves do not coincide, but it can be seen that both curves are nearly parallel.

Fig. 8.3 shows the specimen volumetric strain calculated using the internal strain measurements (Equation 7.1) plotted against the internal axial strain for both tests. It may be seen that both tests show good agreement only at the early stages of shearing; the curves then diverged at larger strains. This may be due to the rubber membrane buckling, which affects the measurements of the lateral strain, as was discussed in Section 7.2.

Figs. 8.4 and 7.20a show the specimen volumetric strain and specific volume measured using the inner cell water volume change unit (Section 5.2.2), plotted against the internal axial strain for both tests. There is a reasonable agreement between the tests, although test FU-A5 (Fig. 8.4) showed more specimen contraction than test FU-A4. This may be due to the fact that test FU-A5 suffered more bedding error than test FU-A4 (Fig. 8.2), as the bedding error causes apparent contraction behaviour of the specimen, as was discussed in Section 7.2. Also it may be due to small variations in soil grading and dry densities (Section 8.3).

Figs. 8.5 and 7.26 show the specimen water content change and specimen water content during the shearing stage, plotted against the internal axial strain for both tests. Both tests have suffered from water leakage, may be through the rubber membrane as explained in Sections 7.2 and 7.3.1.2. This water leakage can be confirmed by looking at Fig. 8.5 and noticing that there is about 0.01% change in the water content at zero internal axial strain. This change occurred before any axial load was applied to the specimen. It should be noted that this 0.01% water content change occurred between the time that the loading machine was switched on, to the time when the piston was put in contact with the centre of the top cap to start shearing, which may have taken about one day or less. Both curves

in Figs. 8.5 and 7.26 showed similar behaviour, despite the water leakage, as water was initially draining out of the specimen and then was drawn back into it. Fig. 8.5 shows that there is a small difference (about 0.008%) between both curves, which may attributed to variation in water leakage, soil grading and compactive effort. Also Fig. 7.26 shows that there is a difference in the water content, this may be due to the variation in the initial water content (±0.15%) as was discussed in Section 8.3.

It can be concluded from the above discussion, which showed that test FU-A5 gave very similar results to test FU-A4, that tests carried out in the new double-wall triaxial cell, measuring systems, specimen preparation and testing procedures are repeatable.

8.6 The Effect of Combining the Equalisation and Consolidation Stages

A test on an unsaturated granular specimen which has a water content below the optimum water content takes a longer time to complete than a test on a saturated specimen, due to the narrow channels between the soil particles through which the specimen water flows due to any induced pore water pressure gradient. Also, granular soils require larger specimen dimensions than those for fine soils (such as clay) due to the larger grain sizes (Section 3.3), which makes the time for full equalisation or dissipation of pore water pressure even longer. The time for testing an unsaturated specimen increases with increasing suction, because the higher the suction the narrower the channels that the specimen water flows through, and the slower the water flow. Each drained test on an unsaturated granular specimen may take more than a month to complete. Long term tests may suffer from the following effects :

(1) The rubber membrane deteriorates when is left in water for long times and this may increase its permeability. This can affect the measurements of the specimen volume and water content changes. It may also increase membrane slippage as the leaking water may form a lubricating layer between the two rubber membranes used in the

current research (Section 6.3.3), and this may affect the internal strain measurements.

(2) Longer testing times may affect the specimen volume change measurements due to the growth of algae in the triaxial cell. Although de-ionised water was used to prevent such growth, it was found that some algae was starting to grow in some of the longer term tests.

(3) It was also found that the formation of air bubbles below the high air entry ceramic stone increased as the testing time increased. This could affect the accuracy of the measurements of the specimen water content change as these air bubbles had to be flushed every day, especially for high specimen suctions, and measured by a burette (Section 4.3.1)

For the above reasons, and also to increase the number of tests which could be carried out in the research period, it was decided to reduce the time for each of the unsaturated specimen tests by combining the equalisation and consolidation stages into one stage (which will be called *The Combined Stage*). This reduced the total test time by about 7-10 days. This combined stage was carried out for all drained tests in series A, except tests FU-A3 and FU-A12 (Table 6.4), and for one of the constant water content tests (FU-B2, Table 6.5) in series B.

To investigate whether this combination of stages had any effect on the test results, test FU-B1, during which this combination was used, was followed by test FU-B2, during which separate equalisation and consolidation stages were used. The suctions for both tests were brought up to 25 kPa before the shearing stage by allowing some water to drain out of the specimen (drained test), and then they were sheared at a rate of strain of 0.00011 %/min with no more change in the specimen water content allowed (constant water content test). The test initial conditions and test results are shown in Tables 6.5, 7.4 and 7.5.

Figs. 7.29 and 7.30 show the deviator stress and Young's modulus respectively plotted against the internal axial strain for both tests. It can be seen that there is a reasonable agreement between the tests, the slight discrepancy is probably due to specimen test FU-B1 having a higher initial dry density than test FU-B2 (Table 6.5). Fig. 8.6 shows the deviator stress plotted against external axial strain for both tests. It can be seen that test FU-B2 suffered a more severe bedding error than test FU-B1. This led to larger errors in the measurements of the lateral strain in test FU-B2, as the specimen moved more at the start of shearing than the specimen in test FU-B1 (Section 7.2). This in turn affected the volumetric strains calculated using the internal strain measurements (Equation 7.1), as can be seen in Fig. 7.31a(2). Fig. 7.31a(2) shows that the tests have similar volumetric strain behaviour up to about 0.4% internal axial strain; then they showed different behaviour at larger internal axial strains, which may be due to membrane buckling (Section 7.2) affecting the measurements of the lateral axial strain. The similarity in the volumetric strain behaviour below 0.4% internal axial strain may also indicate that combining the equalisation and consolidation stages did not affect the specimen volumetric strain behaviour.

The bedding error in test FU-B2 has also affected the measurements of the specimen volumetric strain (Section 7.2) measured by the volume change unit as shown in Fig. 7.31a(1), which shows that the specimen in test FU-B2 appeared to have contracted more than that in test FU-B1. The Figure also shows that, despite the bedding error, the tests exhibit similar behaviour, which may also support the above conclusion that combining the equalisation and consolidation stages did not affect the specimen volumetric strain behaviour. Fig. 7.31b shows the specific volume for both tests during the shearing stage. The Figure shows that both tests exhibit similar behaviour as both curves are nearly parallel. The Figure shows that the specific volume for test FU-B1 lower than that for test FU-B2, this is due to the fact that test FU-B1 had slightly higher value of dry density than that for test FU-B2 (Table 6.5). Fig. 7.32 shows the suction change during shearing. The Figure shows that specimens in both tests exhibited similar behaviour and the difference in

suction measurements between both tests may be due to the variation in soil grading or may be due to a small water leakage through the rubber membrane or fittings.

It would appear that combining the equalisation and consolidation stages does not affect the soil behaviour during shearing. This may be due to the low values of net cell pressures (<114 kPa) used in the current research.

8.7 Isotropic Compression

During the equalisation and consolidation or combined stages, the changes in the specimen volume and water content for drained tests, or suction for constant water contents tests, were recorded.

The reasons why values of calculated volumetric strain using the internal strain measurements, CVS, differ from those of the measured volumetric strain using the volume change unit, MVS, have been discussed in Section 7.3.1.1, and it was concluded that during the equalisation and consolidation stages or the combined equalisation and consolidation stage, measurements of the specimen volume change using the internal strain devices were better than those of MVS. This was because the volume change unit used to measure the specimen volume change by measuring the volume changes in the inner triaxial cell water, could produce errors due to the compression of the two membranes that surround the specimen and the silicone grease and any trapped air in between the two membranes, due to step changes of the cell pressure. For this reason it was also decided to calculate the specimen specific volume using measurements of the internal strains.

It is interesting to examine the relationship between the values of CVS and MVS, to see if it is possible to correct the MVS. Fig. 8.7 shows a graph of MVS for the combined equalisation and consolidation stage of test series A and B, plotted against CVS. The Figure shows a best fit line through all the points. Although the Figure shows some

scatter (0.24% maximum), it may be concluded that there is a relationship between CVS and MVS. It may also be seen that the slope of the best fit line is close to 45°, which indicates that there is a constant error, which was not corrected, affecting the measurements of MVS. This constant error may be due to the compression of the two rubber membranes, silicone grease and trapped air, as was discussed in Section 7.3.1.1, due to step changes of the cell pressure.

Fig. 8.8a shows the specific volume determined using the internal strain measurements at the end of the consolidation stage or equalisation and consolidation combined stage (i.e. just before starting the shearing stage) for the fine grading unsaturated specimens of test series A, B and C (Table 7.1, 7.4 and 7.6), plotted against the net cell pressure, $(\sigma_3 - u_a)$, or net mean stress, $p - u_a$, on a logarithmic scale. Excluding tests FU-A1 and FU-A2, which they have very low initial dry densities lower than the average dry density for the other specimens, and test FU-C2 which have very high dry density higher than the average dry density (Section 8.3), Fig 8.8a shows that the specific volume decreases at low rate as the net cell pressure increases. The effect of suction during the isotropic compression tests is not clear from Fig. 8.8a, as all lines cross each other, which may be due to variation in the initial dry density and inaccuracies in the measurements of the initial conditions of the specimens, as was discussed in Section 8.3.

Another reason which may be considered to explain the reason why the effect of suction is not clear from Fig. 8.8a, by considering the role of suction in granular soils. The effect of increasing suction in granular soils, with water menisci at grain contact points, is to stabilise the contacts and inhibit grain slippage. This means that there is insignificant volume change when changing the suction in granular soils (Burland, 1965). So if there is particle re-arrangement within the specimen during isotropic compression test, suction will resist this movement, the higher the suction the larger the resistance. With no particle re-arrangement the effect of suction can not be detected, i.e. invisible effect. If the volume change seen in Fig. 8.8a is mainly due to particle crushing and not particle re-arrangement,

the effect of suction will not be activated, i.e. invisible. This is because there is no or little particle movement to be resisted by suction. Vesic and Clough (1968) and Al-Hussaini (1983) showed that there was particle crushing during isotropic compression tests and the smaller the particle size the larger the particle crushing. Further discussion on this will be given in the following Subsection.

To avoid the effect of the inaccuracies in the measurements of the initial soil conditions, the average initial specific volume should be assumed same for all specimens which may help reduce data scattering. A similar method is to consider the total volumetric strain up to the shearing stage. The total volumetric strain is calculated by dividing the volume change during the equalisation and consolidation combined stage or the sum of the volume changes during the equalisation and consolidation stages for tests during which these stages were not combined, by the initial specimen volume, as seen in Equations 8.1 and 8.2 respectively:

(1) For tests with combined equalisation and consolidation stage:

$$v_t = [(\Delta V_{ec} + \Delta V_s)/V_i]\ 100 \qquad (8.1)$$

(2) For tests with uncombined equalisation and consolidation stages:

$$v_t = [(\Delta V_e + \Delta V_c + \Delta V_s)/V_i]\ 100 \qquad (8.2)$$

where the v_t is the total volumetric strain, ΔV_e , ΔV_c , ΔV_{ec} and ΔV_s are the volume changes during the equalisation, consolidation , combined and shearing stages respectively, and V_i is the initial specimen volume (after compaction).

Fig. 8.8b shows the total volumetric strain up to the shearing stage for tests series A to C of the unsaturated fine grading specimens, plotted against the net cell pressure $(\sigma_3 - u_a)$ or net mean stress, $p - u_a$ (logarithmic scale). Similar behaviour as that seen in Fig. 8.8a, is seen in Fig. 8.8b, which shows that specimen total volumetric strain decreases as net cell pressure increases. The effect of suction is also not clear from

Fig. 8.8b as there is data scatter which may be due to variation in the initial dry density (Section 8.3). It can also be seen that there is expansion behaviour for specimens tested at net cell pressures below about 80 kPa. This may be due to specimen not getting enough support at these low values of low net cell pressures.

A linear best fit line is drawn through all tests shown in Fig. 8.8b for the fine grading specimens, is shown in the same Figure, to be able comparing the behaviour of soil used in the current research with that found by other authors for granular soils. Similar behaviour to that shown in Fig. 8.8b (best fit line) was also shown by Lee and Seed (1967), Vesic and Clough (1968), Marachi et al. (1972) and Hagerty et al. (1993) for saturated loose and dense granular soils. Atkinson and Bransby (1978) redraw the results of Vesic and Clough (1968) as shown in Fig. 8.9, and indicated that the isotropic compression lines of the initially loose and dense specimens meet at high stress levels. Similar behaviour was also shown for granular soils with different initial densities (or void ratios) by Lee and seed (1967), who also showed that particle crashing occurred at high stresses. More discussion on the behaviour of the isotropic compression line will be given in the following Subsection 8.7.1.

Fig. 8.10 shows the results of specific volume calculated from the internal strain measurements at the end of the consolidation stage or equalisation and consolidation combined stage (i.e. just before starting the shearing stage) for the unsaturated fine and course grading specimen tests series A to D, plotted against the net cell pressure, (σ_3-u_a), or net mean stress, $p-u_a$, on a logarithmic scale. As can be seen that drained isotropic compression tests FU-B1 and FU-B2 and the constant water content test FU-C1, which have suctions of 25 kPa, 25 kPa and 32.7 kPa respectively, have specific volume close to what would be expected for drained tests carried out at the above values of suction. The Figure also shows that test FU-C2 (which has a 34.7 kPa suction) has lower specific volume than what would be expected for drained tests carried out at 34.7 kPa suction. This is due to its very high initial dry density (Table

6.6), as discussed in Section 8.3, which affected the specific volume. It can be concluded that drained and constant water content tests can give similar results. Similar conclusion was also shown by Wheeler and Sivakumar (1992) for unsaturated clay soils, and by Been et al. (1991) for saturated sand.

Fig. 8.10 also shows that the coarse grading specimens have lower values of specific volume than that for the fine grading specimens. This is due to their dry densities being higher than those for the fine grading specimens (Section 8.3). The Figure also shows that the three coarse grading specimens have close values of suction (± 1.7 kPa), and their specific volume decreases with increasing net cell pressure at a rate close to that for the fine grading specimens. This may indicate that the fine and coarse grading soils may have similar behaviour. More work is needed on coarse grading soil to further investigate the behaviour of this soil.

Fig. 8.11 shows the specimen water content of the unsaturated fine grading specimens at the end of the consolidation stage or combined stage of drained test series A and B plotted against the net cell pressure (logarithmic scale). From the Figure it can be seen that there is a relationship between the specimen water content, suction and net cell pressure. The higher the suction and net cell pressure the more water was drained out of the specimen. Due may be to water leakage during testing and inaccuracies in the calculation of the initial water content due to water lost during specimen preparation (Section 8.3), the Figure shows some degree of scatter, especially those for tests series B and tests carried out at 75 kPa suction.

8.7.1 Isotropic Compression Line for the Fine Grading Soil

Different authors in past have shown that there was an isotropic compression line for saturated normally consolidated clay soils, when plotting specific volume against logarithm of applied stress, where all specimens at different applied stresses reach at the end of isotropic compression tests. For unsaturated normally consolidated clay

soils, Wheeler and Sivakumar (1992, 1995) have shown that the slope of this line is suction dependent. The isotropic compression lines for the over-consolidated clay soil meet that for the normally consolidated clay once the maximum stress that was applied to soil in the past is reached.

When dealing with granular soils, the behaviour during the isotropic compression test is different to that for clay soils. Authors such as Lee and Seed (1967) and Vesic and Clough (1968) showed that there were different isotropic compression lines each starts from the initial specific volume of the specimen under test as shown in Fig. 8.9. These lines meet at high stresses due to particle crashing (in clay soils the swelling lines for the over-consolidated clays with different over-consolidation ratios, meet the normally consolidated line when the maximum applied stress in the past is reached). Muir Wood (1990) stated that the lines shown in Fig. 8.9 illustrate the difficulty of exploring the compression plane using any isotropic stresses for granular soil. He also indicated that considerable particle re-arrangement is required for the initial structures of loose and dense granular soils to become the same, and this particle re-arrangement can occur readily only in the presence of shear stress. He also concluded from the results of tests carried out by Lee and Seed (1967) that the isotropic compression lines for saturated sand soils had smaller slopes than that at critical state, at the same stress levels. Muir Wood (1990) stated that volume changes only occur in isotropic compression at very high applied stresses when particle crushing becomes a major feature of the response, and at very high stress levels, greater than about 10 MPa, the isotropic compression and critical lines may become approximately parallel, and the behaviour starts to resemble the compression behaviour of clay soils.

From the above paragraph it may be concluded that for granular soils under isotropic compression tests at applied stresses less than 10 MPa, the slope of the isotropic compression line is initial void ratio and applied stress dependent. It may also be concluded that the slope of the isotropic compression lines for granular specimens,

tested at different initial void ratios and at extremely low stress levels, are expected to be close to zero. This is because very small or no particle re-arrangement occurs during the tests (Muir Wood, 1990), and particle crashing may not start at extremely low stress levels. This no (or small) particle re-arrangement during the isotropic compression test can lead to the conclusion that the effect of suction is invisible during the isotropic compression test for granular soils. This is because suction in granular soil, which contains water menisci at grain contact points, only helps to stabilise soil structure and inhibit particle slippage (Burland, 1965), so if there is no or small particle re-arrangement occurs when the net cell pressure is increased, the resistance to particle movement due to suction may not be activated. Also for granular soils with water menisci at the grain contact points, Burland (1965) showed that the effect of increasing suction induced very small and insignificant volume change.

The above conclusions may explain the reason why the effect of suction was not clear from Figs. 8.8a and 8.8b. It may also explain the reason why the variation in the initial dry density can affect the isotropic compression behaviour. From the above discussion it may be concluded that when testing granular specimens (with water menisci at the grain contact points) at different initial dry densities and degrees of saturation, the plot of specific volume against the net cell pressures (logarithmic scale) will be similar to that shown in Figs. 8.8a and 8.8b. Also there will be different isotropic compression lines, each starts from the initial specific volume of the specimen under test. These lines will meet at some points at high stresses, due to particle crushing, to form one isotropic compression line, similar to the normally consolidated line for clay soils, and may be parallel to the critical specific volume line. The slope of each line at extremely low stresses may be very small and close to zero, as shown in Figs. 8.8b and 8.9. More work is needed to investigate particle crushing and initial dry density effects.

From the discussion made in this Section, it may be concluded the granular soil behaviour can be modelled to predict the soil behaviour. This is in agreement with the

finding of Wheeler and Sivakumar (1992) who carried out tests on unsaturated kaolin clay soil.

8.8 Axial Strain Measurements of the Fine Grading Specimens

The specimen axial and lateral strains for the unsaturated specimens (series A to D) were measured internally, and also their axial strains were measured externally (Section 4.2.2). No internal strain measurements were made on the saturated specimens (series E), their axial strains being measured externally.

Fig. 8.12 shows a typical graph of the internal and external axial strain measurements plotted against time during the shearing stage of a test. The Figure shows three curves, one for the internal axial strain measurements, the second is for the uncorrected external axial strain measurements, and the third is for the external axial strain measurements corrected for the loading machine compression (Section 5.3.3). Although the loading machine produces a constant rate of strain as shown by the linearity of the external (uncorrected) line, the specimen does not get stressed at a constant rate of strain as shown by the curved nature of the other two lines. The Figure shows that loading machine compression can produce errors in the axial strain measurements of about 0.1%. The Figure also shows the effect of bedding errors on the external axial strain measurements, as the internal axial strain measurements showed zero axial strain until a time of about 20 hours, while the external axial strain measurements showed that there was an apparent axial strain of about 0.2%.

Fig. 8.13a shows the specimen internal axial strain at failure for the unsaturated fine grading tests (series A to C) plotted against the net cell pressure. It should be noted that one of the springs that was holding an axial LVDT for the internal axial strain measurements, snapped during tests FU-A7 and FU-A11 (Section 7.2) the results of both

tests are not shown in this Figure. Fig. 8.13b shows the external axial strain measurements at failure for the saturated (series E) fine grading tests, plotted against the effective cell pressures. Both Figures show that the axial strain at failure increases as the confining (net or effective cell) pressure increases. Similar behaviour was found by Olowokere (1986) for the saturated granular specimens at low stress levels (<100 kPa) and Indraratna et al.(1993) for saturated granular specimens at high stress levels (>100 kPa). Fig. 8.13a does not show clearly the effect of suction on the internal axial strains at failure for the unsaturated specimens, as the three lines for drained tests, carried out at 25 kPa, 50 kPa and 75 kPa suctions, cross each other. This may be due to different factors, such as initial condition variations of the specimens (Section 8.3), or may be due to the tilting of the vertical LVDTs measuring the internal axial strains at failure due to specimen bulging during the shear stage (Section 7.2). These factors may have more significant effect on the axial strain measurements at failure than the effect of suction.

8.9 Poisson's Ratio

A typical graph of Poisson's ratio (the ratio of lateral to axial strains) against the internal axial strain during a shearing stage is shown in Fig. 8.14. Also, the Figure shows a curve of the internal lateral strain plotted against the internal axial strain for the same test. Values of Poisson's ratio below an internal axial strain of 0.05% are not shown in the Figure as they fall within the accuracy of the internal strain measuring devices. Also values of Poisson's ratio above internal axial strain of 0.4% are not shown due to the effect of membrane buckling (Section 7.2). The Figure shows that Poisson's ratio appears to have a fairly constant value during shearing. This indicates that the relationship between the internal axial and lateral strains is constant, as shown in the Figure.

Values of the Poisson's ratio at 0.3% internal axial strain for the unsaturated fine grading specimens (series A to C) are plotted against the net cell pressure in Fig. 8.15. It should be noted that specimen tilting at the start of the shearing stage can cause an error of about

±0.03 to the calculation of Poisson's ratio, as was discussed in Section 7.2. Also due to the breakage of one of the axial LVDT springs for the internal axial strain measurements (Fig. 4.4) during tests FU-A7 and FU-A11, the results from these tests are not shown in this Figure. The Figure shows a trend for Poisson's ratio to decrease, from a value higher than 0.5, as the net cell pressure increases up to a net cell pressure of about 80 kPa. Beyond this value, Poisson's ratio decreases, below a value of 0.5, at very slow rate. Similar behaviour was also shown by Olowokere (1986) for saturated granular soil. He showed that the value of Poisson's ratio decreased from a value of 0.82 at effective cell pressure of about 10 kPa to 0.03 at an effective cell pressure of about 200 kPa and then became almost constant above this value of effective cell pressure.

Fig. 8.15 also shows that the three lines drawn through tests carried out at 25 kPa, 50 kPa and 75 kPa suction cross each other, i.e. any effect of suction on Poisson's ratio is not clear. This may be due to the effect of variation in the initial conditions (Section 8.3) and specimen tilting at the start of the shearing stage (Section 7.2). More work is needed to investigate this effect.

Fig. 8.15 shows that the value of Poisson's ratio for tests carried out at net cell pressures lower than 50 kPa are higher than 0.5. This is not possible for an isotropic and elastic material, unless the soil is anisotropic, under plastic behaviour or there are some errors in the measurements of the internal strains. Such errors may be caused due to specimen shape change due to non-uniform deformation (such as barrelling).

The results shown in Fig. 8.15 are taken at internal axial strain of 0.3%, while the peak stresses are at about 1% internal axial strain. Authors such as Ueng et al. (1988) and others (Section 3.3.2) showed that there was no significant difference in the uniformity of the volume change within the specimen at strains below the peak stress, regardless of the end conditions, lubricated (uniform deformation) or unlubricated. From this it

can be concluded that errors due to the effect of non-uniform deformation due to specimen end friction may not be significant.

It was indicated earlier in this Section that errors due to specimen tilting at the start of the shear stage due to piston misalignment (Section 7.2) which affected the internal lateral strain measurements, can cause an error of about ±0.03 in the calculation of Poisson's ratio at 0.3% internal axial strain. This, although small, may be one of the reasons for the high values of Poisson's ratio.

It was shown in Section 7.3.2.2 and Figs. 7.20 to 7.22, that the volume of specimens carried out at very low values of net cell pressure (tests FU-A1, FU-A6 and FU-A10) expanded rapidly soon after a small initial compression during the shearing stage. This means that these specimens reached the plastic behaviour at internal axial strains lower than those carried out at higher values of net cell pressure. This plastic behaviour of the soil at low values of net cell pressure can explain the reason why such values of Poisson's ratio higher than 0.5 are seen in Fig. 8.15.

Soil anisotropy may also affect Poisson's ratio. Arthur and Menzies (1972) and Ricceri and Soranzo (1981) showed that there was an inherent anisotropy in compacted saturated sand soils. Arthur and Menzies (1972) showed from isotropic compression tests that the ratio of the volumetric strain to the axial strain was between 4 and 7, with radial strains larger than the axial strains. In isotropic compression test, this ratio should be 3 for isotropic soils according to Equation 7.1, i.e. the axial strain should be equal the lateral strain. Similar values for the above ratio were also obtained during the consolidation stage that was carried out on the specimens in the current research. This indicates that the specimens used in the current research behaved anisotropically.

From above it may be concluded that both plastic behaviour and soil anisotropy were the main reasons for the high values of Poisson's ratio higher than 0.5. However, Fig. 8.15 shows that these high values of Poisson's ratio occurred only at very low applied net cell pressures. Knowing that the soil expanded rapidly at these values of net cell pressures, it may be concluded that the effect of plastic behaviour was more significant than the effect of soil anisotropy.

8.10 Young's Modulus of the Fine Grading Soil

The internal strain measurements for the unsaturated specimens showed that the value of Young's modulus, between axial strains of about 0.1% to 0.3%, was nearly constant, as was discussed in Section 7.3.2.1 and shown in Figs. 7.16 to 7.18 (for drained tests), 7.30 and 7.38 (for constant water content tests). Values of the secant Young's modulus at 0.25% internal axial strain for unsaturated fine grading specimens (series A to C) are plotted against the net cell pressure ($\sigma_3 - u_a$), in Fig. 8.16. The lines shown in the Figure are the best fit lines for the drained tests at 25, 50 and 75 kPa suctions. It should be noted that tests FU-A7 and FU-A11 were not included due to breakage of one of the springs holding the axial LVDT (Section 7.2). Tests FU-A1 and FU-A2 are not used when calculating the best fit line for tests carried out at 75 kPa suction, due to their very low initial dry densities. Also test FU-A13 has very high initial dry density and not included when calculating the best fit line for tests carried out at 25 kPa suction.

Considering the results of drained tests, the Figure shows there is a relationship between Young's modulus, suction and net cell pressure, such that the Young's modulus increases with increasing suction and net cell pressure. The increase in Young's modulus (soil stiffness) as suction increases indicates that the soil becomes stiffer with increasing suction as was discussed in Sections 2.4 and 2.5. Little work has been done on the effect of suction on Young's modulus. Authors such as Wu et al. (1984, 1985) and Alonso et al.

(1987) have indicated that there was a relationship between the dégree of saturation (suction) and the shear modulus.

The results of the two constant water content fine grading specimen tests (series B) sheared at a rate of strain similar to that of drained tests (0.00011 %/min), are shown as solid circles in Fig. 8.16. Both tests (FU-B1 and FU-B2) had suctions of about 20 kPa at 0.25% internal axial strain. The results of the other two constant water content fine grading specimen tests (series C) sheared at a faster rate of strain (0.00093 %/min) are shown as solid triangles in Fig. 8.16. Both of these tests (FU-C1 and FU-C2) had suction values of about 23 kPa and 28 kPa respectively (Fig. 7.40) at 0.25% internal axial strain. Tests FU-B1, FU-B2 and FU-C1 showed values of Young's Modulus close to what would be expected for drained tests carried out at 20 kPa, 20 kPa and 23 kPa suctions. Due to the fact that test FU-C2 have very high dry density (Section 8.3), this specimen shows higher value of Young's modulus than what would be expected for drained tests carried out at 28 kPa suction. It follows that drained and constant water content tests can lead to similar results, in other words, stress path may not affect the results. It may also be concluded that the effect of rate of strain during constant water content test is insignificant. This may not be the case for drained test. This is because specimen water may not have to move from the top to the bottom of the specimen due to suction gradient during constant water content test as that during drained test.

Due to the effect of bedding errors which affected the measurements of the external axial strains for the saturated specimen tests (Series E), discussion of the Young's modulus values for the saturated tests taken at a certain value of external axial strain will not be considered. Instead, values of the secant Young's modulus taken at 30% of the failure stress will be discussed. Fig. 8.17 shows the secant Young's modulus of the saturated drained tests (Series E) taken at 30% of the failure stress plotted against the effective cell pressure. It should be noted that test FS-E2 showed a lower value of Young's modulus than expected; this may be due to an improper clamping of the LVDT used to measure the

external axial strain (Section 7.7). The dotted line is the best fit line through the test results except test FS-E2. From Fig. 8.17 it can be seen that saturated specimens exhibited similar behaviour to that was shown in Fig. 8.16 for unsaturated drained specimen tests, in that as the effective cell pressure increases the Young's modulus increases. Marachi et al. (1972) and Indraratna et al. (1993) showed similar behaviour for saturated granular soils when plotting the initial Young's modulus against the effective cell pressure.

8.11 Peak Stress of the Fine Grading Specimens.

Most of the tests were stopped two to three days after the peak stress was reached, i.e. the critical state of the soil was not reached. The reason was to investigate the soil behaviour at different values of suction and net cell pressure, especially at the early stage of the shearing process and to find the validity of Fredlund's Equation (Equation 2.3) to predict the shear strength of the unsaturated granular soils at low stress levels. Discussion of the critical state of granular soil will be given in Section 8.14.

The specimens tested in the current research showed similar behaviour to the over-consolidated clay soil during shearing stage. The specimen deviator stress reached a peak stress before they decreased to the critical state, as shown in Figs. 7.13-7.15, 7.29, 7.37, 7.45 and 7.50. In this Section a discussion of the soil behaviour at peak stress (failure) will be given.

The non-uniform deformation that occurs during the shearing stage due to specimen end friction (Section 3.3.2) can induce an effect on the stress-strain-volume change behaviour (Section 3.3.2). This is because part of the specimen (middle part) reaches the peak stress before the rest of the specimen, and the soil particles of this part of the specimen can move freely, while the other parts cannot move due to end friction. The

specimen dimensions chosen for the current research is so that the value of peak stress is unaffected by the end friction, as was discussed in Section 3.3.

To show the shape of the state boundary surface (Hvorslev Surface) at the peak stress (by considering a family of drain tests) is difficult because the specific volume of the specimen is changing throughout the tests. The projections of the failure points into q vs. $p-u_a$ space then refer to different constant specific volume sections of the state boundary surface (Atkinson and Bransby, 1978). It is expected that each constant specific volume of the state boundary surface is of different size and of the same shape. The most convenient way of investigating the shape of the state boundary surface, which is used for clay soils (Atkinson and Bransby, 1978 and Muir Wood 1990) is to scale the stresses to allow for changes in specific volume that occur during the tests.

Scaling the stresses requires information about the isotropic compression and critical state lines (Atkinson and Bransby, 1978), which is not possible in the current research. This is because the critical state was not reached for most of the tested specimens, as they were stopped shortly after they passed the peak stress. Also, as was discussed in Section 8.7.1, an isotropic compression line for granular soil similar to that for normally consolidated clay soils, may only obtained at high applied stress, >10 MPa (Muir Wood, 1990).

Fredlund et al. (1978) proposed Equation 2.3 as an extension to the Mohr-Coulomb failure theory for shearing of unsaturated soils. This equation

$$\tau=c'+(\sigma-u_a)\tan\phi'+(u_a-u_w)\tan\phi^b$$

will give a planar failure envelope if ϕ' and ϕ^b are constant (Fig. 2.10). Some authors, e.g. Escario and Sa'es (1986), have stated that the failure envelope cannot be regarded as planar. However, these authors carried out their tests at high stress levels (>100 kPa),

while in this research the stress levels were low, so the investigation of the validity of Fredlund's equation at low stress levels will be discussed in this Section.

Figs. 8.18 and 8.19 show the deviator stress, q, at failure (peak stress) plotted against the net cell pressure, (σ_3-u_a), and net mean stress, $(p-u_a)$, respectively for drained test series A on the unsaturated fine grading specimens, and against the effective cell pressure, (σ_3-u_w), and the effective mean stress, $(p-u_w)$, for the drained test series E on the saturated fine grading specimens. The lines shown in the graphs are the best fit lines. Test FU-A13 was not included when calculating the best fit line for tests carried out at 25 kPa suction, as it had a much higher dry density than the average dry density for the specimens in this series of tests (Table 6.1).

Considering the drained tests on unsaturated specimens, it can be seen that, despite the low values of suctions used for these tests (25, 50 and 75 kPa), the peak stress increased as suction increased, and also as the net cell pressure increased. This indicates that suction can increase the soil strength as it makes the soil structure more stable. Also a small increase in suction can produce an effect on the shear behaviour of granular soil at low stress levels. This conclusion is important, because it may encourage some researchers to consider carrying out further investigations on the effect of suction on the granular soil behaviour, since previously it was thought that suction would have an insignificant effect on the granular soil behaviour. This may only be true when considering tests at high stress levels.

The unsaturated drained test specimens were sheared at three values of suction (25, 50 and 75 kPa). Although three values of suction may not be sufficient to show clearly whether the three dimensional failure envelope (Fig. 2.10) is planar or not, the lines through the unsaturated drained test results are straight and they pass through most of the test results. This means that the value of ϕ' (Equation 2.3 and Fig. 2.10) may be considered constant for each value of suction. This is in agreement with the works of

Escario and Sa'es (1986) for unsaturated sand tests carried out at high stress levels and values of suction up to 500 kPa. The Figure shows that the slopes of failure envelope for tests carried out at suctions 25 kPa and 75 kPa are approximately similar with a value of ϕ' about 39.9°. The Figure also shows that the slope of the failure envelope of tests carried out at 50 kPa suction is lower that that for tests carried out at 25 kPa and 75 kPa suctions. It is not known why the tests at 50 kPa suction showed this behaviour. Escario and Sa'es (1986) showed that from tests at high stress levels on unsaturated sand that ϕ' increased as suction increased. Alonso et al. (1987) stated that the increase in strength due to suction can not continue indefinitely, in the limiting case of dry soil the failure envelope will coincide basically with the saturated failure envelope, this means that the suction effect on strength must peak at some intermediate value of degree of saturation.

The reason why the value of ϕ' for tests carried out at 50 kPa suction (Figs. 8.18 and 8.19) is less than that for tests carried out at 25 kPa and 75 kPa suctions, may not be explained as was stated in the previous paragraph by Alonso et al. (1987), because the values of ϕ' for tests carried out at 25 kPa and 75 kPa suctions are approximately same. The reason may be due to the variation in the soil grading of the batch that was used for testing unsaturated specimen at 50 kPa suction. However, from the results of the tests carried out at 25 kPa and 75 kPa suctions, it can be postulated that ϕ' is constant at different values of suction. Further tests are required to find whether the value of ϕ^b (in Equation 2.3 and Fig. 2.10) is constant at different values of suction to confirm the validity of Fredlund's Equation.

Figs. 8.18 and 8.19 show that the value of ϕ' for the saturated specimens (series E) is constant, at 38.0°. This confirms the findings of Olowokere (1986), Bathurst and Karpurapu (1993) and Indraratna et al. (1993) who showed that ϕ' was constant for the saturated granular soils at low stress levels. Figs. 8.18 and 8.19 also show that the value of ϕ' for the saturated specimens is lower than that found from drained tests on unsaturated specimens (series A). This may be due to the removal of all the menisci that linking the

soil particles before saturation, and also it may be due to the softening of the soil particles due to saturation for some time (Goodwin, 1991) and this weakened the soil structure. Similar behaviour was also found by Yoshida et al. (1991). They carried out tests on silty sand specimens which were compacted at a certain water content and then each specimen was placed in a triaxial cell and water was permitted to flow in to obtain the desired water content. The specimens were then sheared with a cell pressure of 98 kPa. Fig. 8.20 shows a graph of the deviator stress plotted against the axial strain for the tests that were carried out by Yoshida et al. (1991). It can be seen that there is a large drop in strength when the degree of saturation was increased from 80 % to 100 %.

From the above, it may be concluded that the value of ϕ' for the saturated specimens cannot be used in Fredlund's Equation (Equation 2.3) to predict the shear strength of unsaturated specimens (Section 2.6) as was suggested by Fredlund et al. (1978). It can also lead to another conclusion that Fredlund's Equation cannot be used to predict the shear strength of unsaturated and saturated soils, if specimens are compacted with degrees of saturation below about 80%, due to the removal of all menisci that linking the soil particles, resulting in a lower value of ϕ' for saturated specimens than that of the unsaturated specimens.

Fig. 8.21 shows the results of the two constant water content tests (series B) carried out at a rate of strain similar to that of drained tests (0.00011 %/min). Both tests failed at suction of about 34 kPa (Table 7.5). The Figure also shows best fit lines taken from Fig. 8.19 for the drained test results of unsaturated and saturated fine grading specimens. It may be seen that both tests have values of failure deviator stress which are close to what would be expected from drained tests at 34 kPa suction. This indicates that drained and constant water content tests on unsaturated soils may give similar values of the failure stress. This conclusion for granular soils agrees with that of Wheeler and Sivakumar (1992) for clay soils.

Fig. 8.21 also shows the results of the two constant water content tests on the unsaturated fine grading specimens (series C) sheared at faster rate of strain (0.00093 %/min) than that for the drained tests (series A). Both tests, FU-C1 and FU-C2, failed at 28 kPa and 31 kPa suction respectively. The dry density of test FU-C2 was very high (2.047 Mg/m^3), higher than that of the average dry density for most of the tested specimens (1.962 Mg/m^3), as was discussed in Section 8.3. This test showed a higher value of deviator stress at failure than what would be expected for a drained test sheared with 31 kPa suction. This was almost certainly due to its higher dry density. Test FU-C1 had a dry density close to the average dry density of other tests, and it gave a value of deviator stress close to what would be expected for a drained test sheared with 28 kPa suction. This may indicate that the rate of strain during constant water content test may have a very small effect on the unsaturated soil shearing behaviour. It should be noted that this effect of rate of strain may not be the case for drained test. This is because the specimen water may not need to move from the top to the bottom of the specimen due to suction gradient during constant water content test as that happens during drained test.

8.12 Volume Behaviour at Peak Stress

The measurements of the specimen volume change using the volume change unit was not used when discussing the volume behaviour during the equalisation and consolidation stages or the combined stage (Section 8.7), that because errors were introduced due to the step changes of the cell pressures (Section 7.3.1.1). During the shearing stage, the cell pressure was constant, i.e. errors due to step changes of the cell pressures during the shearing stage were not introduced. And due to the membrane buckling effect and formation of slip planes and other non-uniform deformation, which affected the measurements of the internal lateral strains above about 0.3% internal axial strain (Section 7.2) during the shearing stage, the specimen volume change measured using the volume change unit, will only be used in discussing the volume behaviour at failure. It should be

noted that the specific volume at the start of the shearing stage is calculated from measurements of the internal strains for the unsaturated specimens, and from measurement of the volume change unit for the saturated specimens as no internal strain measurements were carried out for the saturated specimens.

Authors such as Chu and Lo (1993) stated that in triaxial testing of dense granular soils, significant non-uniform deformation would develop prior to approaching the critical state. Ueng et al. (1988) showed for sand soil that there was no significant difference in uniformity of the volume change within the specimen at strains below the peak stress for the lubricated and unlubricated specimen ends. This may indicate that the effect of non-uniform deformation may be very small at peak stress and significant at critical state. Also due to the non-uniform deformation of the specimen due to specimen end friction, part of the specimen (middle part) is changing in volume higher than the other parts, this indicates that the measured volume change is the average volume change of the specimen. Further discussion on the behaviour of specimen volume at the critical state will be given in Section 8.14.

Fig. 8.22 shows the specimen specific volume at failure (peak stress) for the unsaturated and saturated drained test specimens (series A and E) is plotted against $p-u_a$ and $p-u_w$, (logarithmic scale) for the unsaturated and saturated specimens respectively. The Figure shows that there is scatter in the data due may be to the variation in the initial dry density of the specimen and inaccuracies in the measurement of the initial specimen conditions (Section 8.3). This makes the interpretation of the volume behaviour at peak stress (Fig. 8.22) difficult as all lines cross each other.

To avoid this inaccuracies in the initial measurements of the soil conditions, the initial average specific volume will be assumed same for all fine grading specimens. The method described in Section 8.7 will be used to interpret the volumetric behaviour at peak stress. In this method the total volumetric strain up to the peak stress will be

calculated according to Equations 8.1 and 8.2 (total volumetric strain up to the peak stress is the sum of the volume change during the equalisation and consolidation stages or the equalisation and consolidation combined stage and the volume change during the shearing stage up to the peak stress, divided by the initial specimen volume).

Fig. 8.23 shows the total volumetric strain up to the peak stress plotted against the net mean stress, $p-u_a$, and effective mean stress, $p-u_w$ (logarithmic scale) for the unsaturated and saturated fine grading specimen tests series A to C. The Figure shows that the specimen volume at peak stress decreases as net and effective mean stresses increase up to net and mean stresses of about 300 kPa, from where the specimen volume becomes approximately constant. Similar behaviour was also found by Marachi et al. (1972) for saturated granular soils. It may also be seen that as the suction increases the specimen volume at the peak stress increases, i.e. expands. This behaviour of specimen expansion due to suction increase in granular soil is similar to the increase in the over-consolidation ratio (OCR) for the over-consolidated clays. This means that the suction makes the soil stiffer. Fig. 8.23 shows that the change in specimen volume when reducing suction from 25 kPa to zero (saturated specimen) is larger than that when reducing suction from 50 kPa to 25 kPa, or 75 kPa to 50 kPa. This may be due to the fact that values of volume change during the isotropic compression tests for the saturated specimens are taken from measurements of the volume change unit which suffered errors due to step changes of the cell pressures (Section 8.7). While those for the unsaturated specimens are taken from measurements of the internal strains, which may not suffered this type of error.

Fig. 8.24 shows the results of specific volume at peak stress for all specimens tested in the current research for the unsaturated fine and coarse grading specimens (series A to D) and saturated fine grading specimens (series E), plotted against the logarithm net and effective mean stresses ($p-u_a$ and $p-u_w$) for the unsaturated and saturated specimens respectively. The Figure shows that the constant water content specimen

tests FU-B1, FU-B2 and FU-C1, which were failed at 34 kPa, 34 kPa and 28 kPa suctions respectively, are close to what would be expected for drained tests carried out at these values of suctions, it should be noted that test FU-C1 was sheared at faster rate of strain than the other two tests. This indicates that the effects of rate of strain (during constant water content test) and stress path are insignificant, similar behaviour can also be seen in Fig. 8.23. Similar conclusion was also obtained when discussing Young's modulus and shear behaviour at peak stress (Sections 8.10 and 8.11). The effect of changing the rate of strain, which was found insignificant for the constant water content tests, may be significant for drain tests. This is because specimen water may not have to move from the top to bottom of the specimen due to suction gradient during constant water content test as that during drained test.

Fig. 8.24 also shows that the specific volume at failure for the constant water content fine grading specimen test FU-C2, which was failed at 31 kPa suction, is lower than what would be expected for drained test carried out at 31 kPa suction. This is due its high value of initial dry density, 2.047 Mg/m^3, higher than the average dry density for most of the specimens, 1.962 Mg/m^3 (Section 8.3). The dependence of the volumetric behaviour at peak stress on the initial dry density indicates the difficulty in modelling the volumetric behaviour at peak stress. This is because at peak stress the specimen volume continues to change towards the critical state. However, for known compactive effort, which gives small variation in the dry density, it is possible to model the soil volumetric behaviour at peak stress. Authors such as Ponce and Bell (1971) and Fukushima and Tatsuoka (1983), who carried out triaxial tests on saturated sand at low stress levels, and Marachi et al. (1972) and Al-Hussaini (1984) who carried out triaxial tests on saturated rockfill materials at high stress levels, showed that there was a relationship for the specimen volume of granular soil at peak stress.

Fig. 8.24 also shows the results of constant water content tests on coarse grading specimens (series D) at peak stress. Due to their high initial dry densities, the specific

volume of the coarse grading specimens at peak stress is lower than that for the fine grading specimens. The line through the results of the coarse grading specimen tests, which have close values of suction (11.9 kPa ±1.7) is approximately parallel to those for the fine grading specimens. This may indicate that the coarse grading soil has similar volumetric behaviour at peak stress to that for the fine grading soil.

8.13 Specimen Water Content at Peak Stress

Fig. 8.25 shows the specimen water content at peak stress for the unsaturated fine grading drained test specimens (series A), plotted against $p-u_a$ (logarithmic scale). As can be seen that as suction and $p-u_a$ increase, the water content decreases. The decrease in water content as suction increases was already discussed in Section 2.4 and shown in Figs. 2.4 and 2.5. The decrease in water content as $p-u_a$ increases, is due to the fact that in drained test, during which the suction is kept constant, an increase in $p-u_a$ causes a decrease in specimen volume (void ratio) as shown in Fig. 8.22, this leads to an increase in degree of saturation, which will also leads to a decrease in suction. To keep the suction constant, water should be expelled out of the specimen to increase the suction to the value where it was before the change in volume occurred. It should be noted that the change in specimen water content and volume not always of the same sign, for example soil collapse can occur due to wetting.

Fig. 8.25 shows that the variation in the initial dry density has less effect than that shown for the specific volume (Fig. 8.22). This is in agreement to the results of Olson and Leonard (1965) and Krahn and Fredlund (1972) who showed that variation in dry density for clay and sandy clay soils had little effect on suction.

The major problem that affects the change in specimen water content is water leakage. This water leakage could be through specimen membrane, fittings and air line (as

vapour). Fig. 8.25 shows that results of test carried out at 75 kPa are scattered which may be due to water leakage. From the results of tests carried out at 25 kPa and 50 kPa suctions, the relationship between specimen water content at peak stress and $p-u_a$ (logarithmic scale) is approximately linear. Further tests are needed to investigate the relationship between water content and suction for this soil, which may be similar to that shown in Fig. 2.4.

8.14 Critical State of the Fine Grading Soil

The specimens were stopped before reaching the critical state (Section 8.11). Some specimens were sheared at large strained towards the critical state. These specimens will be used in this Section to give an initial interpretation of the granular soil behaviour at the critical state. More tests are needed to fully understand the unsaturated and saturated granular soils at the critical state.

8.14.1 Introduction

The critical state for dense granular or over-consolidation soil is difficult to reach due to the non-uniform deformation after the peak stress (Craig, 1984). Chu and Lo (1993) suggested a new method which can be used to bring the saturated dense granular soil to the critical state in the uniform deformation region by switching the stress path at peak stress from drained to undrained test, i.e. imposing no volume change after the specimen has passed the peak stress. This method was not tested on unsaturated soils, and imposing no volume change on unsaturated soil is impossible due to the compressibility of pore air and the difficulty of controlling air leakage during unsaturated specimen test.

Approaching the critical state of the specimens used in the current research can take long time (approximately 70 days) as this occurs at internal axial strain higher than 9%

(see test FU-C2 in Figs. 7.37 to 7.40). Long time tests can affect the accuracy of the volume change and water content change measurements as was discussed in Section 8.6. Increasing the rate of strain after peak stress is reached, to approach the critical state at shorter time, may not allow time for the suction to equalise within the specimen, which in turn may affect the measurement of deviator stress, volume change and water content change. Yamamura and Lade (1993) showed that increasing the rate of strain for saturated granular soil could affect the test results. However, for unsaturated soils the effect on test results due to an increase in the rate of strain can be more significant than that for the saturated soils, due to the fact that water dissipation is slower than that for saturated soils. Also due to the small amount of water content and large specimen dimensions used in the current research, the water pressure dissipation can take long time.

In Section 8.7.1 and Fig. 8.9, it was shown that a single isotropic compression line for granular soils, similar to that for normally consolidated clay, could only be obtained at very high stress levels (>10 MPa). At applied stresses less than 10 MPa, there are different isotropic compression lines, each starts from the initial void ratio of the specimen under tests, and these lines meet at some points due to particle crushing, forming one isotropic compression line, which may be parallel to the critical void ratio line, and resemble the behaviour of clay soils. Muir Wood (1990) stated that considerable particle re-arrangement is required for the initial structures of the loose and dense granular soils (Fig. 8.9) to be come the same, and this particle re-arrangement can occur readily only in the presence of shear stresses.

Authors such as Been et al. (1991) showed that there was a critical void ratio line for the saturated sand soil, and was linear up to values of effective mean stress (logarithmic scale) of about 1 MPa. Muir Wood (1990) showed from results that was carried out by Vesic and Clough (1968) that the critical void ratio line for saturated sand was non-linear at low stress levels. For unsaturated clay soils at high stress

levels, Wheeler and Sivakumar (1992,1995) showed that the critical void ratio and critical shear strength lines were linear and their slopes were suction dependent.

Toll (1990) showed that there was linear critical void ratio and critical shear strength lines for unsaturated lateritic gravel soil (8-9% clay content) at high stress levels. He developed Equations 8.3 and 8.4 to describe the shear strength and specific volume at the critical state respectively.

$$q = M_a (p - u_a) + M_w (u_a - u_w) \qquad (8.3)$$

$$v = \Gamma_{aw} - \lambda_a \ln(p - u_a) - \lambda_w \ln(u_a - u_w) \qquad (8.4)$$

where M_a , M_w , Γ_{aw} , λ_a and λ_w are functions of the degree of saturation. Toll (1990) state that the contribution of suction to the critical state surface (M_w and λ_w) decreased with decreasing degree of saturation until it became zero at 55% saturation. While the contribution due to total stress (M_a and λ_a) continued to increase with decreasing degree of saturation due to the fact that the number of dry particle/packet contacts increases as the degree of saturation decreases.

Fig. 7.50 and 7.52a show the deviator stress and volumetric strain during the shearing stage of the saturated fine grading specimen tests (series E). From the Figures it can be seen that the deviator stress and volumetric strain for test FS-E3 show constant values at external axial strains higher than about 1.5%. This indicates that this specimen has reached the critical state. Also test FS-E5 is close to the state where the volumetric strain becoming constant (Fig. 7.52a). However, this does not mean that this test has reached the critical state. This test will be assumed that it reached the critical state, as the error involved is small. This is because the specimen already reached constant volume, also the difference in deviator stress between that at the peak stress and critical state is small for saturated specimens, as can be seen in Fig. 7.50 for test FS-E3 which reached the critical state. This difference in deviator stress is about

65 kPa for test FS-E3, which was sheared at 75 kPa effective cell pressure, and this difference is expected to be smaller for test FS-E5, because the specimen was sheared at higher effective cell pressure ,125 kPa (Muir Wood, 1990) than that for test FS-E3. Similar discussion can be used to assume that test FS-E2 has reached the critical state.

In addition to the three saturated fine grading specimen tests FS-E2, FS-E3 and FS-E5 which will be assumed that they reached the critical state, test FU-C2 has also reached the critical state as can be seen from Figs. 7.37, 7.39 and 7.40, for the deviator stress, volume change and suction respectively, although Fig. 7.39 shows that constant volume for this specimen was not reached, despite the fact that the deviator stress and suction (Figs. 7.37 and 7.40) show constant values at the end of the shearing stage. This may be due to the non-uniform deformation that occurs prior to the critical state and affects the specimen volume change, as discussed earlier in this Section.

Figs. 8.26 and 8.27 show the shear strength and specific volume at the critical state respectively, for the drained saturated fine grading specimen tests FS-E2, FS-E3 and FS-E5 and one unsaturated constant water content test FU-C2. The stress paths for these tests are also shown in the Figures. Also shown in the Figures the stress paths of the drained saturated specimen test FS-E1, constant water content specimen test FU-B1, drained specimen tests FU-A1 and FU-A4 which were sheared at 75 kPa suction, and drained tests FU-A10 and FU-A14 which were sheared at 25 kPa suction. The shearing stages for these specimens were stopped before they reached the critical state, and these tests were chosen as representatives for the other fine grading specimens. The point marks shown in Figs. 8.26 and 8.27 are the results at the end of the shearing stage.

8.14.2 Critical Shear Strength

Fig. 8.26 shows that the stress paths for the saturated and unsaturated drained and constant water content tests exhibit similar behaviour to that for the over-consolidated

clay soils. The deviator stress increases until it reaches a peak stress then it decreases on the same stress path until it reaches the critical path.

The dotted line shown in the Fig. 8.26 is the best fit line through the three saturated specimen tests FS-E2, FS-E3 and FS-E5, which they reached the critical state, i.e. this line is the saturated critical shear strength line. The Figure also shows that the saturated specimen test FS-E1, which is close to the critical state as seen in Figs. 7.50 and 7.52, is close to the saturated critical shear strength line (Fig. 8.26). This may indicate that the saturated critical shear strength line is linear, which is in agreement to the finding of the authors mentioned in the previous Subsection 8.14.1. It may also seen that the saturated critical shear strength line is very close to the origin, with more tests a better fitted line may be obtained that passes the origin as was shown by Muir Wood (1990) and Toll (1990) for the saturated grading soil.

Fig. 8.26 also shows that the unsaturated constant water content specimen FU-C2, which reached the critical shear strength at about 40 kPa suction, is close to the saturated critical shear strength line. This may confirm the finding of Toll (1990) who showed that the effect of suction decreased as the degree of saturation decreased until the effect of suction became zero for degrees of saturation below about 55%, as was discussed in the previous Subsection 8.14.1. It should be noted that the degree of saturation for test FU-C2 is about 28%

8.14.3 Critical Specific Volume

Fig. 8.27 shows the results of specific volume against $p-u_a$ and $p-u_w$ (logarithmic scale) at the critical state for the three saturated drained specimen tests FS-E2, FS-E3 and FS-E5, and one unsaturated constant water content specimen test FU-C2. The critical state was not reached for the other tests shown in Fig. 8.27. the dotted line shown in the Figure is the best fit line through the three saturated specimen tests which reached the critical state, i.e. this line is the saturated critical specific volume.

The Figure shows that the behaviour of the of the stress paths during the drained and constant water content shearing stage are same. This indicates that the effect of suction variation during the constant water content test is very small. the Figure also shows that the result of the saturated specimen FS-E1, which is close to the critical state (Figs. 7.50 and 7.52) is above the saturated critical specific volume line (dotted line). It may be concluded that the critical specific volume (void ratio) line for the saturated fine grading soil at low stress levels is non-linear. This in agreement to the conclusion made by Muir Wood (1990) from tests that were carried out by Vesic and Clough (1968), that the critical void ratio for saturated sand was non-linear at low stress levels (Section 8.14.1)

Fig. 8.27 shows that unsaturated fine grading specimen tests FU-B1, FU-A1, FU-A5, FU-A10 and FU-A14, which they did not reach the critical state, are heading above the saturated critical specific volume line. This may indicate that the critical specific volume line for the unsaturated soil is above that for the saturated soil. The unsaturated specimen test FU-C2, which reached the critical state does not show this behaviour as it is below the saturated critical specific volume line (Fig. 8.27). This may be due to the non-uniform deformation that occurs prior the critical state due to specimen end friction (Section 8.7.1). Another reason may be that the effect of suction is very small, as was shown by Toll (1990). He showed the suction contribution to the critical state decreased as the degree of saturation decreased until it became zero at 55% saturation (Section 8.14.1). Further tests are required to understand the unsaturated soil behaviour at the critical state.

8.15 Suggested Model for Unsaturated Granular Soil at Failure

From the discussions made in Sections 8.11 to 8.13, a relationship between the variables that can affect behaviour of the unsaturated granular soil at low stress levels at failure

(peak stress) and at a particular initial dry density, may be proposed. These variables are q, $p-u_a$, suction, specimen specific volume and specimen water content, all at failure. The variation in the initial dry density should be taken into consideration when dealing with the soil at peak stress.

The relationship between q and $p-u_a$, was shown in Section 8.11 to be linear (Fig. 8.19), while the relationship between q and suction needs further investigation to prove whether it is linear or not (Section 8.11). The relationship between specimen volume, suction and $p-u_a$ (logarithmic scale) is shown in Fig. 8.23. This relationship is significantly affected by the initial dry density variation (Section 8.12 and Fig. 8.22). The relationship between water content, $p-u_a$ (logarithmic scale) and suction is shown in Fig. 8.25. Despite the fact that this relationship requires more tests, from tests at 25 kPa and 50 kPa suctions, the Figure shows that the relationship between water content and $p-u_a$ (logarithmic scale) is approximately linear.

It may be concluded that there is a relationship between q, $p-u_a$, suction, specimen specific volume and specimen water content, all at failure. This means that two state surfaces for the specific volume and water content versus $p-u_a$ and suction at peak stress can be drawn. These surfaces require more tests at different values of suction to be able finding the shape of these surfaces. Also a specimen compaction technique should be developed to produce less dry density variation, as this can affect the volume behaviour of the specimens (Section 8.12)

8.16 Comparison between the Coarse and Fine Grading Soils

Three coarse grading specimens (series D) were compacted at the same water content and compactive effort as the fine grading specimens. The specimens were sheared at the same rate of strain as for the fine grading specimen test series C (0.00093 %/min). The values of initial suction that were measured for the coarse grading specimens, were about a third

of those for the fine grading specimens at the same water contents, as shown in Tables 7.8 and 7.9. Also, with the same compactive effort, the coarse grading specimens showed higher dry densities than those for the fine grading specimens. The average dry densities for the fine and coarse grading specimens were 1.962 Mg/m^3 and 2.121 Mg/m^3 respectively (Section 8.3).

The plot of deviator stress at failure against the $p-u_a$ for the coarse grading specimens are shown in Fig. 8.21, together with those for the fine grading specimen tests. The Figure shows that, despite the low values of suction that the coarse grading specimens had, higher values of failure stress than those for the fine grading specimens were recorded. This may be due to the high dry densities of the coarse grading soils. Fig. 8.16 shows that the coarse grading specimens showed higher values of Young's modulus than those of the fine grading specimens. Also due to the high values of dry density, coarse grading specimens failed at lower values of specific volume than those of the fine grading specimens, as shown in Fig. 8.24.

The difference in the initial dry density between the coarse and fine grading specimens makes the comparison between them difficult. Authors such as Marachi et al. (1972), Al-Hussaini (1983) and Indraratna et al. (1993) carried out tests on saturated rockfill materials with different grain sizes. They showed that the initial tangent Young's modulus increased as grain size increased. Indraratna et al. (1993) showed that the volumetric strain of soil with maximum grain sizes between 38 mm and 25 mm at peak stress was independent of the soil grading, while Marachi et al. (1972) showed that the volumetric strain at peak stress became independent of the soil grading for soil grading with maximum grain sizes larger than 50 mm. They showed that the volumetric strain at peak stress for soils with maximum grain size of about 12 mm was less than that for larger grain sizes.

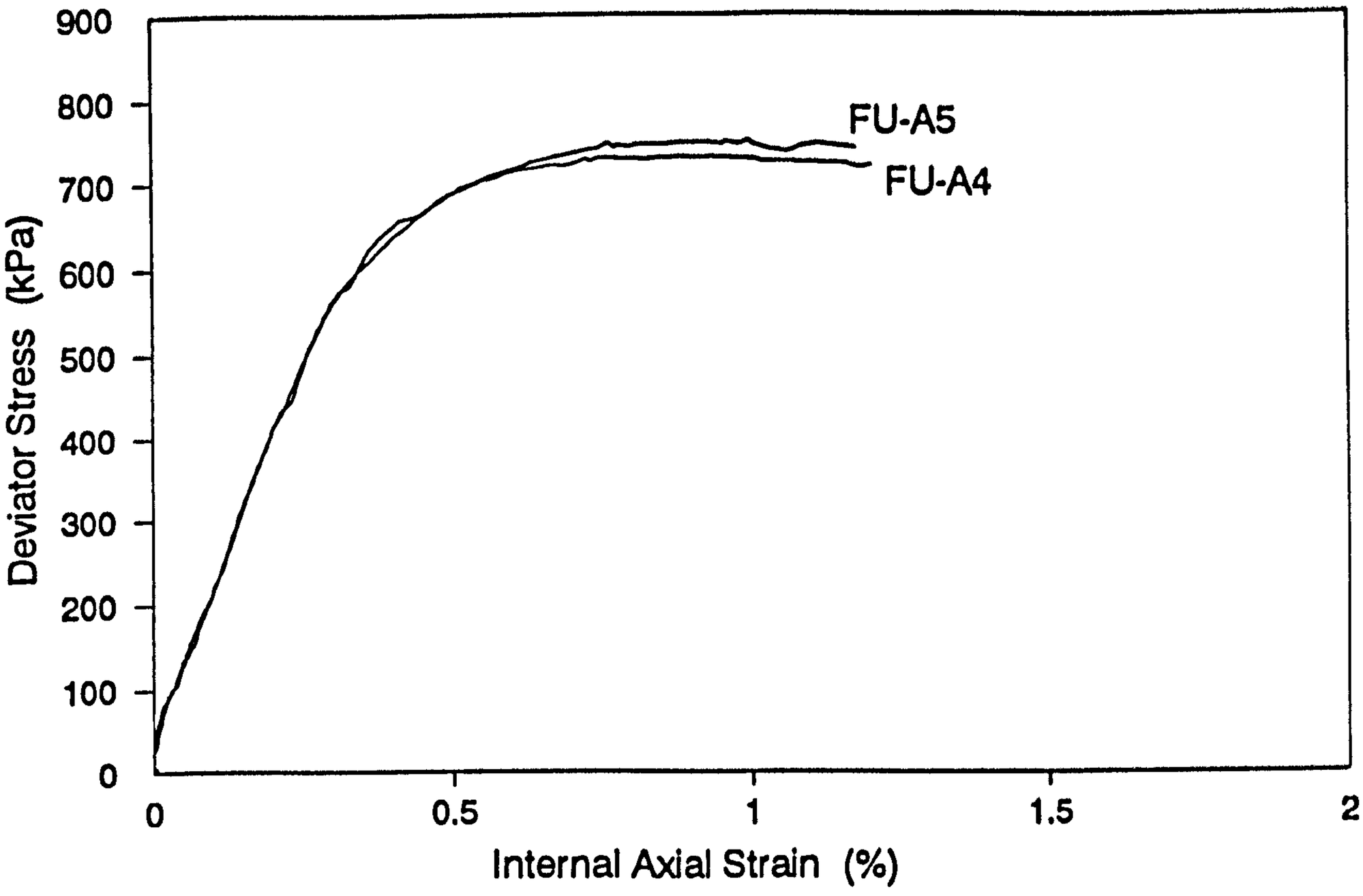

Fig. 8.1- Deviator stress-strain curves for tests FU-A4 and FU-A5 (Suction =75 kPa).

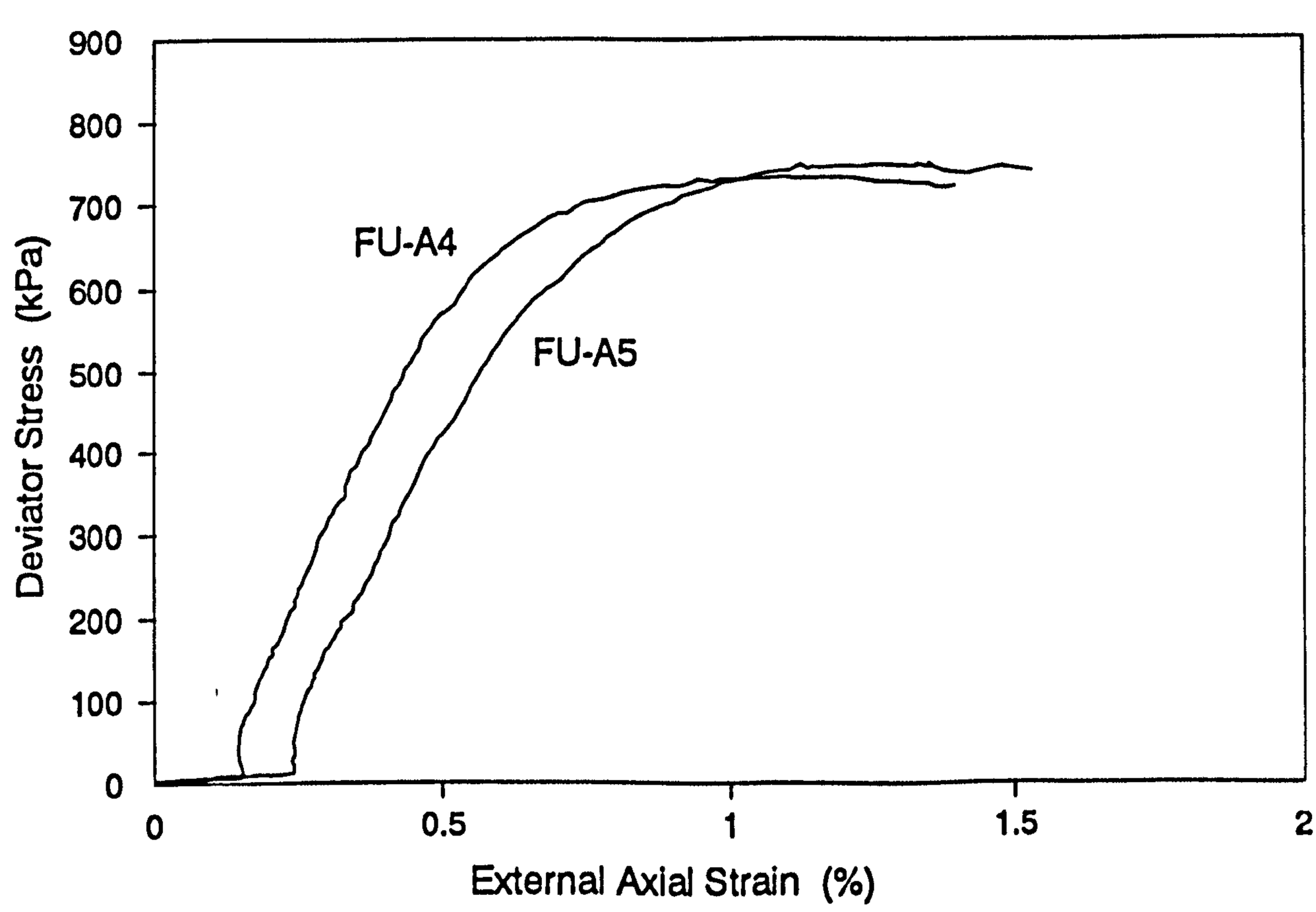

Fig. 8.2- Deviator stress-strain curves of tests FU-A4 and FU-A5, plotted using the external axial strain. (suction= 75 kPa)

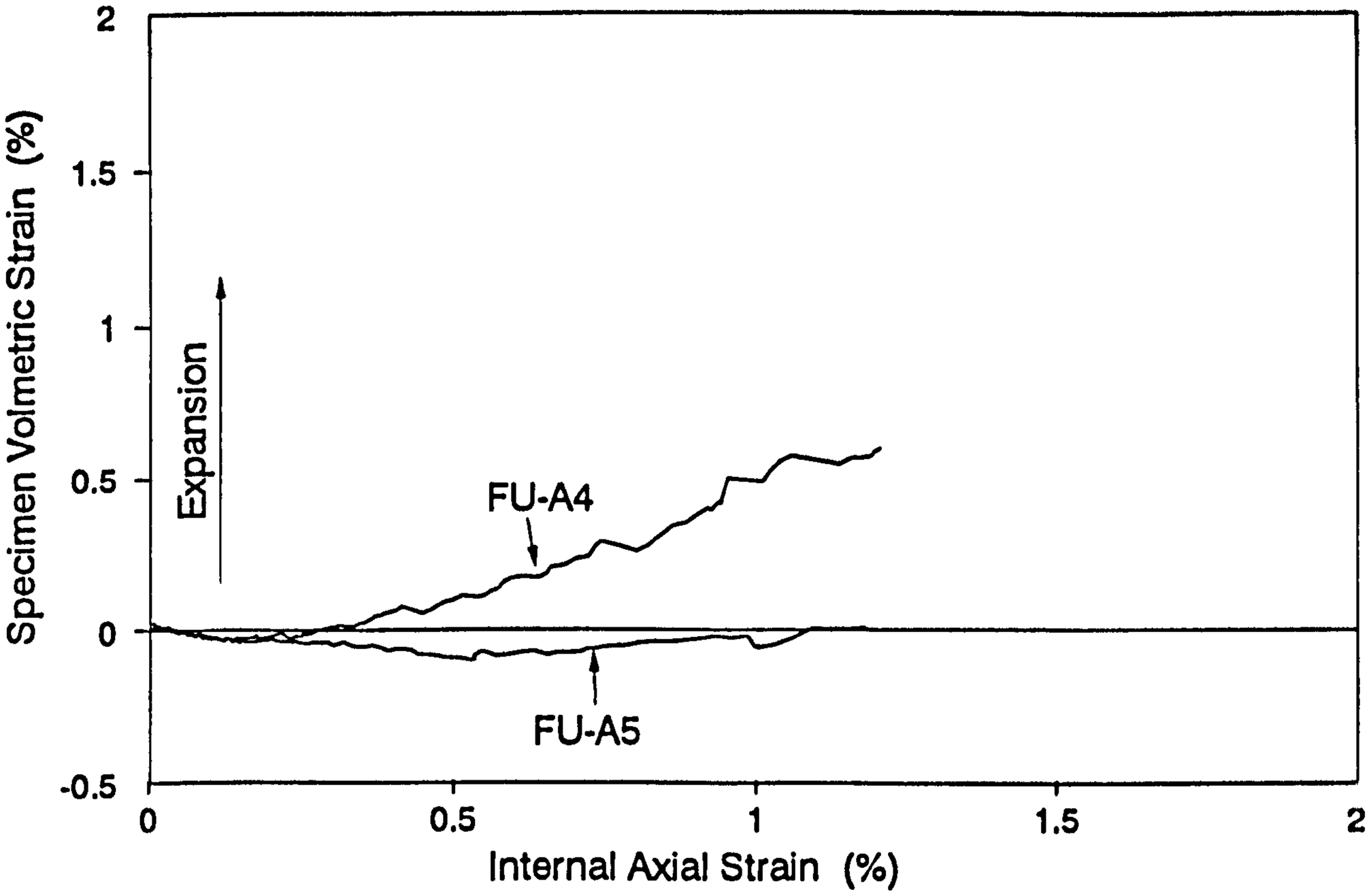

Fig. 8.3- Specimen volumetric strain calculated using the internal strain measurements during shearing for test FU-A4 and FU-A5 (Suction =75 kPa)

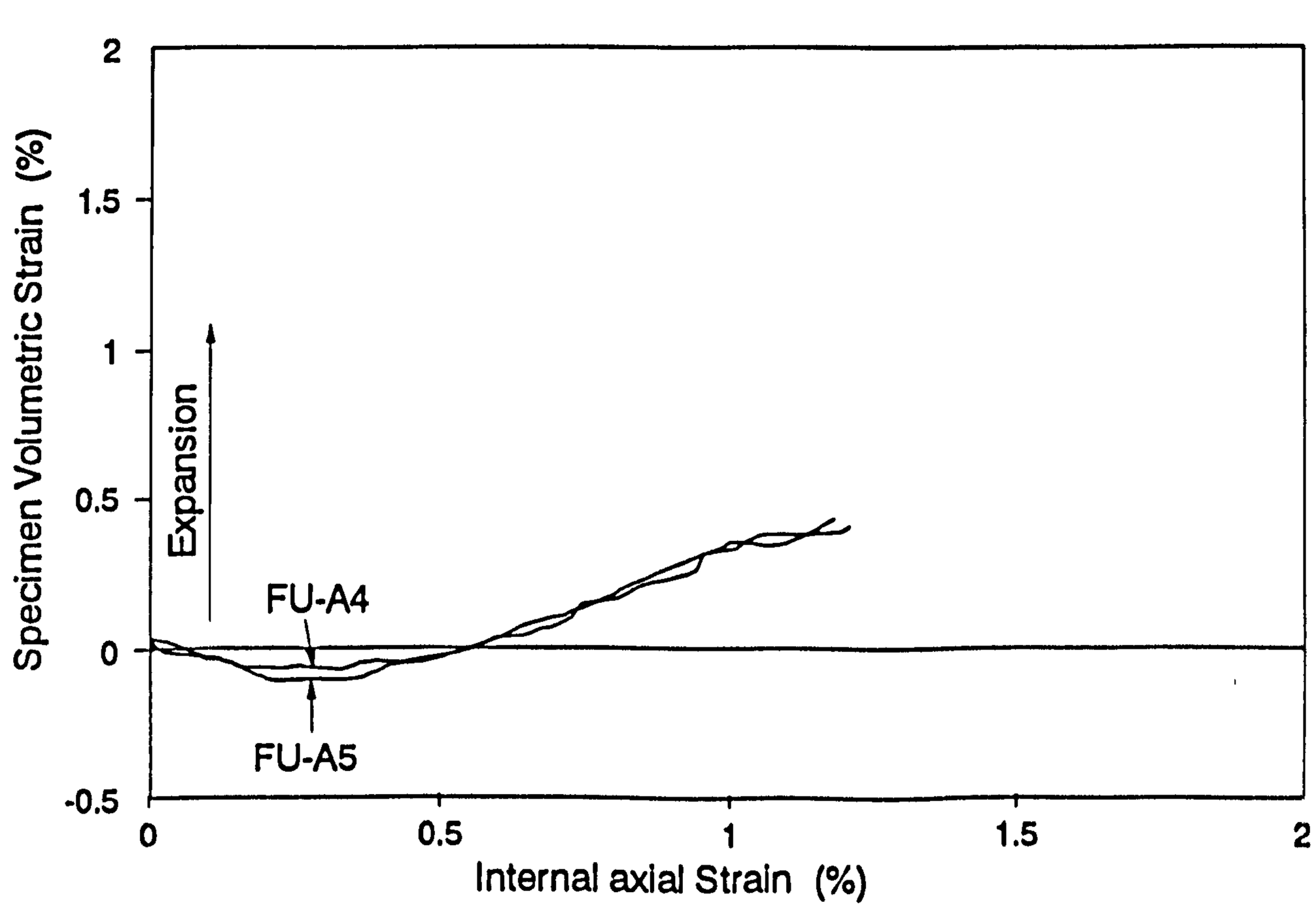

Fig. 8.4- Specimen volumetric strain measured using the volume change unit during shearing for tests FU-A4 and FU-A5 (Suction =75 kPa)

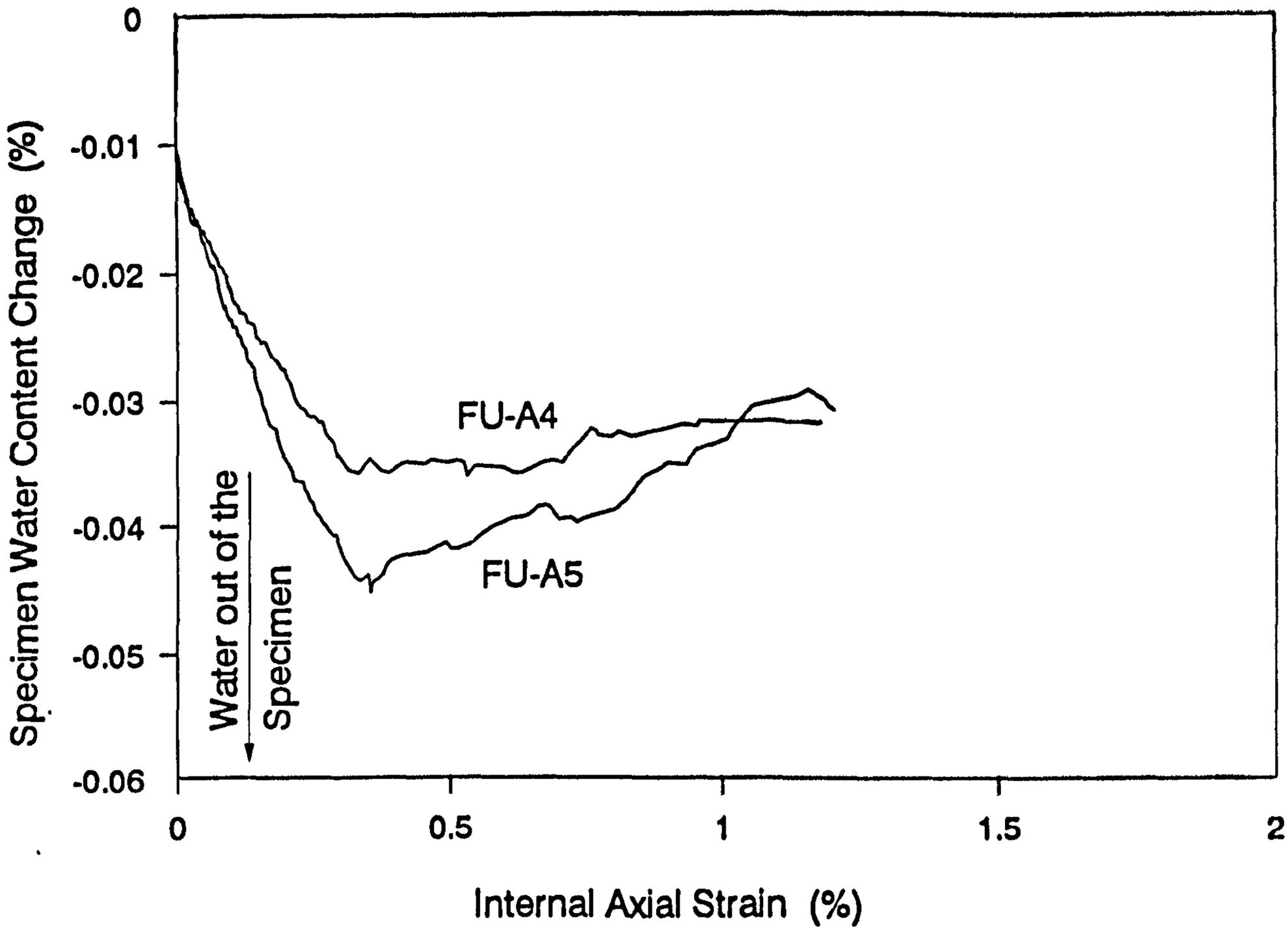

Fig. 8.5- Specimen water content change during shearing for tests FU-A4 and FU-A5 (suction=75 kPa)

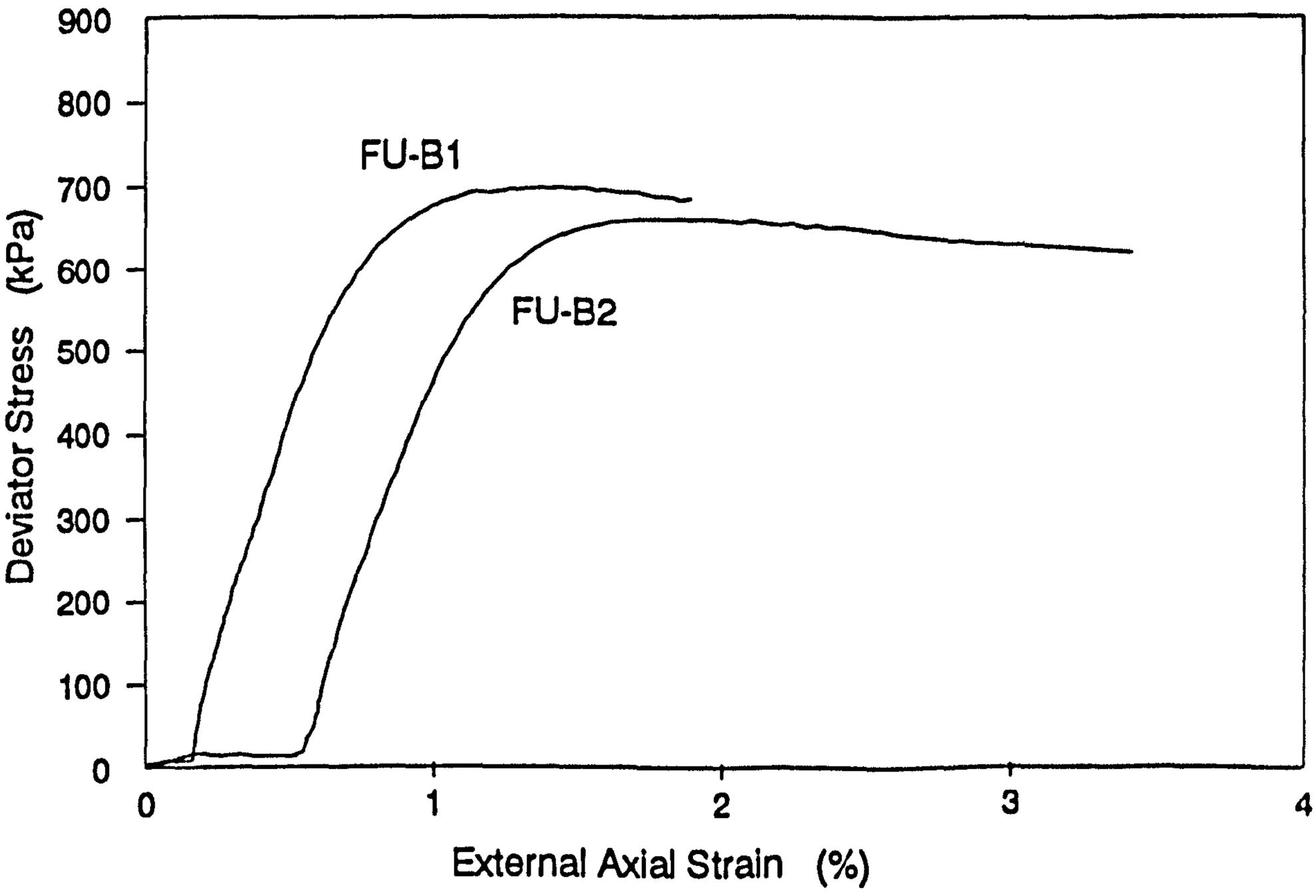

Fig. 8.6- Stress-strain curves of tests FU-B1 and FU-B2 plotted against the external axial strain.

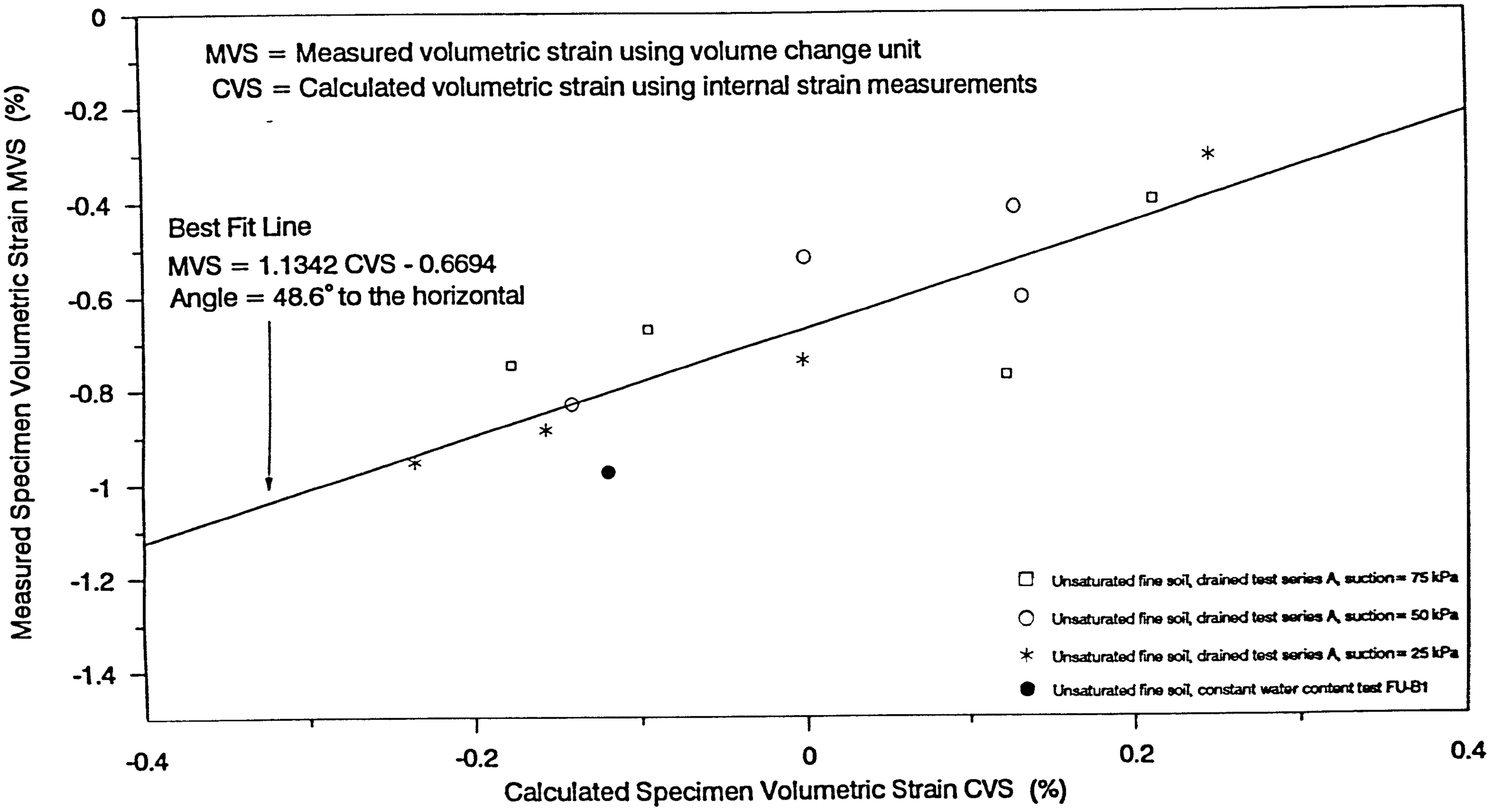

Fig. 8.7 -Comparison between the values of the MVS and CVS

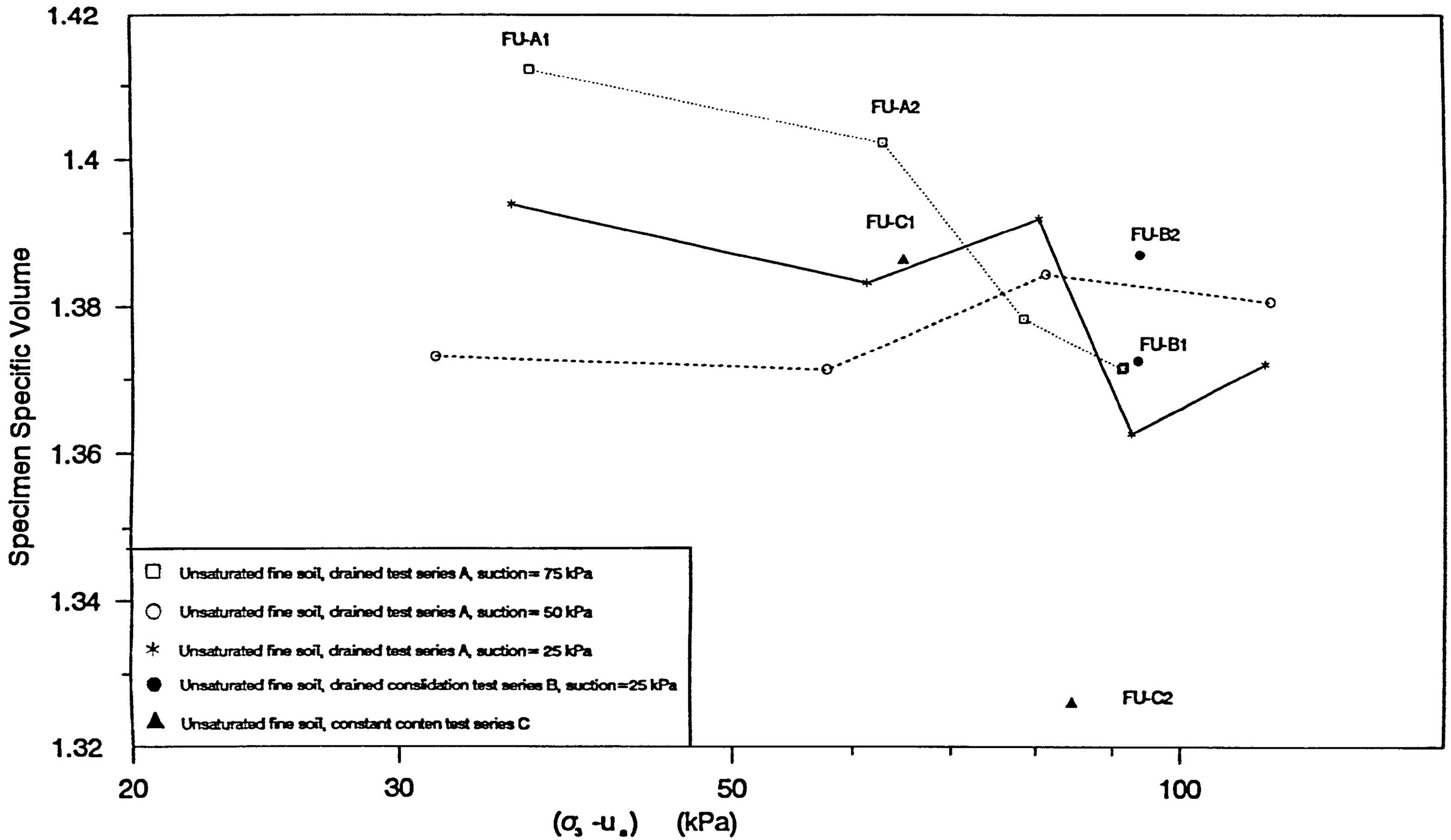

Fig. 8.8a- Specimen specific volume calculated using the internal strain measurements at the end of the consolidation stage and the combined stage for the unsaturated fine grading specimens (test series A to C)

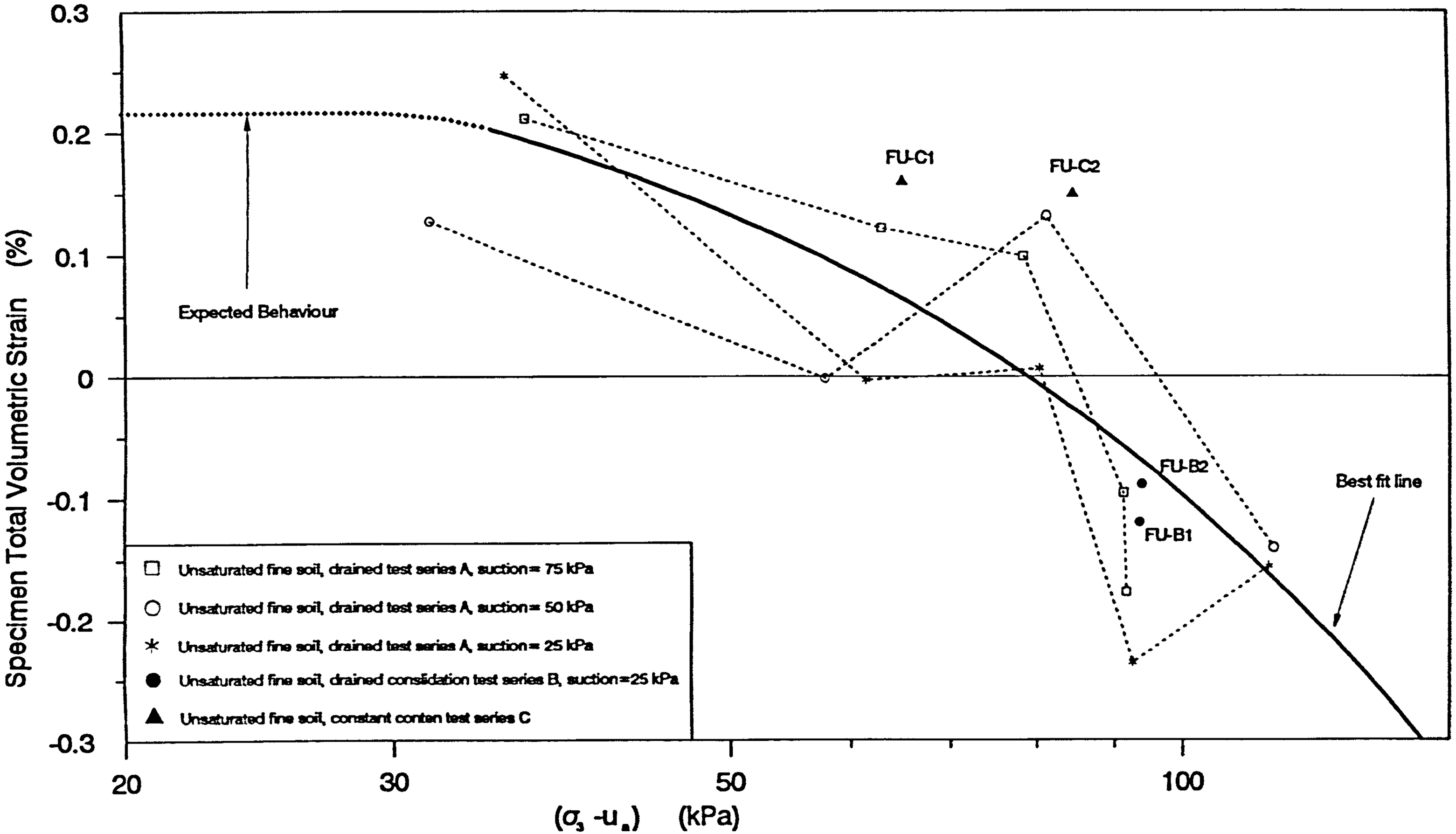

Fig. 8.8b- Specimen total volumetric strain calculated using the internal strain measurements at the end of the consolidation stage and the combined stage for the unsaturated fine grading specimens (test series A to C)

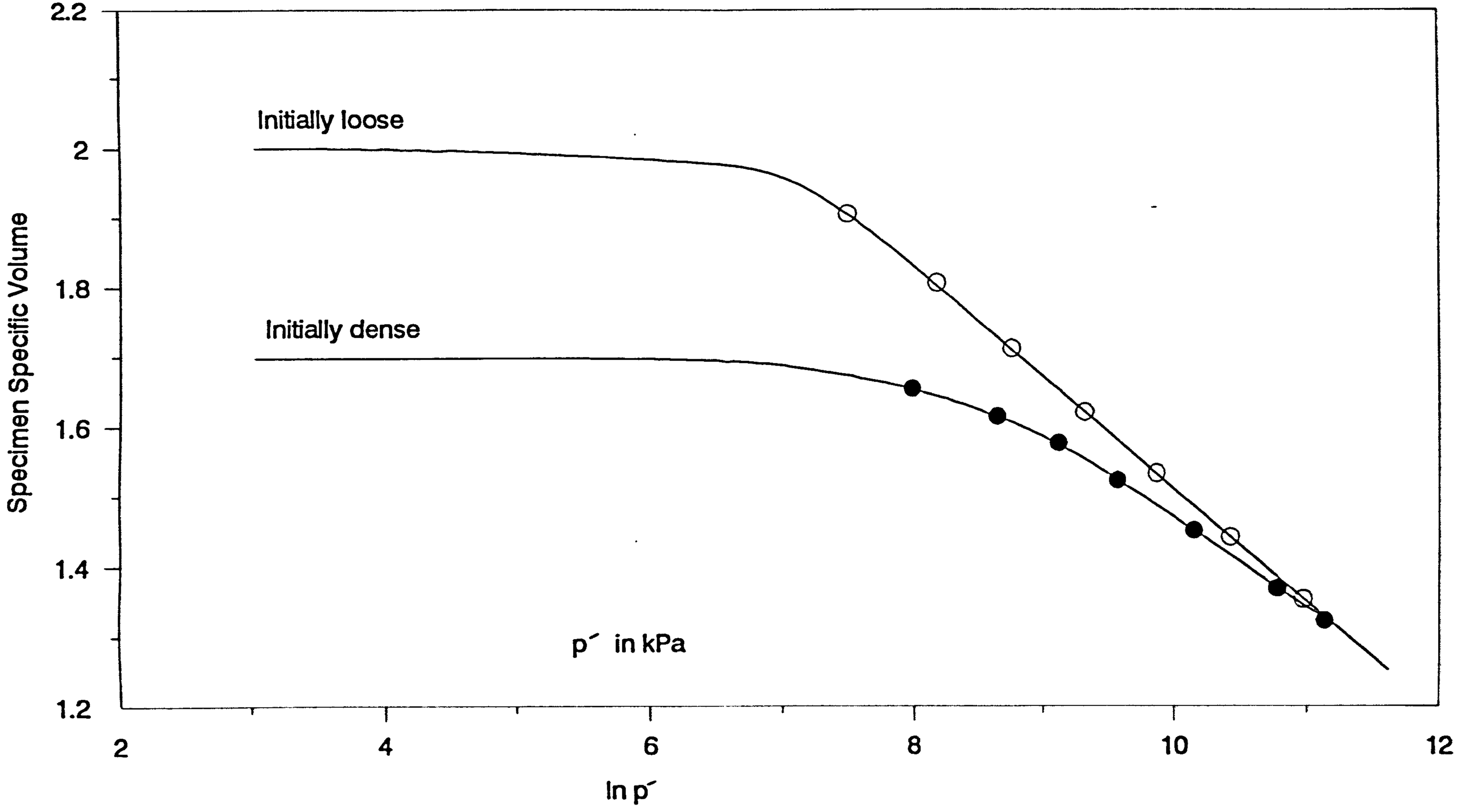

Fig. 8.9- Isotropic compression of Chattahoochee River sand plotted against effective mean stress (after Vesic and Clough, 1968)

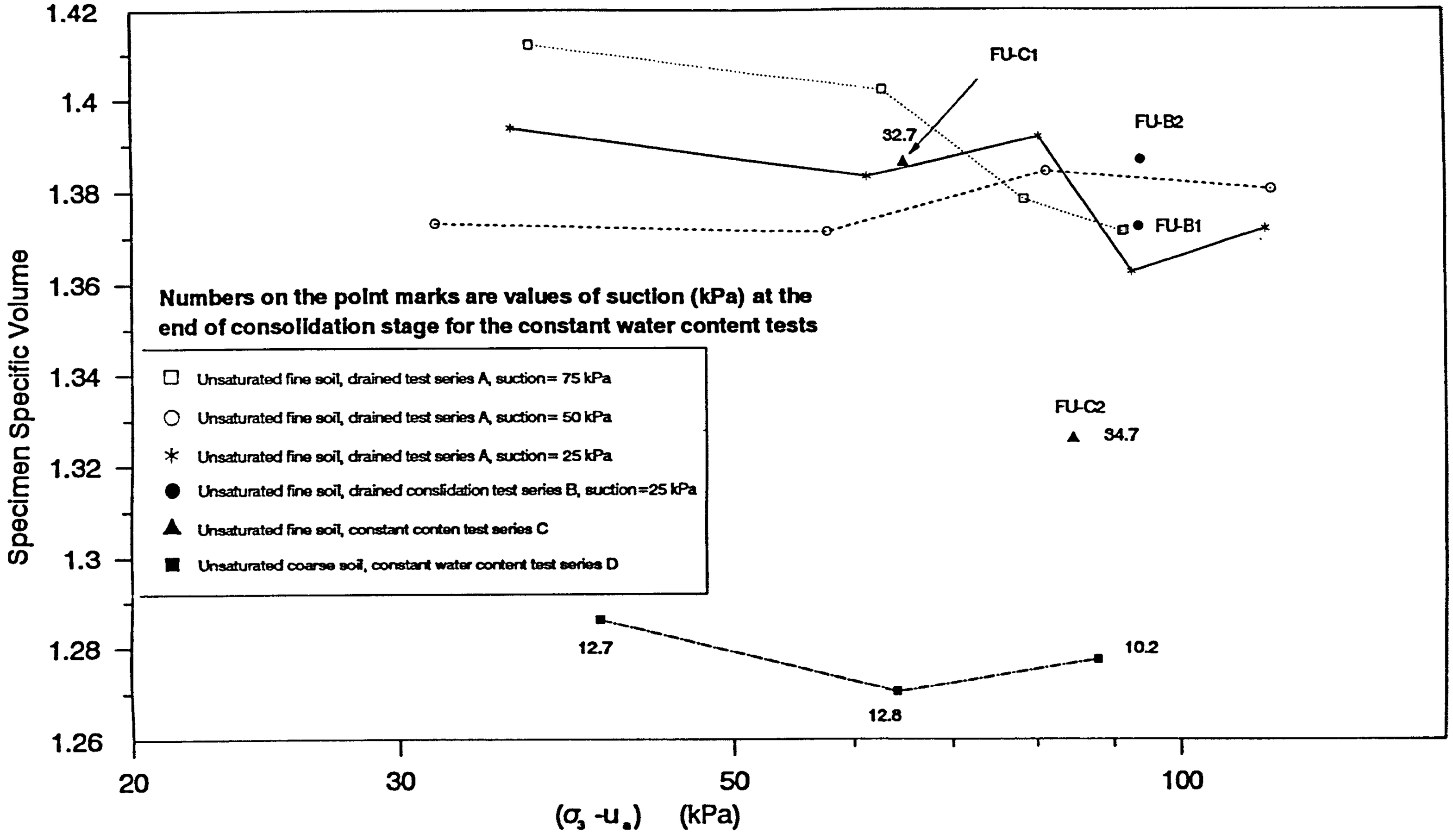

Fig. 8.10- Specimen specific volume calculated using the internal strain measurements at the end of the consolidation stage and the combined stage for the unsaturated fine and coarse grading specimens (series A to D)

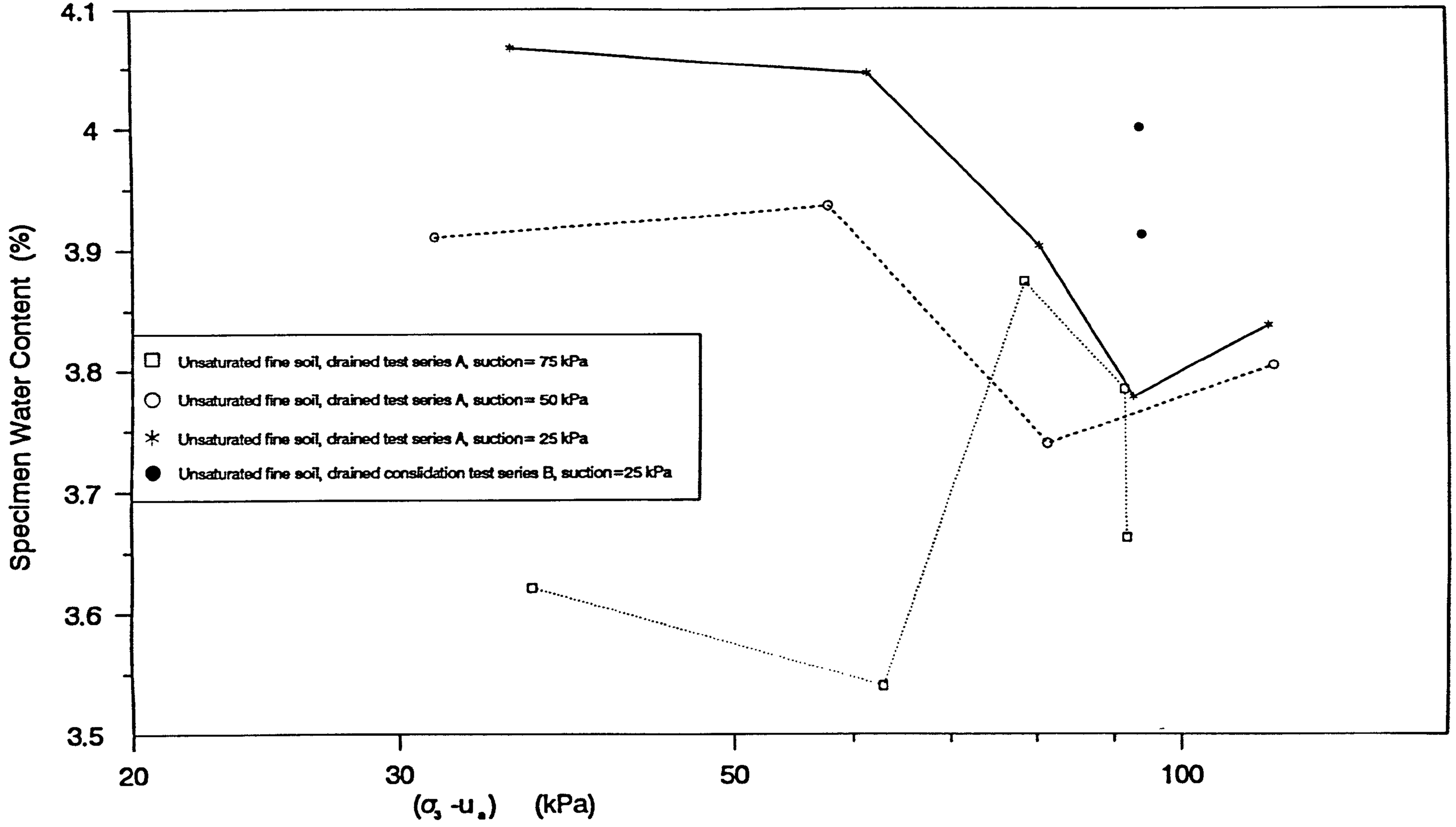

Fig. 8.11- Specimen water content at the end of the consolidation stage and the combined stage for the fine grading specimens (series A & B)

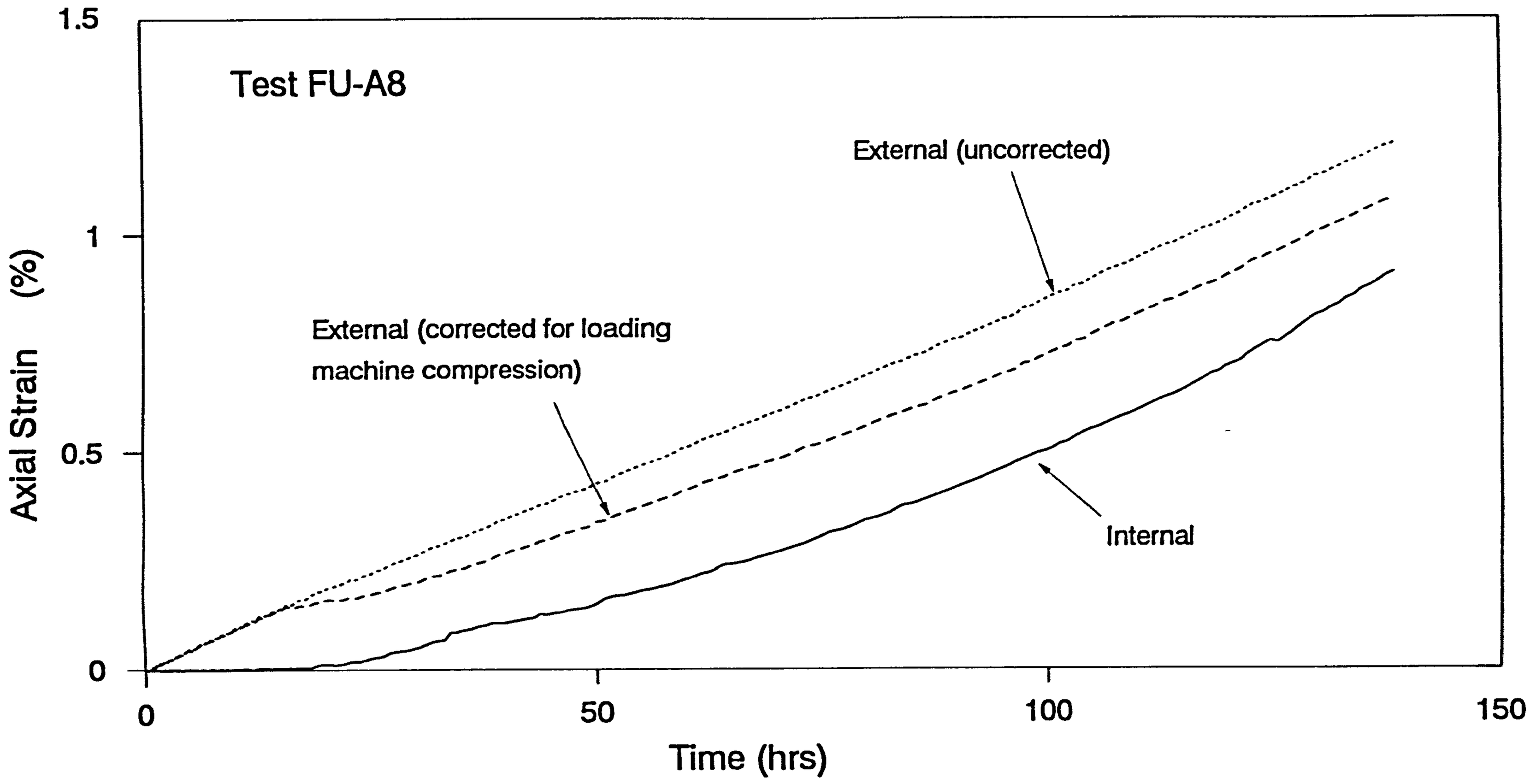

Fig. 8.12- Comparison between the internal and external axial strain measurements

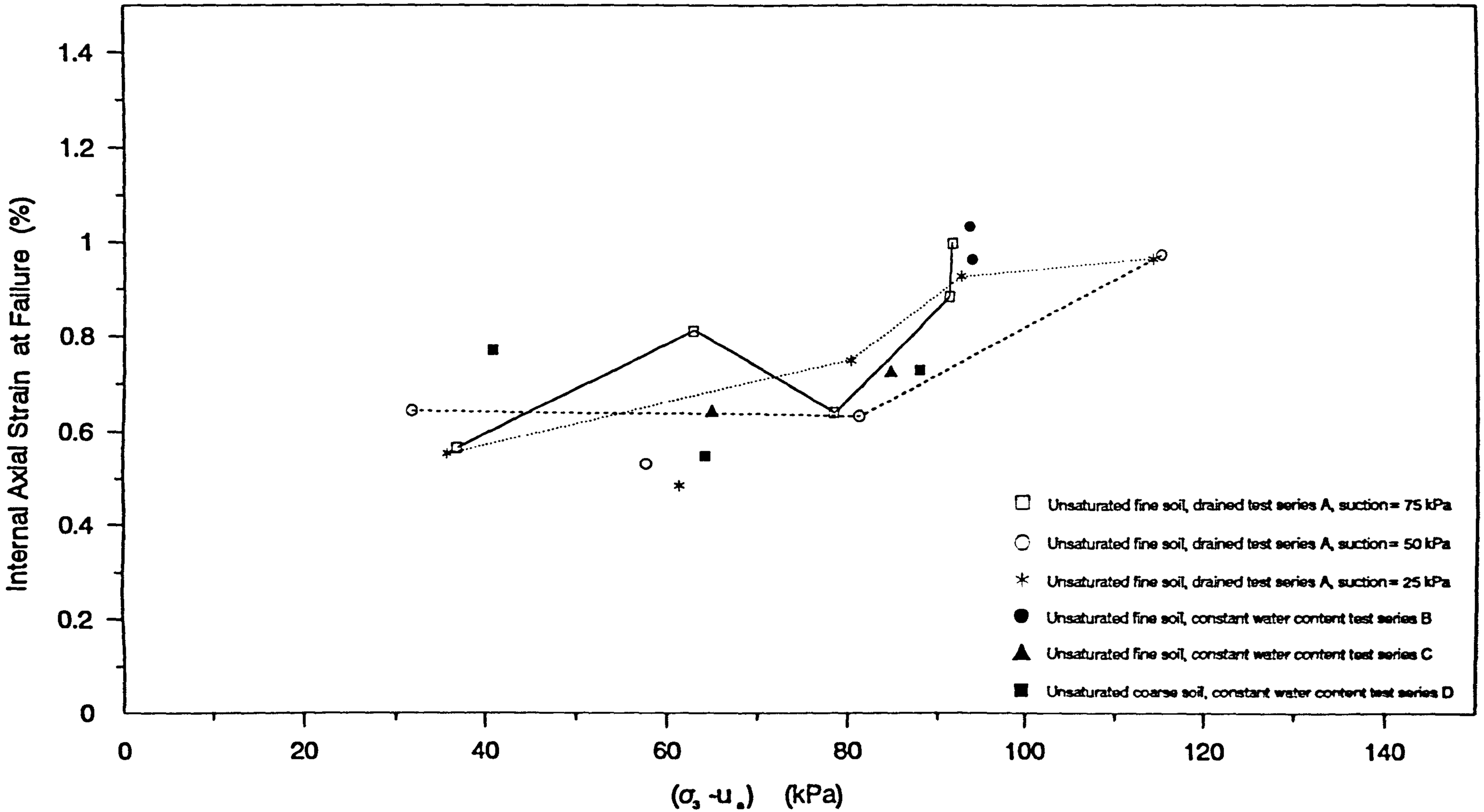

Fig. 8.13a-Values of the internal axial strain at failure for all unsaturated fine and coarse grading specimens, plotted against net cell pressure.

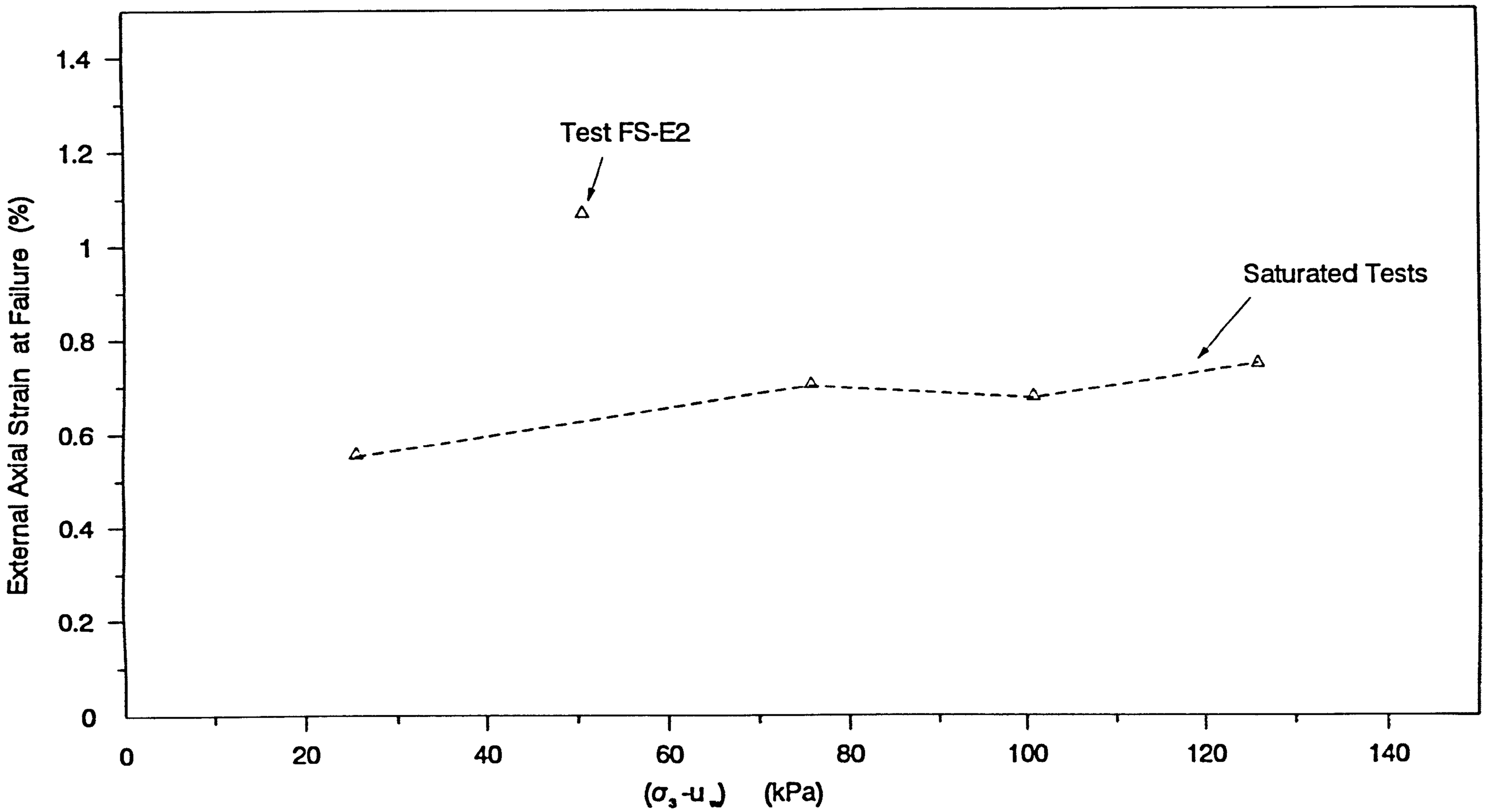

Fig. 8.13b-Values of the external axial strain at failure for the saturated fine grading specimens, plotted against effective cell pressure.

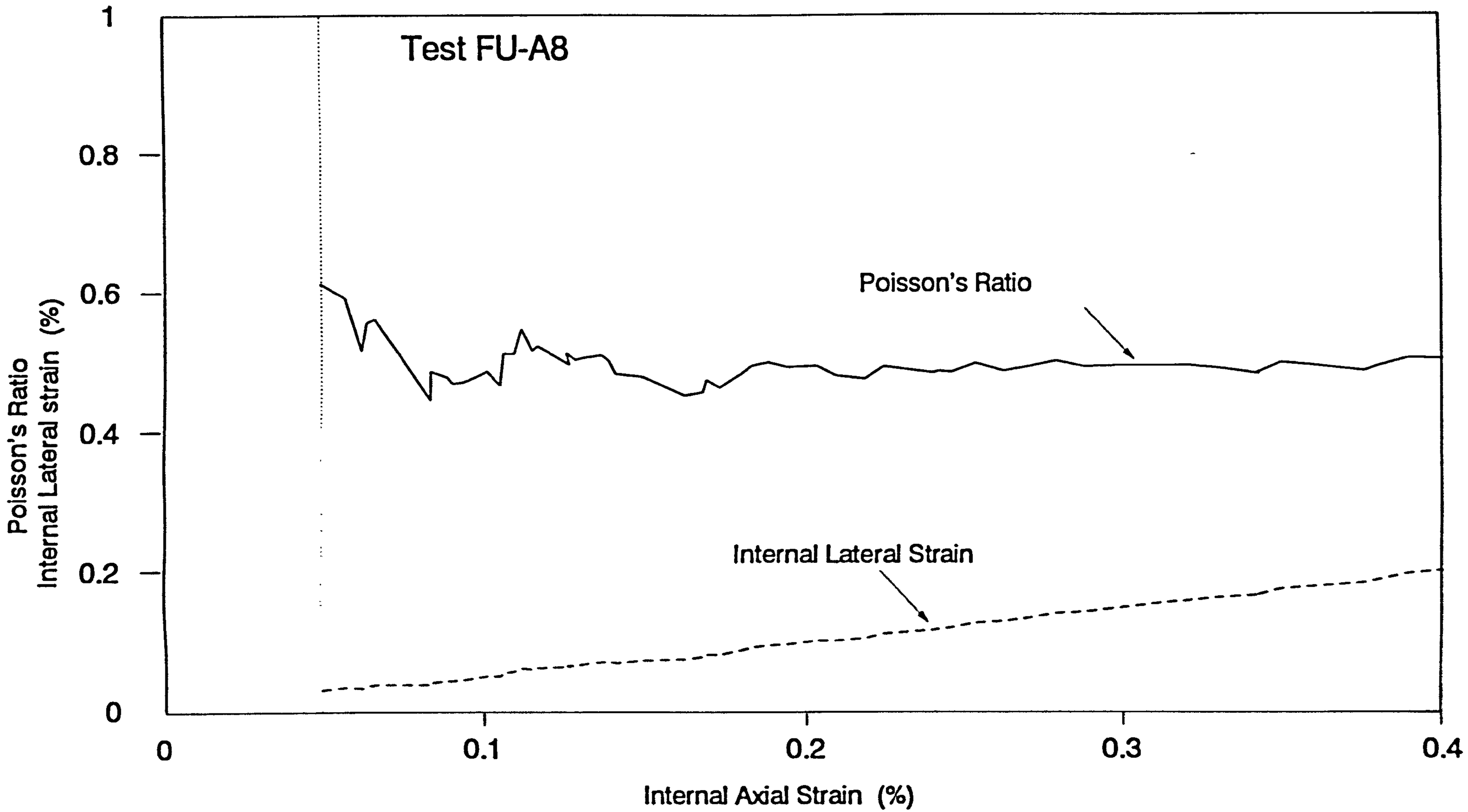

Fig. 8.14 -Typical Values of Poisson's ratio determined from internal strain measurements plotted against internal axial strain (test FU-A8)

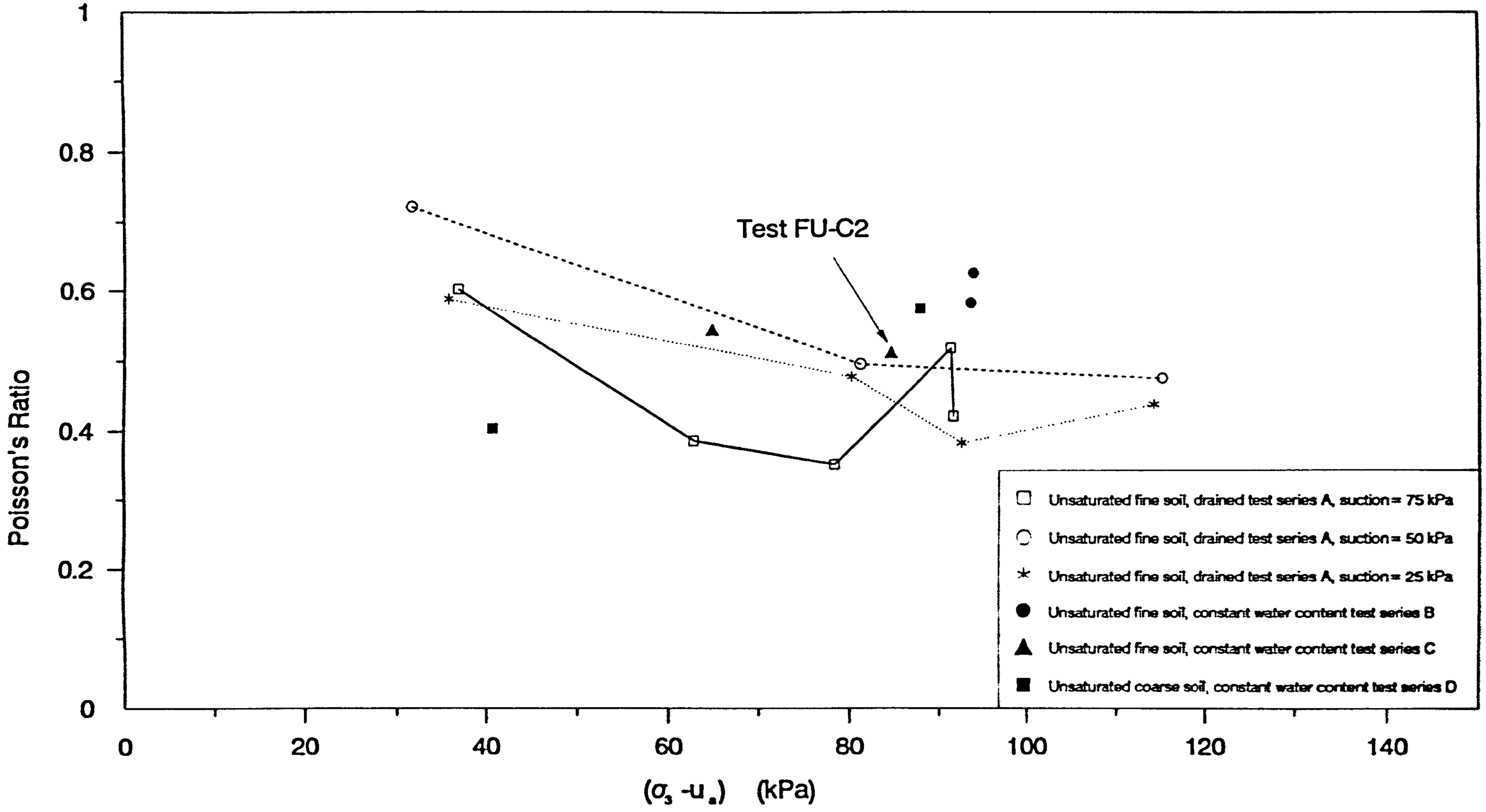

Fig. 8.15 -Values of Poisson's ratio at 0.3% internal axial strain for the unsaturated fine and coarse grading specimens, plotted against net cell pressur.

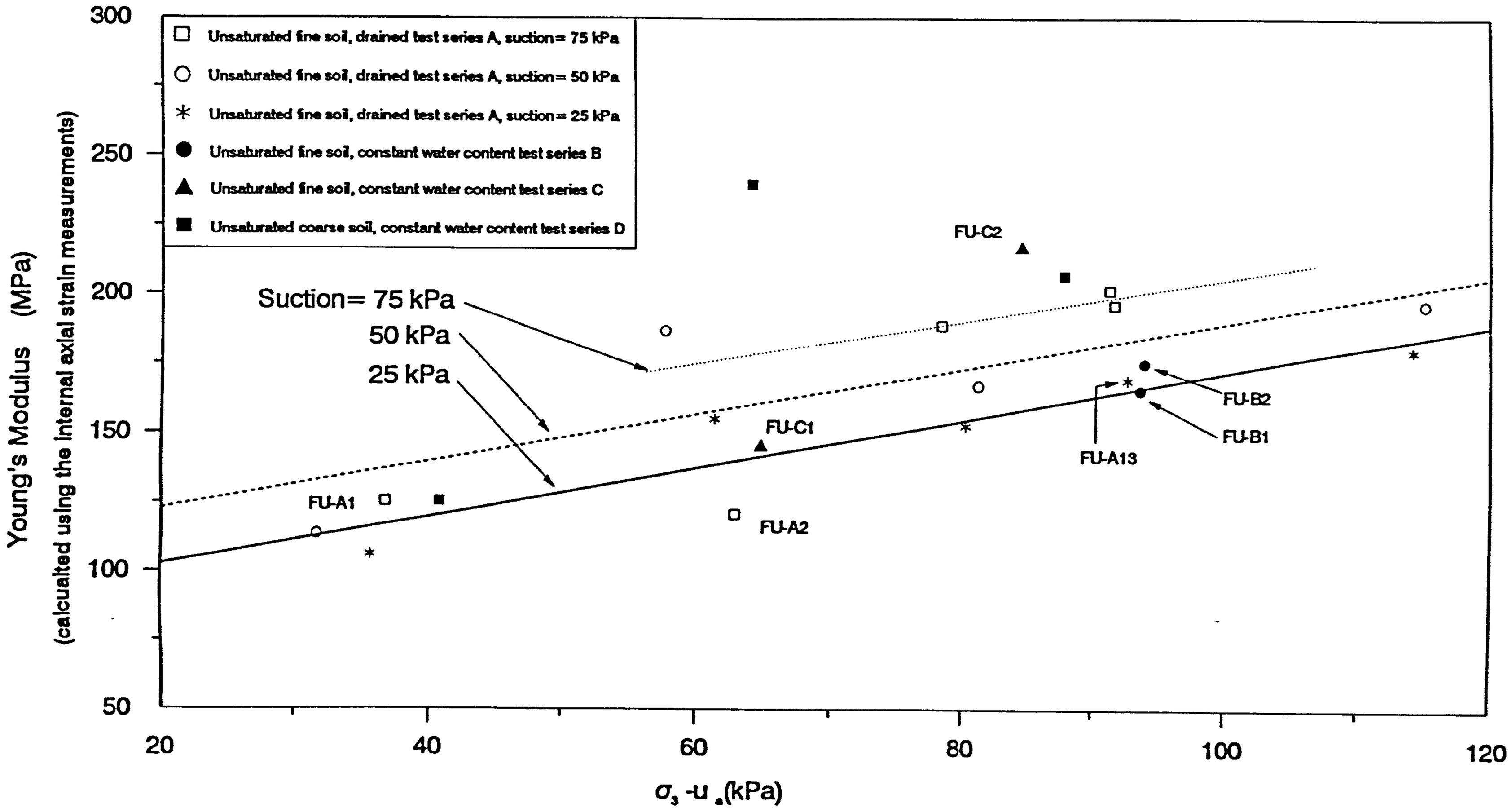

Fig. 8.16 -Values of Young's modulus at 0.25% internal axial strain for all unsaturated fine and coarse specimens plotted against the net cell pressure

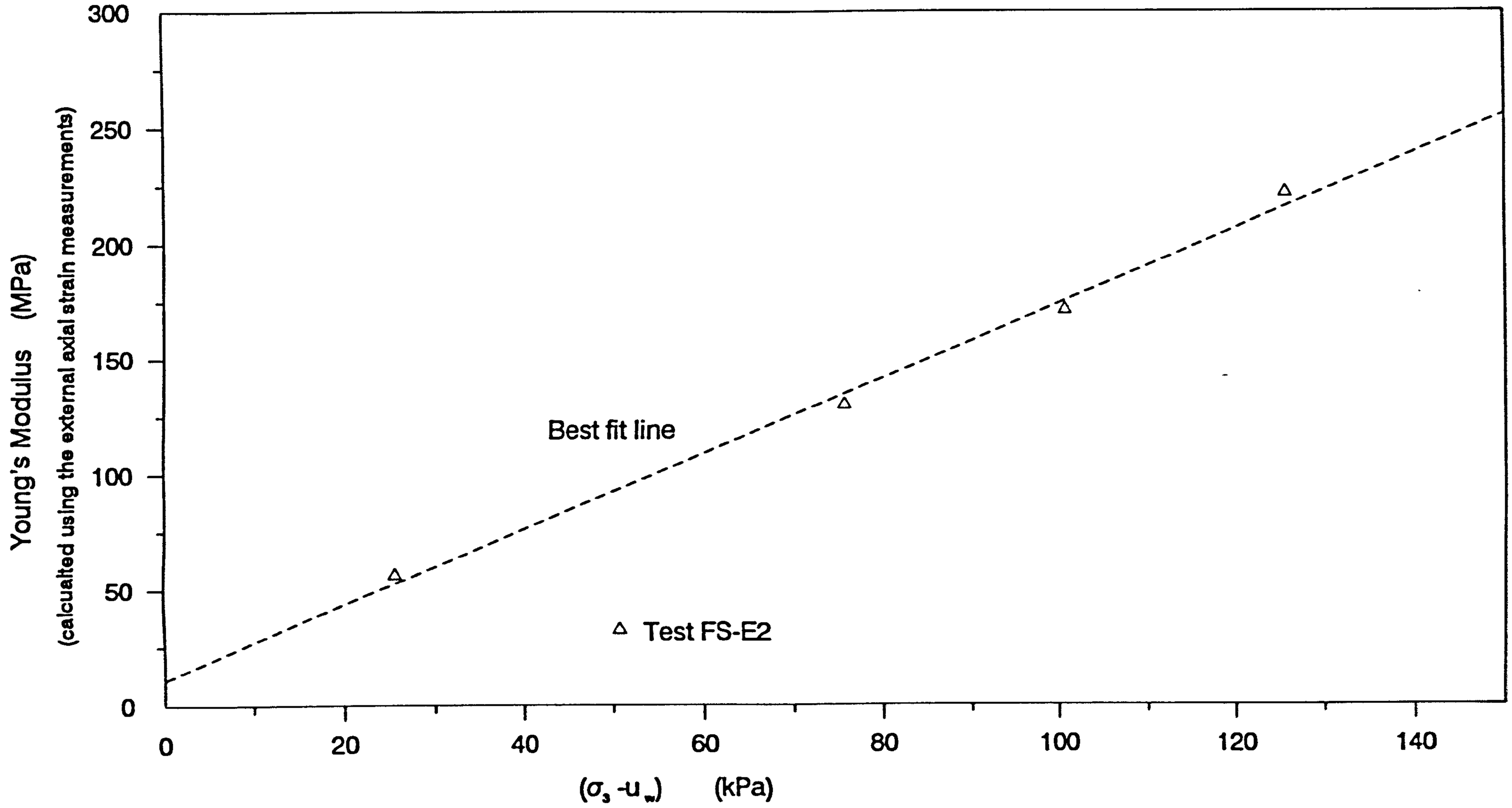

Fig. 8.17-Values of Young's modulus for the saturated fine grading test sereies E at 30% of the failure stress, plotted against effective cell pressure.

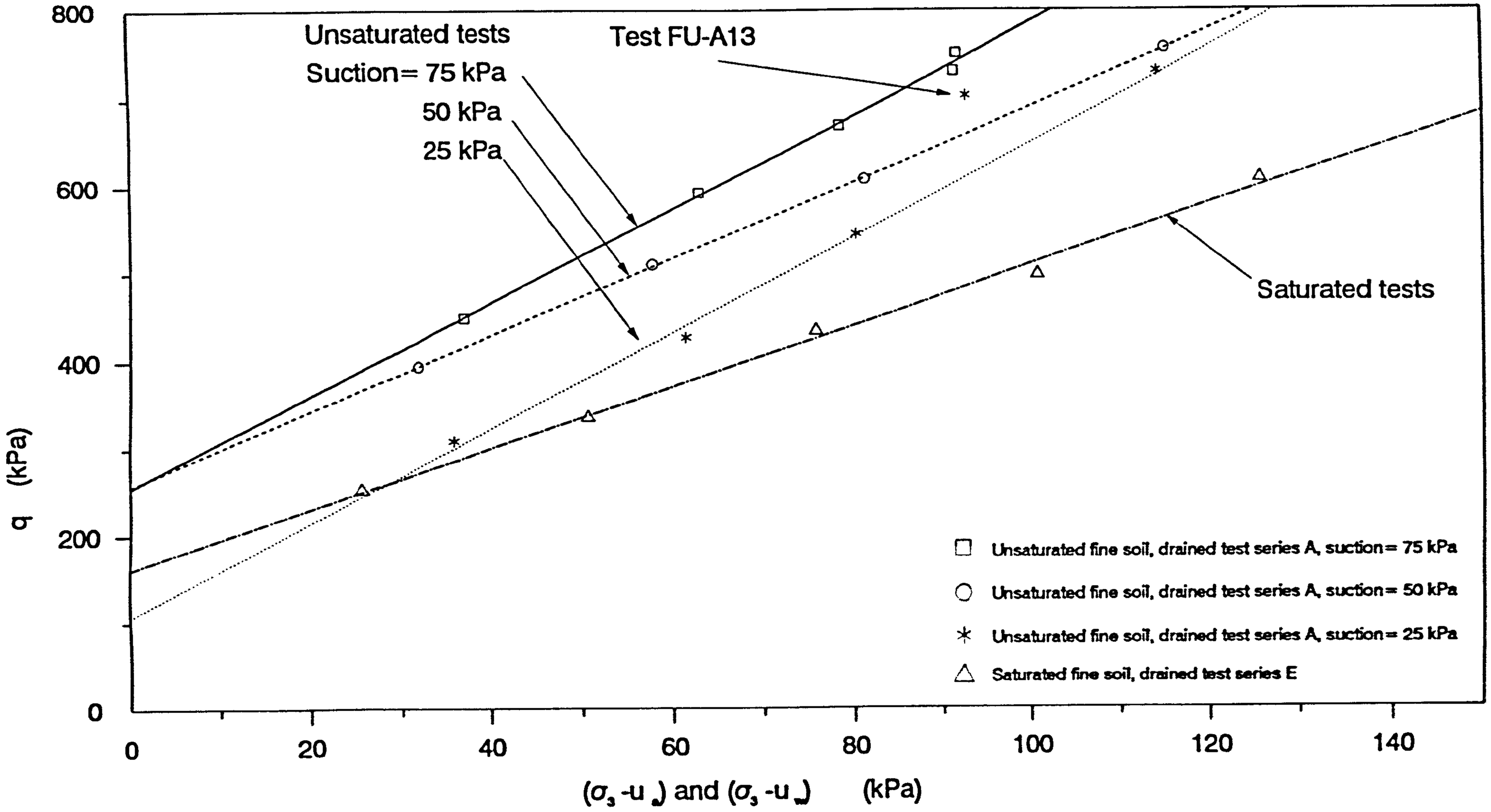

Fig. 8.18-Failure stresses for the drained test series A and E for the unsaturated and saturated fine grading specimens plotted against net and effective cell pressures

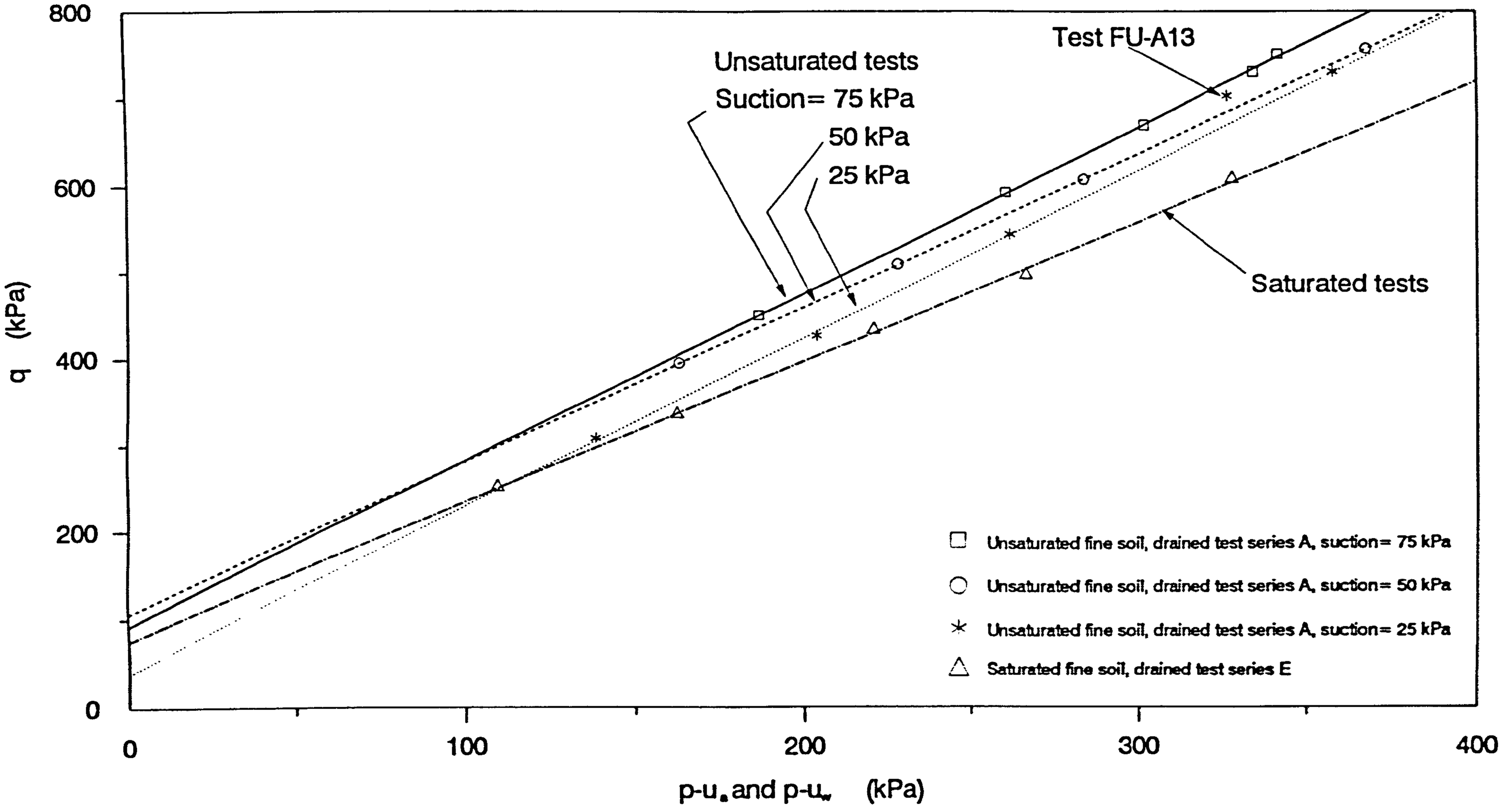

Fig. 8.19-Failure stresses for all drained test series A and E for the fine grading unsaturated and saturated specimens plotted against the net and effective mean pressures.

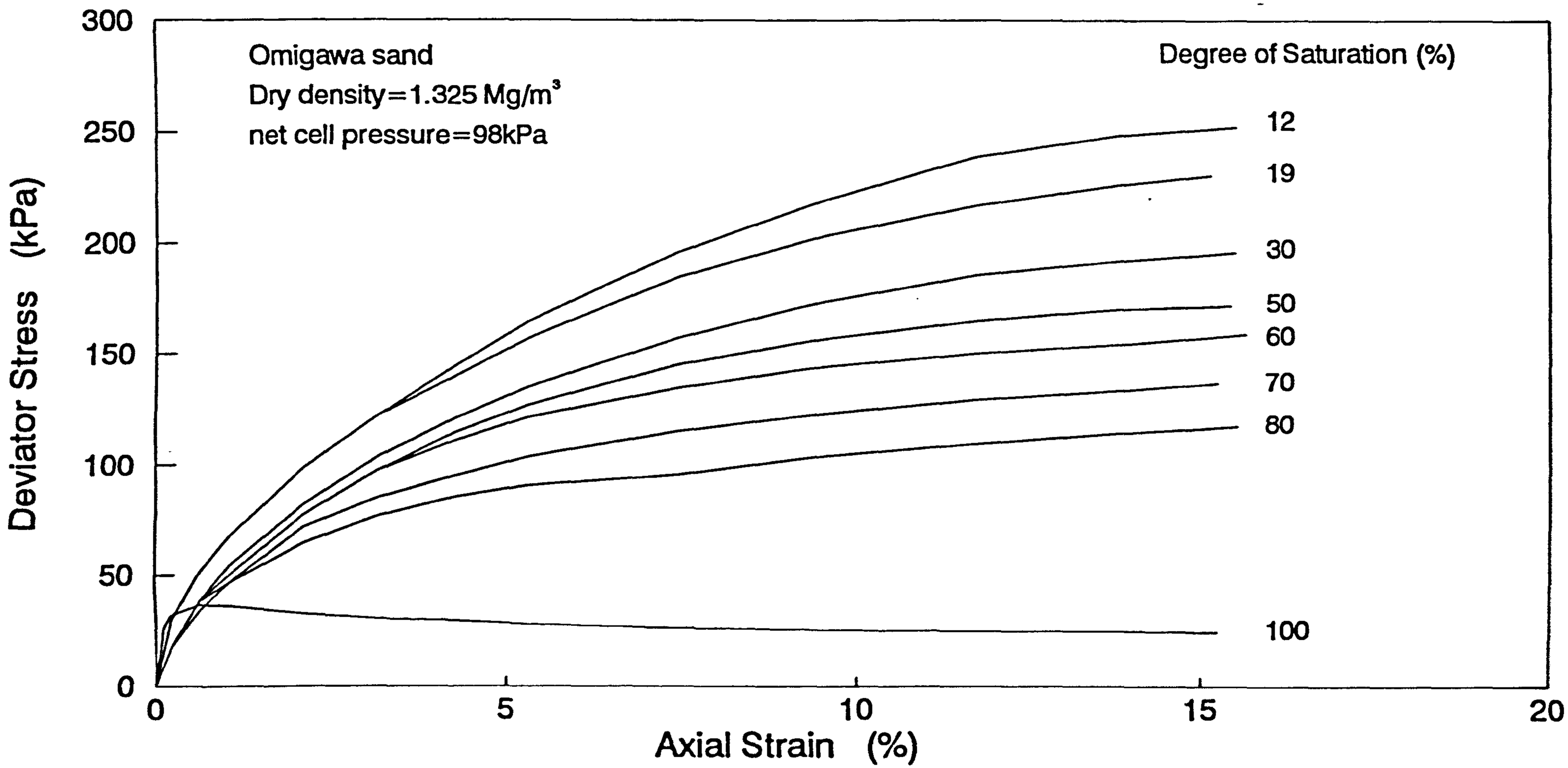

Fig. 8.20- Deviator stress-strain curves obtained from triaxial tests on unsaturated and saturated specimens (after Yoshida et al., 1991)

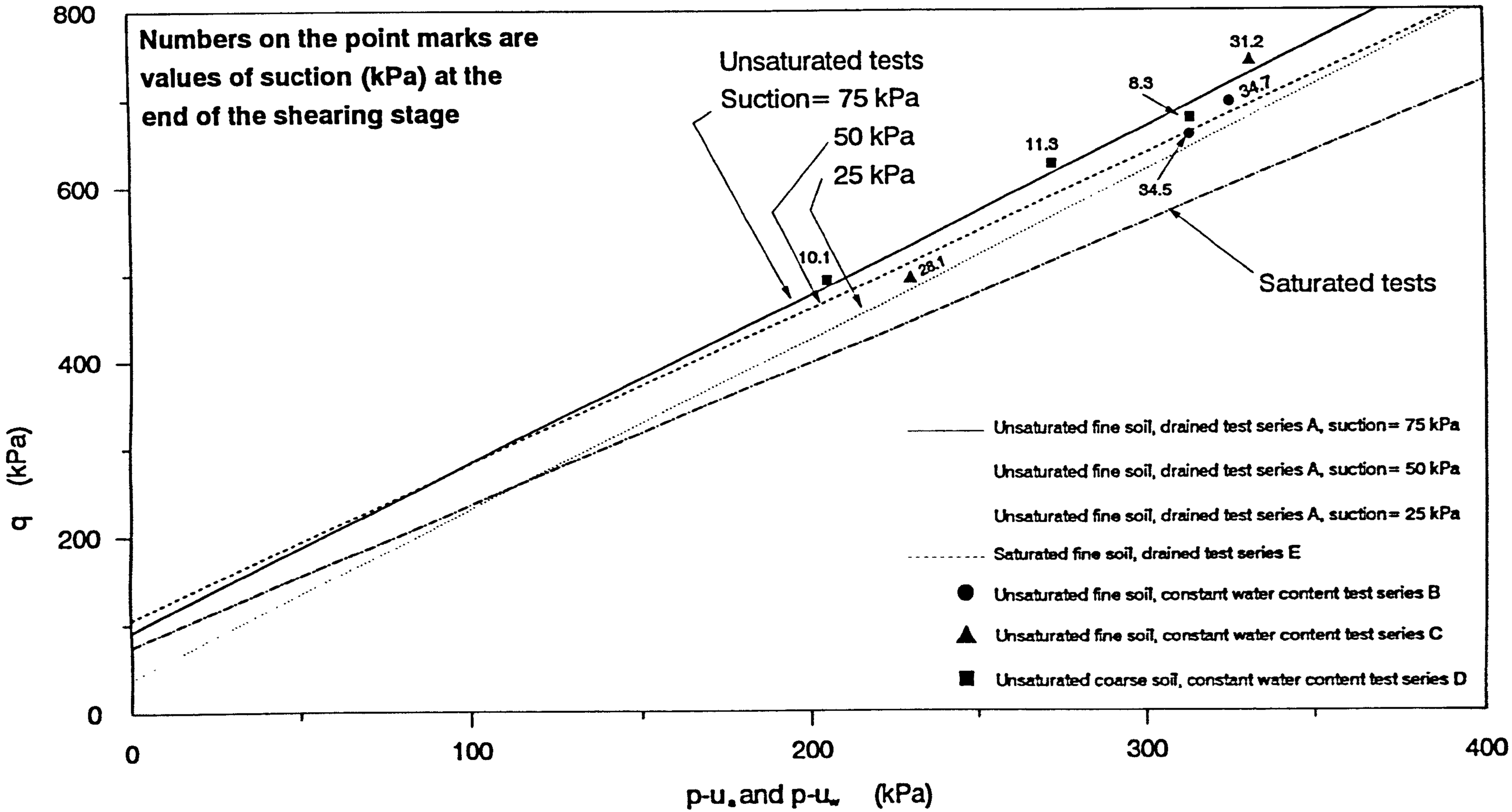

Fig. 8.21-Failure stresses for all specimens, plotted against the net and effective mean pressures.

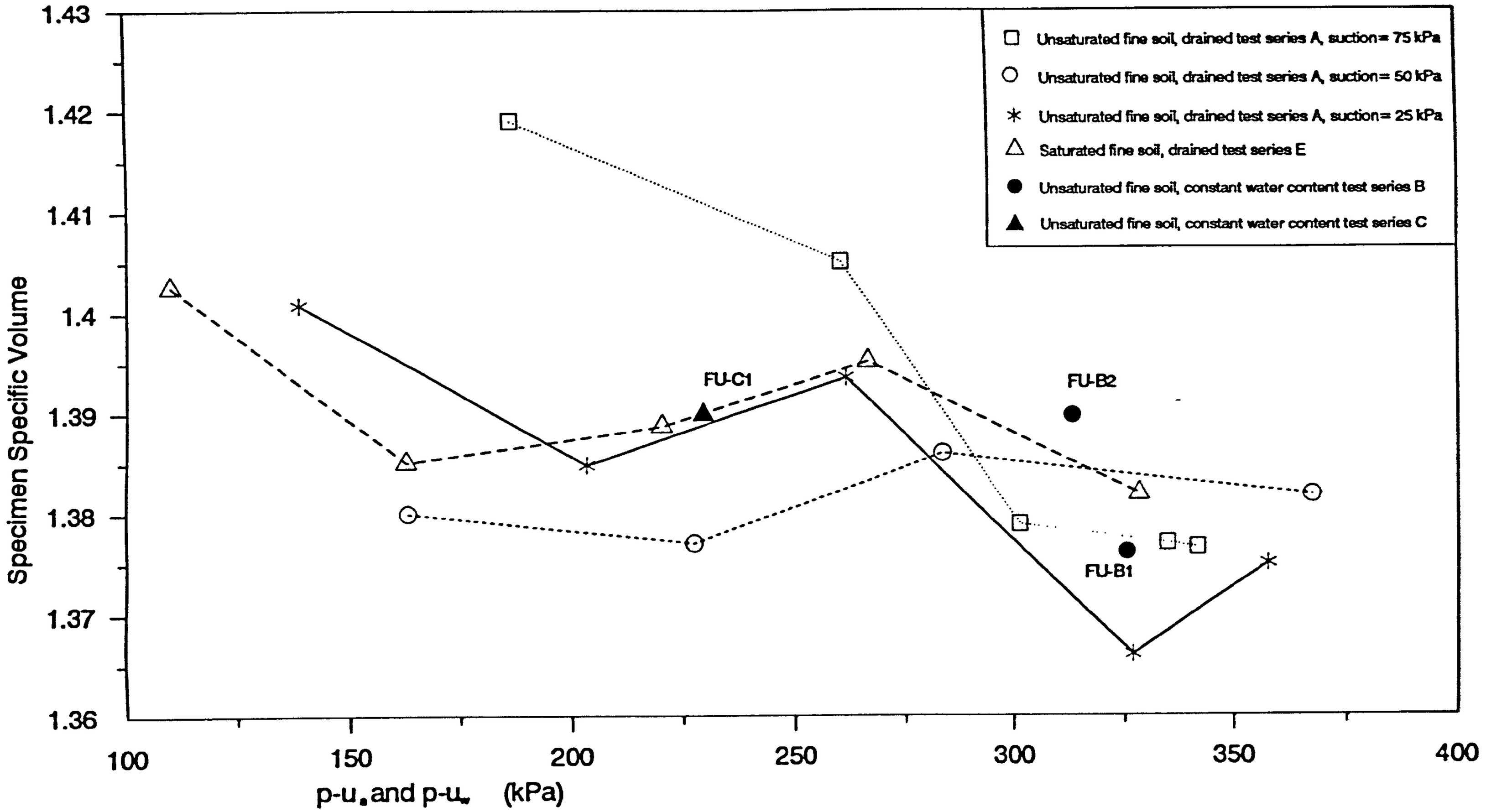

Fig. 8.22- Specimen specific volume calculated using the volume change unit measurements at the peak stress (failure) during the shear stage for the unsaturated and saturated fine grading specimens (series A, B, C & E)

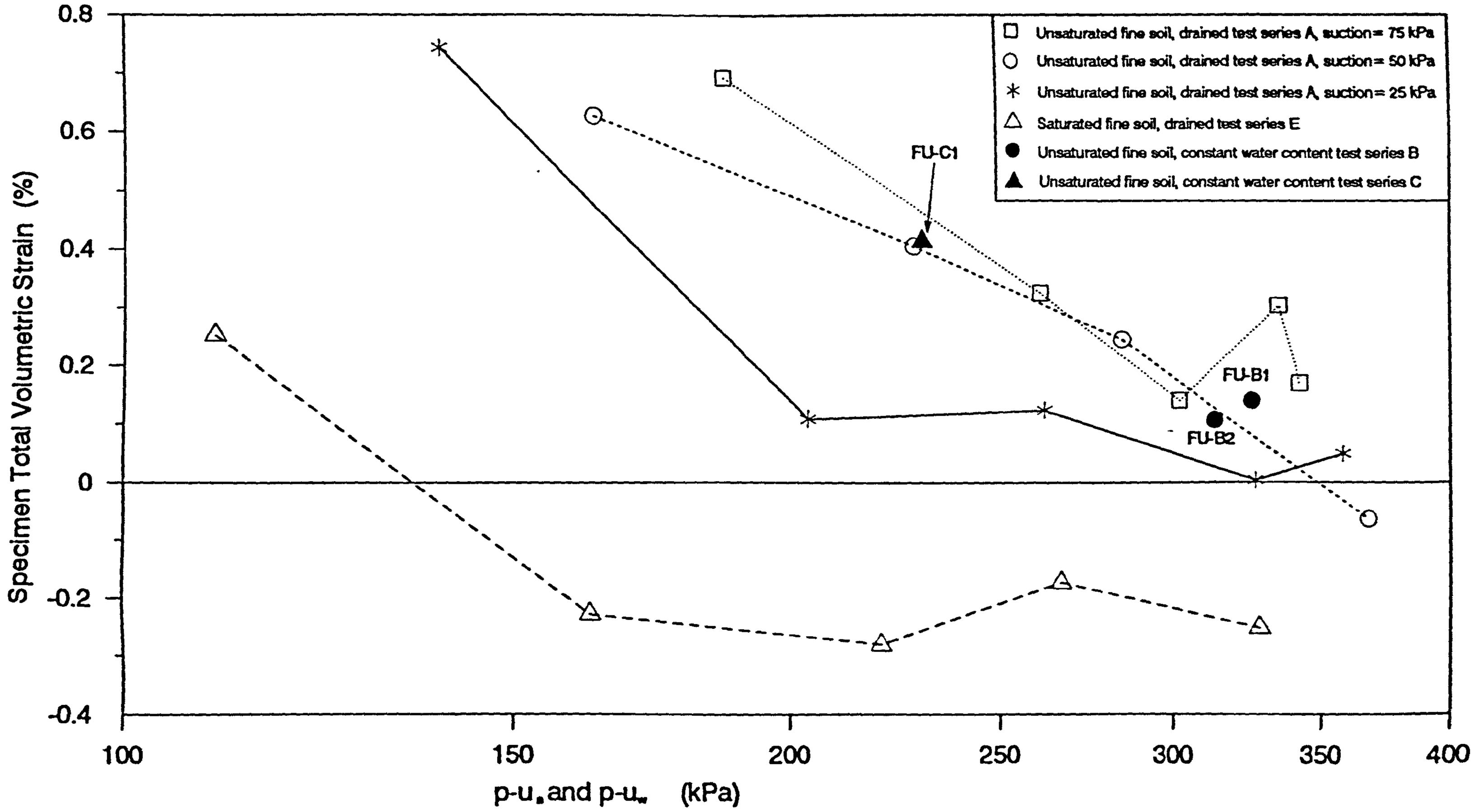

Fig. 8.23- Specimen total volumetric strian calculated using the volume change unit measurements at the peak stress (failure) during the shear stage for the unsaturated and saturated fine grading specimens (series A, B, C & E)

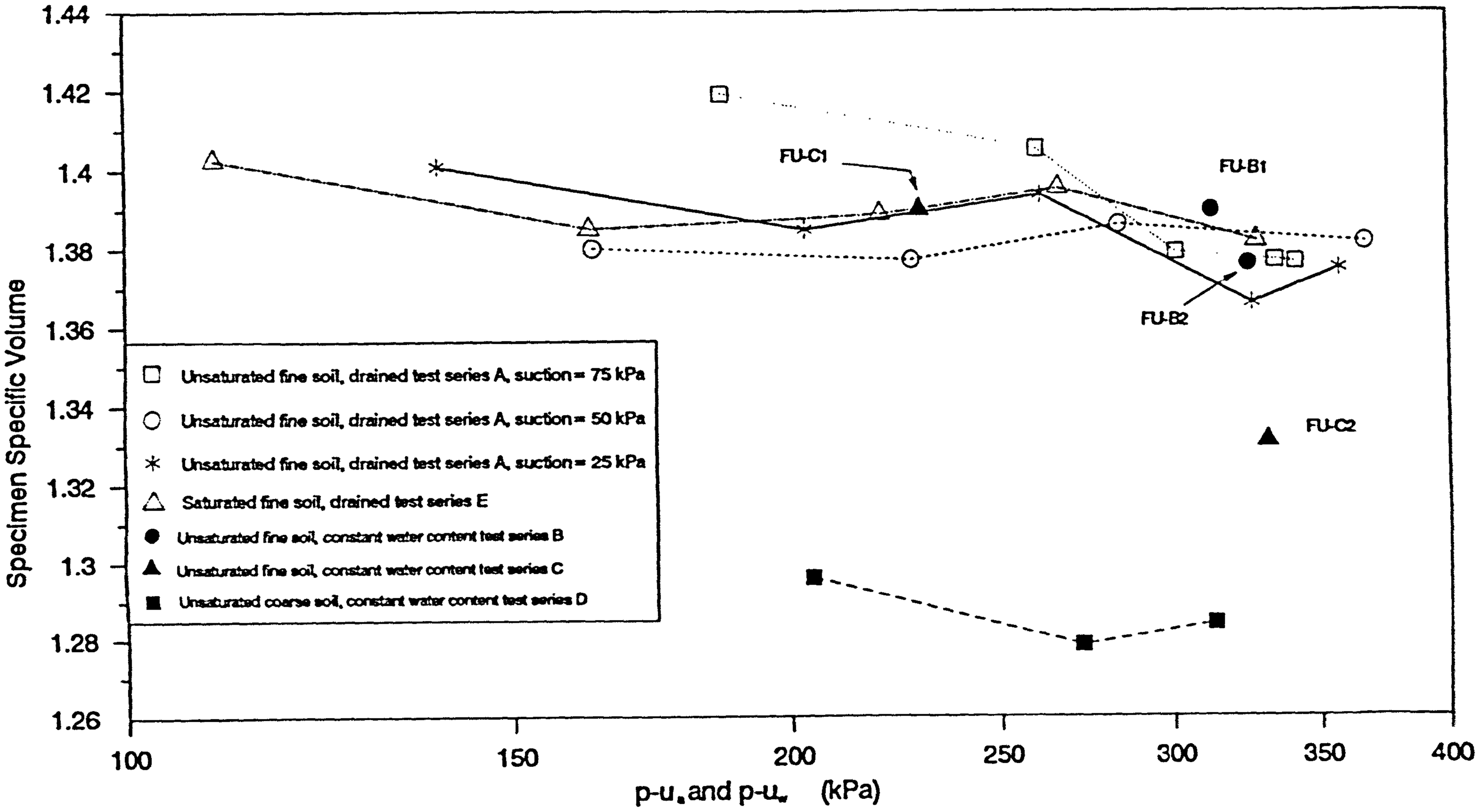

Fig. 8.24- Specimen specific volume calculated using the volume change unit measurements at the peak stress (failure) during the shear stage for the unsaturated and saturated fine and coarse grading specimens (series A to E)

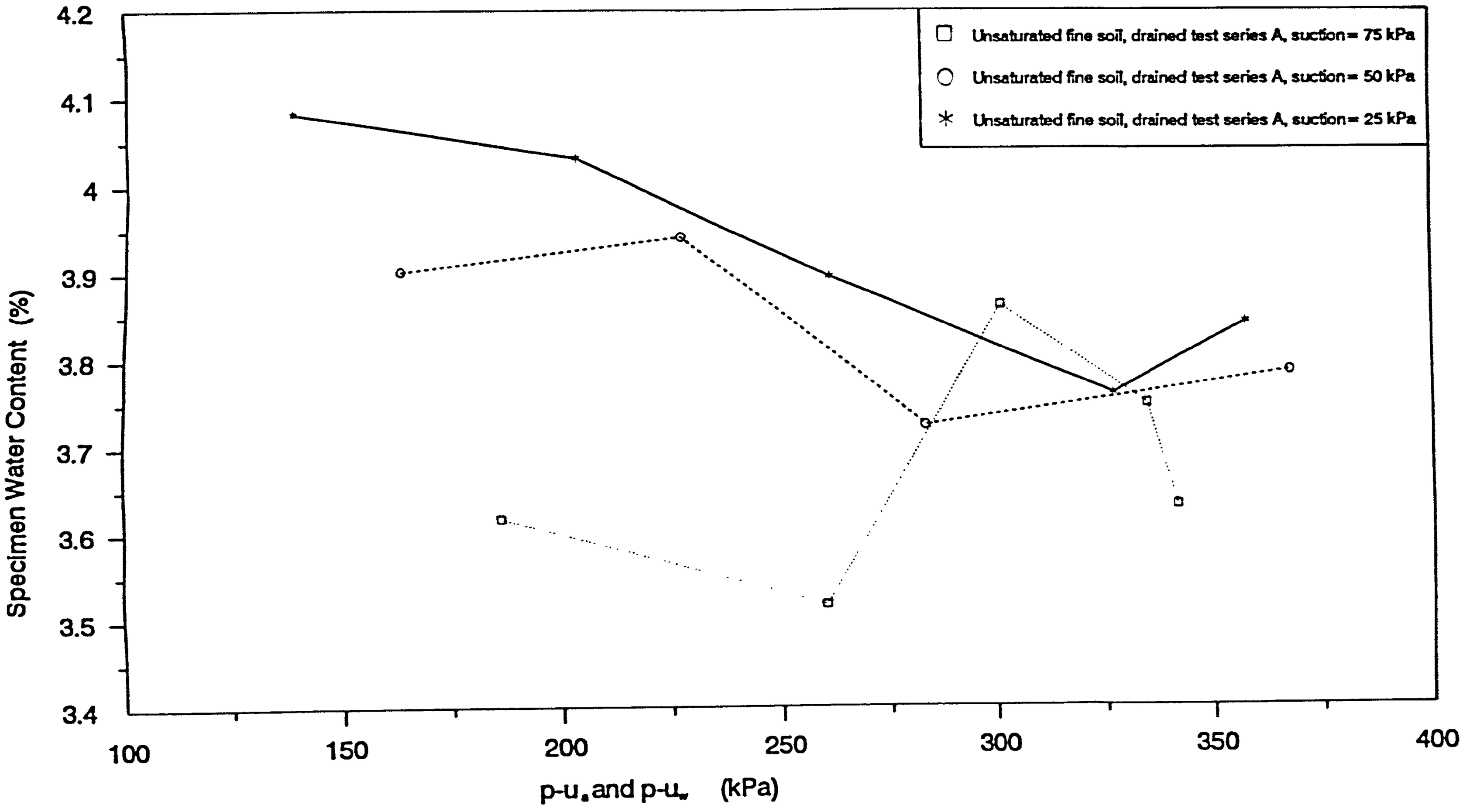

Fig. 8.25- Specimen water content at the peak stress (failure) during the shear stage for the fine grading drained test specimens (series A)

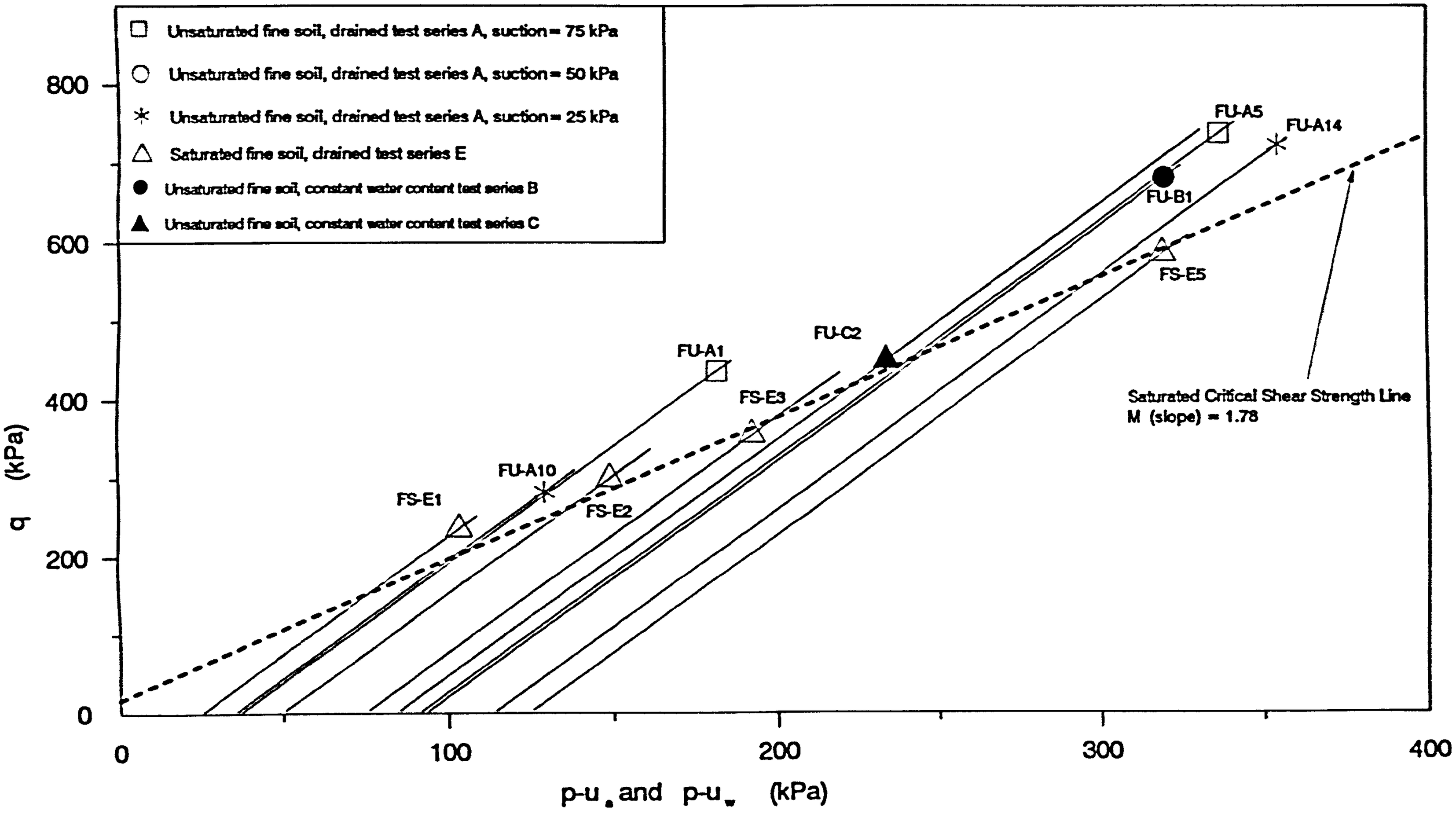

Fig. 8.26- Deviater stress at the end of shearing stage for the saturated and unsaturated fine garding specimens.

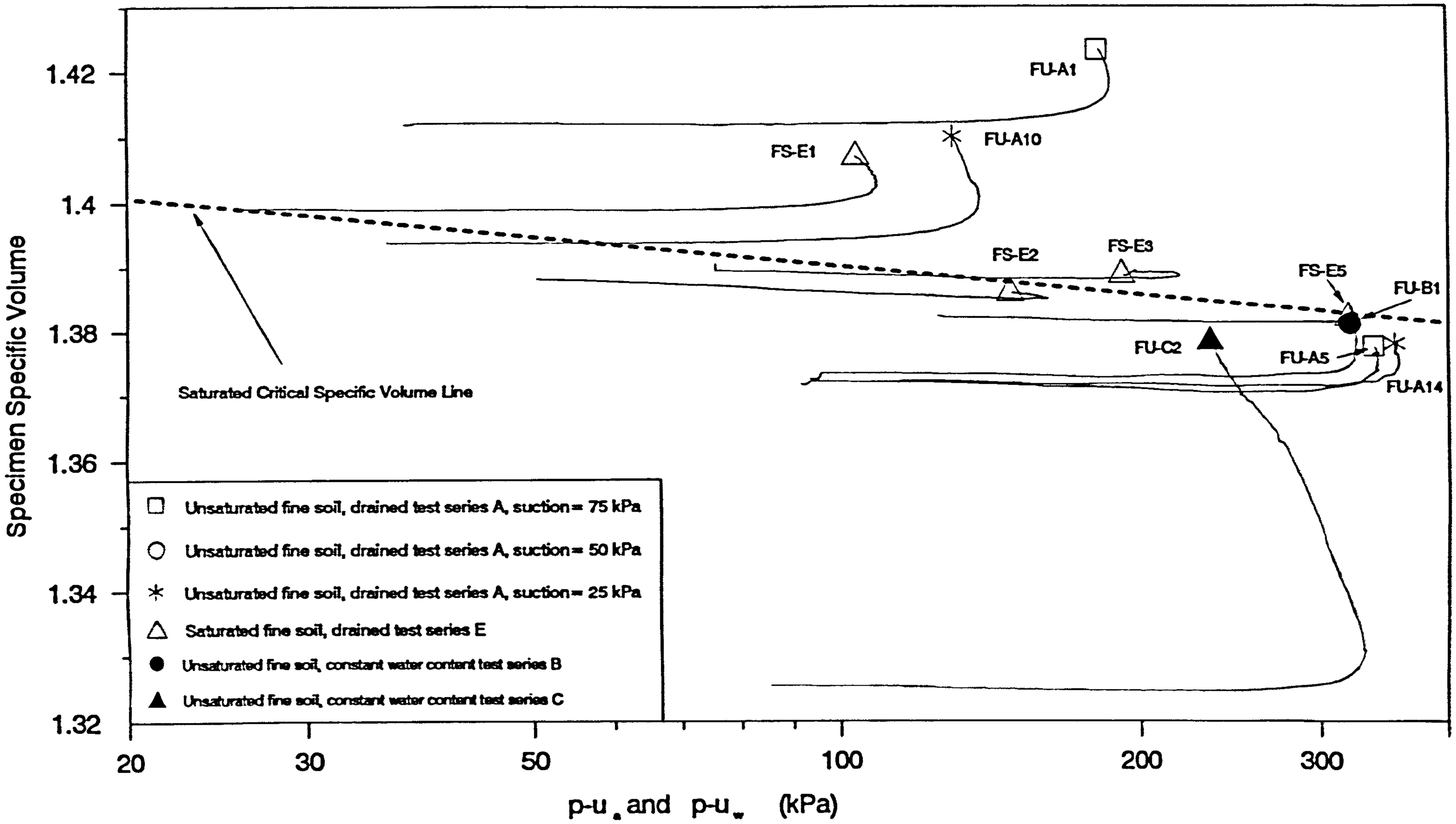

Fig. 8.27- Specimen specific volume at the end of shearing stage for the saturated and unsaturated fine grading specimens.

Chapter 9

Conclusions & Further Work

Work to investigate the triaxial behaviour of partially saturated granular soil at low stress levels (<100 kPa), was carried out on two soil gradings, fine and coarse, with maximum grain sizes of 5 mm and 20 mm respectively. A new double-wall triaxial cell which can accommodate a 150 mm diameter by 375 mm height specimen was designed and constructed for testing partially saturated granular soil. The cell is able to make internal measurements of the specimen stress and strain, and separate measurements and control of the pore air and water pressures. Also an existing conventional triaxial cell was modified to accommodate a specimen with the above dimensions, for testing saturated granular specimens.

The following points summarise the conclusions that were made in chapters 7 and 8:

(1) **Double-Wall Triaxial Cell Performance:** Results from repeatability tests have shown good agreement, which indicate that the techniques and methods used in the new triaxial cell were adequate and can be repeated. The specimen setting up and testing procedures were easy to perform using the new cell. The techniques used in this cell, such as spiral groove, ceramic stone, internal strain measurements, double wall cell and the measurements of pore water, pore air and cell pressures, were found to be working. There were some problems in the measurements of internal lateral strain due to miss-alignment between the piston and top cap which caused specimen tilting at the early stage of the shearing process.

(2) **Suction:** Values of initial suction of about 35 kPa and 15 kPa was measured for the fine and coarse grading soils respectively, at water contents of about 4% (optimum water content was about 6%), which influenced the behaviour of the soil.

(3) **Isotropic Compression:** The specific volume of the soil decreased as the net cell pressure increased, and the effect of suction was not clear. It was suggested that this change in specimen volume might be mainly due to particle crashing and not particle re-arrangement, which may explain the reason why the results did not show the effect of suction. The specimen water decreased as suction and net cell pressure increased. Coarse grained specimens showed lower values of specific volume than that for the fine grading specimens, which was due to their dry densities being higher than that for the fine grading specimens. Similar behaviour was found for the fine and coarse grading soils during the isotropic compression tests.

(4) **Shear Strength:** Drained tests were carried out on the fine grading specimens, at three values of suction 25, 50 and 75 kPa and when saturated. It was found that there was a linear relationship between q and $p-u_a$ for the unsaturated specimen and q and $p-u_w$ for the saturated specimens, i.e. constant value of ϕ'. It was also found that the saturated specimens had lower values of ϕ' than that for the unsaturated specimens. This finding led to the conclusion that the value of ϕ' for the saturated tests may not be used in Fredlund's equation (Equation 2.3) as was suggested by Fredlund's et al. (1978), to predict the shear strength of the unsaturated specimens. This means that the value of ϕ' must be obtained from tests carried out on unsaturated specimens, to be used in Fredlund's equation.

(5) **Soil Stiffness:** Young's modulus was found to increase as the suction and net (σ_3-u_a) and effective (σ_3-u_w) cell pressures increased. The value of Poisson's ratio was found to decrease as the net cell pressure increased, but it became almost a constant above a net cell pressure of about 80 kPa. The effect of suction on Poisson's ratio is not clear.

(6) **Stress Path:** Two types of test were carried out, drained and constant water content tests. The type of test (stress path) was found to have insignificant effect on the unsaturated soil behaviour.

(7) **Dry Density Variation:** Although all the specimens were compacted at the same nominal water content and compactive effort, to try to achieve the same dry density for all of the fine and coarse grading specimens, some variation in dry density (about ±0.015%) was found. This variation had a measurable effect on the Poisson's ratio and specific volume behaviour, and a small effect on soil stiffness and shear strength.

(8) **Axial Strain at Failure:** The axial strain at failure was found to increase as the net or effective cell pressure increased. The effect of suction on failure strain is not clear.

(9) **Relationship between q, $p-u_a$, suction, specific volume and water content all at failure:** A relationship between these variables was found to exist at failure. Two surfaces (three-dimensional diagram) of specimen water content and specific volume at failure against net mean stress, $p-u_a$, and suction may be drawn .

(10) **Critical State:** The critical shear strength for the saturated fine grading soil is linear, while the critical specific volume for the fine grading specimen is non-linear.

(11) **Rate of Strain:** Two rates of strain were used for the constant water content tests, 0.00011 %/min and 0.00093 %/min. It was found that there was insignificant effect on the constant water content test results. The effect of rate of strain on drained tests was not investigated.

As this current work was the first research to carry out triaxial tests on this type of granular soil at low stress levels, more work is needed to further investigate the triaxial behaviour of the partially saturated granular soil at low stress levels. The following recommendations for further work:

(i) More drained and constant water content tests at higher values of suction and using different values of initial total water content should be considered, to further check the validity of Fredlund's equation and to investigate the soil behaviour at higher values of suction.

(ii) More tests at different values of dry density should be carried out to find its effect on the soil behaviour. Also a method for compacting the specimens which gives less dry density variation, should be developed.

(iii) Tests should be carried out for different soil gradings, to see how this affects the soil behaviour.

(iv) The relationship between q, $p-u_a$, suction, specific volume and water content all at failure and at the critical state, needs to be investigated and modelled.

(v) The effect of soil inundation, either from the specimen top or bottom, on the soil behaviour needs to found.

References

[1] Aitchison, G. D. (1960), "Relationship of moisture and effective stress functions in unsaturated soils", Int. Soc. of SMFE, Proc. Conf. on Pore Pressure and Suction in Soils, London, Butterworths : 47-52.

[2] Al-Hussaini, M. (1983), "Effect of particle size and conditions on the strength of crashed Basalt", Canad. Geotech. J., 20(4) : 706-717.

[3] Alonso, E. E., Gens, A. and Hight, D. W. (1987), "Session 5: Special problem soils-General Report", Groundwater Effects in Geotechnical Engineering, Proc. 9th European Conf. on SMFE, Dublin, 3 :1087-1159.

[4] Anderson, W. F., Pyrah, I. C., Goodwin, A. K., Mckingley, A. and Salman, T. H. (1993), "The deformation behaviour of partially saturated fill at low stress levels", Engineered fills, Proc. of the Conf. Engineered Fills, Newcastle : 153-167.

[5] Arthur, J. R. F. and Menzies, B. K. (1972), "Inherent anisotropy in a sand", Geot., 22(1): 115-125.

[6] Atkinson, J. H. and Bransby, P. L. (1978), *The Mechanics of Soils - An Introduction to Critical State Soil Mechanics,* McGraw-Hill, London

[7] Baldi, G. and Nova, R. (1984), "Membrane penetration effects in triaxial testing", JGE, ASCE, 110(3) : 403-420.

[8] Barden, L. (1965), "Consolidation of compacted unsaturated clays", Geotechnique, 15(3) : 267-286.

[9] Barden, L. and Sides, G. R. (1970), "Engineering behaviour and structure of compacted clay", JSMFD, ASCE, 96(SM4) : 1171-1200.

[10] Been, K., Jefferies, M. G. and Hackey, J. (1991), "The Critical State of Sand", Geotechnique, 41(1) : 365-381.

[11] Bishop, A. W. (1959), "The principle of effective stress", Teknisk Ukeblad, 39 : 859-863.

[12] Bishop, A. W., Alpan, I., Blight, G. E. and Donald, I. B. (1960), "Factors controlling the strength of partially saturated cohesive soils", Research Conf. on Shear strength of Cohesive Soils, ASCE, Boulder : 503-532.

[13] Bishop, A. W. and Blight, G. E. (1963), "Some aspects of effective stress in saturated and partially saturated soils", Geotechnique, 13 : 177-197.

[14] Bishop, A. W. and Donald, I. B. (1961), "The experimental study of partially saturated soil in the triaxial apparatus", Proc. 5th ICSMFE, 1 : 10-22.

[15] Bishop, A. W. and Green, G. E. (1965), "The influence of end restraint on the compression strength of a cohesionless soil", Geotechnique, 15(3) : 243-266.

[16] Bishop, A. W. and Henkel, D. J. (1962), *The measurement of soil properties in triaxial test,* Edward Arnold, London.

[17] Blight, G. E. (1965), "A study of effective stresses for volume change", Moisture Equilibria and Moisture Changes in Soils Beneath Covered Areas, Butterworths, Australia : 259-269.

[18] Bocking, K. A. and Fredlund, D. G. (1980), "Limitation of the axis translation technique", Proc. of 4th Int. Conf. on Expansive Soils, Denver : 117-135.

[19] Boyce, J. R. and Brown, S. F. (1976), "Measurement of the elastic strain in granular material", Geotechnique, 26(4) : 637-640.

[20] Brackley, C. J. A. (1973), "Swell pressure and free swell in compacted clay", 3rd Int. Conf. on Expansive Soils, Haifa, Jerusalem, 1 : 169-176.

[21] Brackley, C. J. A. (1975), "A model of unsaturated clay structure and its application to swell behaviour", Proc. 6th Regional Conf. for Africa on SMFE, Durban, South Africa : 71-79.

[22] BS1377 (1990), British Standard Institution.

[23] Burland, J. B. (1965), "Some aspects of the mechanical behaviour of partially saturated soils", Moisture Equilibria and Moisture Changes in Soils Beneath Covered Areas, Butterworths, Australia : 270-278.

[24] Burland, J. B. and Symes, M. (1982), "A simple axial displacement gauge for use in the triaxial apparatus", Geotechnique, 32(1) : 62-65.

[25] Charles, J. A. and Watts, K. S. (1980), "The influence of confining pressure on the shear strength of compacted rockfill", Geotechnique, 30(4) : 353-367.

[26] Chu, J. and Lo, S-C. R. (1993), "On the measurement of critical state parameters of dense granular soils", Geotech. Testing J., ASTM, 16(1) : 27-35.

[27] Criag, R. F. (1984), *Soil Mechanics*, Van Nostrand Reinhold (UK) Co. Ltd., Honk Kong.

[28] Croney, D. (1952), "The movement and distribution of water in soils", Geotechnique, 3 : 1-16.

[29] Croney, D. and Coleman, J. D. (1948), "Soil thermodynamics applied to the movement of moisture in road foundation", Proc. 7th Int. Conf. for Applied Mechanics, 3 : 163-177.

[30] Croney, D. and Coleman, J. D. (1960), "Pore pressure and suction in soil", Int. Soc. of SMFE, Proc. Conf. on Pore Pressure and Suction in Soils, Butterworths, London : 31-37.

[31] Donald, I. B. (1961), "The mechanical properties of saturated and partially saturated soil", PhD thesis, University of London.

[32] Escario, V. (1989), "Strength and deformation of partially saturated soils", Proc. 12th ICSMFE, 1 : 43-46.

[33] Escario, V. and Sa'ez, J. (1986), "The shear strength of partly saturated soils, Geotechnique, 36(3) : 453-456.

[34] Fredlund, D. G. (1979), "Appropriate concepts and technology for unsaturated soils", Canad. Geotech. J., 16 : 121-139.

[35] Fredlund, D. G. and Morgenstern, N. R. (1976), "Constitutive relations for volume change in unsaturated soils", Canad. Geotech. J., 13(3) : 261-276.

[36] Fredlund, D. G. and Morgenstern, N. R. (1977), "Stress state variables for unsaturated soils", JGED, ASCE, 103(GT5) : 447-466.

[37] Fredlund, D. G., Morgenstern, N. R. and Widger, R. A. (1978), "The shear strength of unsaturated soils", Canad. Geotech. J., 15(3) : 313-321.

[38] Fredlund, D. G. and Rahardio, H. (1988), "State-of-development in the measurement of soil suction", Proc. of the Int. Conf. on Engineering Problems of Regional Soils, Beijin : 582-588.

[39] Fredlund, D. G., Rahardio, H. and Gan, J. K. M. (1987), "Non-linearity of strength envelope for unsaturated soils", Proc. of the 6th Int. Conf. on Expansive Soils, New Delhi : 49-54.

[40] Frydman, S., Zeitlen, J. G. and Alpan, T. (1973), "The membrane effect in triaxial testing of granular soils", J. of Testing and Evaluation, 1(1) : 37-41.

[41] Fukushima, S. and Tatsuoka, F. (1984), "Strength and deformation characteristics of saturated sand at extremely low pressures", Soils and Foundations, JSSMFE, 24(4) : 30-48

[42] Gardner, W. R. (1960), "Soil suction and water movement", Int. Soc. of SMFE, Butterworths, London : 137-140.

[43] Gens, A. (1982), "Stress-strain and strength characteristics of low plasticity clay", PhD thesis, University of London.

[44] Goodwin, A. K. (1991), "One dimensional compression behaviour of unsaturated granular soils at low stress levels", PhD thesis, University of Sheffield.

[45] Goto, S. and Tatsuoka, F. (1988), "Effects of end conditions on triaxial compressive strength for cohesionless soil", Advanced Triaxial Testing of Soil and Rock, ASTM, Philadelphia, STP 977 : 692-705.

[46] Gulhati, S. K. and Satija, B. S. (1981), "Shear strength of partially saturated soils", Proc. 10th ICSMFE, Stockholm, 1 : 609-612.

[47] Hagerty, M.M., Hite, D.R. and Ullrich, C.R.(1993), "One-dimensional high-pressure compression of granular media", JGE, ASCE, 119(1), : 1-18.

[48] Head, K. H. (1982), *Manual of Soil Laboratory Testing*, Pentech Press, London.

[49] Henkel, D. J. and Gilbert, G. D. (1952), "The effect of the rubber membrane on the measured triaxial compression strength of clay samples", Geotechnique, 3 : 20-29.

[50] Hilf, J. W. (1956), "An investigation of pore-water pressure in compacted cohesive soils", Technical Memorandum 654, United States Department of the Bureau Reclamation, Denver, Colorado.

[51] Ho, D. Y. F. and Fredlund, D. F. (1982), "A multistage triaxial test for unsaturated soils", Geotech. Testing J., 5(1/2) : 18-25.

[52] Holtz, W. G. and Gibbs, H. J. (1956), "Triaxial shear tests on pervious gravely soils", JSMFD, ASCE, 82(SM1), paper No. 867 : 1-22.

[53] Indraratna, B., Wijewardena, L. S. S. and Balasubramaniam, A. S. (1993), "Large-scale triaxial testing of Greywacke rockfill", Geotechnique, 43(1) : 37-51.

[54] Jardine, R. J., Symes, M. J. and Burland, J. B. (1984), "The measurement of soil stiffness in the triaxial apparatus", Geotechnique, 34(3) : 323-340.

[55] Jennings, J. E. (1960), "A revised effective stress law for use in the prediction of the behaviour of unsaturated soils", Int. Soc. SMFE, Proc. Conf. on Pore Pressure and Suction in Soils, Betterworths : 26-30.

[56] Jennings, J. E. and Burland, J. B. (1962), "Limitation to the use of effective stresses in partially saturated soils", Geotechnique, 12(2) : 125-144.

[57] Jones, R. H. and Hurt, K. G. (1978), "An osmotic method for determining rock and aggregate suction characteristics with application to frost heave studies", Q. J. of Engineering Geology, 11 : 245-252.

[58] Jumikis, A. R. (1962), *Soil Mechanics*, D. Van Nostrand Company, INC., New York, USA.

[59] Kiekbusch, M. and Schuppener, B. (1977), "Membrane penetration and its effect on pore pressure", JGED, ASCE, 103(GT11) : 1267-1279.

[60] Kirkpatrick, W. M. and Belshaw, D. J. (1968), "On the interpretation of the triaxial test", Geotechnique, 18(3) : 336-350.

[61] Kirkpatrick, W. M. and Younger, J. S. (1970), "Strain conditions in compression cylinder", JSMFD, ASCE, 96(SM5) : 1683-1695.

[62] Krahn, J. and Fredlund, D. G. (1972), "On total metric and osmotic suction", Soil Science, 114(5) : 339-348.

[63] Kramer, S. L., Sivaneswaran, N. and Davis, R. O. (1990), "Analysis of membrane penetration in triaxial test", JEM, ASCE, 116(4) : 773-789.

[64] Lambe, T. W. (1953), "The structure of inorganic soil", ASCE, Separate No. 315, 79 : 1-49

[65] Lambe, T. W. and Whitman, R. V. (1979), *Soil Mechanics*, John Wiley & Sons, USA.

[66] La Rochelle, P., Leroueil, S., Trak, B., Blais-Leroux, L. and Tavenas, F. (1988), "Area corrections in triaxial tests", Advanced Triaxial Testing of Soil and Rock, ASTM, Philadelphia, STP 977 : 715-731.

[67] Lee, K. L. (1978), "End restraint effects on undrained static triaxial strength of sand", JGED, ASCE, 104(GT6) : 687-704.

[68] Lee, K. L. and Seed, H. B.(1967), "Drained characteristics of sands", JSMFD, ASCE, 93(SM6) : 117-141.

[69] Leroueil, S., Tavenas, F., La Rochelle, P. and Tremblay, M. (1988), "Influence of filter paper and leakage on triaxial testing", Advanced Triaxial Testing of Soil and Rock, ASTM, Philadelphia, STP 977 : 189-201.

[70] Marachi, N. (1969), "strength and deformation characteristics of rockfill materials", PhD thesis, University of California, Berkeley.

[71] Marachi, N., Chan, C. K. and Seed, H. B. (1972), "Evaluation of properties of rockfill materials", JSMFD, ASCE, 98(SM1) : 95-114.

[72] Maytas, E. L. and Radhakrishna, H. S. (1968), "Volume change characteristics of partially saturated soils", Geotechnique, 18 : 432-448.

[73] Mohamed, A. O., Yong, R. N. and Cheung, S. C. H. (1992), "Temperature dependence of soil water potential", Geotech. testing J., 15(4) : 330-339.

[74] Molenkamp, F. and Luger, H. J. (1981), "Modelling and minimization of membrane penetration effects in tests on granular soils", Geotechnique, 31(4) : 471-486.

[75] Muir Wood, D. (1990), *Soil Behaviour and Critical State Soil Mechanics*. Cambridge University Press, New York.

[76] NIRR Council of Science and Industrial research (1969), "The influence of the ratio of sample to particle diameter on the shear strength of cohesionless soils", VIA 10 (1969), No.1 : 6-7, South Africa.

[77] Norris, G. M. (1981), "Effect of end membrane thickness on the strength of frictionless cap and base tests", Laboratory Shear Strength of Soil, ASTM, STP 740 : 303-314.

[78] Oloworkere, O. (1986), "Behaviour of railway ballast when subjected to triaxial loading", Civil Engineering for Practicing and Design, 5 : 305-321.

[79] Olson, R. E. and Langfelder, l. J. (1965), "Pore water pressure in unsaturated soils", JSMFD, ASCE, 91(SM4) : 127-150.

[80] Ricceri, G. and Soranzo, M. (1981), "Anisotropic behaviour of a saturated uniform sand", Proc. 10th ICSMFE, Stockholm : 759-764.

[81] Raudkivi, A. J. and U'u, N. V. (1976), "Soil moisture movement by temperature gradient", JGED, ASCE, 102(GT12) : 1225-1244.

[82] Ponce, V. M. and Bell, J. M. (1971), "Shear strength of sand at extremely low pressures", JSMFD, ASCE, 97(SM4) : 625-638.

[83] RRL (1968), *Soil Mechanics for Road Engineering*, Road Research Laboratory, London.

[84] Rowe, P. W. and Barden, L. (1964), "Importance of free ends in triaxial testing", JSMFD, ASCE, 90(SM1) : 1-27.

[85] Satija, B. S. and Gulhati, S. K. (1979), "Strain rate for shear testing of unsaturated soil", 6th Asian Regional Conf. on SMFE : 83-86.

[86] Sivakumar, V. (1993), "A critical state framework for unsaturated soil", PhD theses, University of Sheffield.

[87] Skermer, N. A. and Hillis, S. F. (1970), "Gradation and shear characteristics of four cohesionless soils", Canad. Geotech. J., 7(1) : 62-68.

[88] Tadepalli, R., Rahardjo, H. and Fredlund, D. G. (1992), "Measurements of metric suction and volume change during inundation of collapsible soil", Geotech. Testing J., ASTM, 15(2) : 115-122.

[89] Tatsuoka, F., Molenkamp, F., Torii, T. and Hino, T. (1984), "Behaviour of lubrication layers of platens in element tests", Soils and Foundations, JSSMFE, 24(1) : 113-128.

[90] Taylor, S. A. and Cary, J. W. (1960), "Analysis of the simultaneous flow of water and heat or electricity with the thermodynamics of irreversible process", 7th Int. Congress of Soil Science, Madison, USA : 80-90.

[91] Toll, D. G. (1990), "A framework for unsaturated soil behaviour", Geotechnique, 40(1) : 31-44.

[92] Ueng, T-S., Tzou, Y-M. and Lee, C-J. (1988), "The effect of end restraint on volume change and particle breakage of sand in triaxial tests", Advanced Triaxial Testing of Soil and Rock, ASTM, Philadelphia, STP 977 : 679-691.

[93] Vesic, A. S. and Clough, G. W. (1968), "Behaviour of granular materials under high stress", JSMFD, ASCE, 94(SM3) : 661-688.

[94] Wheeler, S. J. (1988), "The undrained shear strength of soils containing large gas bubbles", Geotechnique, 38(3) : 399-413.

[95] Wheeler, S. J. and Sivakumar, V. (1992), "Development and application of a critical state model for unsaturated soil", Wroth Memorial Conf. on Predictive Soil Mechanics, Oxford.

[96] Wheeler, S. J. and Sivakumar, V. (1995), "An elasto-plastic critical state framework for unsaturated soil", Geot., 45(1) : 35-53.

[97] Wu, S., Gray, D. H., Richart, F. E. and JR (1984), "Capillary effect on dynamic modulus of sand and silts", JGE, ASCE, 110(9) : 1188-1203.

[98] Wu, S., Gray, D. H., Richart, F. E. and JR (1985), "Capillary effect on shear strength modulus at high strains", Proc. 11th ICSMFE, 2 : 1091-1094.

[99] Yamamuro, J. A., and Lade, P. V. (1993), "Effect of strain rate on instiblity of granular soils", Geotech. Testing J., ASTM, 16(3) : 304-313.

[100] Yoshida, Y., Kuwano, J. and Kumano, R. (1991), "Effect of saturation on shear strength of soils", Soils and Foundations, JSSMFE, 31(1) : 181-186.